Design of a multifunctional subsea basket for XT operations

Vincent Sondre Førde

Patrick Hjelm Ungvary

Oskar Odland Bø

Bachelor's thesis in Mechanical Engineering

Bergen, Norway 2024

Høgskulen på Vestlandet

Design of a multifunctional subsea basket for XT operations

Vincent Sondre Førde

Patrick Hjelm Ungvary

Oskar Odland Bø

Department of Mechanical Engineering and Maritime Studies

Western Norway University of Applied Sciences

NO-5063 Bergen, Norway

IMM 2024-M05

Western Norway University of Applied Sciences (Høgskulen på Vestlandet, HVL)

Faculty of Technology, Environmental and Social Sciences

Department of Mechanical Engineering and Maritime Studies

Inndalsveien 28

NO-5063 Bergen, Norge

Norsk tittel:	Design av en multifunksjonell undervannskurv for juletreoperasjoner
Author(s), student number:	Vincent Sondre Førde, 587638 Patrick Hjelm Ungvary, 599100 Oskar Odland Bø, 599108
Study program:	Mechanical Engineering
Date:	05.2024
Report number:	IMM 2024-M05 (where XX: group ID.nr)
Supervisor at HVL:	Mariusz Domagala, HVL
Assigned by:	DeepOcean AS
Contact person:	Maria Teige
Antall filer levert digitalt:	None

Preface

This bachelor thesis is written in the Mechanical Engineering program at the Department of Mechanical Engineering and Maritime Studies of Western Norway University of Applied Sciences (WNUAS). The bachelor course this spring, 2024, is set to 20 ECTS points.

The thesis is written in collaboration with DeepOcean, which provided several task options. Given our bachelor's program in Mechanical Engineering, we were especially interested in the opportunity to design a subsea basket for the company. It is relevant to our program and aligns with the group's interests.

In the starting process, the project mainly consisted of reading relevant standards and looking at similar products in the market. This gave an idea of design options and what rules and limitations the subsea industry operates with. In addition, DeepOcean provided a specification list that was important for designing the best possible subsea basket.

We want to express our gratitude to our university supervisor, Professor Mariusz Domagala, for his guidance and valuable knowledge, which he generously shared with us this spring. We are also thankful to Maria Teige, Anders Haga, and Maria Lie Lotsberg from DeepOcean for their supervision and industry expertise, which significantly contributed to the completion of our project. Throughout this period, we have expanded our knowledge and are appreciative of the opportunity to write this thesis.

Abstract

This thesis examines the design of a subsea basket that meets the specifications of the oil service company DeepOcean, aiming to enhance operational efficiency in subsea tree operations. Subsea baskets are typically used in subsea operations to store equipment on the seabed. The thesis explores a solution that allows the basket to be used as a Dead Man's Anchor (DMA), a requirement from clients for the installation of subsea structures.

The solution combines this with the ability to use a crane device with a lower weight capacity, making it easier for deck personnel to handle. The proposed solution in the thesis involves integrating a detachable weight into the subsea basket. This design will make the basket multifunctional, which will be unique in the market.

The subsea basket is designed according to a specification list and complies with relevant standards and regulations. The design process is conducted using Creo Parametric software, and the basket is constructed according to Det Norske Veritas (DNV) and Eurocode standards. These standards provide clear guidelines for structures in the offshore environment and form the basis for weight limit calculations.

Manual calculations have been used to ensure that the subsea basket meets the weight requirements. Additionally, various design and lifting factors have been considered, including quality control of the subsea basket and the selected lifting arrangement. This is done with the help of numerical methods for strength calculations using the simulation program Ansys. Structural analyses, both manual and numerical, have been carried out in accordance with Eurocode standards to ensure that the subsea basket can withstand the loads during lifting operations.

The results from the analyses show that the subsea basket meets the requirements for allowable stress loads, confirming that the design is ready for further certification and testing required for subsea tree operations.

Sammendrag

Denne oppgaven undersøker designet av en undervannskurv som oppfyller spesifikasjoner fra oljeserviceselskapet DeepOcean, og bygger på selskapets mål om å forbedre operasjonseffektiviteten innen juletreoperasjoner. Undervannskurvene brukes normalt i undervannsoperasjoner for oppbevaring av utstyr på havbunnen. Oppgaven vil se på en løsning som gjør at kurven operasjonelt kan brukes som et dødmannsanker (DMA), som er et krav stilt av kunder for installasjon av undervannsstrukturer.

Løsningen vil kombinere dette med muligheten til å bruke en kraninnretning med lavere vektkapasitet, som gjør den lettere å håndtere for dekkspersonell. Den presenterte løsningen i oppgaven innebærer integrering av en avtagbar vekt til undervannskurven. Med dette vil designet kunne definere seg som en multifunksjonell, noe som vil være unikt i markedet.

Undervannskurven er designet etter en spesifikasjonsliste, og overholder relevante standarder og forskrifter. Designprosessen er gjennomført ved hjelp av Creo Parametric programvare, og kurven er konstruert etter Det Norske Veritas (DNV) og Eurocode standarder. Disse standardene gir klare retningslinjer for strukturer i offshoremiljøet, og legger grunnlaget for beregninger av vektbegrensninger.

Manuelle beregninger har blitt brukt for å sikre at undervannskurven oppfyller vektkravene. I tillegg har ulike design- og løftefaktorer blitt vurdert, som kvalitetskontrollerer undervannskurven og valgt løftearrangement. Dette med hjelp av numeriske metoder for styrkeberegninger ved bruk av simuleringsprogrammet Ansys. Strukturanalyser, både manuelle og numeriske, er utført i henhold til Eurocode standardene, for å sikre at undervannskurven tåler belastningene under løfteoperasjoner.

Resultatene fra analysene viser at undervannskurven tilfredsstiller kravene til tillatte spenningsbelastninger, som bekrefter at designet er klart for videre sertifisering og testing som kreves av juletreoperasjoner.

Table of contents

Nomenclature

Symbol	Explanation (Unit)
γ_{Weight}	Margin factor
$\gamma_{Weighing}$	Margin factor of weighed weights of an object
SKL	Skew load factor
DAF	Dynamic amplifying factor
SHL	Static hook load (N)
DHL	Dynamic hook load (N)
SHL_1	Static hook load found from DHL_1 (N)
DHL_1	Dynamic hook load used to establish the maximum weight of the basket (N)
W_{ud}	Upper bound weight (tons)
$W_{rigging}$	Weight of rigging (tons)
$W_{A-frame}$	Weight of A-frame (tons)
W_{basket}	Weight of basket (tons)
W_{Tools}	Weight of tools (tons)
W	Weight sum of basket, A-frame, and tools (tons)
W_1	Desired weight of the entire structure without the extra weight (tons)
F	Design load (kN)
F_{sub}	Design load for subsea lifts (kN)
F_{air}	Design load for air lifts (kN)
$F_{extraWeight}$	Design load of extra weight (kN)
MGW	Mean gross weight of the entire structure (tons)
$MGW_{extraWeight}$	Mean gross weight of the extra weight (tons)
g	Gravitational acceleration (m/s^2)

LL	Resultant lifting load (kN)
LL_{main}	Resultant lifting load for the main lifting point (kN)
$LL_{AFrameSub}$	Resultant lifting load for the A-frame lifting points for subsea lifts (kN)
$LL_{AFrameAir}$	Resultant lifting load for the A-frame sling lifting points for air lifts (kN)
$LL_{extraWeight}$	Resultant lifting load for extra weight bolted connection points (kN)
DF	Design factor
PL	Percentage loading factor
v	The angle between the A-frame sling leg and vertical)
σ_e	von Mises stress caused by the design load (MPa)
σ_{ea}	Allowable Stress (MPa)
R_e	Yield stress of material (MPa)
F_{F1}	Design load for forklift pockets on the extra weight (kN)
F_{F2}	Design load for forklift pockets on the basket (kN)
e	distance between stiffeners at an end post (mm)
h_w	Height of beam cross section (mm)
E	Modulus of elasticity (MPa)
D_H	Diameter of pinhole (mm)
t	Thickness (mm)
R_{pad}	Radius of padeye (mm)
t_{ch}	Thickness of cheek plate (mm)
UF	Utilization Factor (%)
$d_{allowed}$	Minimum diameter allowed (mm)
d	Diameter (mm)
β_p	Reduction factor
t_p	Total plate thickness (mm)

$F_{v,Rd}$	Shear resistance of bolts (kN)
a_v	Cross area factor
f_{ub}	Ultimate tensile strength (MPa)
A	Area (mm^2)
γ_{M2}	Partial factor for resistance of cross-section
$F_{v,Ed}$	Design ultimate shear load (kN)
$F_{p,Cd}$	Design preload (kN)
A_s	Stress area of threaded part (mm^2)
γ_{M7}	Safety factor for preload of high strength bolts
M_A	Tightening torque (Nm)
M_G	Friction moment in screwed in thread section (Nm)
M_K	Friction moment in contact area between bolt head and plate (Nm)
d_2	Pitch diameter (mm)
P	Thread pitch (mm)
μ_{Gmin}	Friction coefficient in threads
D_{Km}	Mean bearing diameter of bolts or nuts (mm)
μ_K	Coefficient of friction
XT	Subsea Tree
IMR	Inspection Maintenance and Repair
Hs	Significant Wave Height
SHS	Square Hollow Section
RHS	Rectangular Hollow Section
EC3	Eurocode3
DNV	Det Norske Veritas
ROV	Remoted Operated Vehicle
DMA	Dead Mans Anchor
MHS	Module Handling System
POU	Portable Offshore Unit

FEM	Finite Element Method
ASD	Allowable Stress Design
ULS	Ultimate Limit State
LRFD	Load and Resistance Factor Design
LTB	Lateral Torsional Buckling
SLS	Serviceability Limit State
γ_{M0}	Partial material safety factor
$W_{pl,} W_y$	Plastic section modulus
f_y	Yield strength (N/mm^2)
M_{Ed}	Bending Moment design value (kNm)
$M_{c,Rd}$	Bending Moment resistance (kNm)
F_{sub}	Design load for subsea POU
ε	Strain Ratio in EC3, classification of cross-sections
V_{Ed}	Shear Force design value (kN)
$V_{c,Rd}$	Shear Force resistance (kN)
A_v	Shear Area of cross-section (mm^2)
M_{cr}	Critical Buckling Moment (kNm)
μ_{cr}	Relative dimensionless critical moment
G	Shear modulus (MPa)
I_z	Moment of inertia by z-axis (mm^3)
I_t	Torsion constant (mm^3)
L_b	Buckling length (mm)
C_1	Load factor
K_{wt}	Torsional parameter
I_w	Warping constant (mm^6)
$\overline{\lambda}_{LT}$	Slenderness of cross-section

ky, kz, kw	Constraints correction factor
a	Effective throat thickness (mm)
β_w	Correlation factor for fillet welds
$\sigma_\perp$	Normal stress perpendicular to the throat (MPa)
$\sigma_\parallel$	Normal stress parallel to the axis of the weld (MPa)
$\tau_\perp$	Shear stress (in the plane of the throat) perpendicular to the axis of the weld (MPa)
$\tau_\parallel$	Shear stress (in the plane of the throat) parallel to the axis of the weld (MPa)
η	Permissible usage factor
$W_{eff,x,z}$	Effective section modulus for major(x) and minor(z) axis, in the elastic region (mm^3)
W_{el}	Elastic section modulus(mm^3)
A_{eff}	Effective Area of cross-section for HEB (mm^3)
l_{weld}	Length of the weld (mm)
CoG	Center of Gravity
F_{SD}	Sling design load (kN)
γ_{sf}	Design factor for slings and grommets
γ_h	Lifting factor
γ_c	Consequence factor

1. Introduction

This chapter provides an overview of subsea baskets and their role in subsea operations. It introduces DeepOcean's motivation for a multifunctional subsea basket. The chapter highlights the innovative design features of the proposed basket and describes the capabilities of the construction vessel Normand Ocean used in these operations.

1.1. Background

Subsea Baskets are used to store various tools and equipment needed for subsea operations. They serve as support by safely storing tools and equipment while lowered down to the seabed or recovered up to deck. One instance is subsea tree operations (XT operations), where these subsea baskets are deployed with equipment for the module and necessary tools for a Remotely Operated Vehicle (ROV). This increases the ROV's efficiency of accessing the tools and equipment needed to install the subsea trees.

In the oil and gas industry, a subsea tree is a module that sits on top of the well and regulates the production flow. It also connects the well with tubing, other devices, as well as the topside. The trees are heavy constructions that can weigh up to 70 tons, which leads to challenges when deploying them from a construction vessel. If the subsea tree module is accidentally dropped due to calculation deviation or other unforeseen circumstances, the consequences could be catastrophic for the environment and operational assets. In the worst case, it can cause risks to the safety of personnel.

To ensure safety in case of any accidents, it's crucial to use an offset method of landing the tree, as illustrated in Figure 1. This offset method is a requirement from operators in the oil and gas industry and is used in the installation of all types of subsea structures.

The method involves a dead man’s anchor (DMA), which is a heavy object placed on the seabed to create a stable anchoring point. In XT operations the DMA is connected to guidewires passing through the funnels of the subsea tree structure. The DMA is placed on the seabed with an offset of 10% of the sea depth away from the structure manifold. Once the guidewires are connected to the DMA, the tree is gradually lowered to 30 meters above the seabed. Then, one guidewire at a time is transferred to guideposts at the tree's landing area for accurate positioning. The vessel is then moved over to the manifold position, and the tree is lowered the remaining 30 meters to be positioned at the landing area.

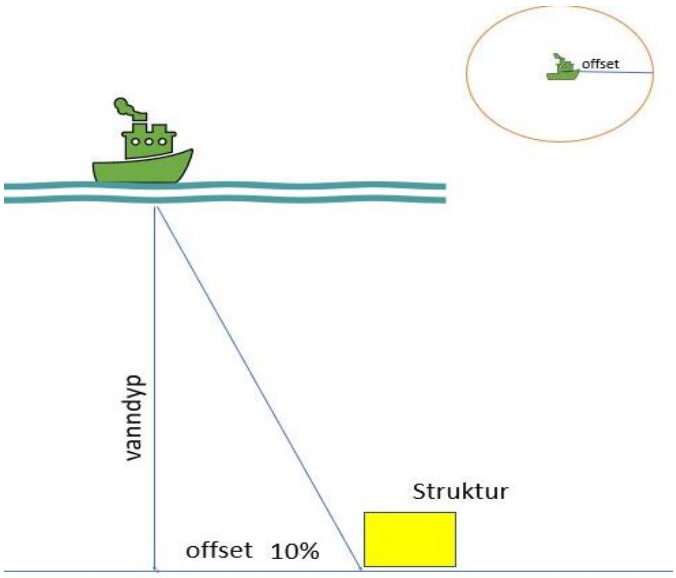

Figure 1 - Illustration of a procedure for the offset method, obtained from DeepOcean.

1.2. Motivation

According to feedback from DeepOcean supervisors, a shortage of subsea baskets in the market has led to high rental costs. The company is considering conducting further research to determine the feasibility of manufacturing its own subsea basket with multifunctional features for XT operations. Specifically, the basket shall be operational for transporting tools and as a DMA. It will be designed for the construction vessel Normand Ocean, where there are two types of lifting cranes for subsea lifts. When practical, it is desirable to use the crane with a lower lifting load capacity because of its time efficiency. This could be solved with a subsea basket equipped with the capability of changing its mean gross weight (MGW) by adding/removing additional weight.

The company's target is to achieve a 45% reduction in CO2 emissions before 2030 and by 2040, further aiming to become carbon neutral [1]. A subsea basket with the mentioned features would help operations to become more cost-efficient and sustainable by reducing the amount of time. This design concept would be a unique product on the market, with customizations that specifically meets the company's requests.

1.3. Novelty

Given the existing subsea baskets in the market, the novelty of the subsea basket is established in its multifunctional design and adaptability to various operational needs within the subsea industry. Unlike traditional subsea baskets that serve limited purposes, this innovative design aims to integrate the ability to fulfill multiple roles.

This implies including features such as regulated weight to meet requirements and enabling the use of a whip-line system (1.4). The basket can be used as an independent module or in combination with the integrated DMA. The structure is also designed to fit the basket without affecting the passthrough of water in any significant way. Additionally, the basket's design enhances efficient ROV handling and sea fastening for XT equipment, making it ideal for IMR operations.

1.4. Construction Vessel and MHS Overview

Normand Ocean is a multipurpose subsea construction vessel owned by Solstad Offshore, which DeepOcean charters for its wide IMR use. The vessel, presented in Figure 2, is designed to ensure safe and efficient subsea operations. The key vessel feature is a 1020-square-meter working deck plan, which accommodates a large amount of equipment and tooling. It is equipped with a 160te subsea crane configured with a main block hook and a secondary system called whip-line, capable of handling loads up to 12te. A 40te module handling system (MHS) equipped with a skidding mechanism is fitted, allowing efficient module handling during operations. The vessel also contains two ROVs which can be operated under the limitation of 5-meter significant wave height (Hs) [2].

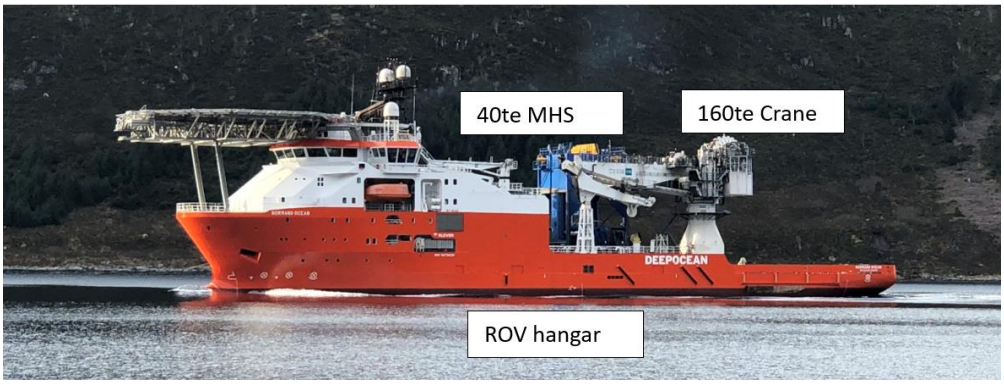

Figure 2 - Normand Ocean, obtained from DeepOcean.

MacGregor provides the MHS designed for installing and maintaining subsea installations, as shown in Figure 3. This system ensures accurate and safe handling in challenging weather conditions. The key components include an integrated tower on deck, housing the main lift winch, guidewire, cursor, and moonpool doors system. The guidewire system ensures precise load handling and accurate positioning of the subsea modules on the seabed, which is particularly crucial during operations in rough weather. In addition, the cursor system plays a vital role in securely constraining subsea modules during deployment and recovery through the moonpool. This prevents swinging due to controlled handling that minimizes the risk of damage to the load [3].

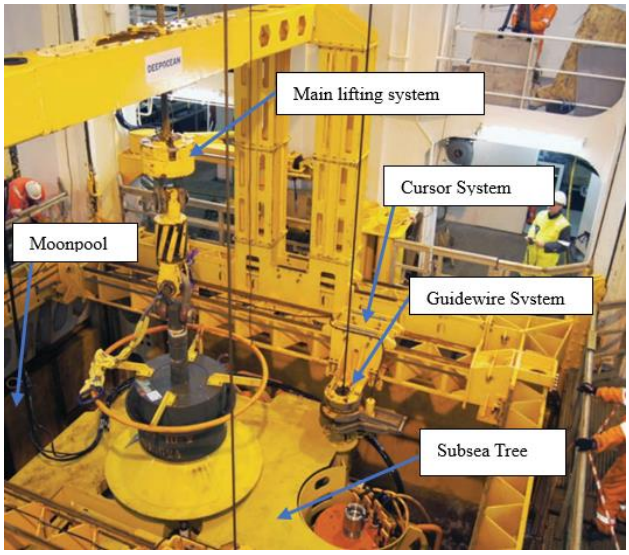

Figure 3 - MHS system, MacGregor. [3]

2. Methodology

Methodology concerns the different methods used to gather and approach information. When using the proper methods, the article is well-supported and with correct information. This chapter includes the methods of gathering information and the research approach of the project.

2.1. Research Approach

When there is not a substantial amount of information on a topic on the internet, interviewing engineers in different disciplines is a suitable method for acquiring knowledge. Interviewing experts is an inductive and qualitative method and a reliable and primary source of information.

Another inductive and qualitative method is document analysis. This is done when reading articles and documents found on the internet, in literature, or in other sources. When analyzing documents, it is essential to be critical of potential misinformation. This can be checked by confirming that the sources are backed up by research and professionals. As an example, standards from DNV are well-known and used by all companies operating in the jurisdiction of these standards.

In addition to the research team's experience, the group includes an educated ROV pilot who has experience with various subsea basket alternatives in operation. This experience provides insights into the practical aspects of design choices and helps the group understand subsea operations.

2.2. Research of Design Alternatives

There are a variety of subsea baskets on the market, where the different designs have certain advantages and disadvantages during subsea operations. A few features that are crucial for such baskets are time efficiency, safety, and easy management by the deck crew and ROV. The lifting of the basket is achieved using different types of lifting mechanisms, where the most common types are presented in Figure 4 to Figure 6.

Figure 4 - Subsea basket 4-leg rigging. [4]

Figure 5 – Subsea basket with A-frame. [4]

Figure 6 - Subsea basket with Center pole. [4]

2.2.1. Pros and Cons of Existing Designs

Pros and cons of existing designs in Table 1 presents the different alternatives, outlining their advantages and disadvantages. This comparison affected the final decision regarding the design choice, as discussed in chapter 2.2.2.

Table 1 - Pros and cons of existing designs.

Alternatives	Advantages	Disadvantages
4-Leg Rigging	Require less structural analysis during the engineering process.	Challenges for handling rigging components for ROV and deck personnel due to several lifting slings, potentially leading to operational delays.
	Provides a large storage area.	The lifting slings may interfere with other subsea equipment, leading to the potential risk of damage to high-cost operational assets.
	Components can be designed with minimal complexity for efficient manufacturing, potentially lowering production costs.	Uneven weight distributions would lead to increased dynamic forces.
A-frame	Spreader bar of the A-frame design helps distribute loads more evenly.	Potentially higher production costs due to the A-frame.
	Efficient handling of rigging components for ROV and Deck personnel, reducing operational delays.	A-frame application increases overall weight (advantage for DMA option).
	Better accessibility to tooling and equipment for ROV and Deck personnel, leading to increased operational efficiency.	
Center Pole	Center Pole has fewer dynamic forces during lifting operations.	Reduced accessibility to tooling and equipment for ROV and deck personnel.
	Center Pole provides centralized support for the subsea basket, contributing to stability during subsea positioning.	Center Pole reduces basket area for tooling and equipment.
	One lifting point, the center pole arrangement simplifies the rigging dure to single lifting point.	Increased risk of tether entanglement for ROV, leading to operational delays.

2.2.2. Final Design Selection

To conclude the further design choice of lifting appliances, a case survey was conducted among personnel involved in operations onboard the construction vessel. This was initiated through a survey in a Facebook group dedicated to Normand Ocean staff. The aim was to map the most suitable alternatives for IMR operations.

Given the results illustrated in Figure 7, 83% of the respondents chose A-frame applications out of the 17 responses received. This preference contributed to the decision-making process, considering the advantages and disadvantages. The selected lifting application will be the A-frame due to its effective handling for deck and ROV personnel.

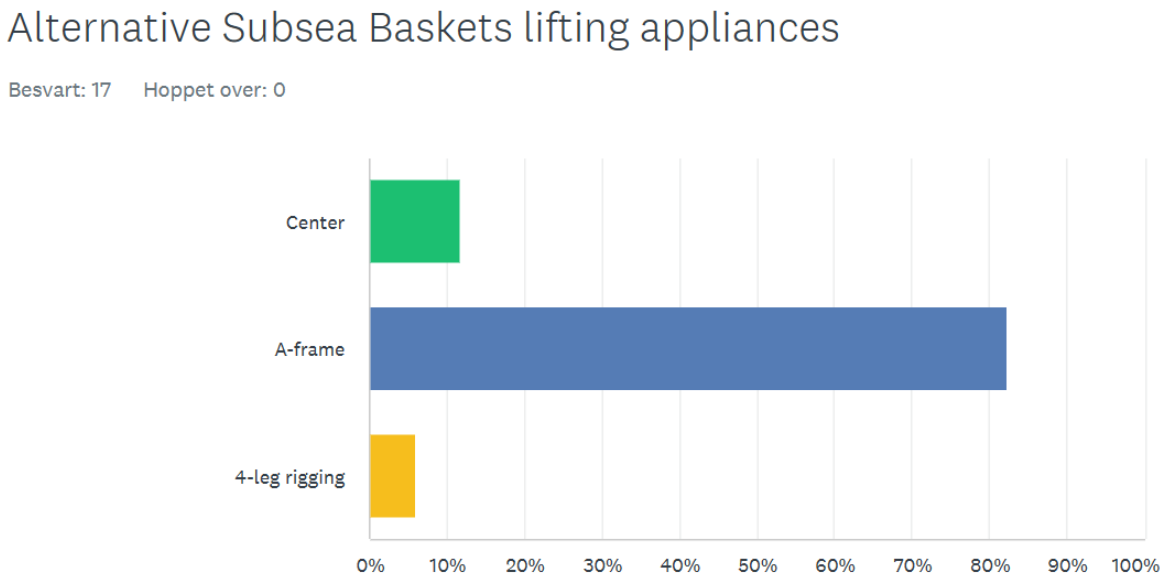

Figure 7 - Survey results for lifting applications preferences.[5]

2.3. Design Tools and Software

In the engineering approach to designing a subsea basket, using computer-aided design (CAD) is essential for delivering a complete product. Results from simulations using finite element method (FEM) will reveal the structural integrity and push the design process in the right direction. Information from software is a primary source and a deductive and quantitative design approach.

2.3.1. Design and Simulation Method

Several software programs were used to design and simulate the subsea basket. Creo Parametric was used in the 3D design, using the Framework application for the structural frame. Other parts were modeled using sketching commands and feature commands (extrude, revolve, sweep, and blend). These were used for creating and dimensioning 2D profiles and creating and modifying 3D shapes.

The simulation software Ansys, with the Static Structural analysis module, provided the simulations of the different components. Because of a limitation of nodes in the student version, the full-size basket was converted to a shell model through the geometry editing tool SpaceClaim in Ansys. The shell model provided a lower number of nodes and elements. The shell was only applied to the full-size basket and A-frame, as the other parts could be simulated as 3D models.

3. Project Description

The task is to design a multifunctional subsea basket that can be used in subsea tree operations. In a typical offset operation, the subsea basket and DMA are handled separately. However, if the DMA is integrated into the subsea basket design, only one lifting operation would be required before deploying the subsea trees. This would enhance operational efficiency, resulting in considerable time and cost savings. The company has provided a detailed list of specifications and preferences for the project. This will guide the process of creating a multifunctional subsea basket that adheres to relevant standards and guidelines and meets the requirements of an integrated DMA function.

3.1. Design Specifications

From the key aspects of the subsea basket, the company has provided a specification list outlining requests and expectations that should be met:

- DMA option, respecting the minimum weight requirement and adding GW receptacles
- Minimal deck space
- Transportability on a car with a width of 2.5m
- Size equivalent to a 13-foot container
- Zinc galvanization for corrosion resistance
- Compliance with relevant standards and guidelines
- Accessibility for a pallet jack
- Consideration of a weight limit under 12te for use with whip-line
- ROV accessibility
- Fastening points for equipment inside the basket
- Attachment points for grating
- Fastening points for securing subsea basket on deck
- Forklift pockets
- Dynamic Amplitude Factor (DAF) set to 2

Based on these specifications, the final design proposition aims to generate innovative solutions for a multifunctional subsea basket. Throughout meetings with the company, the requirements have been reviewed and discussed to prioritize the essential aspects for the primary purpose. This includes weight requirements, with a specified limit of 10 tons for the DMA option and a maximum of 12 tons for using the whip-line. These considerations are highly prioritized to ensure the design effectively meets all other specifications.

3.2. Standards

In the subsea industry, there is a wide range of standards and guidelines that need to be strictly followed. The subsea basket must comply with these standards to be certified and meet the specifications set by the company. Standards provide specifications, characteristics, and requirements that act as guidelines during the product design process. These standards comply with industry norms and contribute to the safety and integrity of operational assets. Relevant standards for this project include:

- Eurocode3
- DNV-STN001Marine operations and warranty
- DNV-ST-E273 2.7-3 Portable offshore units

3.2.1. Eurocode 3

Eurocode 3 is a European standard for the design of steel structures. It provides guidelines and specifications for material properties, design of steel members, connections, and the overall stability of structures. Eurocode 3 covers a wide range of structural elements, including beams, connections, welds, and bolted joints.

3.2.2. DNV-ST-N001

DNV-ST-N001 is a standard that focuses on a large aspect of marine operations and warranty. The standards provide several different aspects in the design process of structures used in marine operations, such as transportation and installation. The standard is also used extensively in the establishment of the loads used in the design calculations [6].

3.2.3. DNV-ST-E273 2.7-3

DNV-ST-E273 2.7-3 contains information about the requirements and design principles for portable offshore units and is highly suitable for the design of subsea baskets [7]. In this design, the standard is mainly used in the structural design process and material selection.

3.3. Material

3.3.1. Material Selection

Choosing a material that can withstand the different load scenarios that can appear is essential. The natural material for a subsea basket is construction steel because of its strength and durability. However, there are many different types of steel with different attributes. In this case, the steel should be ductile to manage sudden loads, and weldable. A low-carbon steel is the most suitable option for these two characteristics [8].

The basket should also be suitable for low temperatures to ensure that it can manage the North Sea climate. There is a test for determining the characteristics of materials under different temperatures called the Charpy V-notch test [9]. It uses a pendulum that hits a piece of steel with a V-notch from a given height. This shows how much impact load the steel can absorb when fracturing. Given from this test are steel subgrades: JR, J0, and J2. JR can absorb 27 Joules of energy at room temperature, J0 at 0 degrees Celsius, and J2 at -20 degrees Celsius. The standard DNV-ST-E273 states that in the absence of a design temperature designation, the design temperature should be -20 degrees Celsius [7, Ch. 3.2.1]. These factors yield the basis for choosing the material S355J2, with properties as shown in Table 2. This is a strong low-carbon steel with impact durability at -20 degrees Celsius.

Table 2 - Material properties for S355J2 steel. [10]

Material Property S355J2	Value
Density	7850 kg/m^3
Modulus of elasticity	210000 MPa
Shear modulus	81000 MPa
Yield strength	355MPa

Ultimate strength	510MPa
Poisson's ratio in elastic range	0,30

3.3.2. Galvanization

According to DNV standards for portable offshore units (POU), suitable corrosion protection shall be applied to the material [7, Ch. 4.6]. The company will choose the best-suited corrosion protection, and galvanization of the subsea basket is a good option. Although this procedure is costly, it provides superior durability and maintains a better appearance over time compared to other coating alternatives.

3.3.3. Allowable stress

According to the POU standards, the von Mises equivalent stresses produced by the design load should not exceed 85% of the selected materials' yield stress [7, Ch. 3.4.3]. For the selected material S355J2 steel grade, an allowable stress of 301,75 MPa is used as a maximum allowable value in the structural analysis, unless anything else is stated.

$$\sigma_e \leq \sigma_{ea} = 0,85 \cdot R_e = 0,85 \cdot 355MPa = 301,75\ MPa$$

Where:

R_e : Yield stress of the material

3.4. DNV Calculations

DNV standards state guidelines used to calculate various factors and loads. These calculations create the basis for design choices and simulations.

3.4.1. Factors

Several factors are used in the calculation of forces that the subsea basket must be able to withstand. These factors contribute to establishing the most extreme scenarios to which the structure theoretically can be subjected.

Weight margin factor

A center of gravity (CoG) envelope is applied to accommodate for uncertainties and variations of the actual CoG. The lifting points which are closest to the CoG will normally be subjected to the highest loads [6, Ch. 5.6.2.3]. There will also be deviations due to the weight distribution of the cargo.

A weight margin factor is applied to the MGW, which is an alternative way to accommodate for the uncertainties mentioned above [6, Ch. 5.6.2.3.2]. A factor of 1,10 is found in Table 3, which is suitable in cases with an estimated MGW of low certainty.

Table 3 - Unweighted object weight margin factors. [6, Ch. 5.6.2.2.2]

	γ_{Weight}
Weighed weights of parts of the object	$\gamma_{Weighing}$
Estimated weights - high confidence in weight report	As agreed with the MWS company but generally not less than 1.05
Estimated weights - low confidence in weight report	1.10

Skew load factor

The skew load factor (SKL) considers additional loading which can occur from fabrication tolerances in the rigging and lifting structures. This includes asymmetry and the distribution of forces in the rigging arrangement. The skew load factor is set to 1,33 which is suitable for 4 leg sling set. A 4-leg sling set is used as it resembles the A-frame structure the most [7, Ch. 3.5.5].

Dynamic amplifying factor

The dynamic amplifying factor (DAF) is a factor that accommodates the influence of a variety of dynamic elements. In subsea operations, such influences include, among others, wave dynamics, buoyancy, etc. These elements affect the overall load subjecting the basket [6, Ch. 16.17.2.1]. A customer requirement is to set the DAF to 2, which is higher than the value found using DNV standard calculations for offshore lifts. The calculations below are found using the formula in Supplementary Table 6.

$$DAF = 1 + 0,25\sqrt{\frac{100}{SHL}} = 1,75 < 2,0$$

3.4.2. Weight calculations

The hook loads are calculated using the following formula [6, Ch. 16.3.2]:

$$SHL = W_{ud} + W_{rigging}$$

$$DHL = SHL \cdot DAF$$

$$Where:$$

$$SHL = static\ hook\ load$$

$$W_{ud} = upper\ bound\ design\ weight$$

$$W_{rigging} = rigging\ weight$$

$$DHL = dynamic\ hook\ load$$

$$DAF = dynamic\ amplification\ factor$$

The rigging weight is the sum of the weights of the entire rig, excluding the A-frame, which is a part of the upper bound weight. The rigging includes shackles, wires, chains, etc. [6, Ch. 5.6.2]. An upper bound design weight (W_{ud}) is used in the calculations to cover expected weight deviations, whether the structure is weighed or not. The upper bound design weight can be determined by multiplying the estimated weight (W) with an appropriate weight margin factor (also known as the weight contingency factor).

As shown in Table 3, the margin factor is 1,10. The estimated weight value is set to be ten tons. The actual weight of the structure is estimated using Creo Parametric. The upper bound design weight becomes:

$$W = W_{basket} + W_{Frame} + W_{Tools}$$

$$W_{ud} = W \cdot \gamma_{weight}$$

where

$$weight\ margin\ factor: \gamma_{weight} = 1,10$$

Because the crane has a maximum weight limit of 12 tons, the dynamic hook load is set to 12 tons. The maximum weight of the structure including the A-frame and tools becomes 5,45 tons as shown in the calculations below. This weight value is used in the dimensioning of the basket design.

$$Max.\ crane\ load = 12\ tons = DHL_1$$

$$DHL_1 = SHL_1 \cdot DAF = 12\ tons \rightarrow SHL_1 = 6\ tons$$

$$SHL_1 = W_1 \cdot \gamma_{weight} = 6\ tons$$

$$W_1 = \frac{SHL_1}{\gamma_{weight}} = \frac{6\ tons}{1,10} = 5,45\ tons$$

where

DHL_1: *Dynamic hook load used to establish the weight of the structure* $\left(DHL_1 = 12 tons\right)$

W_1: *desired weight of the structure without the extra weight*

SHL_1: *Static hook load from* W_1

3.4.3. Design Loads

The design load used in the simulations and dimensioning of the subsea basket is based on the design load basis values, which are established for both the subsea basket and the extra weight.

Design Load Basis

The design load (*F*) is the highest design loading which is found based on subsea lifts and the dynamic loading regarding POUs. For subsea lifts the design load can be found using a design factor of 2,5 [7, Ch. 3.5.1]. By adding the weight of the extra weights, the MGW is 10 tons. By adding the weight margin factor the MGW becomes 11 tons (upper bound value).

$$F_{sub} = 2,5 \cdot MGW \cdot g = 2,5 \cdot 11\ tons \cdot 9,81 {}^{m}/_{s^2} \approx 270\ kN$$

The extra weight has a desired weight of 4,55 tons. By adding the weight margin factor of 1,1, the total weight is 5 tons. A design load for the pad-eyes which connect the extra weight to the subsea basket is calculated below. Here, only the subsea design load is relevant.

$$F_{extraWeight} = 2,5 \cdot MGW_{extraWeight} \cdot g = 2,5 \cdot 5\ tons \cdot 9,81\ {}^{m}/_{s^2} \approx 122.7\ kN$$

Lifting Point Design Loads

As mentioned, the lifting points that are nearest the CoG will carry the most loads. The highest vertical reactional force in a lifting point is calculated in the most extreme scenario possible. For a 4-point lift, the following equation can be used to calculate the highest vertical reaction load [3, Ch. 16.3.3] [4, Ch. 3.5.5]:

Lift point loads

$$LL_{main} = 1,2 \cdot F_{sub} = 1,2 \cdot 270kN = 324kN$$

$$LL_{AFrameSub} = DF \cdot SKL \cdot F \cdot PL \cdot \frac{1}{\cos v}$$

$$= 1,2 \cdot 1,33 \cdot 270kN \cdot 0,25 \cdot \frac{1}{\cos 30°}$$

$$= 124,4kN$$

$$LL_{extraWeight} = DF \cdot SKL \cdot F_{extraWeight} \cdot PL = 1,2 \cdot 1,33 \cdot 122,7kN \cdot 0,25 = 49kN$$

where

LL: *resultant lifting load*

LL_{main}: *resultant lifting load for main lifting point*

$LL_{AFrameSub}$: *resultant lifting load for the A − frame lifting points for subsea lifts*

$LL_{extraWeight}$: *resultant lifting load for extra weight bolted connection points*

DF = *Design factor for lift points*

F = *Design load basis*

PL = *Percentage loading for F*

SKL = *skew load factor*

v = *angle between A − frame legs and vertical*

Forklift Pocket Loads

The design loads for the forklift pockets are found using a design factor of 1,65 multiplied by the MGW of the subsea basket with the extra weight and without the extra weight, respectively [7, Ch. 3.5.7]:

$$F_{F1} = 1,65 \cdot MGW_1 \cdot g = 1,65 \cdot 11\ tons \cdot 9,81 {}^{m}/_{s^2} = 178,1\ kN$$

$$F_{F2} = 1,65 \cdot MGW_2 \cdot g = 1,65 \cdot 5,45\ tons \cdot 9,81 {}^{m}/_{s^2} = 88,3\ kN$$

3.5. Guidelines for Calculations

3.5.1. Structural Analysis

General

The guidelines outlined in Eurocode3: Part 1-1, Design of steel structures. Are applied in the structural analysis of the bottom beams within the subsea basket's framework. The objective is to evaluate the structural integrity of the beams under the two different member loads illustrated in Figure 8. This is commonly encountered for a subsea basket with different dimensions of tooling and equipment [11].

According to EC3 applications, the most used member load criteria are concentrated and uniformly distributed loads, as illustrated in Figure 5. The member loads working on the bottom beams will mainly be caused by tooling for ROV handling. During mobilization preparation, the deck crew tries to achieve an evenly distributed load.

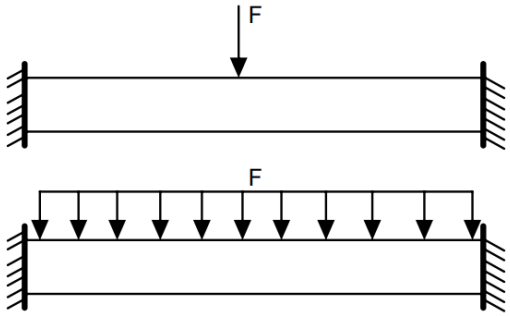

Figure 8 - Concentrated and uniformly distributed loads on the bottom beam section.

The bottom beams, constructed of Rectangular Hollow Section (RHS) 250x150x12.5, were originally designed as forklift pockets, as mentioned in chapter 4.1.1. However, these beams are the main load-bearing elements for supporting loads from the operational tool's equipment in this application. The forklift pockets are supported by 3x3 HEB100 beams to obtain structural integrity and stiffness in the bottom structure.

Classifications of cross-sections

The purpose of classifying cross-sections is to evaluate the behavior of their limitations on resistance and rotational capacity by local buckling resistance. As an underlying factor affecting cross-sections, the subsea basket will primarily be classified as class 1 and 2 cross-sections [11, Sec. 5.5.2].

Class 1: These cross-sections can form a plastic hinge with high rotation capacity according to plastic analysis, without reducing resistance. They sustain plastic deformation without any loss of strength.

Class 2: Cross-sections that can develop plastic moment resistance but have a limited rotation capacity due to the occurrence of local buckling. These resist plastic deformation to some extent, and local buckling limits the ability to rotate.

Figure 9 shows the dimensions and axis of the bottom beams of the subsea basket, which are used for Eurocode3 part 1-1 calculations.

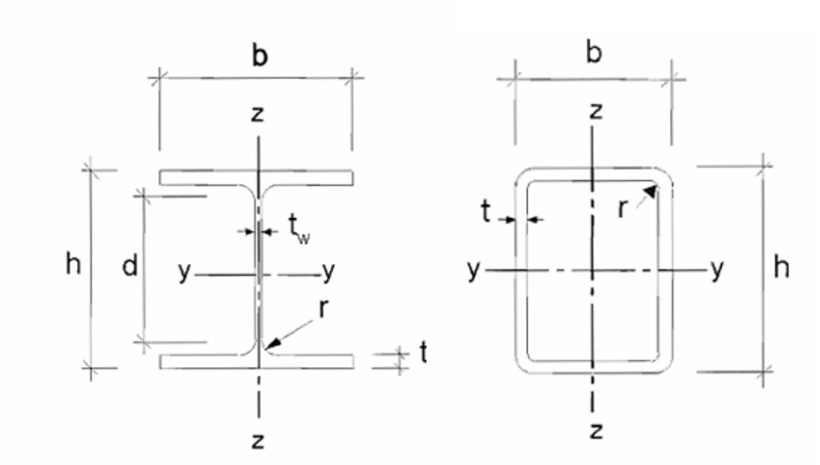

Figure 9 - Dimensions and axis of cross-sections used in calculations. [11]

Ultimate Limit State

According to the plastic global analysis approach in EC3, the ultimate limit state (ULS) principle verifies when a structure reaches its ultimate capacity to resist loads before global failure occurs. This implies that the structural state is in the elastic region, avoiding further plastic deformation. This can lead to permanent deformation over time, resulting in fracture. It means that if the bending, shear, and buckling stresses are below the calculated resistance, the structure will satisfy the ULS criteria according to [11, Sec. 6]

Lateral Torsional Buckling

Lateral torsional buckling (LTB) is a buckling phenomenon that occurs within structural members under specific loading conditions. When critical forces are reached, it can result in both lateral displacement and torsional twisting [12].

There are three methods for determining the cross-section capacity against LTB in EC3 [14, Sec. 6.3.2].

1. General case
2. For rolled sections or equivalent welding sections
3. Simplified assessment methods for beams with restraints in buildings

For the structural behavior, the general case will be used to determine if the bottom profiles will be subject to buckling.

Critical buckling moment

In this analysis, the EC3 does not provide guidelines on how to calculate the critical buckling moment for cross-sections. However, the method of determining the critical buckling moment is obtained from a previous master thesis [13, Ch. 4.3].

3.5.2. Welding

General

The subsea basket's structure behaves like trusses consisting of various nodes that form the basis for welding calculations. The structural analysis, based on a Staad.Pro analysis provided by a supervisor from the company, is found in Supplementary Table 11. The welding calculations are conducted according to Eurocode3: part 1-8, Design of joints [14]. DNV provides guidelines related to EC3, which are considered later in the chapter.

Guidelines from Eurocode

The standards cover different principles of welding features. The most common types of welds intended for use in the structure are fillet welds and butt welds. Fillet welds are considered valid when the angle of the cross joints is between 60 and 120 degrees. However, angles under 60 degrees are also acceptable but should be considered for partial penetration butt welds [14, Sec. 4.3]. For fillet welds, an all-around weld is effective for transferring shear forces to avoid potential shear lag, meaning that there can be a loss in the strength of the structure if the cross-section is not directly connected [15].

Figure 10 and Figure 11 illustrate various types of cross joints within the frame. Angles at KT and N-joints are less than 60 degrees but greater than 30 degrees, which makes them suitable for welding [14].

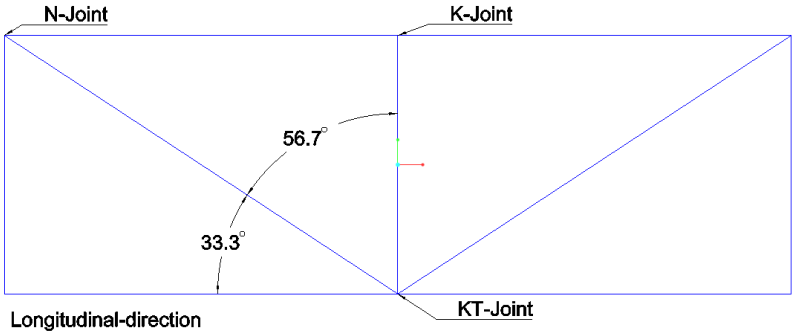

Figure 10 – Joints at the right and left side of the basket.

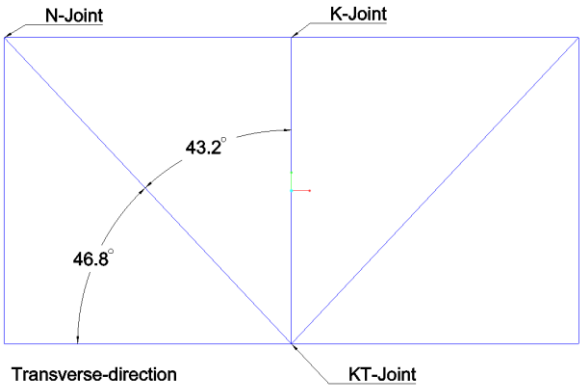

Figure 11 - Joints at the back of the basket.

The effective throat thickness (a) determines the structural strength of a welded joint and should not be less than 3mm. The effective throat size represents the height of the largest triangle that can be inscribed in the cross-section of the fillet weld. It is dimensioned sufficiently to ensure the welds support the structural load [14, Sec. 4.5.2].

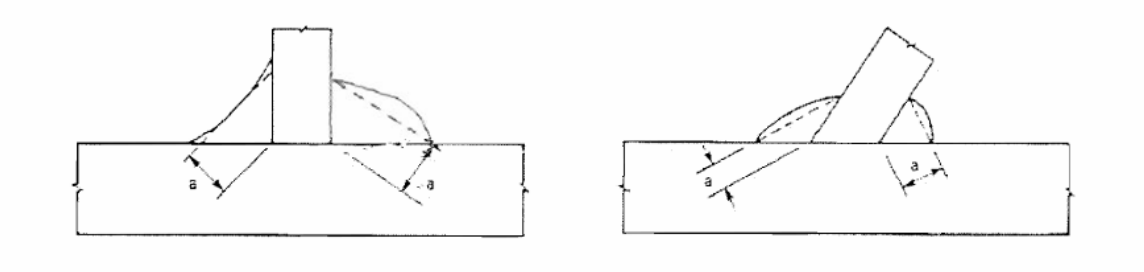

Figure 12 - Fillet weld throat thickness. [14, Sec. 4.5.2]

The design resistance of fillet welds is determined by using the directional method, where uniform stress is assumed to be evenly distributed for the internal forces of the fillet weld. Resulting in normal and shear stresses, leading to equivalent stress values compared against the criteria.

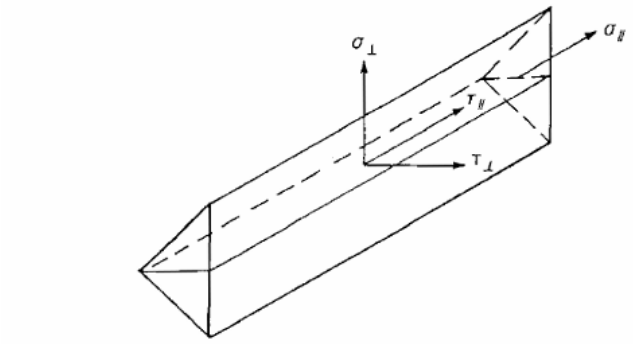

Figure 13 – Stresses that are located on the throat section of fillet welds. [14, Sec. 4.5.3.2]

The design resistance of fillet welds will be validated if both criteria are satisfied:

$$\sigma_{eq} = \sqrt{\sigma_{\perp}{}^2 + 3\left(\tau_{\perp}{}^2 + \tau_{\parallel}{}^2\right)} \leq \frac{f_u}{\beta_w \gamma_{M2}} \text{ and } \sigma_{\perp} \leq \frac{0{,}9 \cdot f_u}{\gamma_{M2}}$$

$$\sigma_{eq} = \sqrt{\left(\sigma_{norm} + \sigma_{bend}\right)^2 + 3\left(\left(\tau_{norm} + \tau_{bend}\right)^2 + \left(\tau_{par,flange}\right)^2\right)} \leq \frac{f_u}{\beta_w \gamma_{M2}}$$

Where:

$\sigma_{\perp}$: Normal stress perpendicular to the throat $\sigma_{\parallel}$

$\sigma_{\parallel}$: Normal stress parallel to the axis of the weld $\tau_{\perp}$

$\tau_{\perp}$: Shear stress (in the plane of the throat) perpendicular to the axis of the weld

$\tau_{\parallel}$: Shear stress (in the plane of the throat) parallel to the axis of the weld

γ_{M2} : Partial safety factors for resistance of welds = 1,25

β_w: Correlation factor for fillet welds, S355J2 = 0,9 (EC3)

Guidelines from DNV

According to DNV for portable offshore units, the allowable stresses in the welds shall equal the design load criteria for allowable stresses mentioned in section 3.3.3. However, the permissible stress in the structure does not need to be less than 355MPa for fillet welds in structures [7, Ch. 3.4.5].

The normal stress parallel to the axis is not considered when verifying the design resistance of the weld. Perpendicular stress conditions to the axis of the welds may be equal in cases where the load acting on the cross-section is applied parallel to the axis of the weld [6, Ch. 5.3.9.4]. The design resistance of fillet welds will be validated if both criteria are satisfied:

$$\sigma_{\perp} = \tau_{\perp}$$

$$\sqrt{\sigma_{\perp}^2 + 3(\tau_{\perp}^2 + \tau_{\parallel}^2)} \leq f_u \eta \qquad \text{ASD/WSD}$$

$$\sqrt{\sigma_{\perp}^2 + 3(\tau_{\perp}^2 + \tau_{\parallel}^2)} \leq \frac{f_u}{\gamma_m} \qquad \text{LRFD}$$

Where:

η = Permissible usage factor applicable to the welding condition for ASD/WSD

γ_m = Material factor applicable to the welding condition for LRFD

4. Design, Calculations, and FEM Simulations

The simulations are done with the software tool Ansys by running a FEM simulation of parts subjected to significant loadings. In this chapter, the results from the FEM analysis will be presented. Assumptions made in the analyses are that the material is linear and isotropic, the welds are not included, and the weight load is included in the simulations instead of gravity.

The subsea basket consists of 3 main sub-assemblies, as illustrated in Figure 14. The A-frame is illustrated in orange, the basket in yellow, and the extra weight in blue. These subassembly terms are used throughout the report, each explained in detail in their own subchapters 4.1 to 4.3.

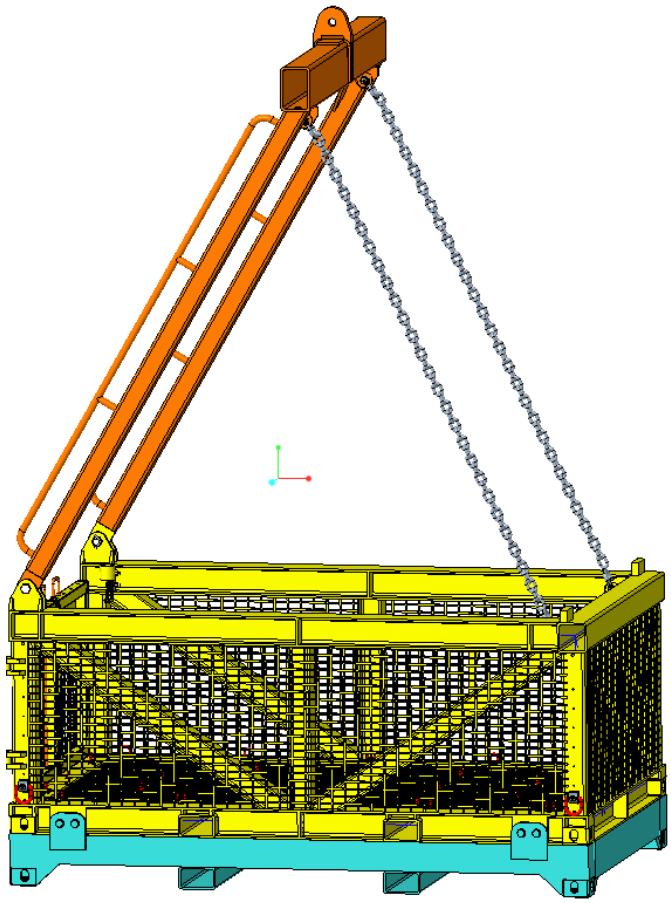

Figure 14 - Subsea basket sub-assemblies.

4.1. Basket

4.1.1. Design Choice

The design of the basket is primarily determined by the specifications set by the company.

Structural Beams

A variety of beam profiles are used in the design of the basket structure. The ones used are HEB, SHS, and RHS beams with varying dimensions. HEB profiles are mainly used in the design as these are easier to handle during the galvanization process, and they have more efficient drainage with no need for additional drainage holes compared to hollow beam sections. SHS profiles are added in each corner of the basket, mainly to simplify the manufacturing process by avoiding complicated beam joints. SHS profiles were also applied at locations where HEB profiles would have shown high stress levels, which is explained in detail in the FEM simulation chapter 4.1.2.

Skeleton

The skeleton of the design was inspired by existing subsea baskets. Features such as forklift pockets and lifting points were considered when designing the frame. The beam placements and orientations enhance the structural integrity and are optimized for the lifting loads. Figure 15 illustrates the skeleton design of the basket.

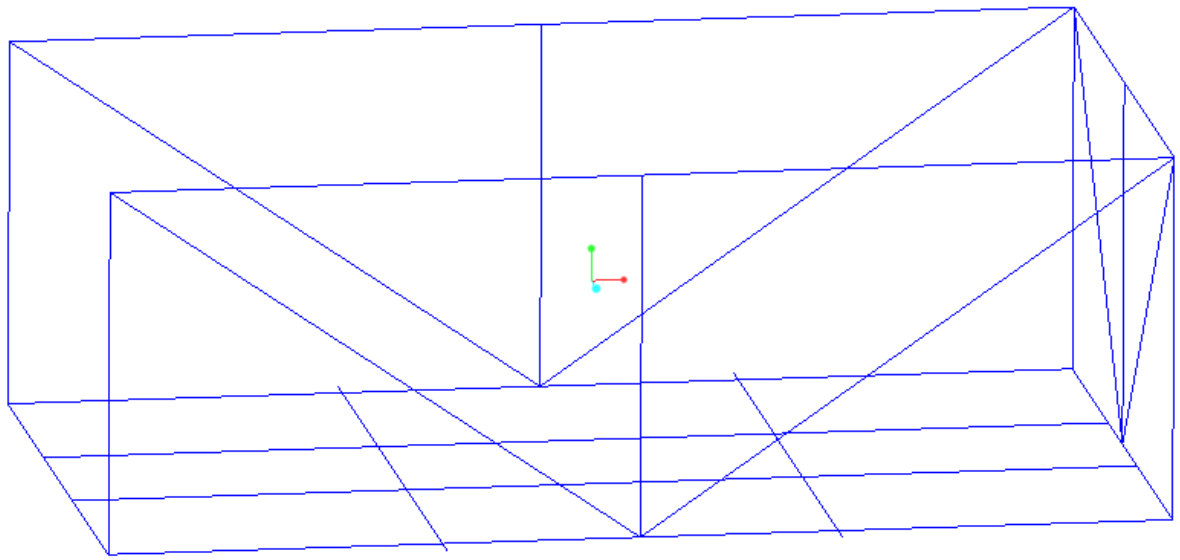

Figure 15 - Skeleton sketch of the basket.

Dimensions

The basket is designed to meet the company's demands regarding the dimensions of the overall structure. As mentioned in the demand list from the company, the basket should take as little deck space as possible. It should also be transportable on a car with a width of 2.5m and be equivalent to the size of a 13-foot container. These demands have been met in the basket design as shown in Figure 16 and Figure 17.

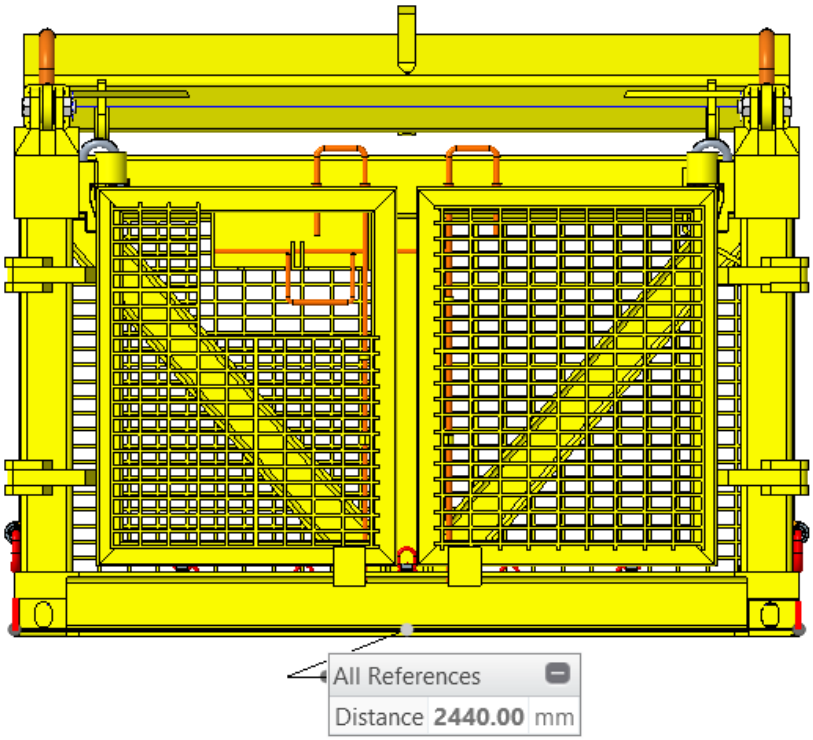

Figure 16 - Width of basket.

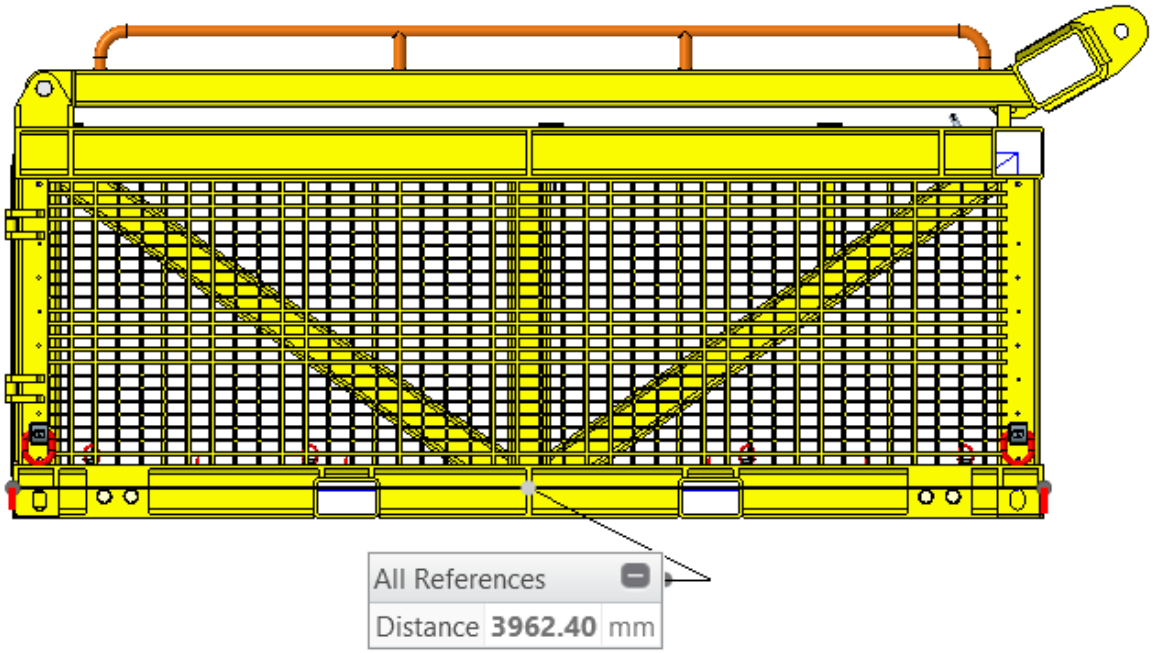

Figure 17 - Length of the basket.

Drainage

Drainage holes are included in the vertical hollow corner beams to prevent implosion. These drainage holes also provide access to the inside of the hollow section during the galvanization process. The drainage holes are shown in Figure 18. The other hollow section does not require any additional drainage holes, as the end sections are kept open, as shown in Figure 19.

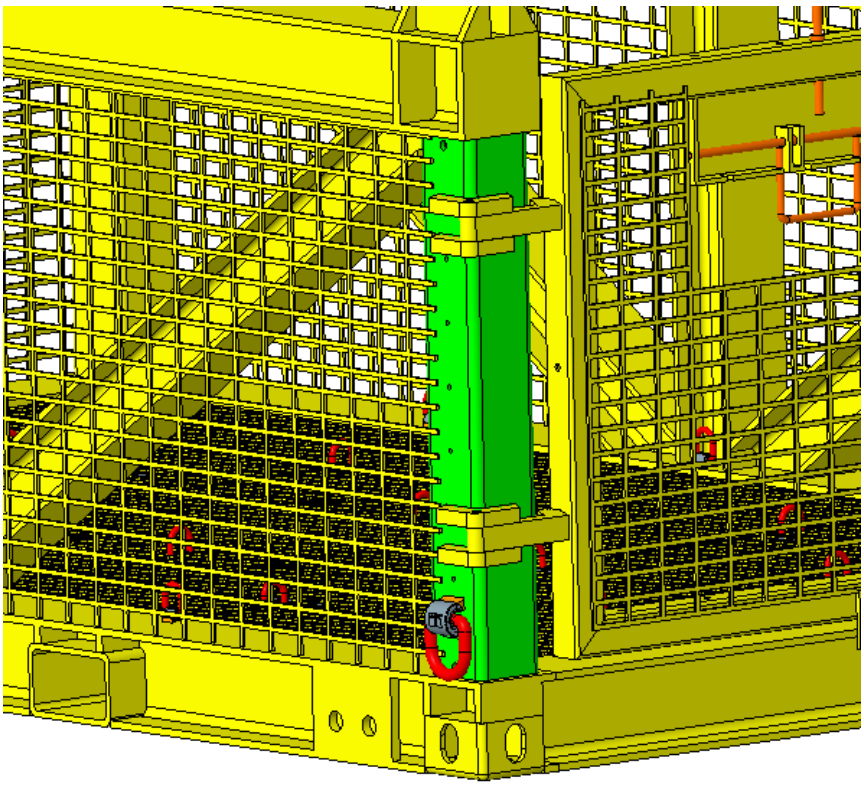

Figure 18 – Square hollow profile with drainage holes and closed ends.

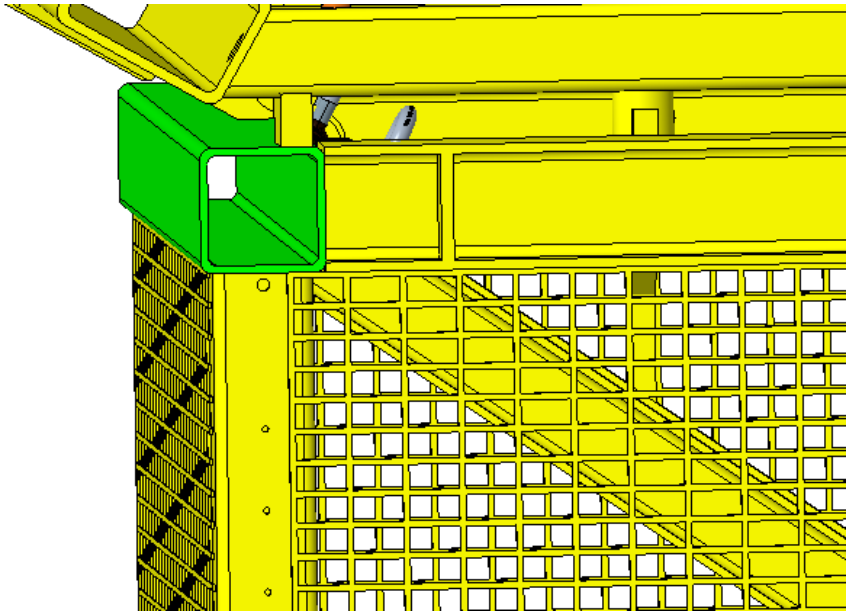

Figure 19 - Square hollow profile with open ends.

Beam Stiffeners

Web stiffeners are added to critical points in the construction to prevent web buckling. The critical sections are sections where the risk of buckling is the highest. Other locations where stiffeners are of interest are sections with point loads, or in beam connections such as K- or T joints. Point loads are the forces exerted by a support, or at the location of lifting loads. Stiffeners also contribute to resisting longitudinal member stresses, which are found in the web plane.

The stiffeners are designed according to EC3 standards and the design at the end posts comprises of two double-side stiffeners. The distance between two stiffeners shall not be less than 10% of the height of the inner section of the beam profile [16, Ch. 9.3.1].

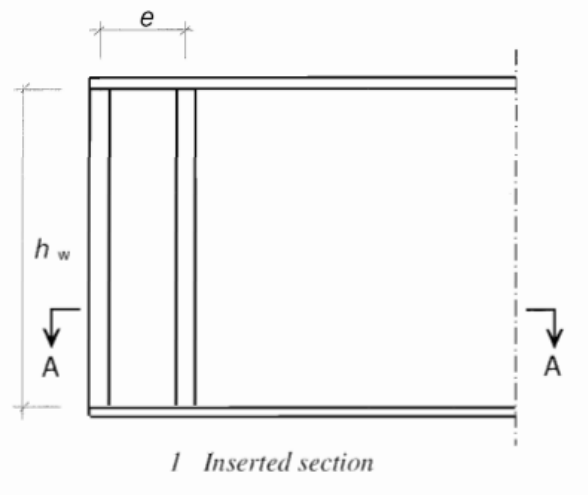

$$e > 0,1 \cdot h_w = 17mm$$

$$crossectional\ area \geq \frac{4 \cdot h_w \cdot t^2}{e}$$

where

$h_w = 170mm$

$t = 9mm$

Forklift Pockets

The forklift pockets are designed to meet the minimum criteria of 200mm x 90mm [7, Ch. 3.9.3]. In both the extra weight and the subsea basket, the forklift pockets go through the base of the structures. As shown in Supplementary Table 1, the center distances of the pockets are designed to be above 25% of the length of the basket. 1400mm is used. Figure 20 shows the forklift pockets mounted on both the basket and the extra weight.

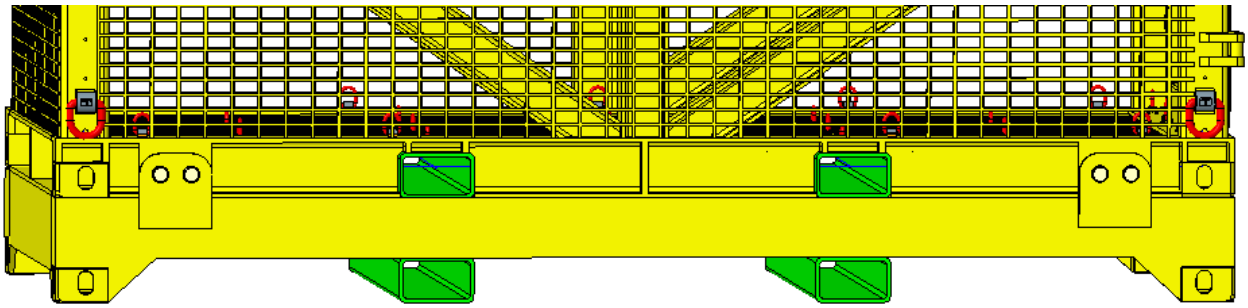

Figure 20 - Forklift pockets on basket and extra weight.

Doors

The doors on the basket are inspired by doors from other subsea baskets, with some customizations. They consist of a frame made of 80x80x5mm hollow steel beams, as well as two hinges, a handle, and a locking mechanism for the left door. This adds up to each door weighing approximately 80kg. Figure 21 shows how the doors look when closed.

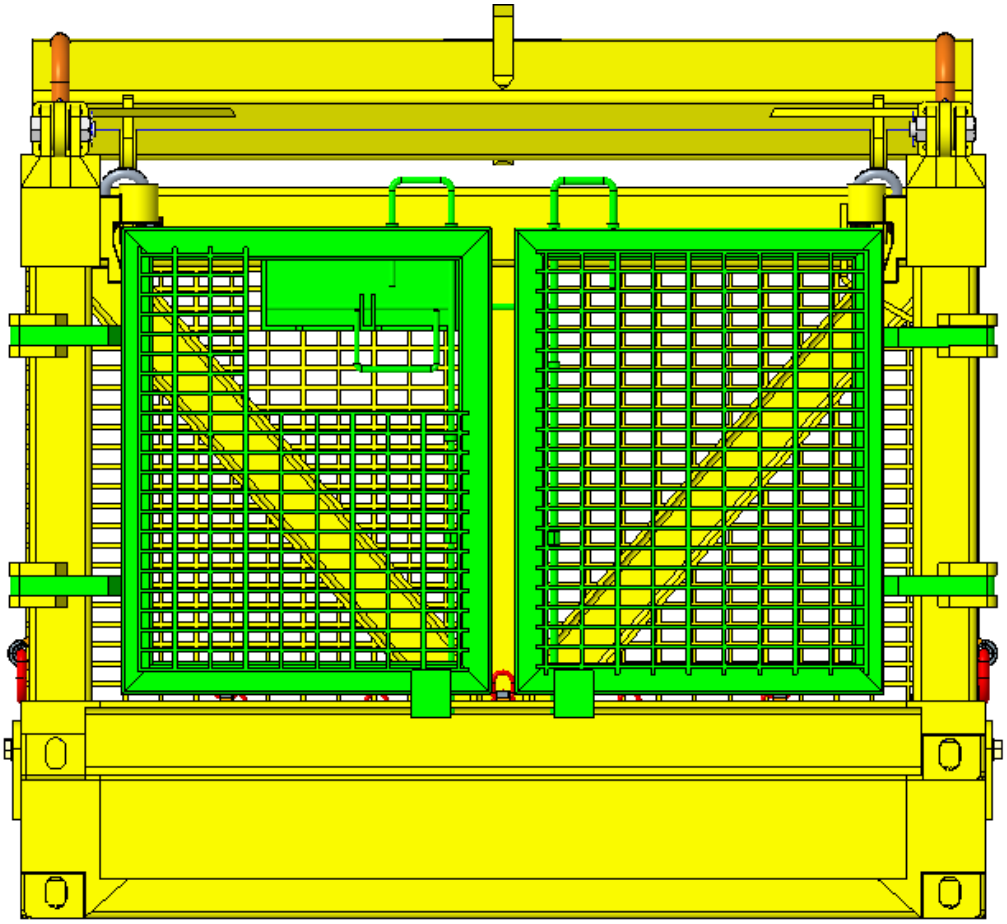

Figure 21 - Subsea basket doors.

The locking mechanism is easy to understand and operate. The handle is turned 90 degrees towards the operator and pushed all the way to the left until it stops. Here, the operator drops the handle, and as shown in Figure 22, the handle locks in place. Then, each of the top handles on the doors can be lifted to open the doors individually. Both locking mechanisms must be unlocked to open the doors, which provides additional safety.

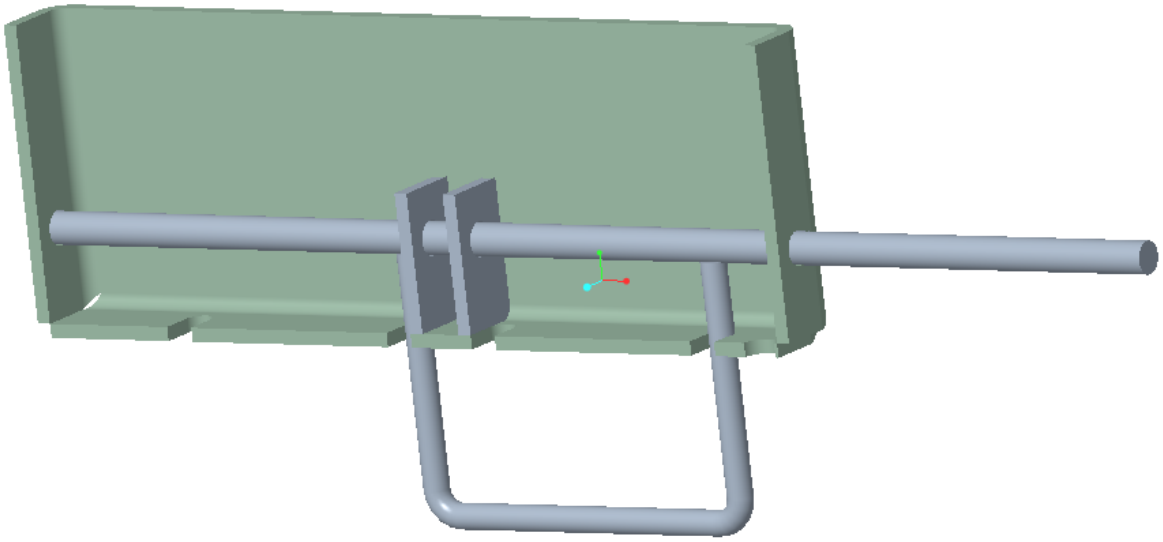

Figure 22 - Locking mechanism.

The small plate at the bottom of each door prevents the door from opening or closing beyond intention. The plate is designed to stop the door when it is entirely parallel with the basket in both locked and opened positions, as can be seen in Figure 23. This stops the hinges from colliding with the corner beams and lines up the hole for the locking mechanism.

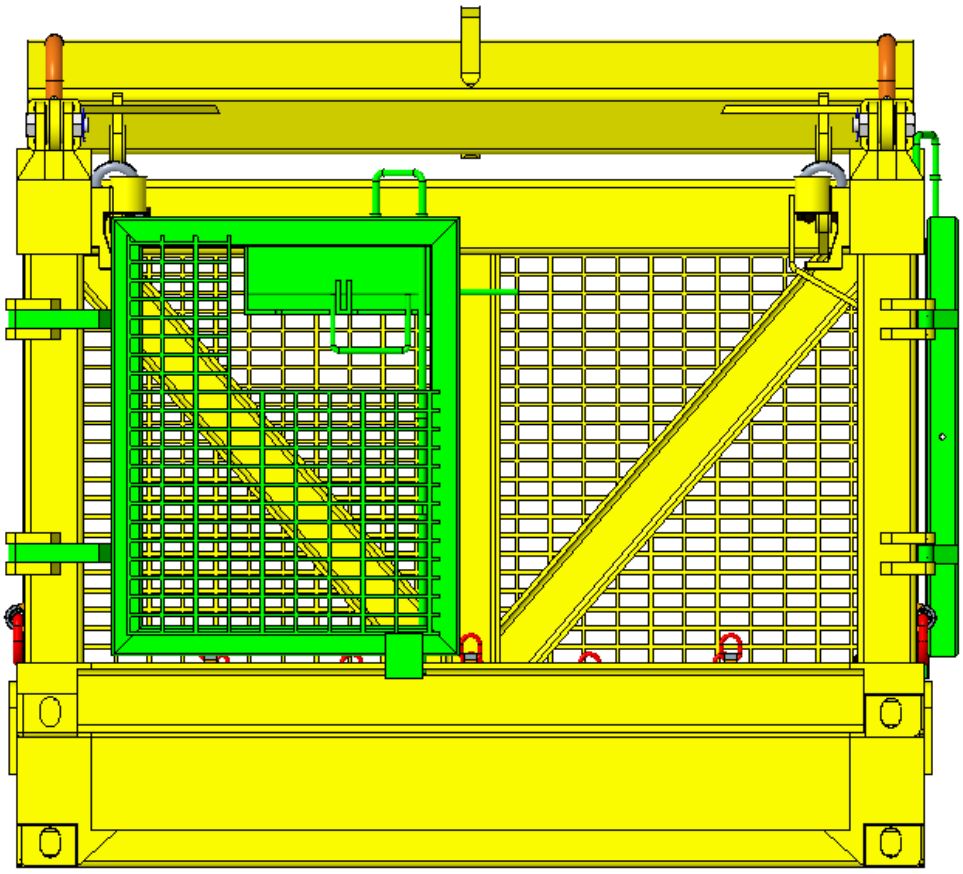

Figure 23 - Right door fully open.

When the door is fully opened, it can be locked in that position. The handle can be lifted to make one of the pipes go out of its hole in the door. When this pipe gets above the beam on the basket, there is a ring on the other pipe that stops the handle from going entirely out of position. This is illustrated in Figure 25 and functions for both doors. When the handle is lifted above the beam on the basket, it can be turned slightly and placed in a hole that will be drilled into the beam. This way, the door can be locked in an open position using a mechanism with only one moving part.

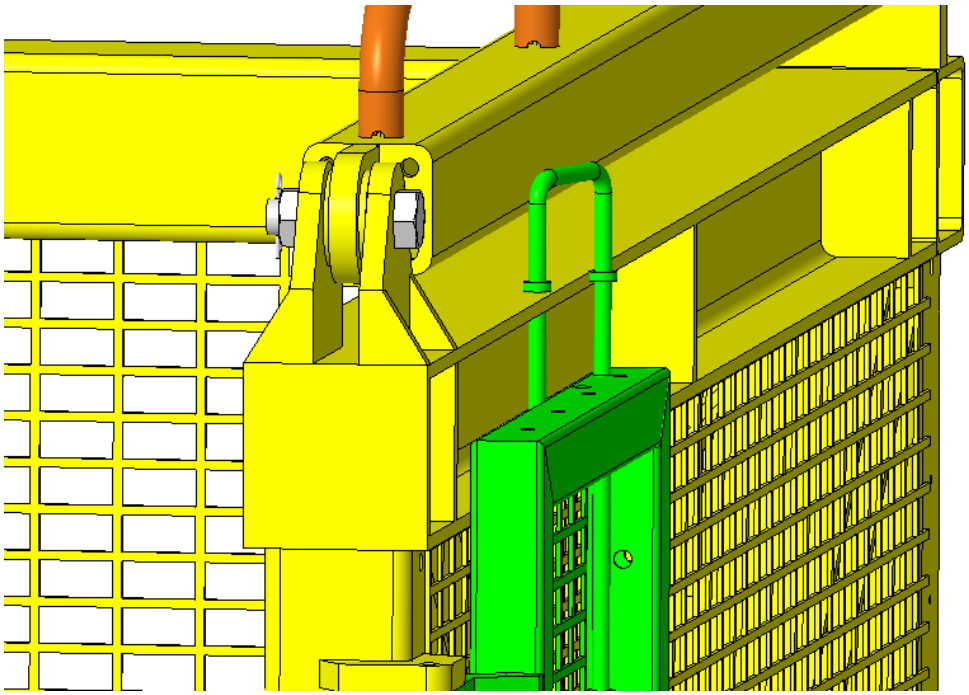

Figure 24 - Locked door in open position.

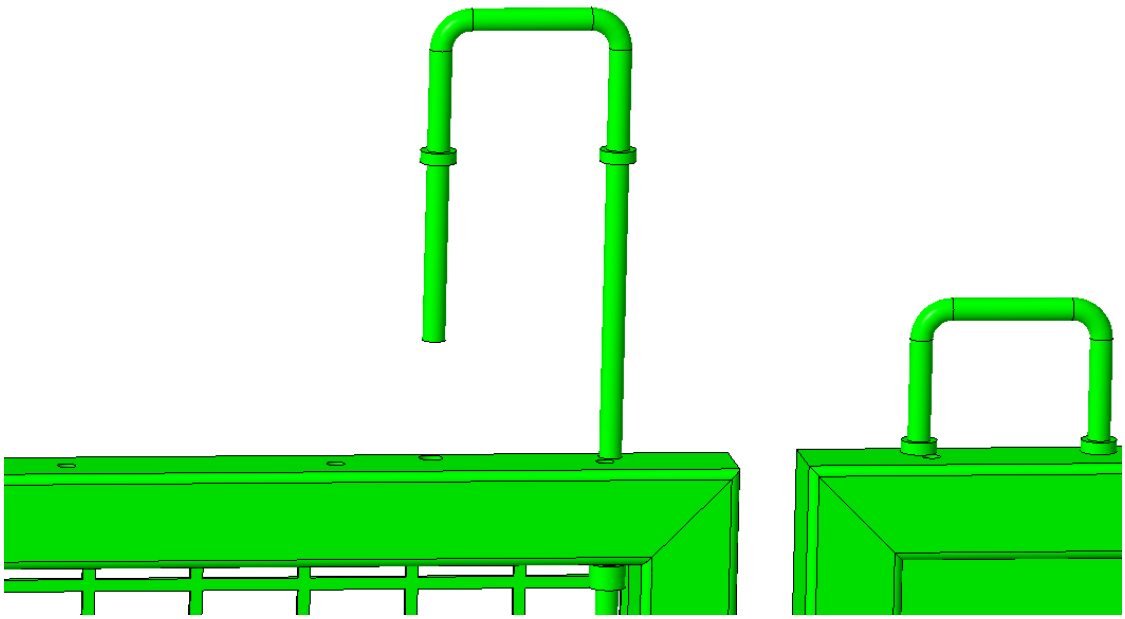

Figure 25 - Stopper when locking door in open position.

4.1.2. Basket FEM Simulation

A method of creating remote points to represent the A-frame was used to simulate lifting the basket, as shown in Figure 26 and Figure 27. The remote points are based on the pad-eyes and have coordinate systems that are fixed in position where the connection points at the A-frame spreader bar would be located. This leads to the simulation showing the basket hanging like in a lifting operation. The force that has been added is the calculated main *LL* of 324kN, presented in Figure 28. *LL* represents the weight of the basket, DMA, and tools, with every safety factor as well as the DAF added. The load was distributed on the beams that make up the basket floor to create the most realistic scenario.

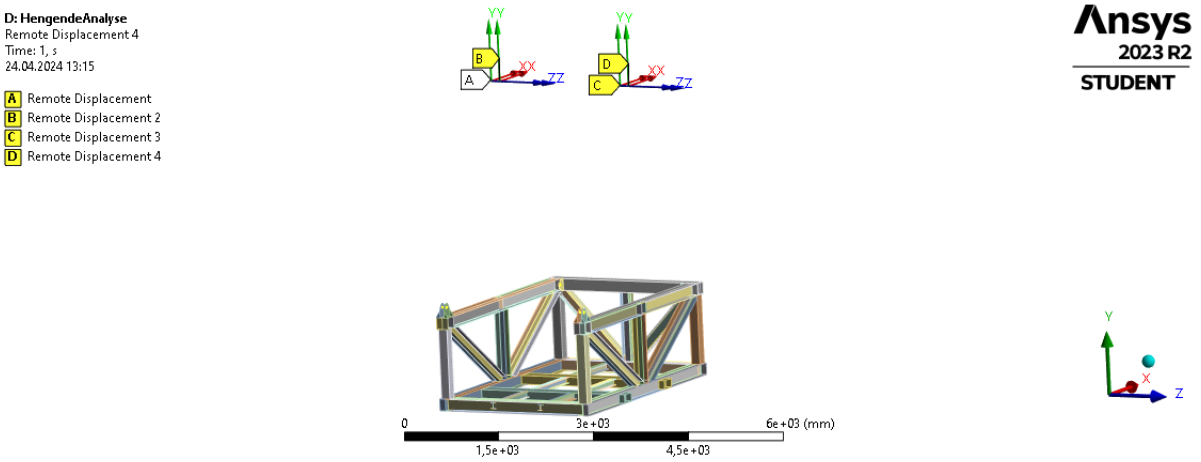

Figure 26 – Remote displacements for basket simulation.

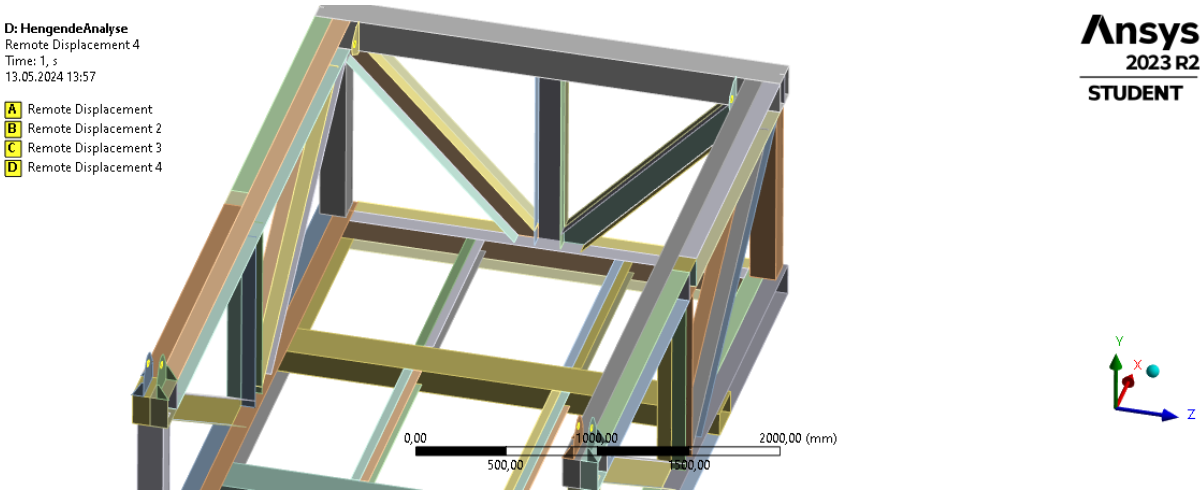

Figure 27 – Pad-eye constraints for remote displacements, highlighted yellow inside each pad-eye.

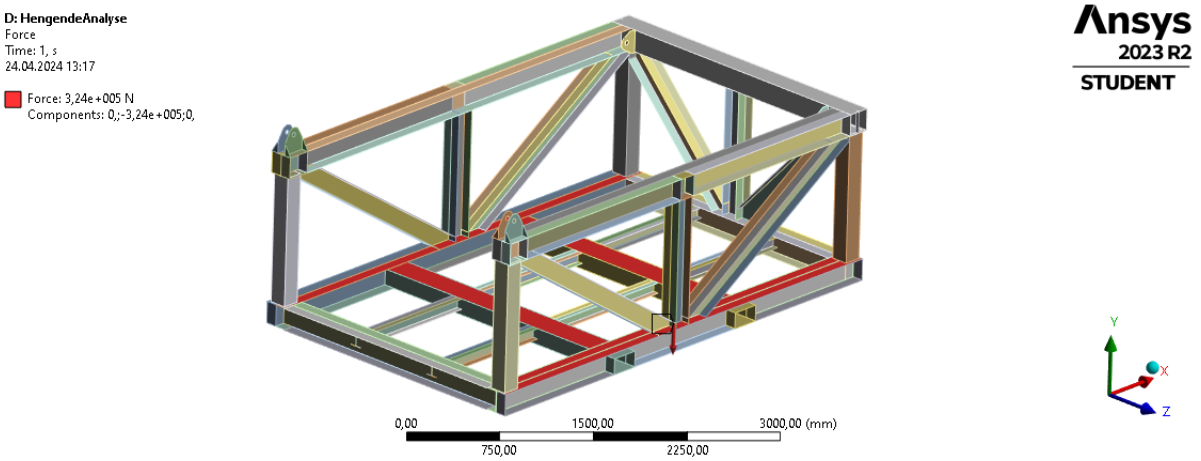

Figure 28 - Force for basket simulation.

Figure 29 shows the von Mises stress results from the basket simulation. The highest concentration of stress appeared at the pad-eyes positioned on the inside of the basket. Here, the stress was 157.11MPa, which is well within the calculated maximum allowed stress value of 301.75MPa. The rest of the basket had evenly distributed stress, with concentrations at the connection points of the beams and in the middle of the basket. These stress concentrations were, however, not significant, showing that the basket would handle the forces with a substantial margin.

Figure 30 shows the stress values at one of the lifting points. SHS profiles result in smaller stress levels around the area of the pad-eye. If the SHS beam were replaced with an HEB beam profile, the stress levels would increase above allowable limits.

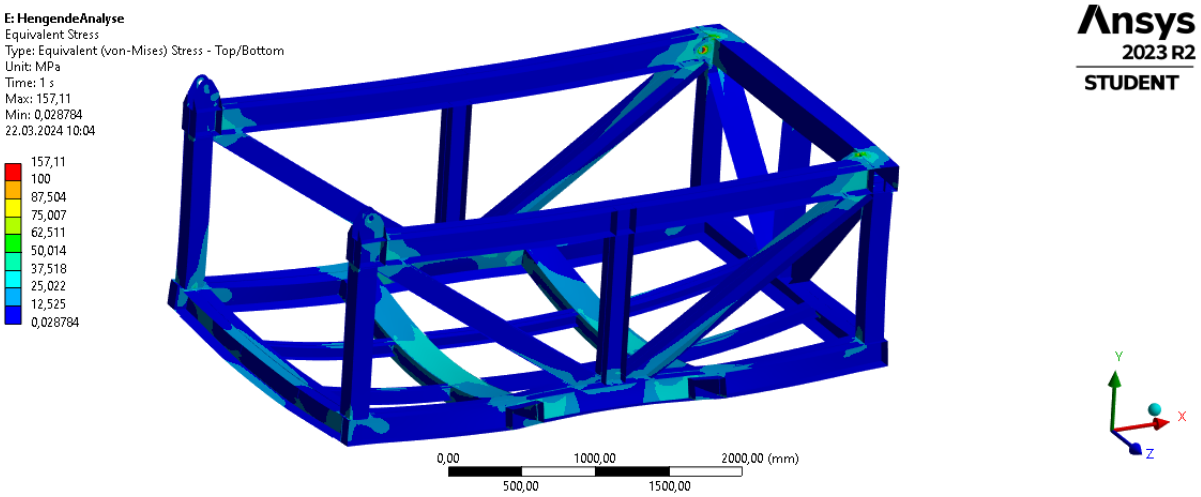

Figure 29 - von Mises stress results hanging simulation.

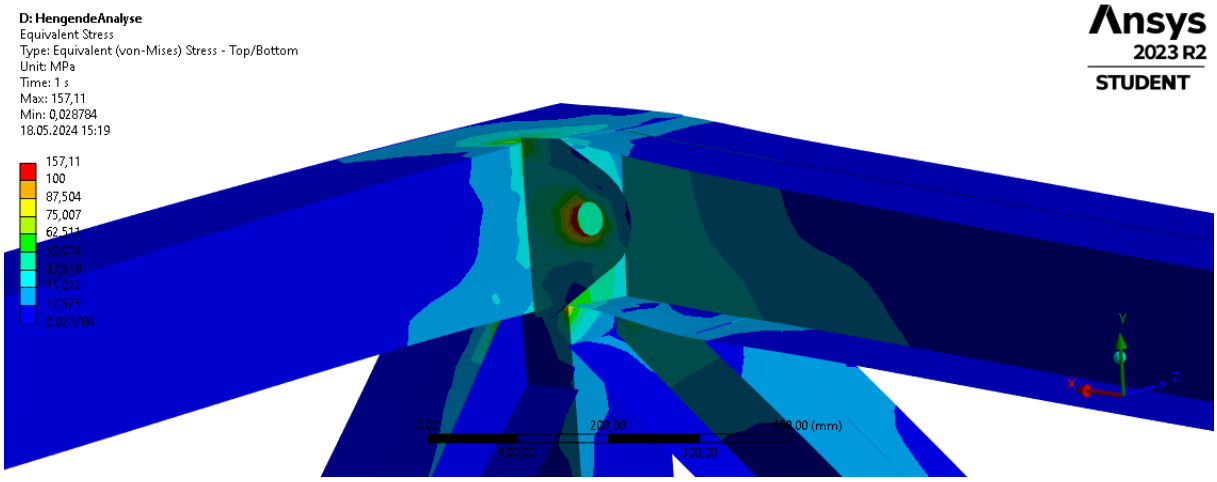

Figure 30 - Stress concentrations in basket corner.

The deformation of the basket can be seen in Figure 31. There was minimal deformation, given the size of the basket. Only a few of the stiffeners were included in the simulation. The resulting deformation is expected to be lower in real-life scenarios.

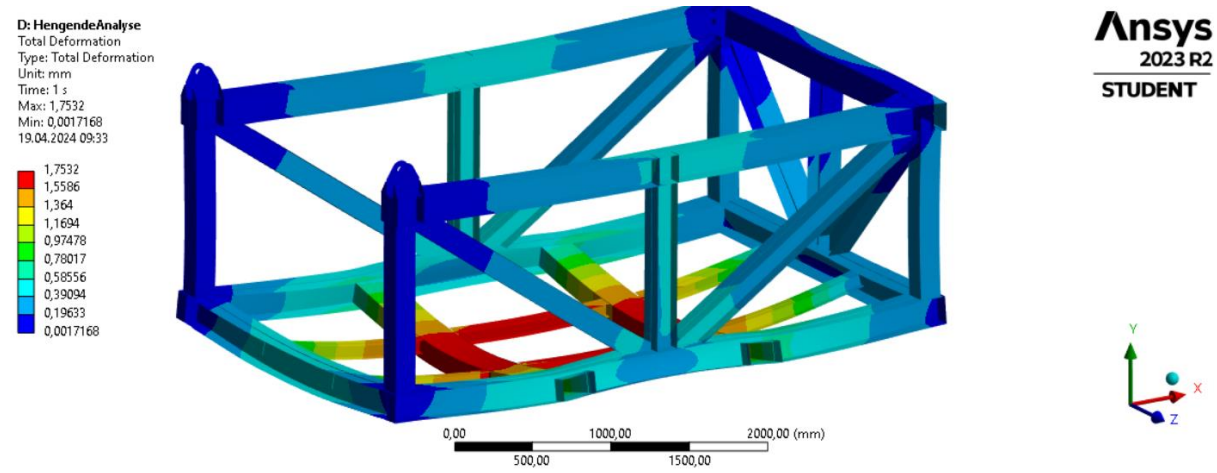

Figure 31 - Basket deformation.

4.1.3. Door FEM Simulation

The structure of the door is built up by strong beams, which can withstand much more force than what realistically will appear. Therefore, only the hinges and the handles are presented in this simulation segment. Figure 32 presents how the door looks fully assembled without grating and shows the hinges and handle that are analyzed in this chapter. The left door is identical to the right, but with a locking mechanism under the handle.

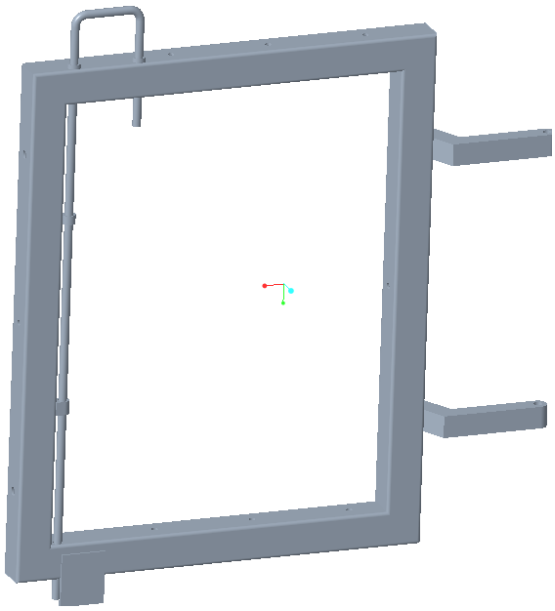

Figure 32 - Right door assembly.

Hinges

Different worst scenarios were simulated to figure out what the hinges on the doors would be able to handle. The first load case was based on something crashing on top of the door in a halfway-opened position, where the hinge would be weakest. A weight of 1 ton was added as a force to the end of the hinge as seen in Figure 33. Because there are two hinges for each door, the weight was divided into two, giving 4905N per hinge.

For load case 1, the constraints were a cylindrical support and a fixed support. The cylindrical support was added to the hole of the hinge, as shown in Figure 34, to allow some movement in the z-axis for a most realistic simulation. Fixed support had to be included to fully constrain the hinge, which was placed at the bottom of the hole, as presented in Figure 35. This made sure that most of the results were realistic, but the lowest part of the hole would most likely get an unrealistic result.

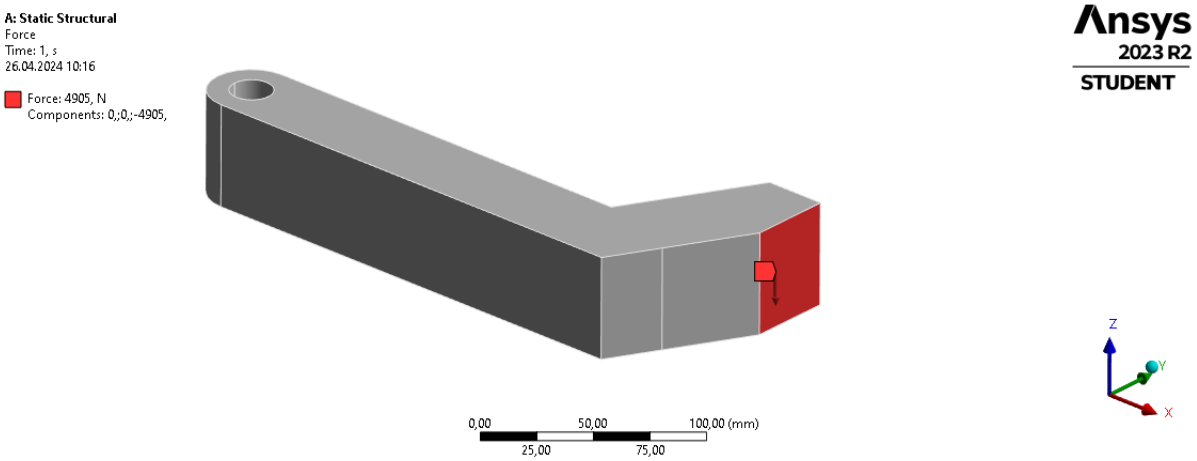

Figure 33 - Hinge load case 1 force.

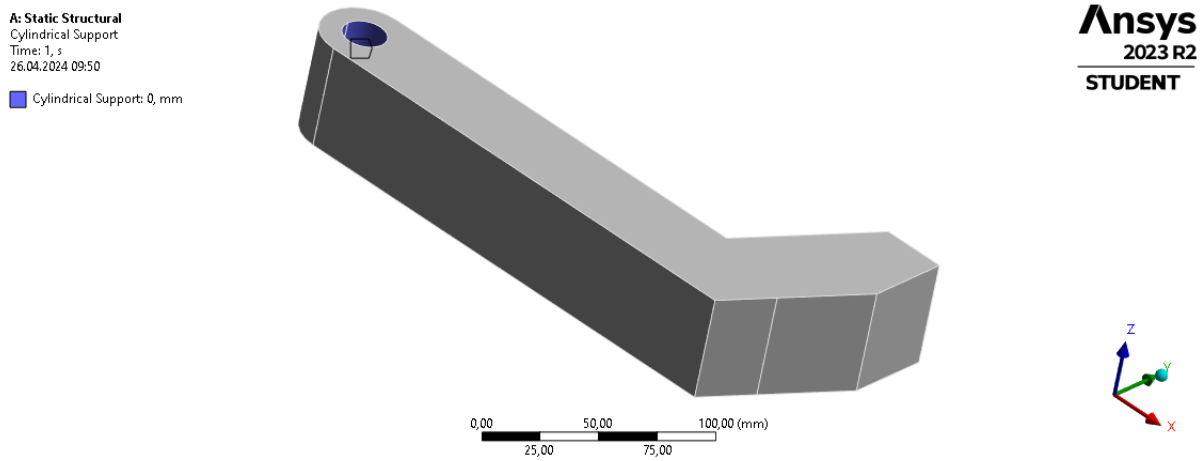

Figure 34 - Cylindrical support hinge load case 1.

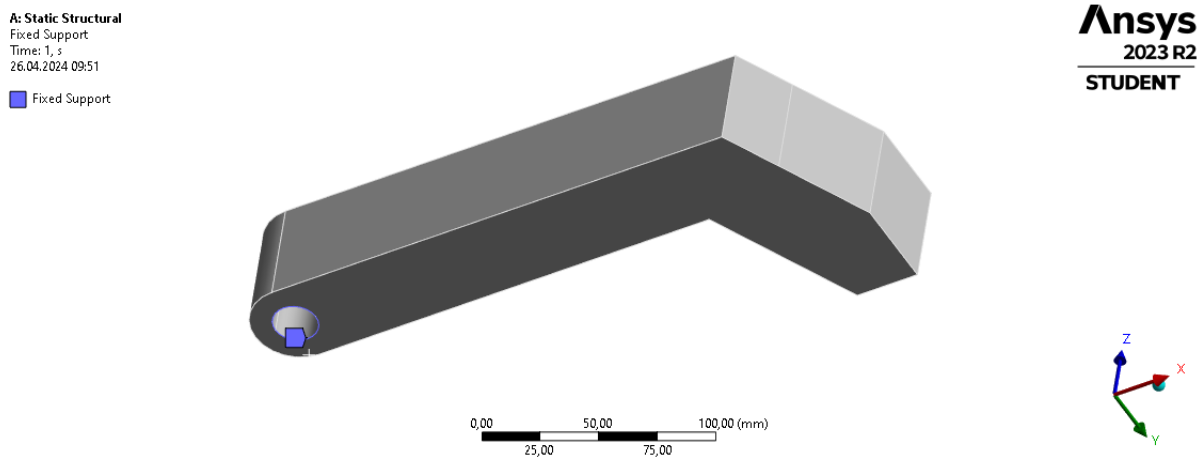

Figure 35 - Fixed support hinge load case 1.

Figure 36 shows the von Mises stress results for the first hinge simulation. 500kg on each hinge leads to a stress of 245,24MPa, which is close but lower than the maximum allowable stress of 301,75MPa. This stress appears where there was added a fixed support as shown in Figure 37, so it is not completely realistic. The stress would realistically be lower, but the hinge was able to handle even this worst-case scenario.

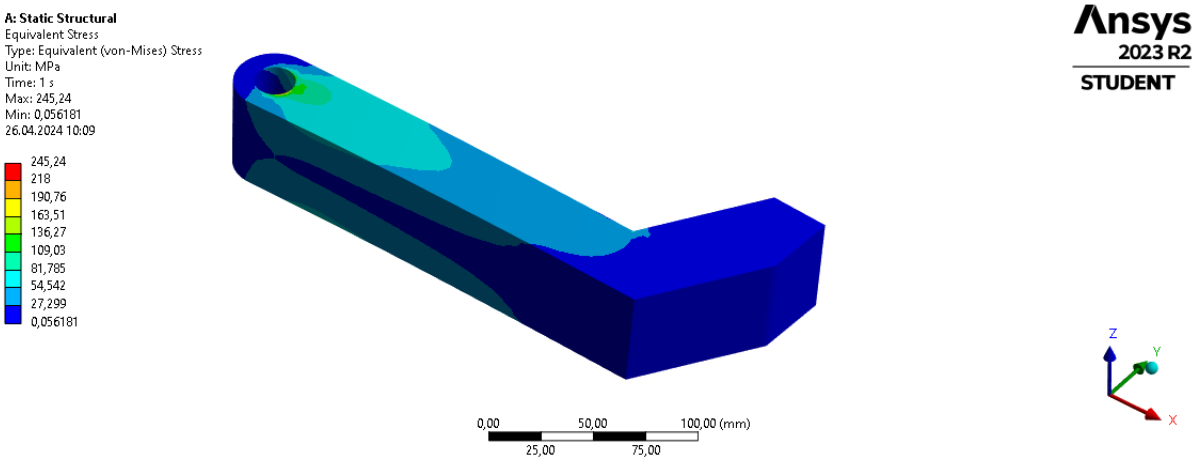

Figure 36 - Hinge load case 1 results.

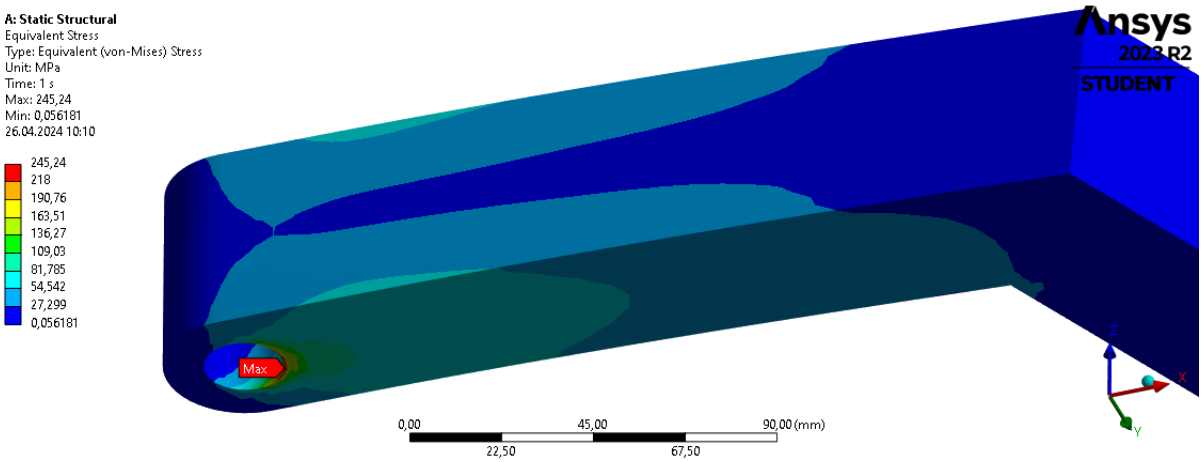

Figure 37 - Max stress hinge load case 1.

For load case 2, the hinge was tested for a pull force equivalent to 200kg. The length of the door is 1045mm, so the moment would be 2050Nm. Given that there are two hinges, the moment was divided by 2, which gave 1025Nm. It was added to the end of the hinge, as shown in Figure 38, around the Z-axis.

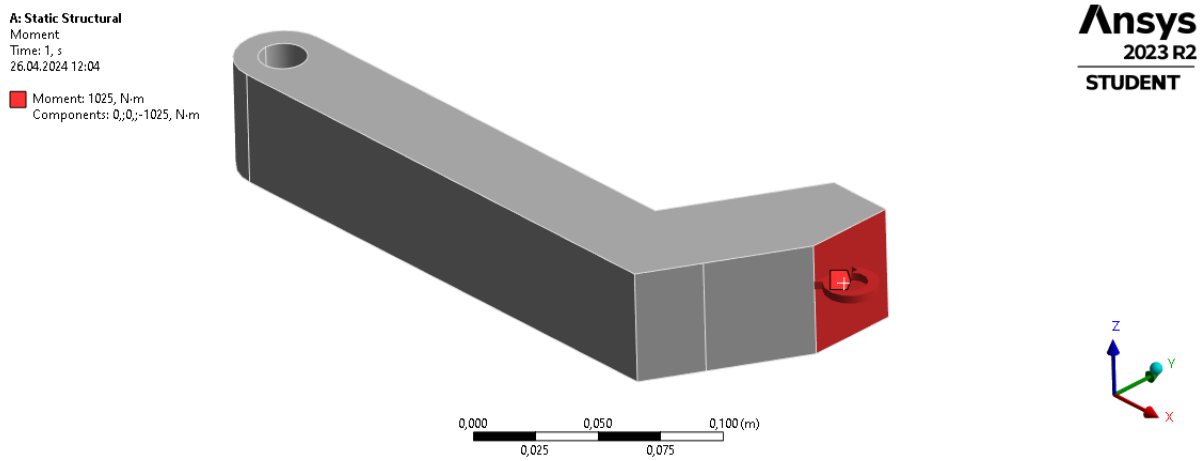

Figure 38 - Hinge load case 2 moment.

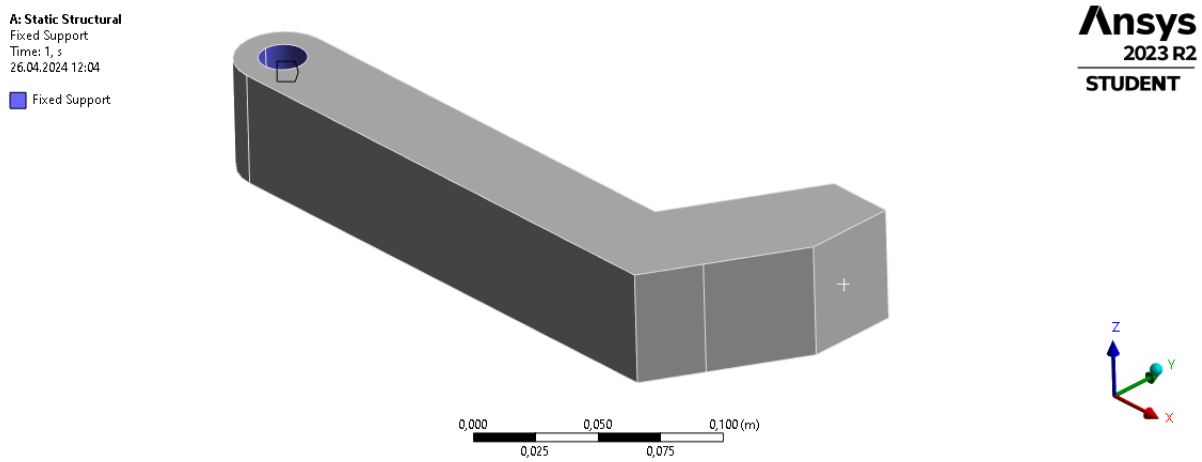

Figure 39 - Hinge load case 2 fixed support.

The results from load case 2 can be seen in Figure 40. Each hinge got a maximum stress value of 131,74MPa, which is much lower than the maximum allowed stress of 301,75MPa. This means they will hold if the hinge is stuck, and the door is pulled by a force equivalent to 200kg.

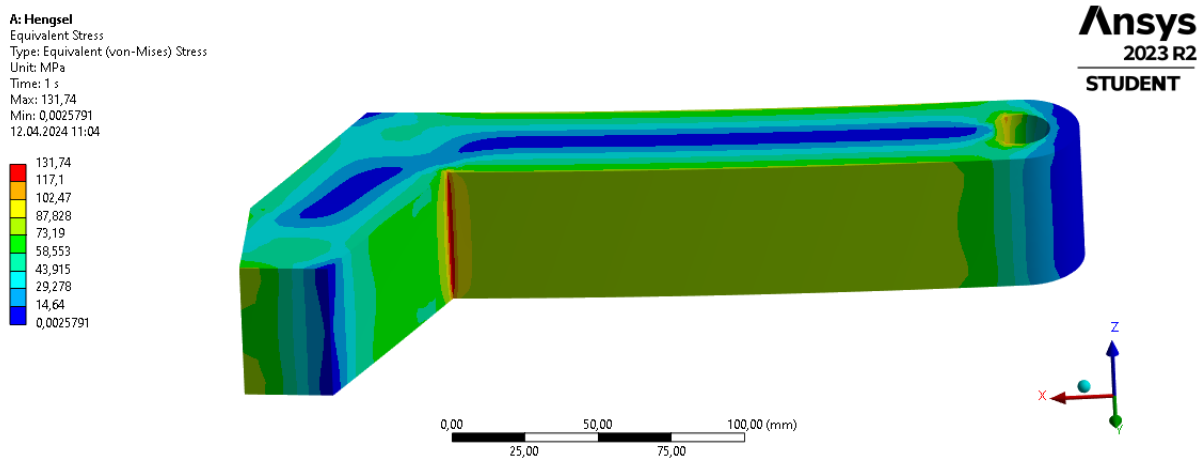

Figure 40 - Hinge load case 2 results.

Handle

The handle would have to endure the same amount of pulling force as the hinges if the hinges got stuck. Therefore, the handles were also tested for a pull equivalent to 200kg or 2050N. Figure 41 shows how the force was applied to run the simulation, and Figure 42 shows the fixed support. The force was placed where the ROV would pull, and a fixed support was placed where the handle is in contact with the door. The locking pin is the same diameter as the handle. Therefore, there is no need to do a simulation on the locking pin as well, as it will withstand approximately the same force.

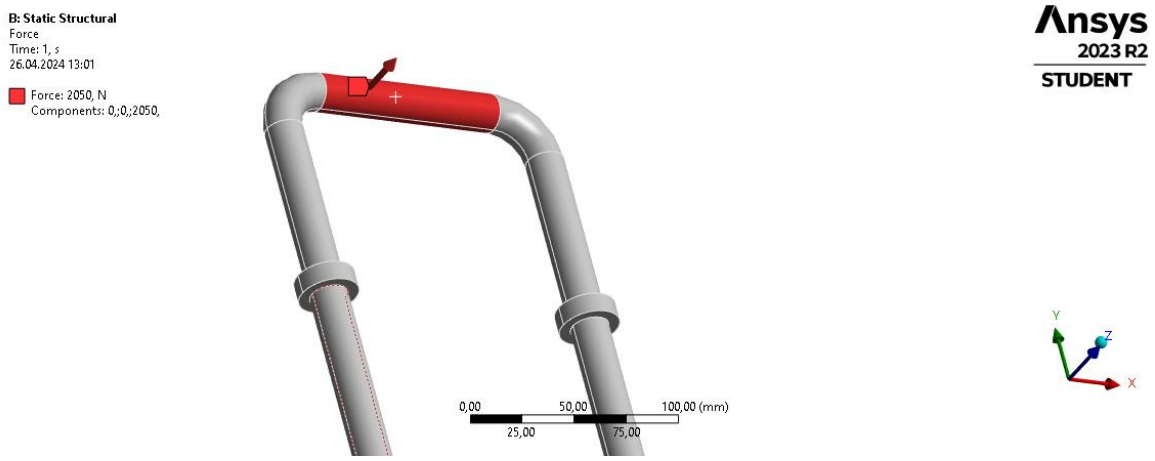

Figure 41 - Force for handle simulation.

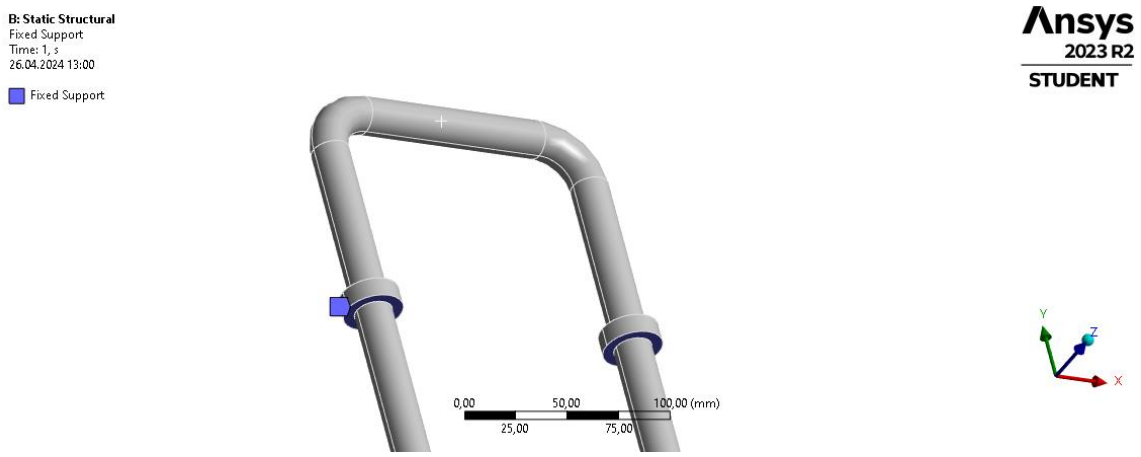

Figure 42 - Fixed support for handle simulation.

Figure 43 shows the results from the handle simulation. The maximum stress was 173,63MPa, which is well within the maximum allowed stress of 301,75MPa. This shows that the handle can manage a pull equivalent to 200kg. Although some deformation occurs, it remains within acceptable limits and is not problematic.

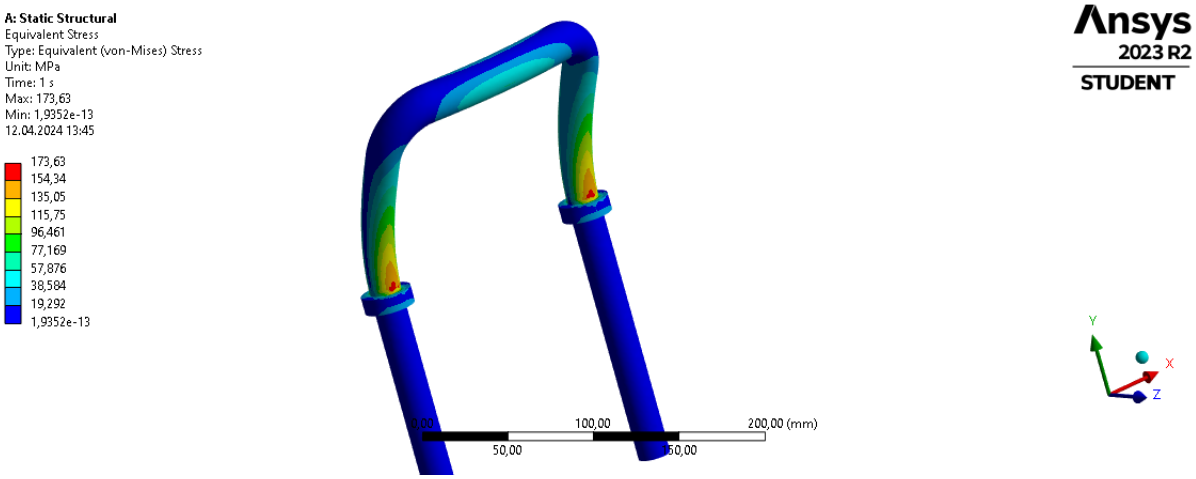

Figure 43 - Results from handle simulation.

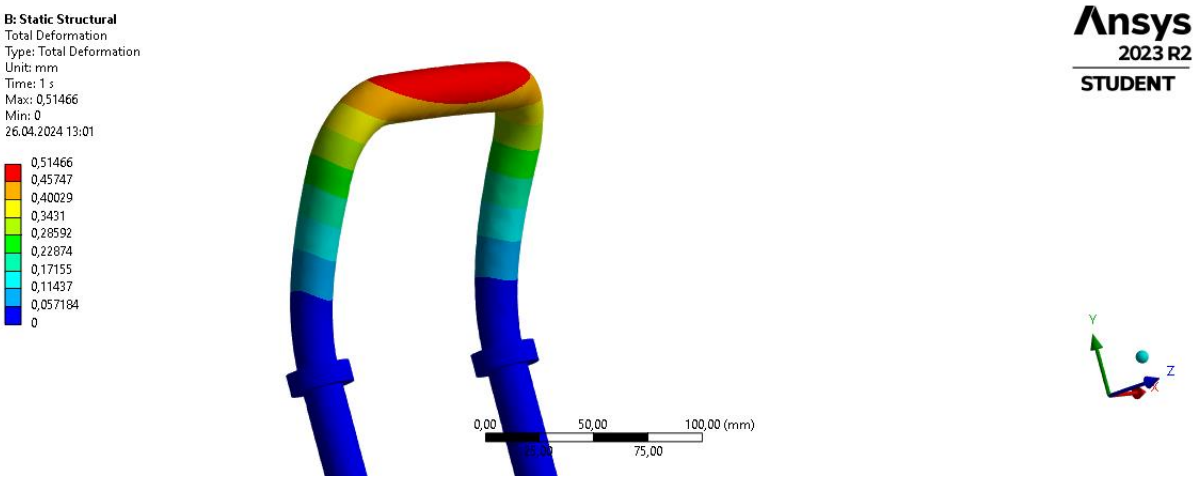

Figure 44 - Deformation handle simulation.

4.1.4. Structural Analysis Calculations

Simplifications

Static calculations regarding the loads on the bottom beams are simplified for FEM, 1D beam simulation. They apply for design values of shear force and bending moment for bottom beam cross sections. These are extracted from the shear bending moment diagrams for the different load cases from Supplementary Figure 7 to Supplementary Figure 10.

Classification of RHS

The epsilon factor is given for further cross-section classification:

$$\varepsilon = \sqrt{\frac{235}{f_y}}$$

$f_y = 355\ \text{N/mm}^2$ [11, Sec.5.6]

$\varepsilon = 0,81$

Internal compression parts(web)

$$\left(\frac{c}{t}\right)_{web} = \frac{(h - 2 \cdot t \cdot r_i)}{t} = \frac{(250 - 2 \cdot 12,5 - 2 \cdot 12,5)}{12,5} = 16,00$$

$\left(\frac{c}{t}\right)_{web} \leq 72\varepsilon \rightarrow$ the web is classified as Class1.

Outstand Flange

$$\left(\frac{c}{t}\right)_{flange} = \frac{\left(\frac{h}{2} - t - r_i\right)}{t} = \frac{\left(\frac{250}{2} - 12,5 - 12,5\right)}{12,5} = 8,00$$

$\left(\frac{c}{t}\right)_{flange} \leq 9\varepsilon$

$\left(\frac{c}{t}\right)_{flange} \leq 10\varepsilon \rightarrow$ the flange is classified as Class 2.

Classification of HEB100

Internal compression parts(web)

$$c = h - 2t_f - 2r = (100 - 2 \cdot 10 - 2 \cdot 12) = 56mm$$

$$\left(\frac{c}{t}\right)_{web} = \frac{56}{5} = 11,20$$

$\left(\frac{c}{t}\right)_{web} \leq 33\varepsilon \rightarrow$ the web is classified as Class1.

Outstand Flange

$$c = \frac{(b - t_w - 2r)}{2} = \frac{(100 - 6 - 2 \cdot 12)}{2} = 35$$

$$\left(\frac{c}{t}\right)_{flange} = \frac{35}{10} = 3,5$$

$$\left(\frac{c}{t}\right)_{flange} \leq 9\varepsilon \rightarrow \text{the flange is classified as Class1.}$$

Table 4 - Result of classification of total cross-section.

Cross-Section	Classification of total cross-section
RHS250x150x12,5	Class 2
HEB100	Class 1

Load Conditions for Bottom Beams

The loads acting on the bottom beams are based on the Design Factor(DF) that is defined for the operational class for POU [7, Ch. 3.5.1]. The member load equals a payload combined with tare weight.

$$F_{sub} = DF \cdot MGW \cdot g$$
$$MGW = (T + P)$$
$$F_{sub} = 2,5 \cdot P \cdot g$$
$$F_{sub} = 120\,\text{kN}$$

Where:

MGW = Maximum Gross Weight

$T = Tare$

$P = Payload$

Table 5 - Total shear and moment forces, from Supplementary Figure 7 to Supplementary Figure 10.

Load Type	Profile type	Length (mm)	Total shear V_{ED} (kN)	Total Moment M_{ED} (kNm)
Concentrated	RHS250x150x12,5	2385	60,00	35,80
Uniformly Distributed			59,90	23,85
Concentrated	HEB100	1150	60,00	17,25
Uniformly Distributed			59,20	11,50

Bending Moment

The design value of the bending resistance verification:

$$\frac{M_{Ed}}{M_{c,Rd}} \leq 1,0 \qquad \text{[11, Sec. 6.2.5]}$$

The design resistance for bending about the major or minor axis of a cross-section:

$$M_{c,Rd} = M_{pl,Rd} = \frac{W_{pl} \cdot f_y}{\gamma_{M0}} \quad \text{for class 1 or 2 cross-section}$$

Where:

γ_{M0} : partial material safety factor

W_{pl}: Plastic section modulus

f_y: Yield strength S355J2

Bending Moment RHS250

For bending about the minor axis z-z:

$$M_{c,z,Rd} = M_{pl,z,Rd} = \frac{W_{pl,z} \cdot f_y}{\gamma_{M0}} = \frac{514 \cdot 10^3\,\text{mm}^3 \cdot 355 \frac{\text{N}}{\text{mm}^2}}{1,05} = 173,8\,\text{kNm}$$

The utilization for the bending resistance verification is equal to:

$$\frac{M_{Ed}}{M_{c,z,Rd}} = \frac{35\,\text{kNm}}{173,80\,\text{kNm}} = 0,20 \leq 1,0 \text{ OK!}$$

Bending Moment HEB100

For bending about the major axis y-y:

$$M_{c,y,Rd} = M_{pl,y,Rd} = \frac{W_{pl,y} \cdot f_y}{\gamma_{M0}} = \frac{104 \cdot 10^3\,\text{mm}^3 \cdot 355 \frac{\text{N}}{\text{mm}^2}}{1,05} = 35,23\,\text{kNm}$$

The utilization for the bending resistance verification is equal to:

$$\frac{M_{Ed}}{M_{c,y,Rd}} = \frac{17,25\,\text{kNm}}{35,23\,\text{kNm}} = 0,49 \leq 1 \text{ OK!}$$

Shear Resistance

The design value of the shear force resistance verification:

$$\frac{V_{Ed}}{V_{c,Rd}} \leq 1,0 \qquad \text{[11, Sec. 6.2.6]}$$

The design plastic shear resistance is given by:

$$V_{pl,Rd} = \frac{A_v \left(\frac{f_y}{\sqrt{3}} \right)}{\gamma_{M0}}$$

Where:

A_v: Shear area

Shear Resistance RHS250

For rolled rectangular hollow sections of uniform thickness, load parallel to depth:

$$A_v = \frac{Ah}{(b+h)} = \frac{9207\,\text{mm}^2 \cdot 250\,\text{mm}}{(150+250)\,\text{mm}} = 5754,40\,\text{mm}^2$$

For the shear force along z-z:

$$V_{pl,z,Rd} = \frac{5754,40\,\text{mm}^2 \left(\frac{355\,\text{N/mm}^2}{\sqrt{3}} \right)}{1,05} = 1123,30\,\text{kN}$$

The utilization for the shear resistance verification is equal to:

$$\frac{V_{Ed}}{V_{c,Rd}} = \frac{60\,\text{kN}}{1123,30\,\text{kN}} = 0,05 \leq 1,0 \text{ OK!}$$

Shear Resistance HEB100

For rolled I and H sections, load parallel to web:

$$A_v = A - 2bt_f + (t_w + 2r)t_f$$
$$A_v = 2604\,\text{mm}^2 - 2 \cdot (100 \cdot 10)\,\text{mm}^2 + (6 + 2 \cdot 12) \cdot 10\,\text{mm}^2$$
$$A_v = 904\,\text{mm}^2$$

For the shear force along y-y:

$$V_{pl,y,Rd} = \frac{904\,\text{mm}^2\left(\frac{355\,\text{N/ mm}^2}{\sqrt{3}}\right)}{1,05} = 176,50\,\text{kN}$$

The utilization for the shear resistance verification is equal to:

$$\frac{V_{Ed}}{V_{c,Rd}} = \frac{60\,\text{kN}}{176,50\,\text{kN}} = 0,34 \leq 1,0 \text{ OK!}$$

Arbitrary cross-section

The general equation for the critical buckling moment:

$$M_{cr} = \mu_{cr}\frac{\pi\sqrt{EI_z GI_t}}{L_b}$$

Where:

μ_{cr}: Relative dimensionless critical moment

E: Modulus of elasticity

G: Shear modulus

I_z: Moment of inertia by z-axis

I_t: Torsion constant

L_b: Buckling length.

The moment factor μ_{cr} is simplified due to a doubly symmetric cross-section:

$$\mu_{cr} = \frac{C_1}{k_z}\left[\sqrt{1+k_{wt}^2}\right]$$

Where:

$$k_{wt} = \frac{\pi}{k_w L}\sqrt{\frac{EI_w}{GI_t}}$$

C_1: Load factor

K_{wt}: Torsional parameter

I_w: Warping constant

	k_y	k_z	k_w	C_1	C_2	C_3
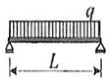	1 1	1 0,5	1 0,5	1,12 0,95	0,46 0,31	0,53 0,67
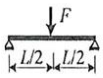	1 1	1 0,5	1 0,5	1,35 1,03	0,55 0,44	0,41 0,52
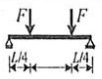	1 1	1 0,5	1 0,5	1,04 0,92	0,43 0,24	0,56 0,77
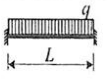	0,5 0,5	1 0,5	1 0,5	2,58 1,49	1,56* 0,83*	-0,86* 0,003*
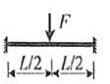	0,5 0,5	1 0,5	1 0,5	1,68 0,94	1,39* 0,84*	-0,72* -0,07*
* Verdiene gjelder for $-0,5 \leq \psi_f 0,5$						

Figure 45 - Load Factor based on given constraints in the beams. [13]

LTB General Case

Non-dimensional slenderness:

$$\bar{\lambda}_{LT} = \sqrt{\frac{W_y f_y}{M_{cr}}} \qquad \text{[11, Sec. 6.3.2.2]}$$

$W_y = W_{pl,y}$ for Class 1 or 2 cross-sections

For rolled sections or equivalent welded sections the slenderness maximum value:

$$\bar{\lambda}_{LT,0} = 0,4$$

For slendernesses $\bar{\lambda}_{LT} \leq \bar{\lambda}_{LT,0}$ or for $\frac{M_{Ed}}{M_{cr}} \leq \bar{\lambda}_{LT,0}^{\ 2}$

Lateral torsional effects may be ignored and only cross sectional checks apply.

Where:

M_{Ed}: Design value of the moment

LTB for HEB100

From the load combination diagram the load factor and correction factors for the member load case:

$k_y = 0,5$

$k_z = 0,5$

$k_w = 0,5$

$C_{1,Concentrated} = 0,94$

$C_{1,Distributed} = 1,49$

For the momentfactor μ_{cr} :

$$k_{wt} = \frac{\pi}{k_w L}\sqrt{\frac{EI_w}{GI_t}} = \frac{\pi}{0,5 \cdot 1150\,\text{mm}}\sqrt{\frac{2,1 \cdot 10^5\ \text{N/mm}^2 \cdot 2475 \cdot 10^6\ \text{mm}^6}{8,1 \cdot 10^4\ \text{N/mm}^2 \cdot 51,99 \cdot 10^3\ \text{mm}^3}}$$

$k_{wt} = 1,92$

$$\mu_{cr} = \frac{C_{1,Concentrated}}{k_z}\left[\sqrt{1+k_{wt}^2}\right] = \frac{0,94}{0,5}\left[\sqrt{1+(1,92)^2}\right]$$

$\mu_{cr,concentrated} = 4,06$

$\mu_{cr,distributed} = 6,45$

Then Critical buckling moment is:

$$M_{cr} = \mu_{cr}\frac{\pi\sqrt{EI_z GI_t}}{L} = 4,06\frac{\pi\sqrt{2,1 \cdot 10^5\ \text{N/mm}^2 \cdot 1,338 \cdot 10^6\ \text{mm}^2 \cdot 8,1 \cdot 10^4\ \text{N/mm}^2 \cdot 51,99 \cdot 10^3\ \text{mm}^3}}{1150\,\text{mm}^2}$$

$M_{cr,concentrated} = 381,52\,\text{kNm}$

$M_{cr,distributed} = 605,60\,\text{kNm}$

Non-dimensional slenderness:

$$\bar{\lambda}_{LT} = \sqrt{\frac{W_{pl,y} f_y}{M_{cr,concentrated}}} = \sqrt{\frac{83,01 \cdot 10^3\ \text{mm}^2 \cdot 355\,\text{N/mm}^2}{381,52 \cdot 10^6\ \text{Nmm}}}$$

$\bar{\lambda}_{LT,concentrated} = 0,277$

$\bar{\lambda}_{LT,distributed} = 0,220$

$\bar{\lambda}_{LT} \le \bar{\lambda}_{LT,0}$

$0,277 \le 0,4$ OK!

or for:

$$\frac{M_{Ed}}{M_{cr}} \le \bar{\lambda}_{LT,0}^{\,2}$$

$$\frac{17,25\,\text{kNm}}{381.52\,\text{kNm}} \le 0,4^2$$ OK!

LTB for RHS250

There were limited literature findings regarding LTB for hollow cross-sections. While the standard provides primarily guidelines for Rolled and Welded I-sections, other cross-sections are also mentioned. However, hollow sections do not have warping properties, which can be an important factor in the approach to the calculation for buckling. With this, the calculations can be ignored as they will not be critical.

ULS summary

The loads analyzed as member loads acting on the bottom beams of the structure indicate that the results from the ULS approach for the subsea basket are validated and considered safe according to the standards and guidelines.

4.1.5. Weld Calculations

The welding calculations are based on the direct method outlined in Eurocode3. While a simplified method is available, the direct method is preferred due to its familiarity within the company. This method follows a load and resistance factor design (LRFD) approach, with criteria provided by DNV for both the LRFD and allowable stress design (ASD) methods.

For the cross-joints experiencing the highest stresses in the structure, calculations are based on T-joints with fillet welds at an angle of 45 degrees. This ensures that calculations comply with the company calculation method, which is based on the direct method. This is to ensure the safety and structural integrity of the overall subsea basket. Detailed welding calculations for pad-eyes are covered in their respective chapter 4.4.4.

Assumptions and Simplifications

The angles in the KT- and N-joints are below the valid angles for using fillet welds. T-butt joints, also known as K-joints, should be considered. The design resistance is determined using the method for a fillet weld. This implies that the effective throat thickness is assumed to be greater than 3mm. Additionally, welding calculations for stiffeners are not taken into consideration.

Fillet Weld Calculations

The stress values in the nodes used to calculate weld dimensions are found in Supplementary Table 7.

HEB160 weld calculations:

Bending stress due to moment about the major and minor axes:

$$\sigma_b = \frac{\mathrm{M_{Ed,x}}}{\sqrt{2}\cdot \mathrm{W_{eff,x}}} + \frac{\mathrm{M_{Ed,z}}}{\sqrt{2}\cdot \mathrm{W}_{eff,z}} = \frac{7\cdot 10^3\ \mathrm{Nmm}}{\sqrt{2}\cdot 247{,}85\cdot 10^3\ \mathrm{mm^3}} + \frac{1.149\cdot 10^6\ \mathrm{Nmm}}{\sqrt{2}\cdot 85{,}48\cdot 10^3\ \mathrm{mm^3}} = 9{,}52 MPa$$

The factor $\frac{1}{\sqrt{2}}$ from trigonometric identity is due to the sine of the 45-degree fillet angle.

The shear stress equals the normal stress due to bending because of the angle of the fillet:

$\tau_b = \sigma_b$

Shear stress parallel to the axis of weld in the web, assuming 5mm throat size:

$$\tau_{\parallel,web} = \frac{\mathrm{V_{Ed,x}}}{2 \cdot a \cdot \mathrm{l}_{weld,z}} = \frac{89,774 \cdot 10^3\,\mathrm{N}}{2(5 \cdot 130)\,\mathrm{mm}^2} = 69MPa$$

Shear stress parallel to the axis of weld for the flanges:

$$\tau_{\parallel,\,flange} = \frac{\mathrm{V_{Ed,z}}}{4 \cdot a \cdot \mathrm{l}_{weld,x}} = \frac{613\,\mathrm{N}}{4(5 \cdot 160)\,\mathrm{mm}^2} = 0,19MPa$$

$$\tau_{\parallel} = \tau_{\parallel,web} + \tau_{\parallel,\,flange}$$

Normal stress due to axial forces of tension/compressive forces acting:

$$\sigma_{\perp} = \frac{\mathrm{N_{Ed}}}{\sqrt{2} \cdot \mathrm{A}_{eff}} = \frac{2,097 \cdot 10^3\,\mathrm{N}}{\sqrt{2} \cdot 4600\,\mathrm{mm}^2} = 0,32MPa$$

Perpendicular stresses are equal due to symmetrical loads acting:

$$\tau_{\perp} = \sigma_{\perp}$$

The combination of the effects of normal stresses and shear stresses in the different directions of the weld gives the equation for von Mises:

$$\sigma_{eq} = \sqrt{\left(\sigma_{\perp} + \sigma_b\right)^2 + 3\left(\left(\tau_{\perp} + \tau_b\right)^2 + \left(\tau_{\parallel}\right)^2\right)} = \sqrt{\left(0,32 + 9,52\right)^2 + 3\left(\left(0,32 + 9,52\right)^2 + \left(69 + 0,19\right)^2\right)}$$

$$\sigma_{eq} = 121,45MPa$$

The permissible usage factor is given as:

$$\eta = \frac{\sigma_{eq} \cdot \beta_w \cdot \gamma_{M2}}{\mathrm{f}_u} = \frac{120,30MPa \cdot 0,9 \cdot 1,25}{510MPa} = 0,267$$

Table 6 - Node calculations for von Mises stress and permissible usage factor, based on welding equations.

Welded Joint profile	**Calculation**	**von-Mises stress (MPa)**	**Permissible usage factor**
HEB160	1	113,94	0,250
	2	119,30	0,263
	3	120,30	0,265
	4	121,45	0,267
SHS140x12,5	5	130,00	0,286
	6	125,40	0,276

Weld Summary

The welding calculations indicate that the von Mises stresses are within acceptable limits while using the direct method in Eurocode3. The various principal stress methods are also acceptable. This means that the effective throat thickness is calculated to be 5mm, which is the required welding dimension for the basket and A-frame. An average permissible usage factor of 26% provides a substantial margin of safety.

Table 7 – Principal Limitation criteria for welding calculations, according to the relevant standards.

Eurocode3: LSD Criteria [MPa]	**DNV:** Allowable stress [MPa]	**DNV:** LRFD Criteria [MPa]	**DNV**: ASD Criteria [MPa]	**Permissible usage factor**
453,33	301,75	392,30	270,30	$\eta \leq 1$

4.2. A-Frame

4.2.1. Choice Of Design

An A-frame is a type of lifting frame often used in subsea baskets. The A-frame consists of a spread bar, beams, shackles, chains, and pad-eyes. The beams are connected to the spread bar at one end and have a hinge mechanism on the other end. This hinge mechanism and gravitational forces allow the A-frame to be laid down flat on the basket when not under load. Figure 46 and Figure 47 show the A-frame position with applied load and without applied load, respectively. This feature effectively saves space during ROV operations and transportation.

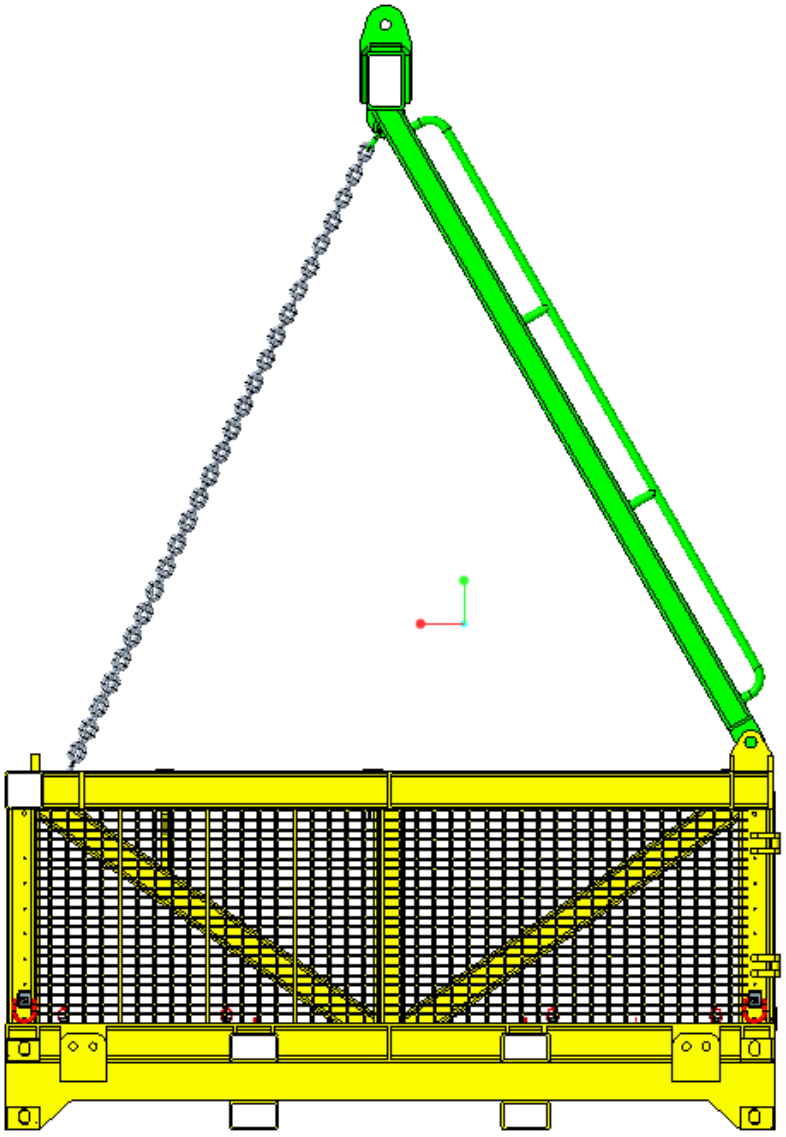

Figure 46 - A-frame position during lifting operation.

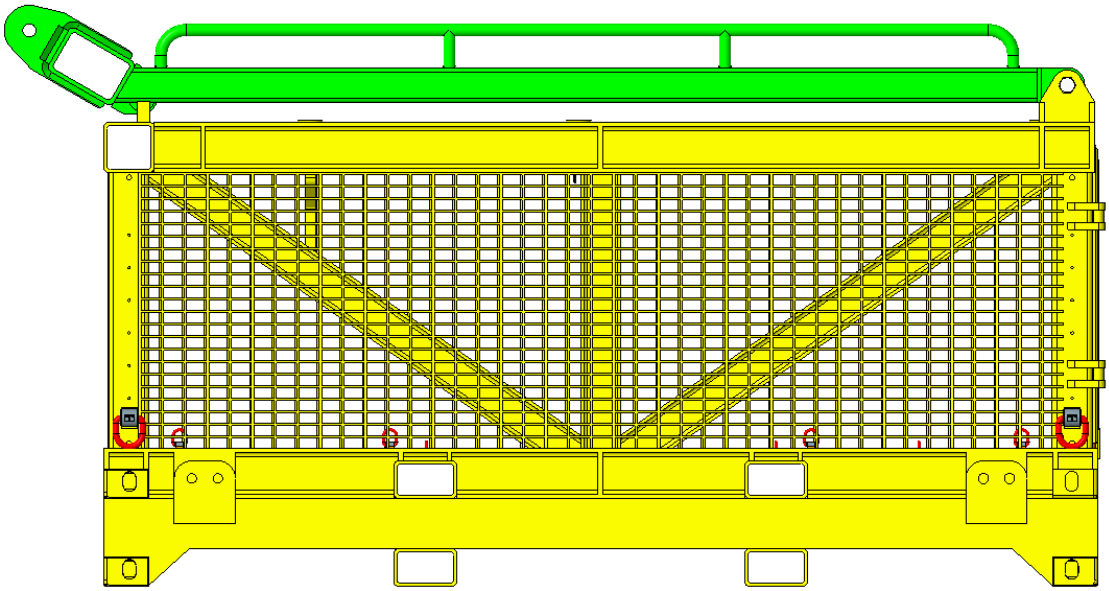

Figure 47 - A-frame position when no load is applied.

The fork-like geometry of the A-frame leaves the basket entirely open. The hinge mechanism is located on the same side of the basket as the doors, which results in unobstructed access into the basket both for the ROV and the deck crew. This is illustrated in Figure 48.

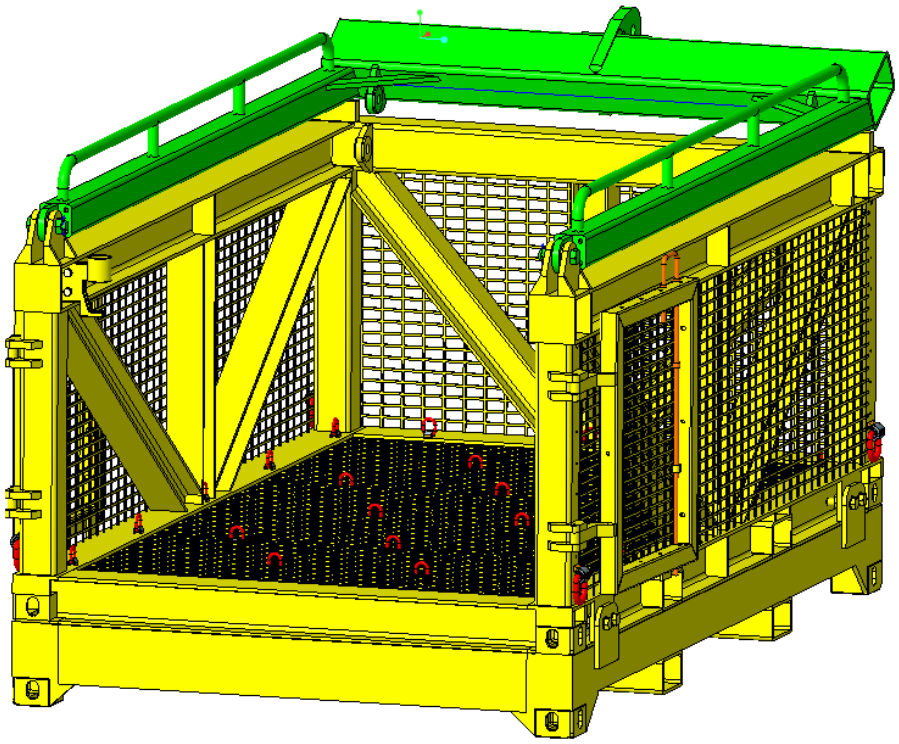

Figure 48 - Basket with A-frame when no lifting load is applied.

The presence of a single connection point centered on the spread bar enhances time efficiency, simplifying operations. Chains are used on the opposite side of the A-frame and are more suitable than wires as they exhibit a more predictable falling pattern when they are not under tension. This prevents potential tangling.

4.2.2. Side beams

To begin with the side beams were designed using HEB profiles. Through an update of the structural simulation using SAP2000, as advised by the supervisor from DO, it became clear that the utilization ratio of longitudinal beams of HEB140 had a utilization ratio above 1. By using hollow profiles such as SHS140, this leads to the desired utilization ration being below 1. This is due to the side loads that may occur during a subsea operation.

Drain holes are added at the end sections to allow water to flow in and out of the beam profiles. This is illustrated in Figure 49.

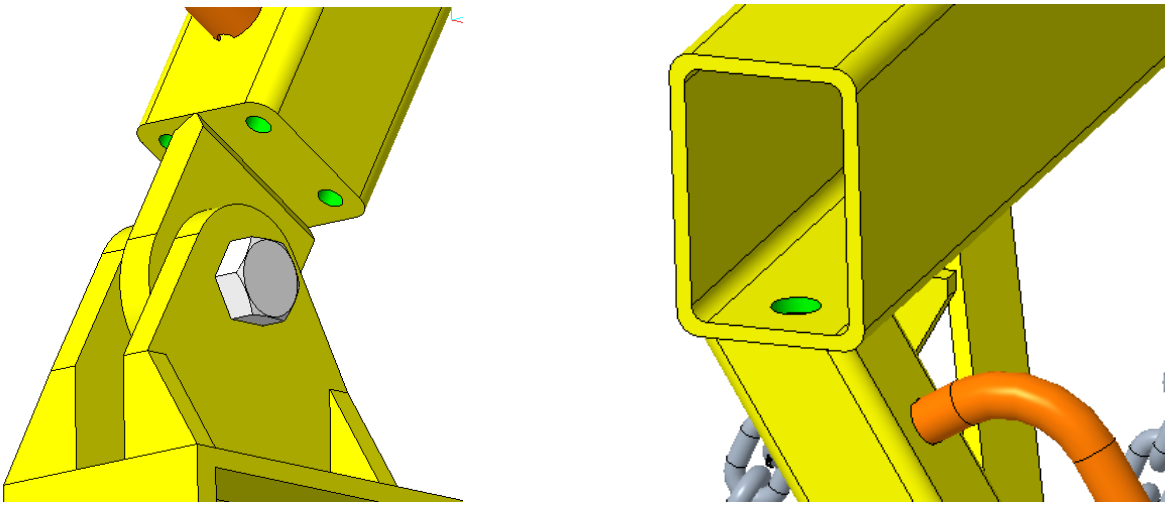

Figure 49 - Drainage holes of end sections of A-frame, highlighted in green.

4.2.3. Spreader Bar

The load point connections on the spreader bar result in uneven load distributions. Many stiffeners would be required to keep the stress levels below yield when using H-profiles. Alternatively, to avoid stiffeners, a larger H-beam size could be used. This, however, would not be suitable for design purposes. Therefore, a hollow profile beam is chosen as a spreader bar. A rectangular profile oriented with the longest surface along the vertical plane results in the highest moment of inertia compared to other hollow sections, such as circular or quadratic hollow sections.

The end sections of the beams are kept open to avoid hydrostatic loading [6, Ch. 16.6.3.5]. Figure 50 shows the spreader beam attached to the rest of the A-frame.

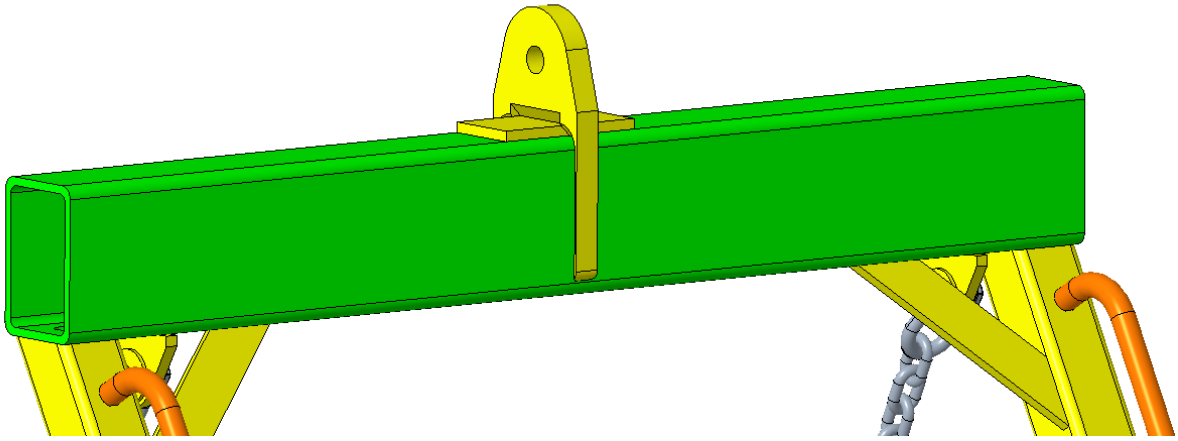

Figure 50 - A-frame spreader beam.

4.2.4. A-Frame Hinge Pins

According to NS-EN ISO 286-1 2010, a clearance fit between the hole diameter and the pin/bolt can be used in the design to allow for an easy assembly and, at the same time, unobstructed movement of the parts when in operation. A tolerance of C11/h11 is used in the design [17, p. 17]. The maximum/minimum clearances for these tolerance grades are calculated in the equations below.

$$Maximum\ clearance = 39,120mm - 38,989mm = 0,131mm$$

$$Minimum\ clearance = 39,280mm - 29,000mm = 0,280mm$$

The bolts used in the design are secured with R-clips to prevent the bolted connections from unscrewing. It is designed with the dimensions of an M39 bolt according to Eurocode 3 and the tolerances given above. The length of the unthreaded section is designed to carry all the shear forces. Figure 51 shows the hinge mechanism where the bolt is placed.

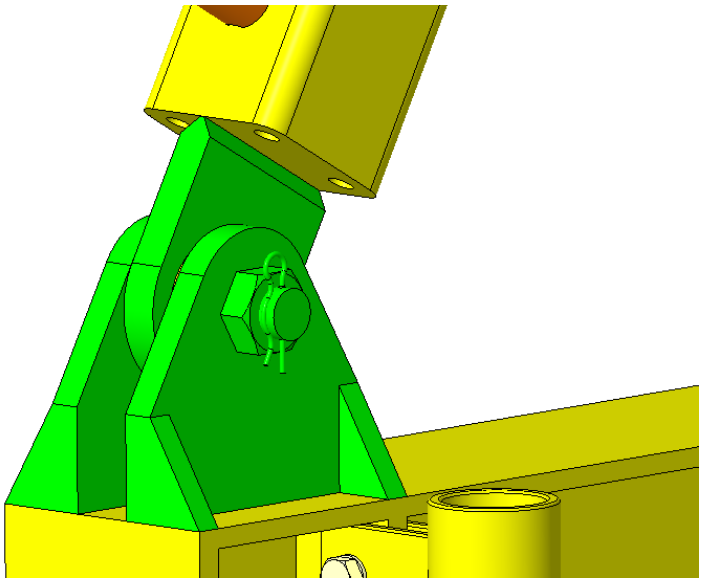

Figure 51 - Hinge mechanism between basket and A-frame.

4.2.5. A-frame FEM Simulations

In the A-frame simulation, the forces added were the same as the pad-eye forces. The main pad-eye on top of the A-frame was fixed, as shown in Figure 52. The pad-eye forces were directed down with an angle to simulate the subsea basket, as can be seen in Figure 53 and Figure 54. Because of the limits to the student version of Ansys, this simulation did not include the stiffeners that were added at the sides of the main pad-eye. The simulation did, however, show to some degree realistic results of the pad-eyes and beams on the bottom side of the A-frame.

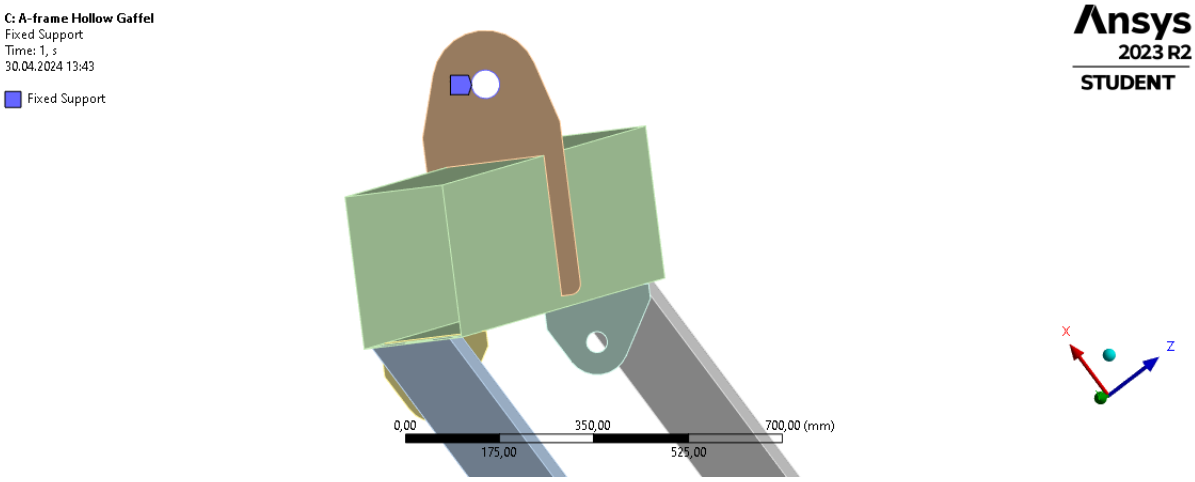

Figure 52 – Fixed support for simulation of A-frame.

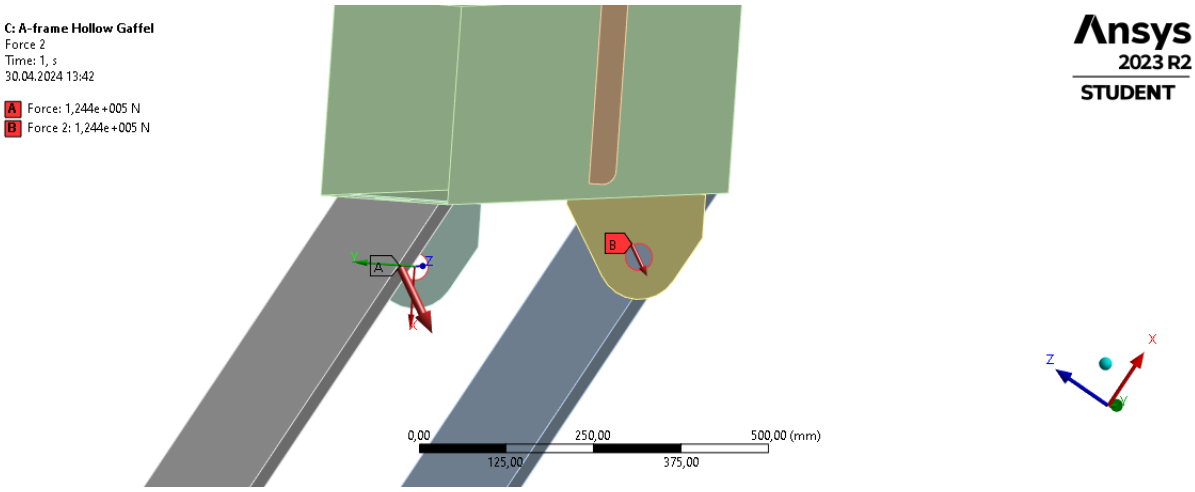

Figure 53 - Upper forces for simulation of A-frame.

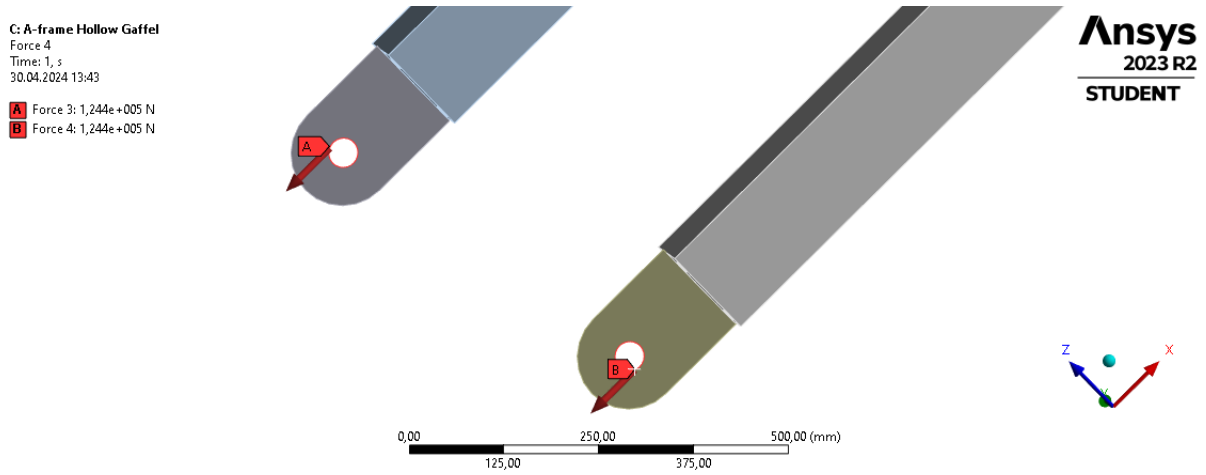

Figure 54 - Bottom forces for simulation of A-frame.

Figure 55 shows the von Mises stress results from the A-frame simulation. The maximum stress is concentrated around the main pad-eye, where the stiffeners will be placed. There are no stress concentrations elsewhere, and the stress looks otherwise well distributed. Even though the maximum stress is not completely accurate because of the lack of stiffeners, a stress of 217,72MPa is within the maximum allowable stress of 301,75MPa.

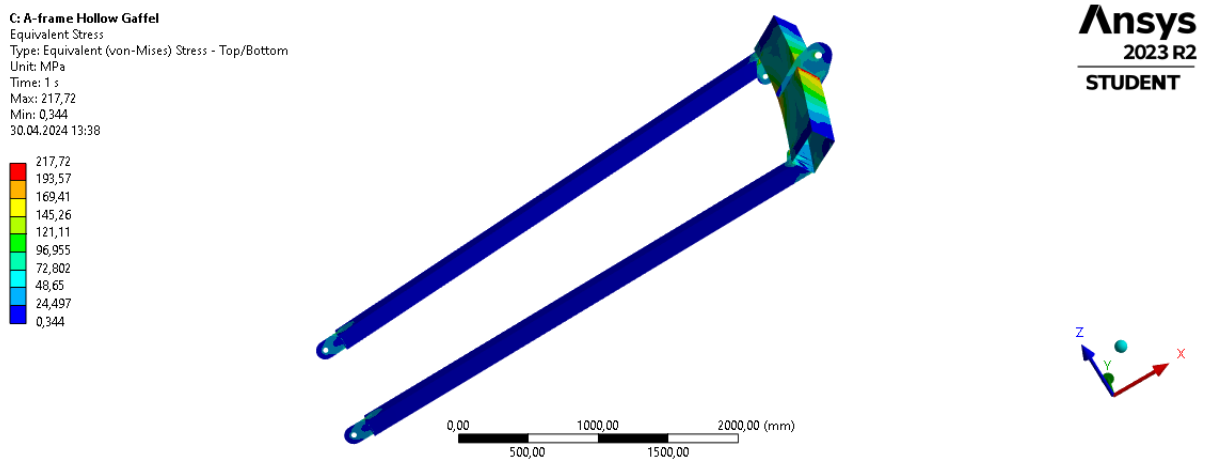

Figure 55 - Results from A-frame simulation.

A simulation of just the spreader beam was also initiated including the stiffeners shown in Figure 56, which would show a more realistic stress distribution for the spreader beam and the top pad-eye. To get a worst-case result for the beam, the ends in this simulation were fixed, and the force was the main pad-eye force of 324,4kN.

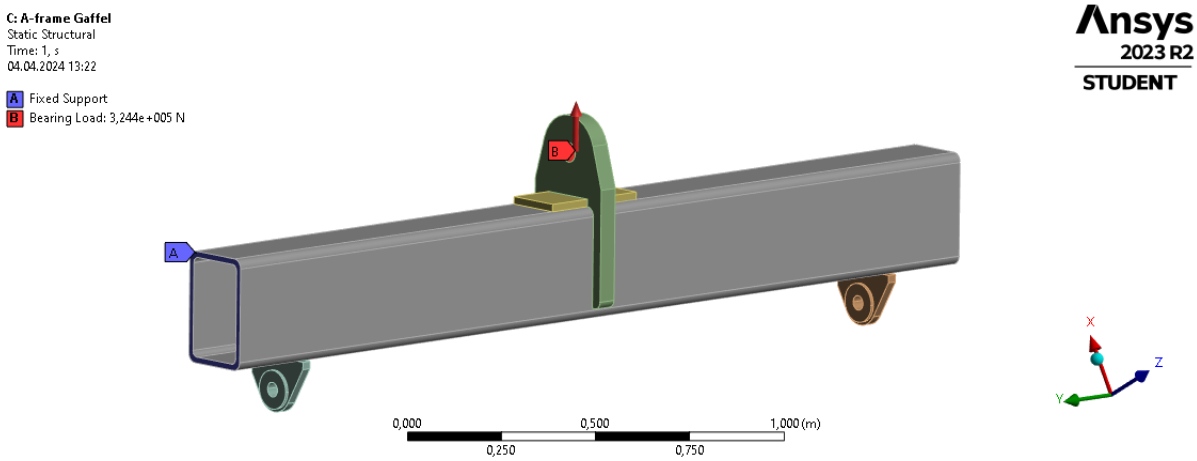

Figure 56 - Force and constraint for spreader beam simulation.

The von Mises stress results from the simulation of the spreader beam are displayed in Figure 57. With the stiffeners added, the maximum stress is inside the hole of the pad-eye. The stress on the rest of the beam is distributed better, and the effect of the stiffeners is good. The maximum stress of 183,24MPa is lower than the maximum allowable stress of 301,75MPa. The deformation is shown in Figure 58.

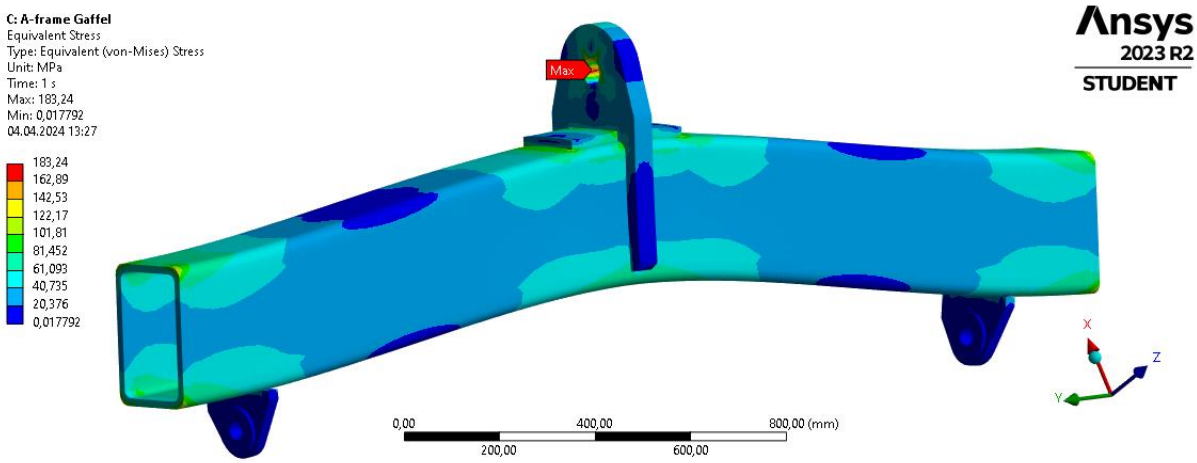

Figure 57 - Spreader beam simulation results.

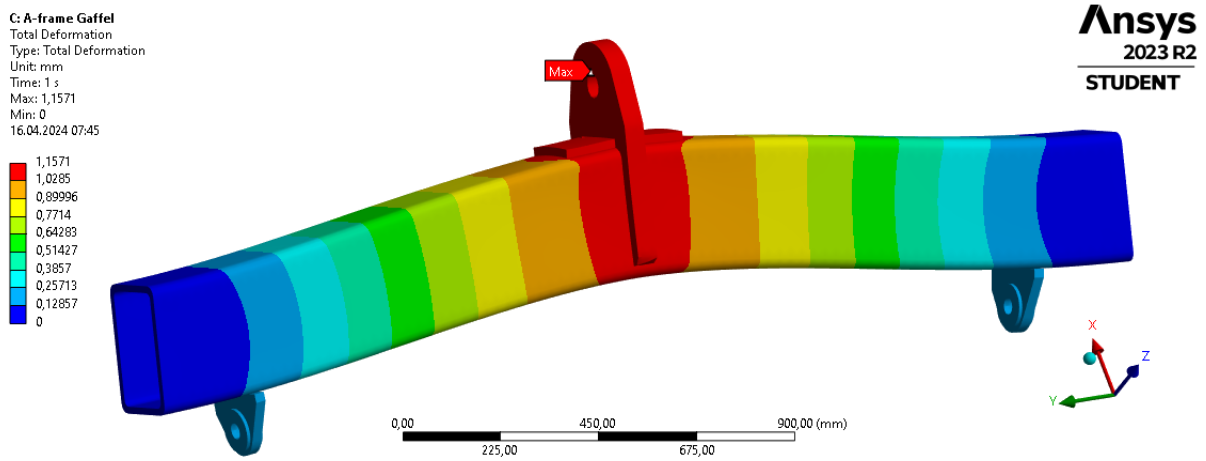

Figure 58 - Deformation for the spreader beam.

4.2.6. Weld Calculations

The values obtained from the node analysis, necessary for calculating the equivalent stresses in the welds, are in Supplementary Table 7. This section includes the calculations for the longitudinal A-frame beams intended for welding to the spreader bar. Following a similar approach as the basket, the final summary of the welding application is presented in chapter 4.1.5.

SHS140 weld calculations:

$$\sigma_b = \frac{\mathrm{M_{Ed,x}}}{\sqrt{2}\cdot \mathrm{W_{el,x}}} + \frac{\mathrm{M_{Ed,z}}}{\sqrt{2}\cdot \mathrm{W}_{el,z}} = \frac{(1.7\cdot 10^6 + 164\cdot 10^3)\,\mathrm{Nmm}}{\sqrt{2}\cdot 236{,}10\cdot 10^3\,\mathrm{mm^3}} = 5{,}60 MPa$$

$$\tau_b = \sigma_b$$

$$\tau_{\parallel,x} = \frac{\mathrm{V_{Ed,x}}}{2\cdot a\cdot \mathrm{l}_{weld,z}} = \frac{109{,}621\cdot 10^3\,\mathrm{N}}{2(5\cdot 150)\,\mathrm{mm^2}} = 73 MPa$$

$$\tau_{\parallel,z} = \frac{\mathrm{V_{Ed,z}}}{2\cdot a\cdot \mathrm{l}_{weld,x}} = \frac{2{,}389\cdot 10^3\,\mathrm{N}}{2(5\cdot 150)\,\mathrm{mm^2}} = 1{,}60 MPa\,,$$

$$\tau_{\parallel} = \tau_{\parallel,x} + \tau_{\parallel,z}$$

$$\sigma_{\perp} = \frac{\mathrm{N_{Ed}}}{\sqrt{2}\cdot \mathrm{A}} = \frac{923\,\mathrm{N}}{\sqrt{2}\cdot 6207\,\mathrm{mm^2}} = 0{,}10 MPa$$

$$\tau_{\perp} = \sigma_{\perp}$$

$$\sigma_{eq} = \sqrt{\left(\sigma_{\perp} + \sigma_b\right)^2 + 3\left(\left(\tau_{\perp} + \tau_b\right)^2 + \left(\tau_{\parallel}\right)^2\right)} = \sqrt{\left(0{,}10 + 5{,}60\right)^2 + 3\left(\left(0{,}10 + 5{,}60\right)^2 + \left(73 + 1{,}60\right)^2\right)}$$

$$\sigma_{eq} = 130 MPa$$

4.3. Extra Weight

4.3.1. Choice Of Design

The extra weight is constructed with the same outer dimensions as the subsea basket. This minimizes the flow restrictions through the construction, as mentioned earlier. As shown in Figure 59, the extra weight is fitted with ISO corners for sea fastening and transportation, connection points for tooling inside the basket, and forklift pockets.

The beam elements used are made from S355J2 steel plates because this is the only option available on the market. Lower-strength steel would have been acceptable, as the assembly is constructed of solid elements with abundant strength. For assembly purposes, when connecting the extra weight to the basket, the steel plates are cut to the same width as the lower beam elements on the basket (200mm). The only relevant thicknesses available are 200mm and 250mm.

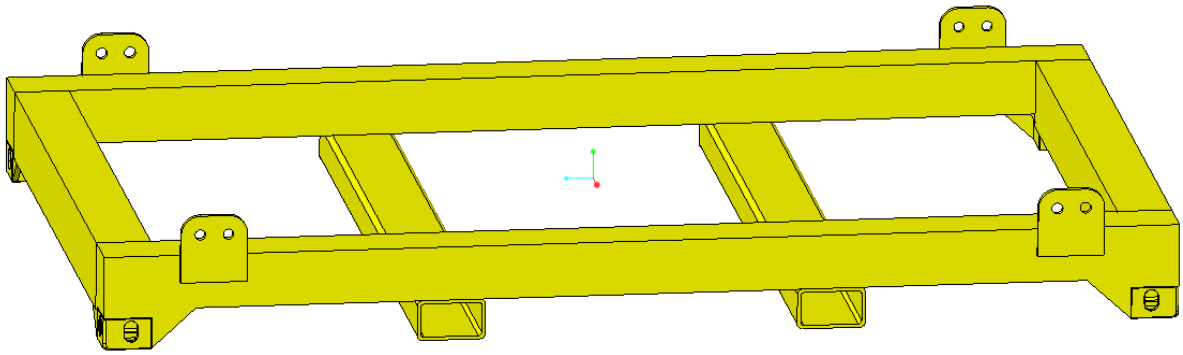

Figure 59 - Extra weight design.

4.3.2. Weight

The desired weight of the extra weight is approximately 4,54 tons. 200x200 and 250x200 rectangular profiles, bolted plates, iso corners, and forklift pockets sum up to a total weight of 4,58 tons, as shown in Figure 60. This is an acceptable weight given the estimated desired weight of 4,54 tons. The weight value is found using Creo Parametric with a material density of 7860$^{kg}/_{m^3}$.

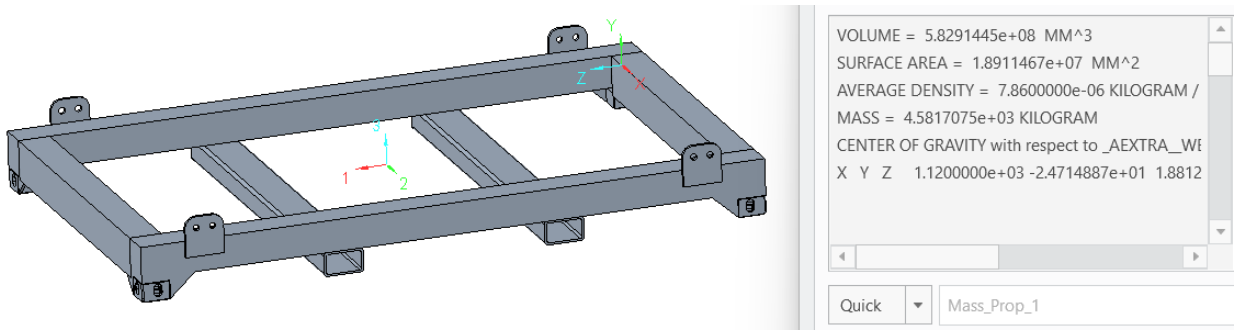

Figure 60 - Mass of extra weight structure.

The extra weight could also be designed using reinforced concrete. However, this would result in a density of 2500 $^{kg}/_{m^3}$, which would require 3,14 times the volume. As the aim is to keep the surface area to a limit, the more expensive option (J355S2 steel plates) was chosen for the design.

4.3.3. Bolted Joints

The extra weight is connected to the basket using bolted joints. This is an effective, cheap, and easy-to-maintain option. The bolt plates are designed to be as short as practical to reduce bending stresses on bolt plates. This is obtained by adding plates/stiffeners parallel to the H-beam of the basket. A bolted joint is located in each corner of the construction, resulting in a symmetrical and evenly distributed load on each joint. The bolt diameter is designed to withstand the shear forces created by the weight load of the extra weight. The bolted connection is illustrated in Figure 61, where the extra weight is colored green, and the basket is colored yellow.

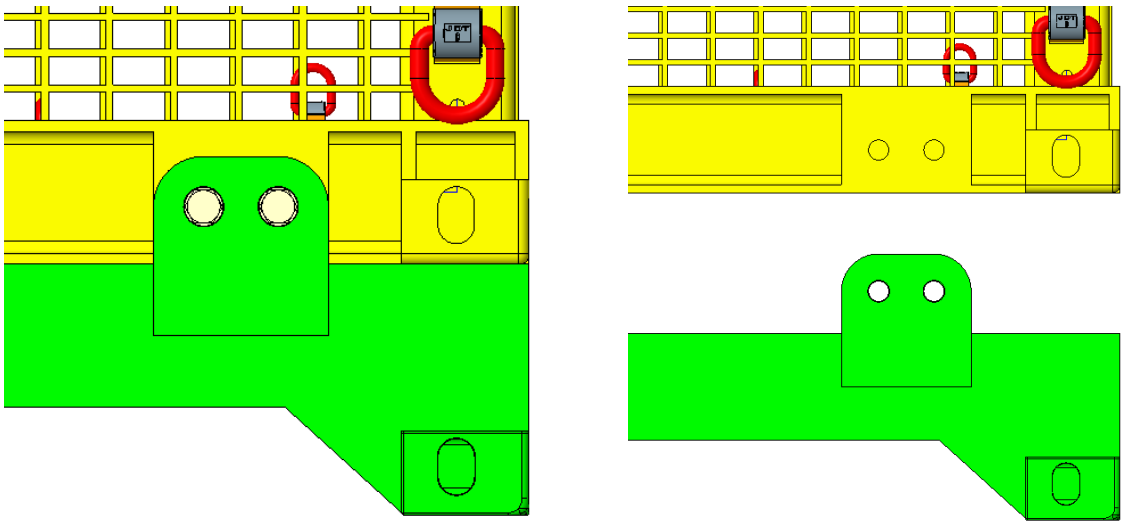

Figure 61 - Bolted joint connection.

Bolted Joint Calculations

Plates and holes

The number of connection points is kept to a minimum to make the assembly of the extra weight to the basket simple. Four connection points are used in total, with a pair of bolts in each connection. To make things easier, oversized round holes are used. According to Eurocode 3, the minimum load-bearing capacity per mm of connected plate thickness for S355 steel is 19,6 kN/mm [18]. For 20mm steel plates, this results in 392kN. Assuming a worst case where the load is carried by only one out of the two bolts in each bolted connection, the largest possible load is 49kN. The bearing capacity of 392kN is therefore considered to be more than adequate for this design.

Bolt Calculations

The bolted connection is mainly loaded with shear forces and is categorized accordingly. For assembly purposes, there is a distance tolerance between the two bolted plates. Because of this gap, an accurate preload calculation is not possible. The bolted connection is categorized as a bearing type [14, Ch. 3.4.1]. Therefore, the design's ultimate shear load shall not exceed the design shear resistance.

Hole Positioning

The locations of the bolt holes concerning the plate edges and the center distances, as illustrated in Supplementary Figure 1, are within the limits stated in Supplementary Table 3. The maximum values are calculated assuming the steel is exposed to weather or other corrosive conditions. The equations listed

below show the respective values. All the dimensions used in the design are within the given values, as shown in the calculations below.

$$e_{1,min} = 1,2 \cdot d_0 = 1,2 \cdot 38mm = 45,6mm$$
$$e_{1,max} = 4 \cdot t + 40mm = 4 \cdot 20mm + 40mm = 120mm$$

$$e_{2,min} = 1,2 \cdot d_0 = 1,2 \cdot 38mm = 45,6mm$$
$$e_{2,max} = 4 \cdot t + 40mm = 4 \cdot 20mm + 40mm = 120mm$$

$$p_{2,min} = 2,4 \cdot d_0 = 2,4 \cdot 38mm = 91,2mm$$
$$p_{2,max} = 14t = 14 \cdot 20mm = 280mm$$

Shear resistance for individual screw:

A reduction factor is added to the shear resistance because the total thickness of the bolted plates is greater than 1/3 of the nominal diameter of the [14, Ch. 3.6.1].

$$\beta_p = \frac{9d}{8d + 3t_p} = \frac{9 \cdot 30mm}{8 \cdot 30mm + 3 \cdot 40mm} = \frac{3}{4}$$

where

d: *nominal diameter of bolt* ($d = 30mm$)

t_p: *total thickness of plated* ($t_p = 40mm$)

$$F_{v,Rd} = \frac{\alpha_v \cdot f_{ub} \cdot A}{\gamma_{M2}} = \frac{0,6 \cdot 800\ MPa \cdot A}{0,3} \geq F_{v,Ed} = 49kN$$

where

α_v: *cross area factor for* 8.8 *through the unthreaded portion* ($\alpha_v = 0,6$ (*table* 3.4))

f_{ub}: *ultimate tensile strength for* 8.8 *bolts* ($f_{ub} = 800\ MPa$)

A: *crossection of the bolt*

γ_{M2}: *partial factor for resistance of cross sections in tension* ($\gamma_{M2} = 1,25$)

$F_{v,Ed}$: *design ultimate shear load* ($F_{v,Ed} = 49kN$)

$$\frac{\alpha_v \cdot f_{ub} \cdot A}{\gamma_{M2}} \cdot \beta_p \geq 49kN \quad \rightarrow \quad d \geq \sqrt{\frac{49kN \cdot \gamma_{M2} \cdot 4}{\alpha_v \cdot f_{ub} \cdot \pi \cdot \beta_p}} = \sqrt{\frac{49kN \cdot 1,25 \cdot 4}{0,6 \cdot 800MPa \cdot \pi \cdot 3/4}} = 14.72mm$$

Bolt and Hole Design

M30 bolts are used in the design. Oversized round holes for M30 bolts have a diameter of 38mm [14, Ch. 3.6.1]. As a redundancy, two bolts are used in each corner. If a bolt connection should fail, a second bolt will hold the load. Safety pins are added in the threaded section to prevent the bolts from being unscrewed. The bolt is designed so that the threaded section is not included in the shear plane. According to Eurocode 3, the length of the threaded section, which is included in the bearing, shall not exceed 1/3 of the thickness of the respective plate, as illustrated in Figure 62.

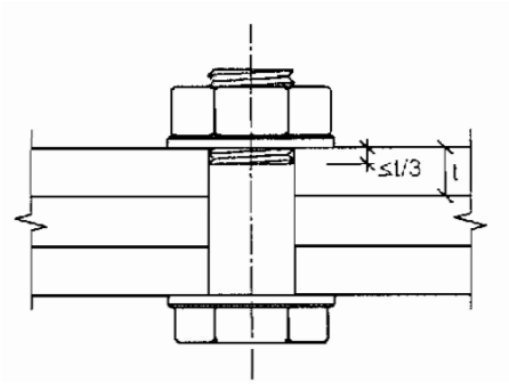

Figure 62 - Length of bearing part of the threaded portion. [14, Ch. 3.6.1]

Every bolted connection is provided with washers both for the nut and the bolt head.

Assembly

Preloading is not required in the bolted connections. However, the same torque as for preloaded connections can be used in the assembly to prevent overtightening of the bolts.

$$F_{p,Cd} = \frac{0,7 \cdot f_{ub} \cdot A_s}{\gamma_{M7}} = \frac{0,7 \cdot 800MPa \cdot 561mm^2}{1,1} = 285,6kN$$

where

$F_{p,Cd}$: *design preload*

A_s: *stress area of the threaded part* $\left(A_s = 561mm^2\right)$

γ_{M7}: *saf ety f actor f or preload of high strength bolts* $\left(\gamma_{M7} = 1,1\right)$

Recommended torque

The torque needed for the tightening of the bolts is made up of the moments needed to overcome the friction in the screwed-in thread, and the friction between the bolt head/nut and the steel plates [19, p. 533]. As shown in the calculations below, the tightening torque is 1379,4Nm. The calculations below are based on the approach of [19].

$$M_A = M_G + M_K = F_{p,Cd}\left(0,16P + 0,58 \cdot d_2 \cdot \mu_{Gmin} + \frac{D_{Km}}{2} \cdot \mu_K\right)$$

$$= 285,6kN\left(0,16 \cdot 3,5mm + 0,58 \cdot 27,727mm \cdot 0,12 + \frac{39mm}{2} \cdot 0,12\right)$$

$$= 1379,4Nm$$

where

M_A: *tightening torque*

M_G: *friction moment in the screwed in thread section*

M_K: *friction moment in the contact area between the bolt head and the steel plate.*

d_2: *pitch diameter of thread* $\left(d_2 = 27,727mm\right)$

P: *thread pitch* $(P = 3,5mm)$

μ_{Gmin}: *smallest coefficient of friction in threads. Values are found in tables for electrolytically galvanized dry bolts and nuts* $\left(\mu_{Gmin} = 0,12\right)$

D_{Km}: *mean bearing diameter for the bolts or nuts* $\left(D_{Km} = 1,3 \cdot d = 39mm\right)$

μ_K: *coefficient of friction* $\left(\mu_K = 0,12\right)$

4.3.4. FEM Simulations

The extra weight is made of strong solid beams that will withstand the stresses that occur during the operations it will be used for. However, the lifting points must be strong enough to hold a weight of 4,5 tons. To simulate this, the $LL_{extraWeight}$ load of 49kN mentioned in chapter 3.4.3, was used. This was added to every lifting point, as shown in Figure 63. Fixed support was added under every corner, presented in Figure 64.

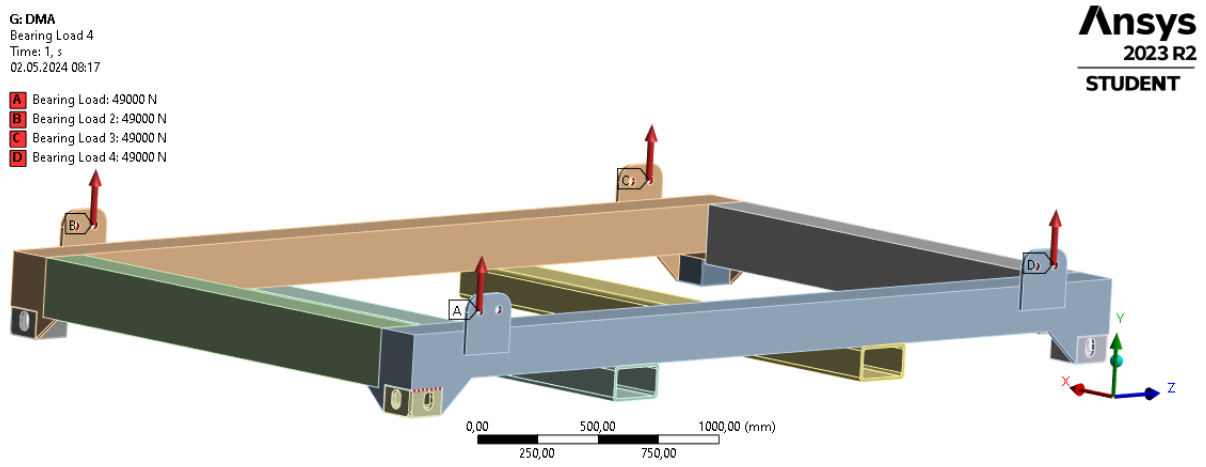

Figure 63 - Extra weight simulation forces.

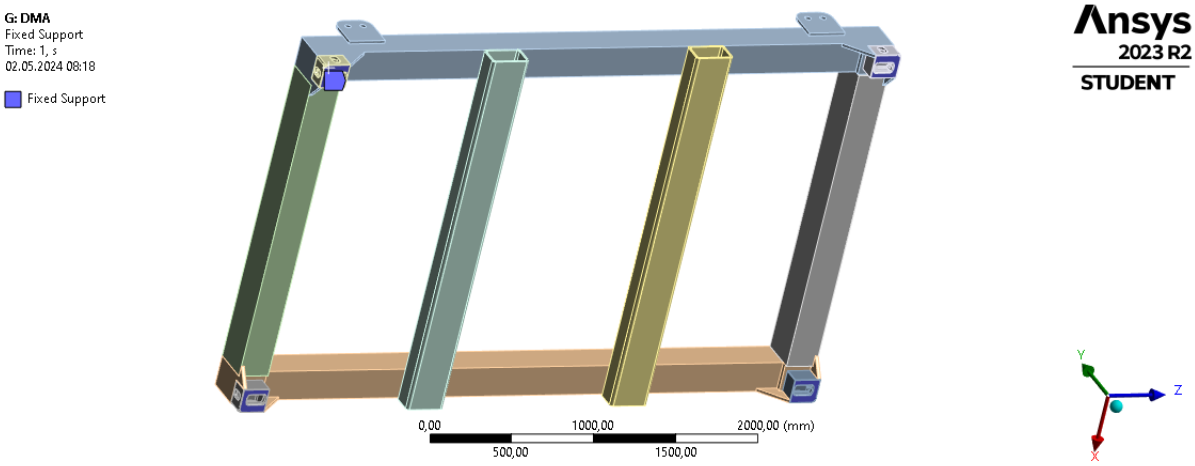

Figure 64 - Extra weight fixed support.

The von Mises stress results from the simulation are presented in Figure 65. As mentioned, the extra weight is designed using solid beam elements. The stress values in the entire extra-weight structure are low, with a maximum value of 122,99MPa found in the connected plate regions and the ISO corners. These values are well under the 301,75MPa max allowed stress. The maximum stress occurs on the bottom of one of the corner stiffeners and looks like a singularity occurrence, as seen in Figure 66. Using fixed support does not give completely realistic results in this simulation. However, this gives an indication of what forces the lifting points are capable of withstanding. When evaluating the lifting point in Figure 67, the max stress is 38,68MPa. This was the maximum value of stress for all the lifting points.

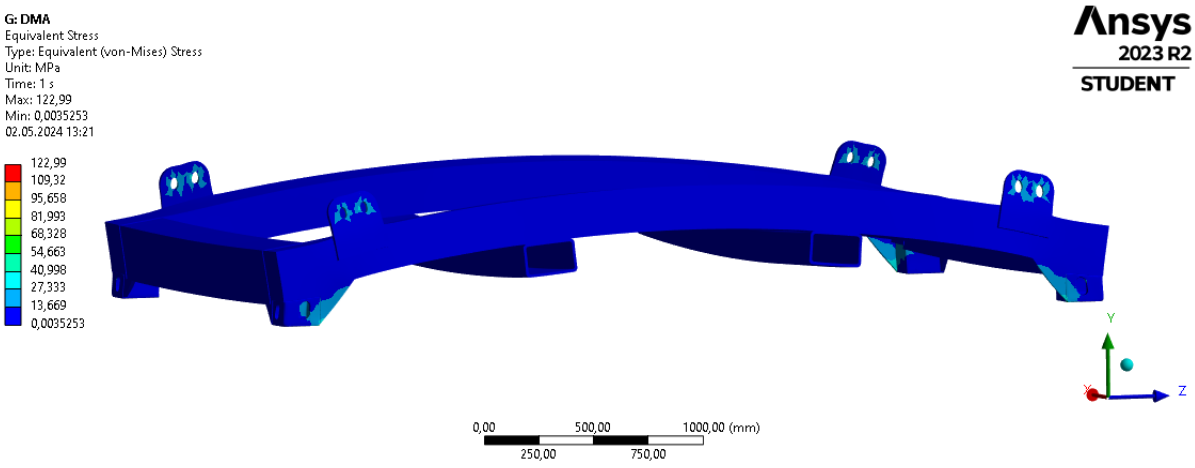

Figure 65 – von Mises stress result for extra weight.

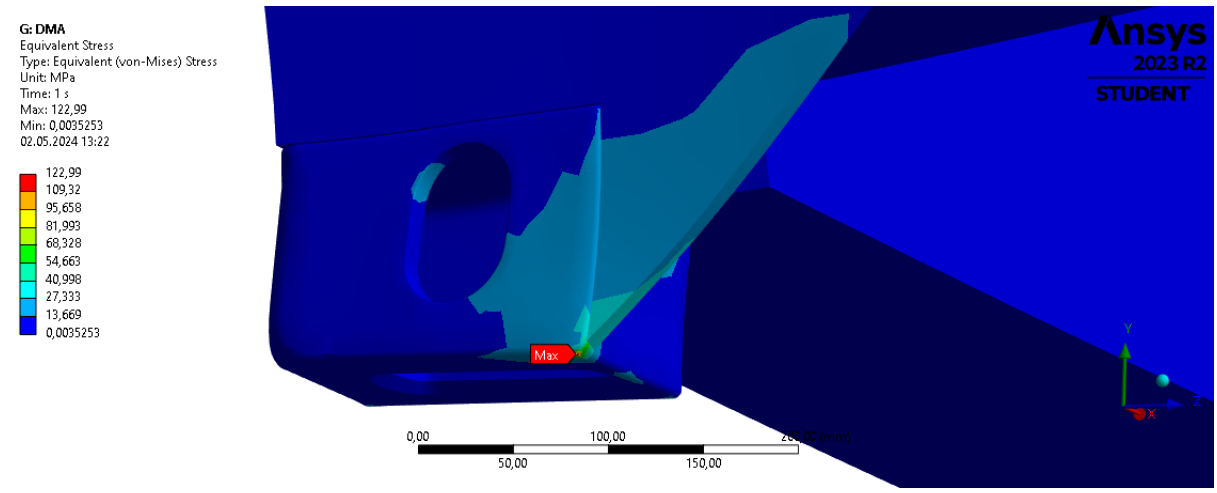

Figure 66 - Max stress value extra weight.

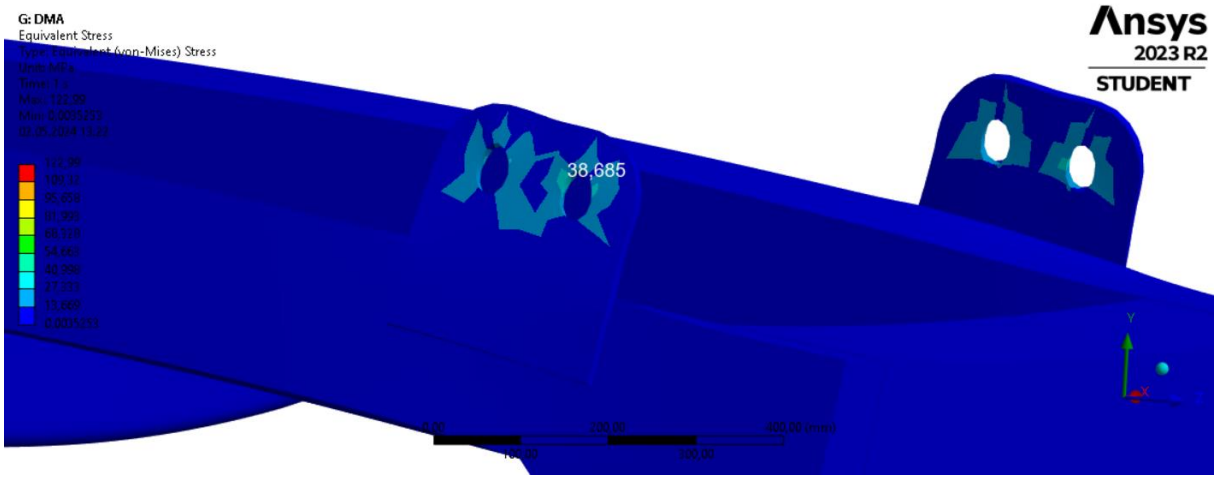

Figure 67 - Stress in lifting point on extra weight.

4.4. Pad-Eyes

4.4.1. General Geometric Criteria

The design of the pad-eyes shall have the following geometry criteria [7, Ch. 3.8.4]:

1. The main plate radius is not less than the pin hole diameter.
2. The pad-eye thickness (including the cheek plates) cannot exceed 75% of the inside width of a shackle. This criterion is also used when shear pins or bolts are used.

4.4.2. Hand Calculations

In the entire construction (basket with A-frame and the extra weight), a total of 7 different pad-eyes are used. All pad-eyes are designed using the tear-out and bearing formula listed below. Here, the pin diameter is designed to be equal to or larger than 94% of the pinhole diameter [7, Ch. A.3] [7, Ch. A.4]. The thickness value, t, is calculated using the highest value found in the bearing and tear-out pressure calculations below. Table 8 shows all the values for the different types of pad-eyes. Figure 68 shows the different pad-eyes and their respective number tags used for the project. The bolted plates of the extra weight are also included in the calculations.

Bearing pressure:

$$\sigma_e \geq 0,045 \cdot \sqrt{\frac{RSF \cdot E}{D_H \cdot t}} \quad \rightarrow \quad \left(\frac{\sigma_e}{0,045}\right)^2 \cdot \frac{D_H}{RSF \cdot E} \geq t$$

Tear out pressure:

$$\sigma_e \geq \frac{2 \cdot RSF}{\left(2 \cdot R_{pad} - D_H\right) \cdot t} \quad \rightarrow \quad t \geq \frac{2 \cdot RSF}{\left(2 \cdot R_{pad} - D_H\right) \cdot \sigma_e}$$

The rest of the pad-eyes are based on the diameter of the pins. These are established in the calculations below, with regards to a S355J2 solid steel shaft and a safety factor of 2.

A-frame pad-eye pins:

$$\sigma = \frac{RSF}{A} = \frac{RSF}{\frac{\pi \cdot d^2}{4}} \quad \rightarrow \quad d_{allowed} \geq \sqrt{\frac{RSF \cdot 4}{\sigma \cdot \pi}} = \sqrt{\frac{124,4\ kN \cdot 4}{177,5\ MPa \cdot \pi}} \approx 29,9mm$$

Table 8 - Results of pad-eye calculations.

	1	*2*	*3*	*4*	*5*	*6*
LL (kN)	324	124,4	124,4	67,2	124,4	109,7
Pin diameter	50	37	37	37	37	28
Hole diameter	53	39	39	39	39	30
Thickness (including cheeks)	50	41	41	25	41	25
Pad-eye radius	100	60	70	60	60	60
Max bearing stress	227,6	181,9	181,9	171,2	181,9	249,4
Max tear out stress	88,2	74,9	60	66,4	74,9	97,5

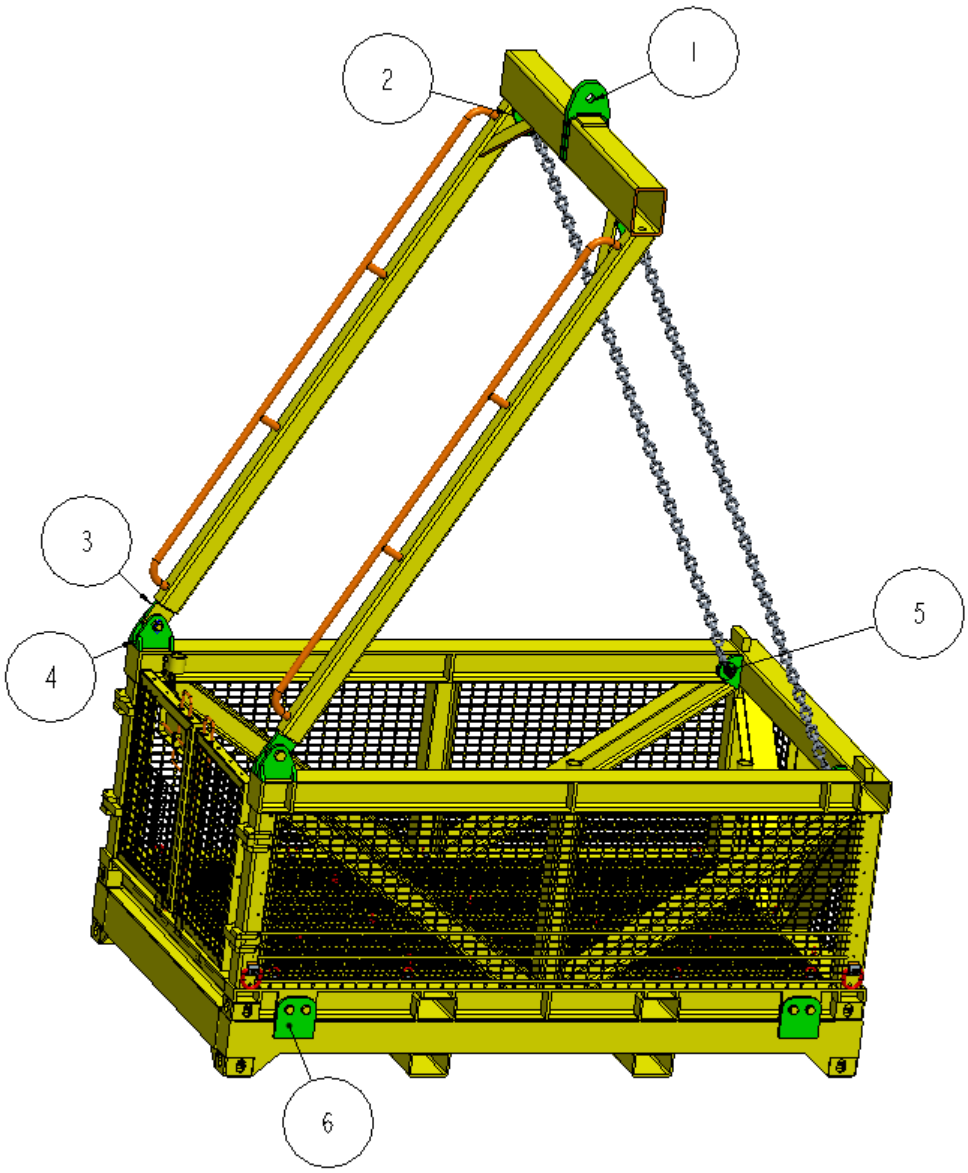

Figure 68 - Number tags for the location of different pad-eyes.

4.4.3. FEM Simulations

The number for each pad-eye from Figure 68 will be used in this chapter. Pad-eye no. 2 and no. 5 have the same dimensions but get different angles on the loads, which is why they have been given different numbers. The force used for every pad-eye except number 1, is the $LL_{AFrameSub}$ which was calculated in chapter 3.4.3.

Pad-eye No. 1

For the top pad-eye, the simulation was run together with the beam on which it is placed. The force of 324.4kN shown in Figure 69 is the LL_{main} from chapter 3.4.3. Fixed support at the ends of the spreader beam gave the needed constraints to evaluate the capabilities of this pad-eye as well as the beam.

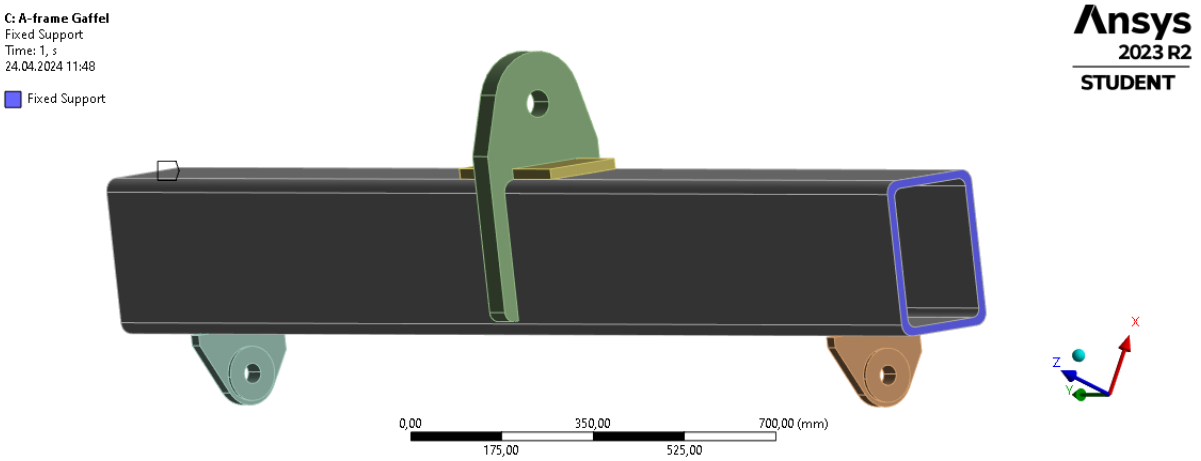

Figure 69 – Fixed support on both sides of the beam.

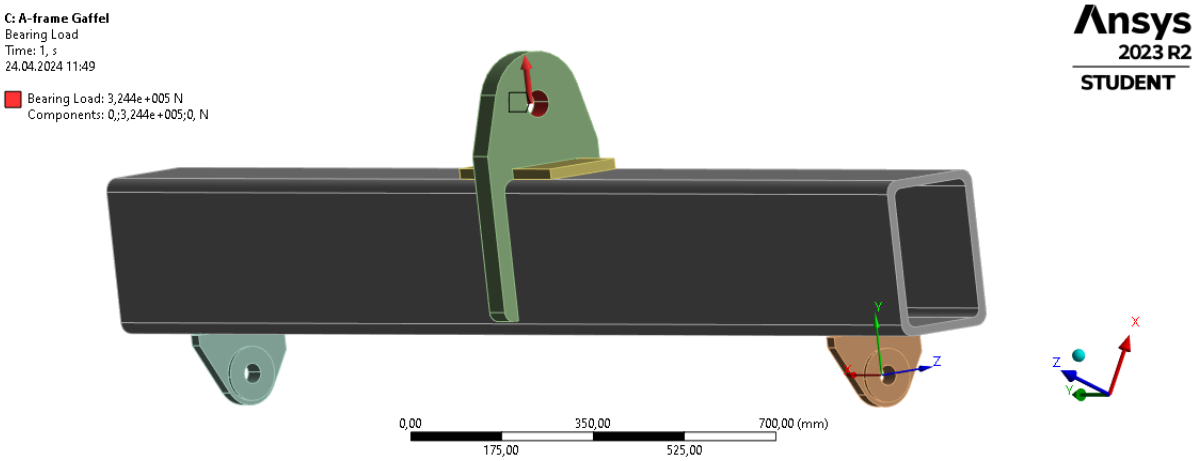

Figure 70 - Bearing load for pad-eye no. 1.

The von Mises stress result from the simulation is shown in Figure 71. There was some stress concentration inside the hole where the shackle should be placed, but this is higher than it would be realistically. The stress of 183,24MPa is however quite below the maximum allowed stress of 301,75MPa. The deformation is 1,157mm as illustrated in Figure 72, but given the length of the beam, this is not a high value.

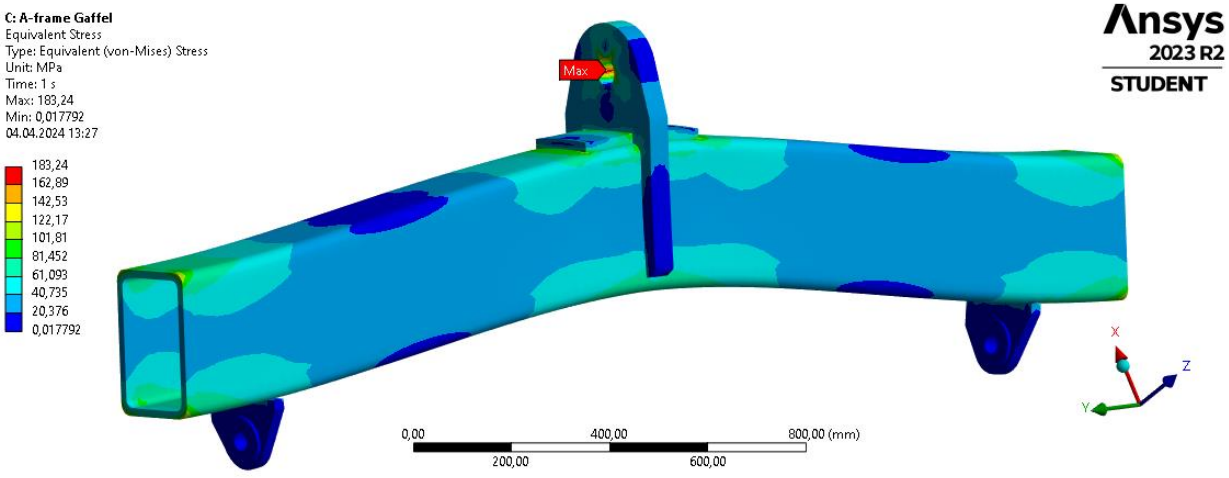

Figure 71 - Pad-eye no. 1 simulation result.

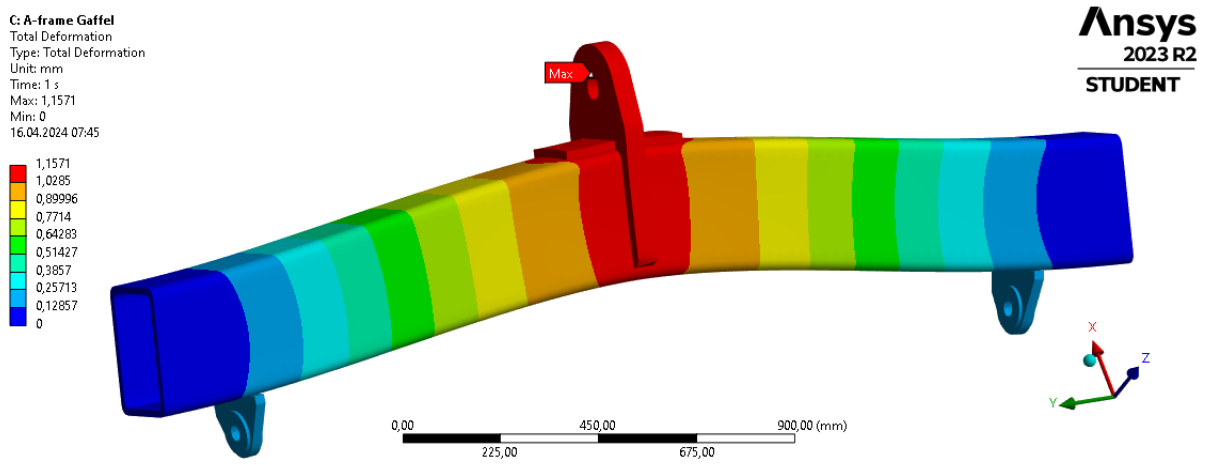

Figure 72 - Deformation for pad-eye no. 1.

Pad-eye No. 2

The force and constraint used in the simulation for pad-eye no. 2 were fixed support and a bearing force of 124,4kN, as shown in Figure 73 and Figure 74. The fixed support simulates the welded connection that the pad-eye has with the A-frame spreader beam. This pad-eye sits under the A-frame spreader beam, and Figure 73 shows how it is oriented in a lifting scenario.

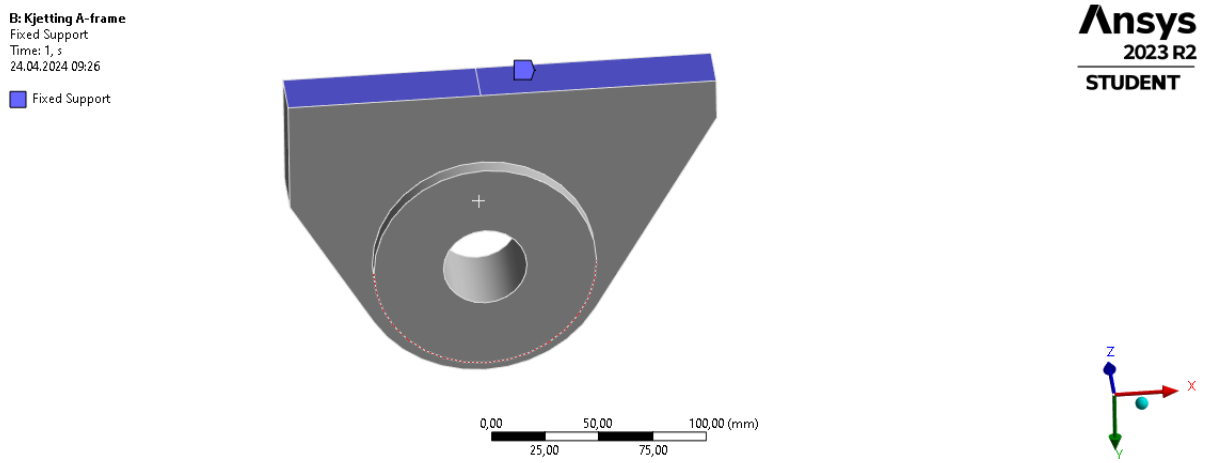

Figure 73 - Fixed support for pad-eye no. 2.

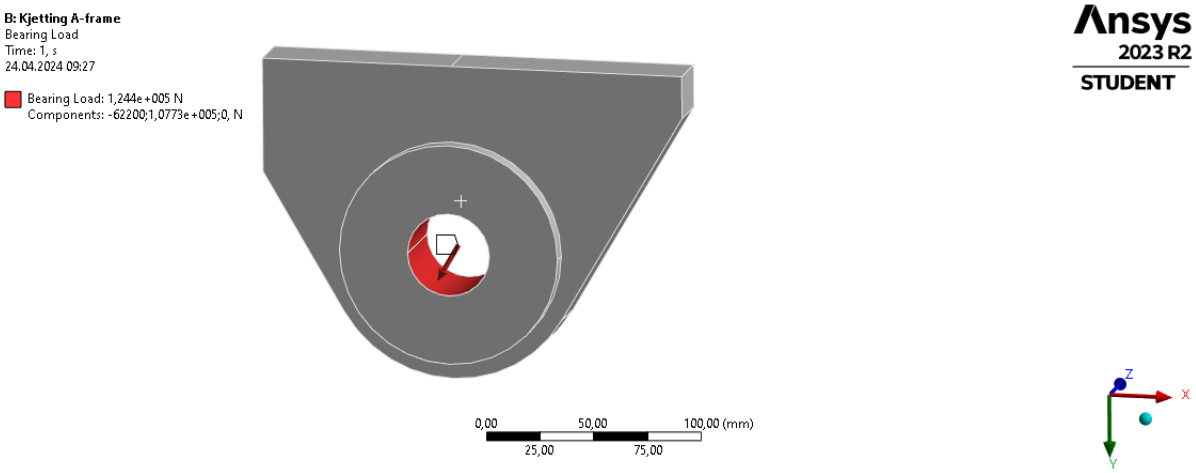

Figure 74 - Bearing load for pad-eye no. 2

Figure 75 shows the von Mises stress results for pad-eye no. 2. The stress of 130,35MPa is much lower than the maximum allowable stress of 301,75MPa, which shows that this pad-eye will hold the forces that can occur. The deformation is not significant, as shown in Figure 76.

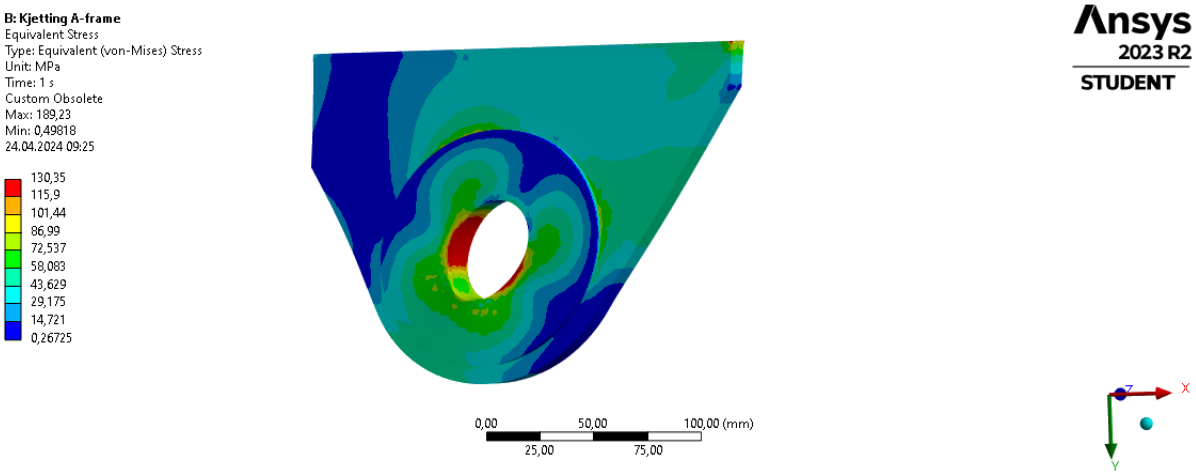

Figure 75 - Pad-eye no. 2 simulation result.

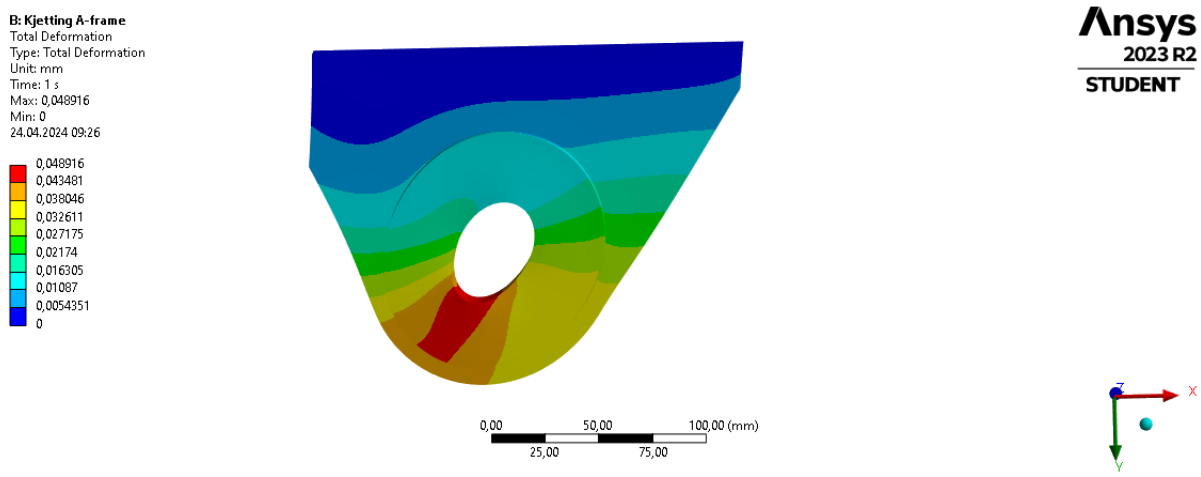

Figure 76 - Deformation for pad-eye no. 2.

Pad-eye No. 3

Figure 77 shows the fixed support used for the pad-eye no. 3 simulations, while Figure 78 shows the bearing load. These are the same as for pad-eye no. 2, but the force for this one is normal to the bottom of the pad-eye. This pad-eye is welded to the end of the side beams of the A-frame.

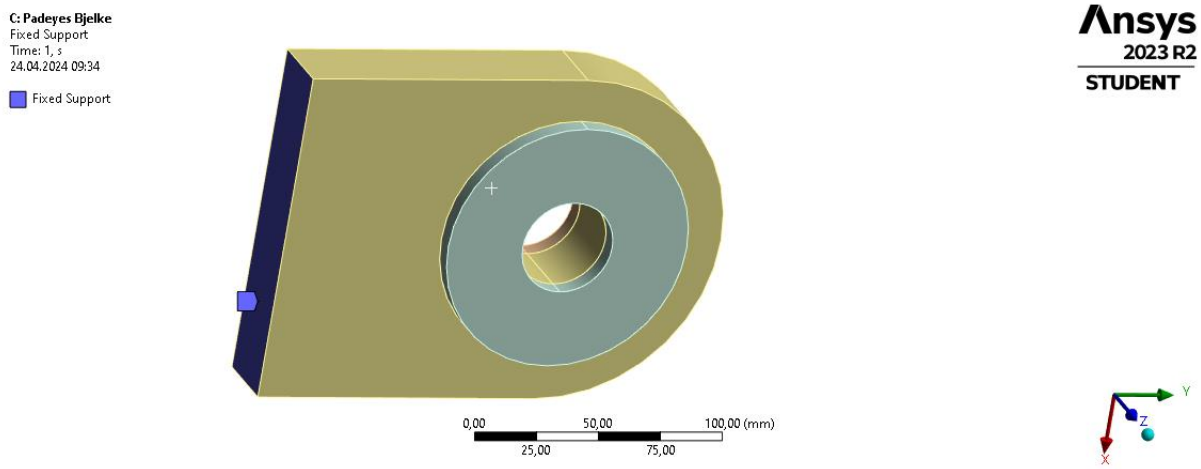

Figure 77 – Fixed support for pad-eye no. 3.

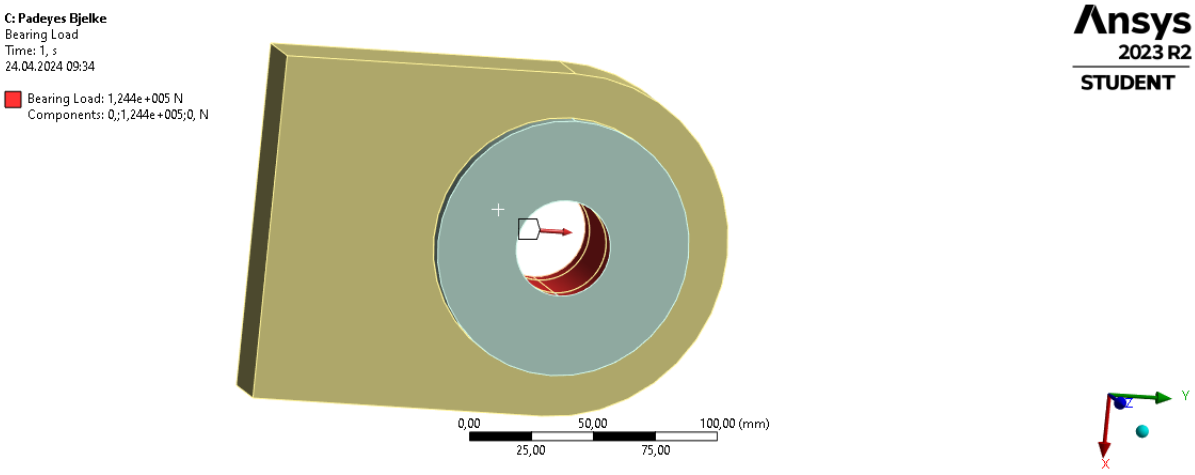

Figure 78 - Bearing load for pad-eye no. 3.

Figure 79 shows the von Mises results from the simulation of pad-eye no. 3. The maximum stress value occurred inside the hole on each side. Other than this, there were no high stress concentrations. The maximum stress of 153,97MPa was within the maximum allowable stress of 301,75MPa. The deformation of this pad-eye was also not significant, as shown in Figure 80.

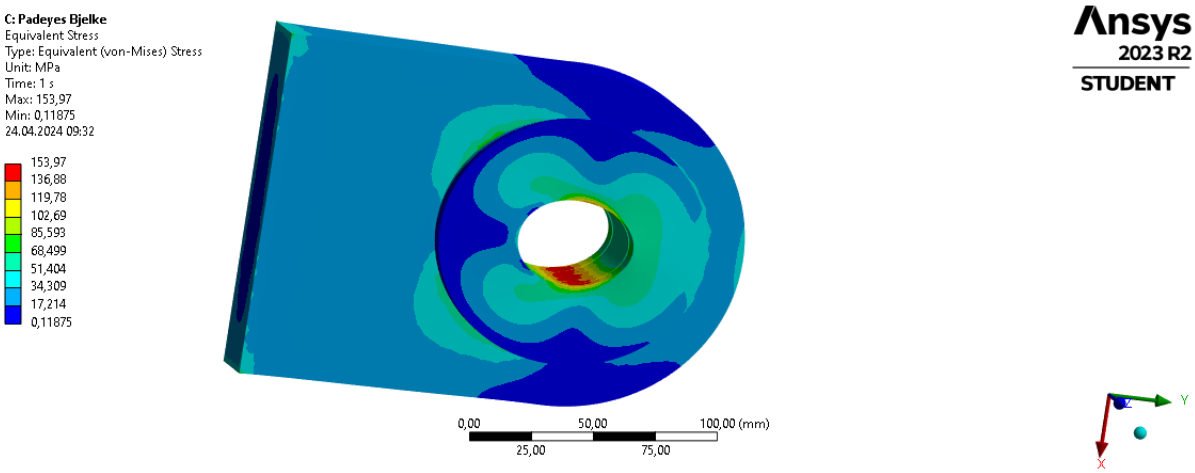

Figure 79 - Pad-eye no. 3 simulation results.

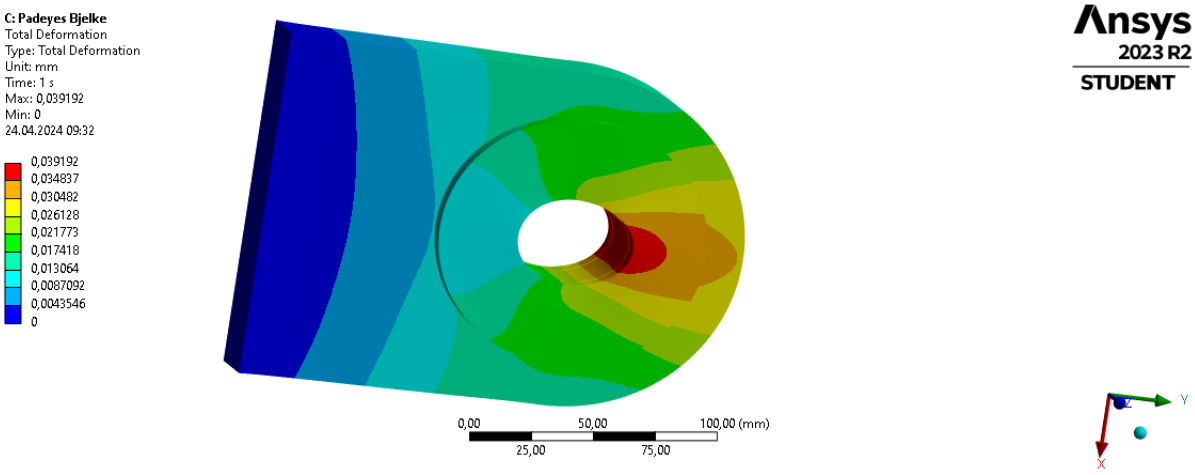

Figure 80 - Deformation of pad-eye no. 3.

Pad-eye No. 4

The fixed support used in the simulation for pad-eye no. 4 is shown in Figure 81, while the bearing load is shown in Figure 82. There are 4 of these pad-eyes, one on each side of the beam. Since there are two on each side of the basket, the force in the pad-eyes was divided by 2, giving 62,2kN. The force was applied with a 60-degree angle to simulate the A-frame. The fixed support simulated the welded contact point.

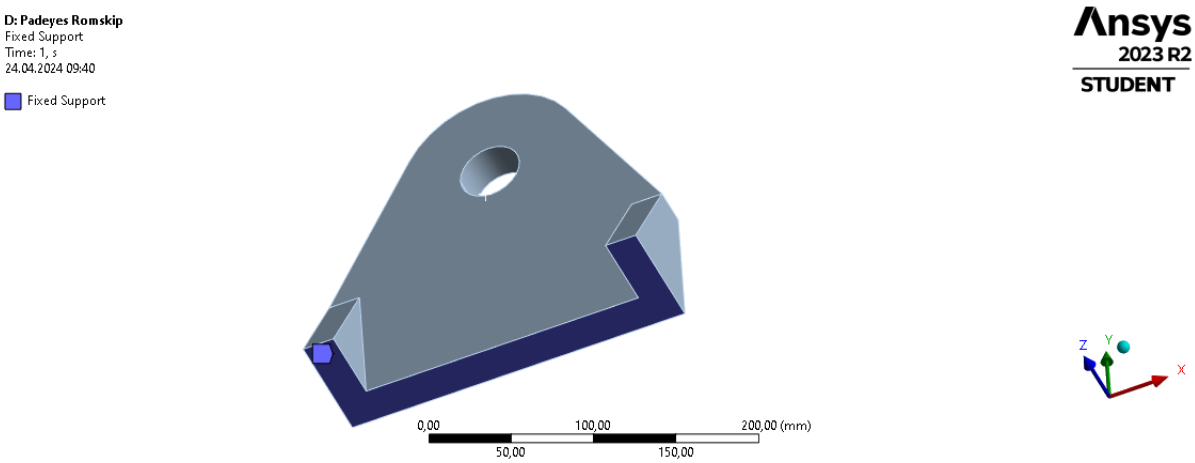

Figure 81 – Fixed support for pad-eye no. 4.

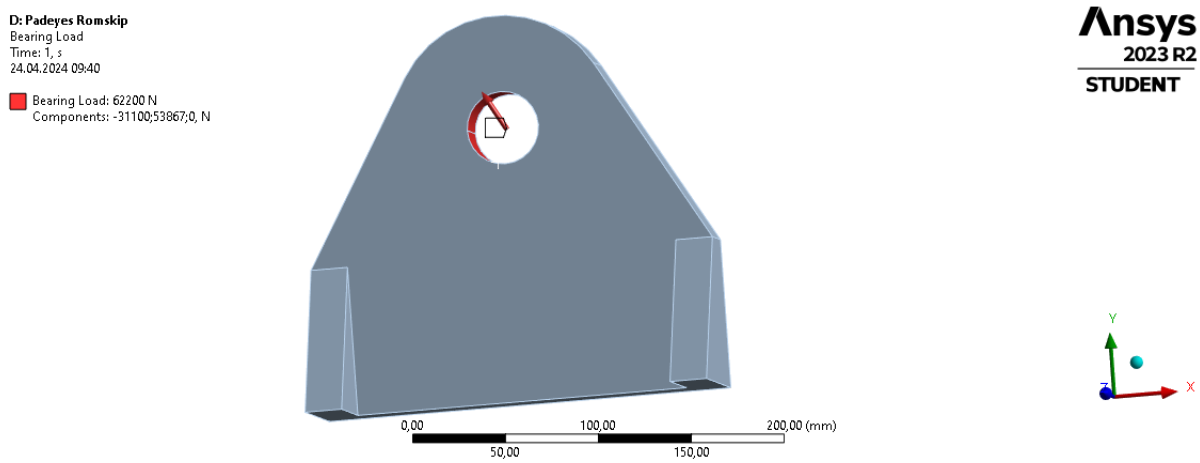

Figure 82 - Bearing load for pad-eye no.4.

For pad-eye no. 4, the maximum stress of 146,97MPa was a good margin below the maximum allowable stress of 301,75MPa. The von Mises stress results are displayed in Figure 83, and the deformation is minimal, as shown in Figure 84.

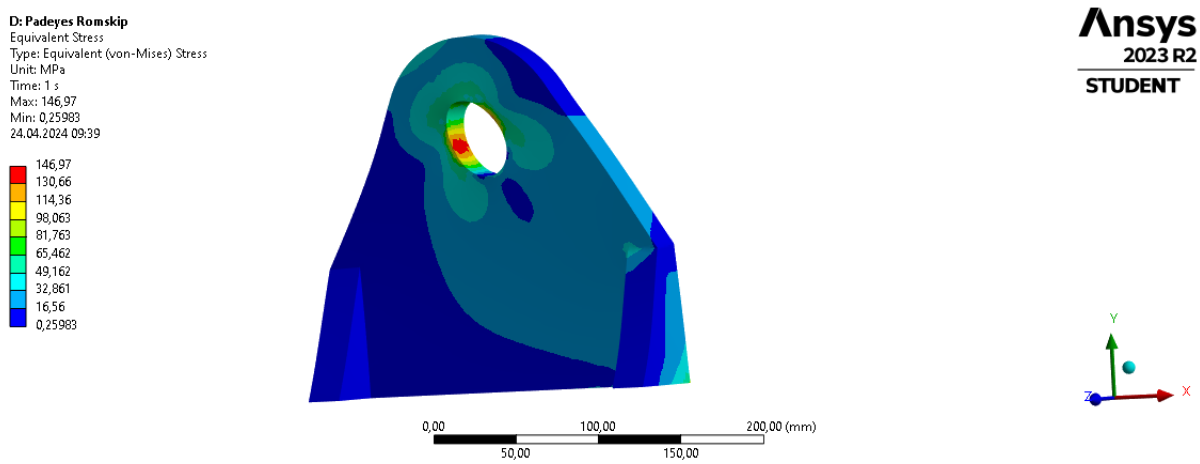

Figure 83 - Pad-eye no. 4 simulation results.

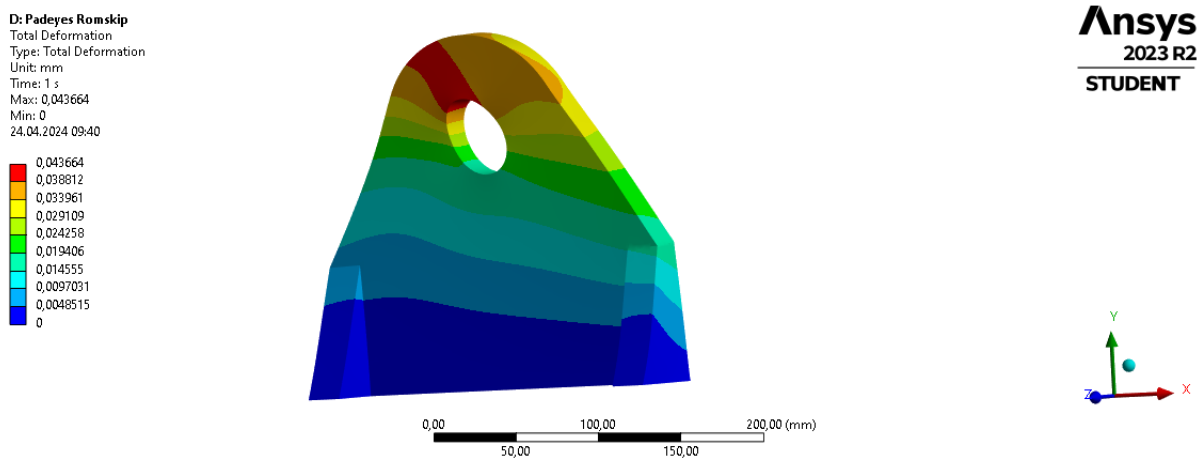

Figure 84 - Deformation for pad-eye no. 4.

Pad-eye No. 5

Figure 85 shows the fixed support for pad-eye no. 5, representing the welded connection. The orientation shows how the pad-eye sits on the hollow section at the back of the basket. The load used in the simulation is a bearing load, which is shown in Figure 86, with a value of 124,4kN in the direction of the A-frame.

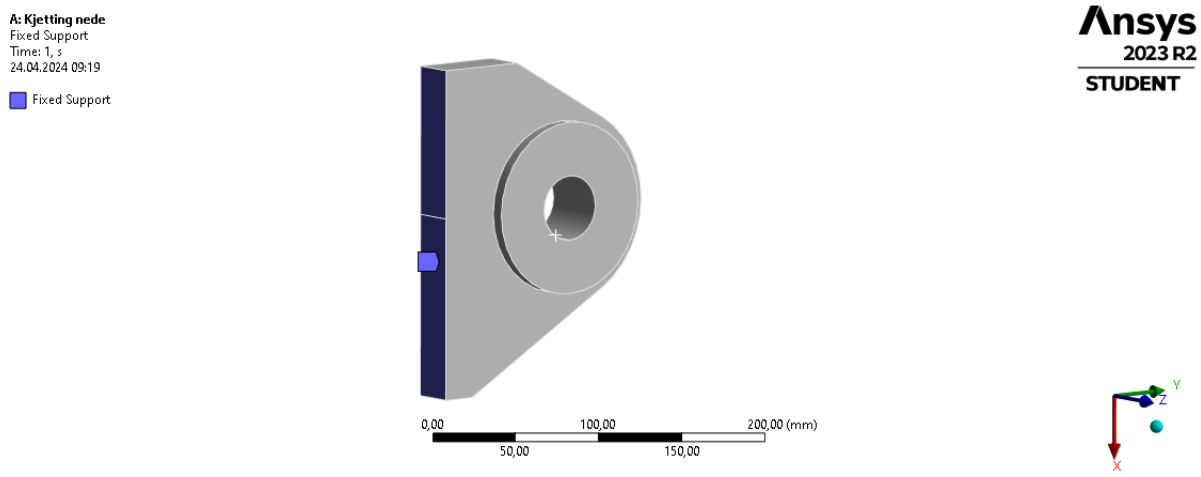

Figure 85 - Force and constraint for pad-eye no. 5.

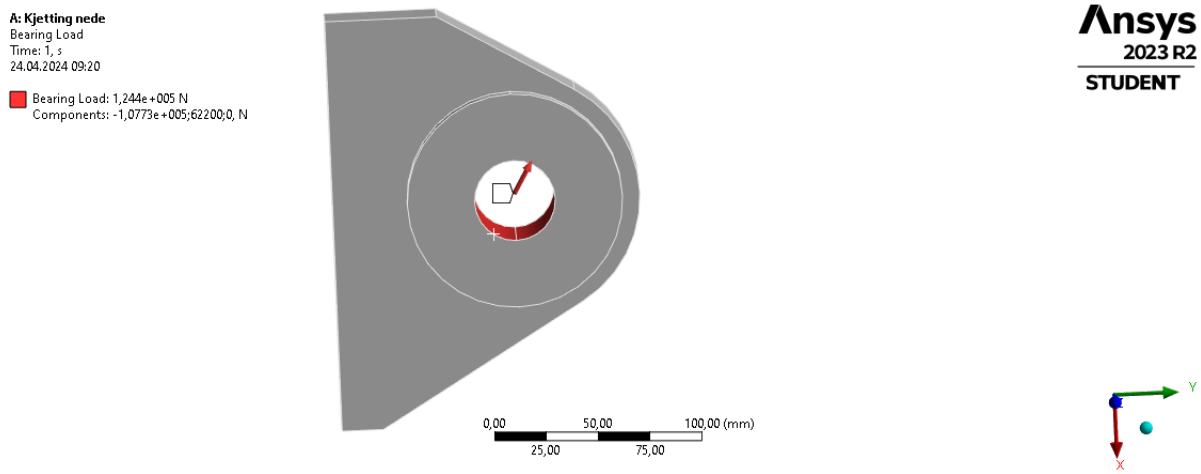

Figure 86 - Bearing load for pad-eye no. 5.

Figure 87 shows the von Mises stress results for the simulation of pad-eye no. 5. The maximum stress of 209,95MPa is below the maximum allowable stress of 301,75MPa, and the deformation is minimal, as shown in Figure 88.

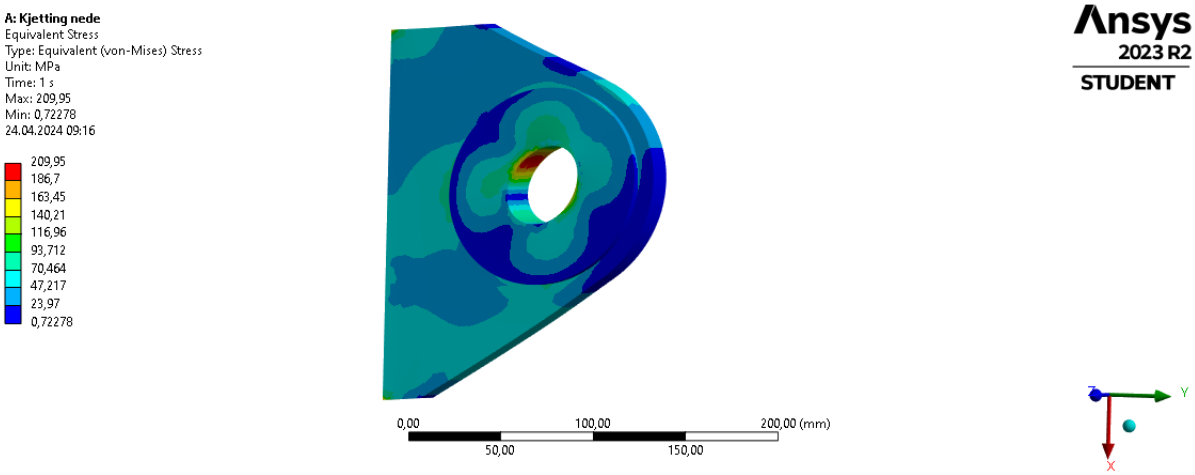

Figure 87 - Pad-eye no. 5 simulation results.

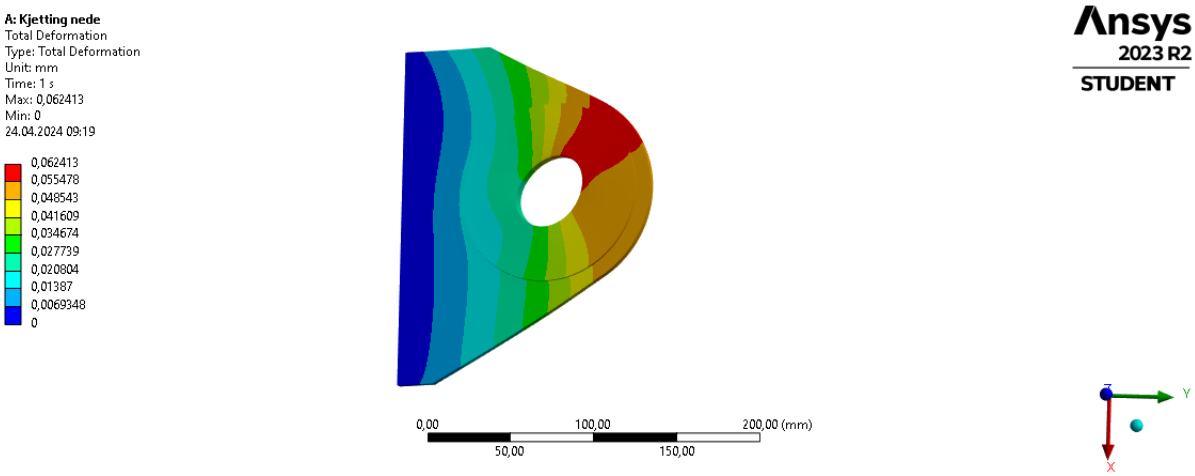

Figure 88 - Deformation for pad-eye no. 5.

4.4.4. Welds

The pad-eyes are welded according to DNV standards, with full penetration T-butt welds [7, Ch. 3.2.4]. The chamfer on the pad-eyes is designed to leave a gap of less than 1/5 of the pad-eye thickness, and the sum of the a-values found on each side of the pad-eye shall not be less than the thickness of the pad-eye as illustrated in Figure 89 [14, Ch. 4.7.3]. The welding parameters and their respective values are given in Table 9. Pad-eye 4 is only welded on one side. This is for assembly purposes because of the limited access to the welding area.

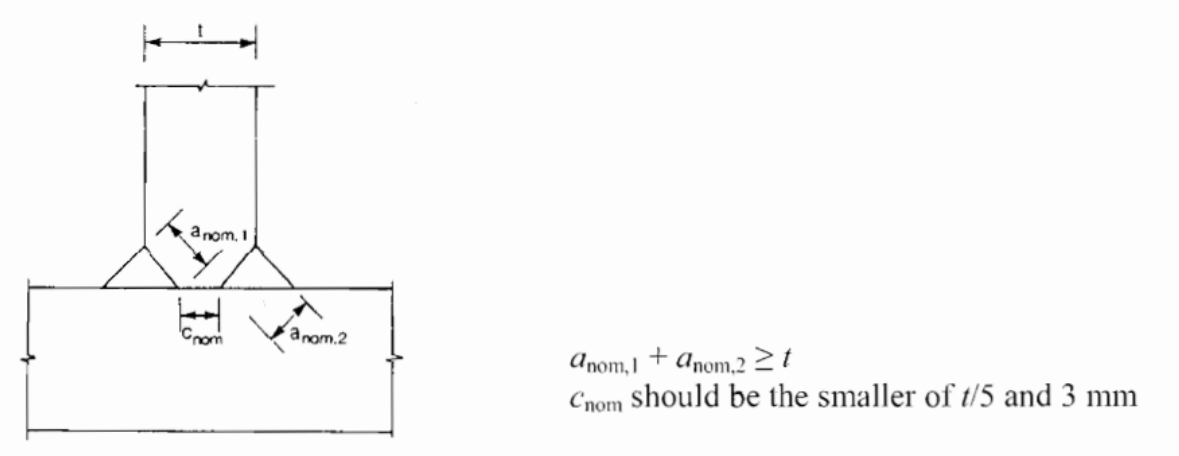

Figure 89 - Full penetration of T-butt welds [14, Ch. 4.7.3]

Table 9 – Pad-eye weld parameters and values

Pad-Eye (*see* Figure 68)	$a_{nom,1}$	$a_{nom,2}$	c_{nom}	t
Pad-eye 1	25mm	25mm	3mm	50mm
Pad-eye 2	12,5mm	12,5mm	3mm	25mm
Pad-eye 3	15mm	15mm	3mm	30mm
Pad-eye 4	25mm	0	3mm	25mm

The cheek plate welds in pad-eyes 2 and 3 are calculated for the a-value with the formula below [7, Ch. A.5]. The results are shown in Table 10. According to Eurocode 3 standards, fillet welds have a minimum throat thickness of 3mm [14, Ch. 4.5.2]. All cheek weld throat thicknesses are set to 3mm to meet this criterion.

Cheek plate welds

$$\sigma_e \geq \frac{LL \cdot t_{ch}}{t \cdot D_{ch} \cdot a \cdot UF} \quad \rightarrow \quad a \geq \frac{LL \cdot t_{ch}}{t \cdot D_{ch} \cdot \sigma_e \cdot UF}$$

where

LL: *Lif inting load applied to the pad – eye*

σ_e: *Allowable stress of the material* $\left(\sigma_e = 301,75MPa\right)$

t_{ch}: *thickness of the cheek plates*

D_{ch}: *Diameter of cheek plates*

a: *Weld thoat thickness*

UF: *maximum allowable f illet weld utilization* $(UF = 0,6)$

t: *total thickness of padeye, including cheeks*

Table 10 - Cheek plate calculation parameters and results

Pad-eye name	*LL (kN)*	t_{ch}	D_{ch}	*UF*	t	σ_e	a
Pad-eye 2	124,4kN	8mm	104mm	0,6	41mm	301,75MPa	1,3mm
Pad-eye 3	124,4kN	8mm	104mm	0,6	46mm	301,75MPa	1,2mm

4.5. Accessories

4.5.1. Guidewire Receptacles

The guidewire receptacles are designed by the company and are included in the subsea basket assembly. They accommodate the guidewire anchors when the subsea basket is used as a DMA. The guidewire anchors are designed to snap at a specific load to prevent the DMA from shifting location during unwanted loadings.

Guidewire receptacles must be installed to use the basket as a DMA. The diagonal distances between the receptacles are based on which guide tubes are used on the XT structure. Normally, XT structures have four guide funnels, of which two are used at a time. The guide funnels are oriented in a square pattern with a diagonal distance of 3657mm and an edge length of 2586mm. During DMA operations, one of the two orientations is used. Figure 90 illustrates the two optional distances between the guidewire receptacles, where one is at 3657mm and the other at 2586mm.

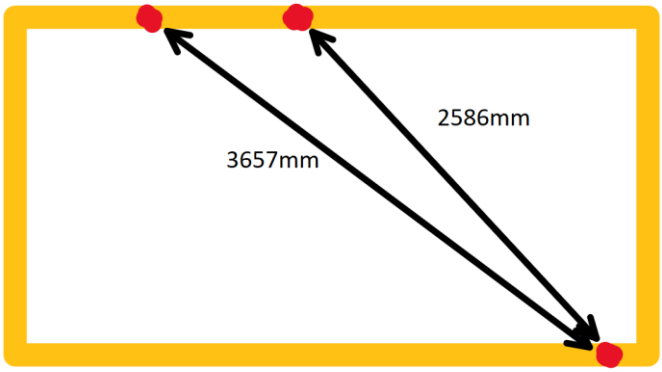

Figure 90 - Guidewire receptacle distances.

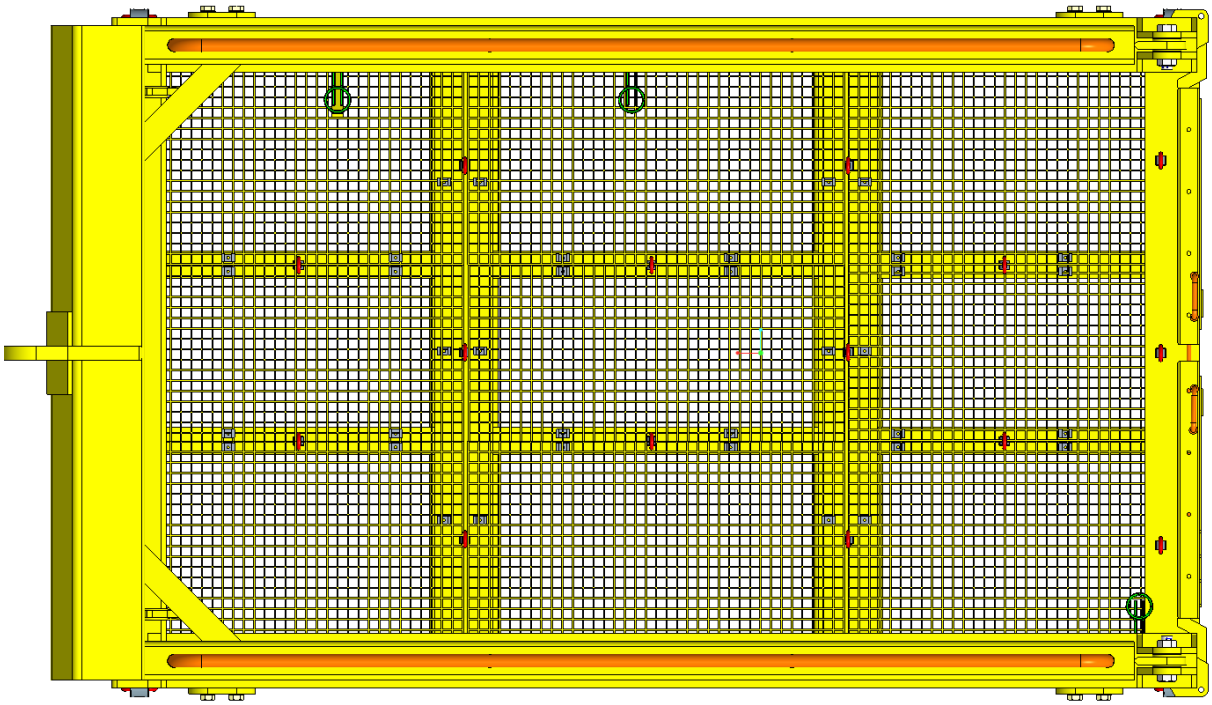

Figure 91 - Top view of the receptacle locations on the subsea basket

Because the chain may come in conflict with one of the receptacles during lifting operations, a cover is designed to prevent the chain from tangling on the receptacle. Figure 92 shows the cover of the conflicting receptacles.

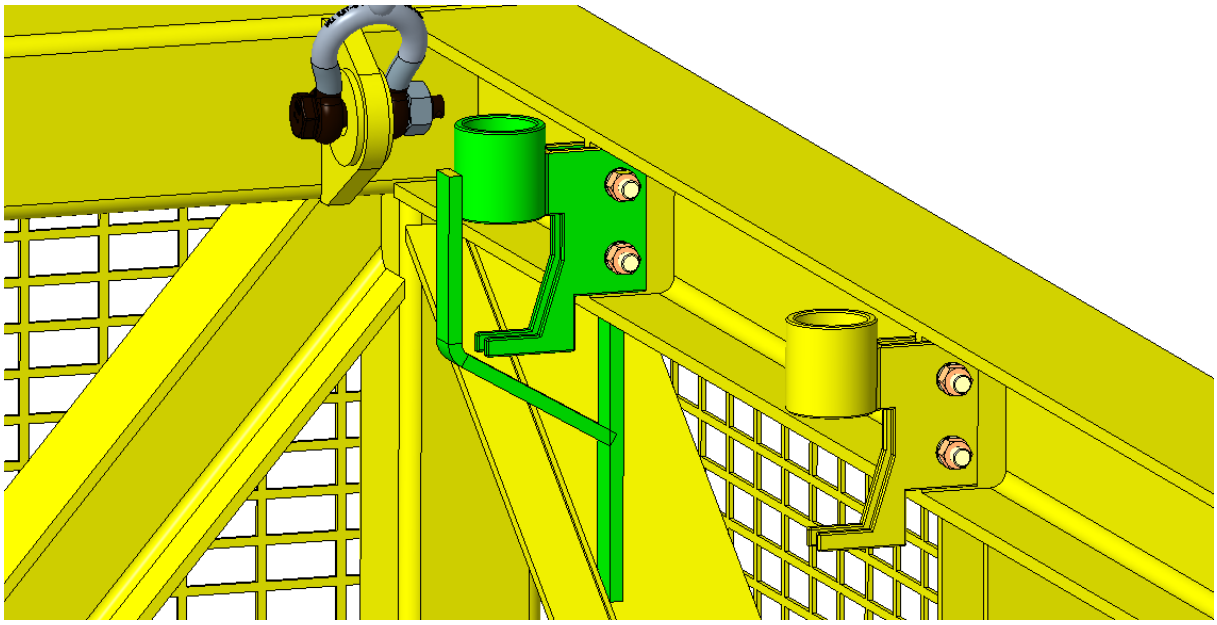

Figure 92 – Receptacles with chain guide to prevent tangling.

Since the design of the receptacle is based on the company's drawings, an assessment with a FEM simulation is something that will validate further use of the design in the subsea basket. The guidewires contain a shear pin that breaks at a load of 2,5 tons. This load is provided in the load conditions for the analysis, which are based on a lifting factor and consequence factor [6, Ch. 16.4.3].

$$\gamma_{sf} = \gamma_h \gamma_c$$

$$\gamma_h = 1,3$$

$$\gamma_c = 1,3$$

$$F_{SD} = \gamma_{sf} \cdot F_{Breakout} \cdot g$$

$$F_{SD} = 1,69 \cdot 2500kg \cdot 9,81\frac{m}{s^2} = 41,45kN$$

Where:

F_{SD} : Sling design load

γ_{sf} : Design factor for slings and grommets

γ_h : Lifting factor

γ_c : Consequence factor

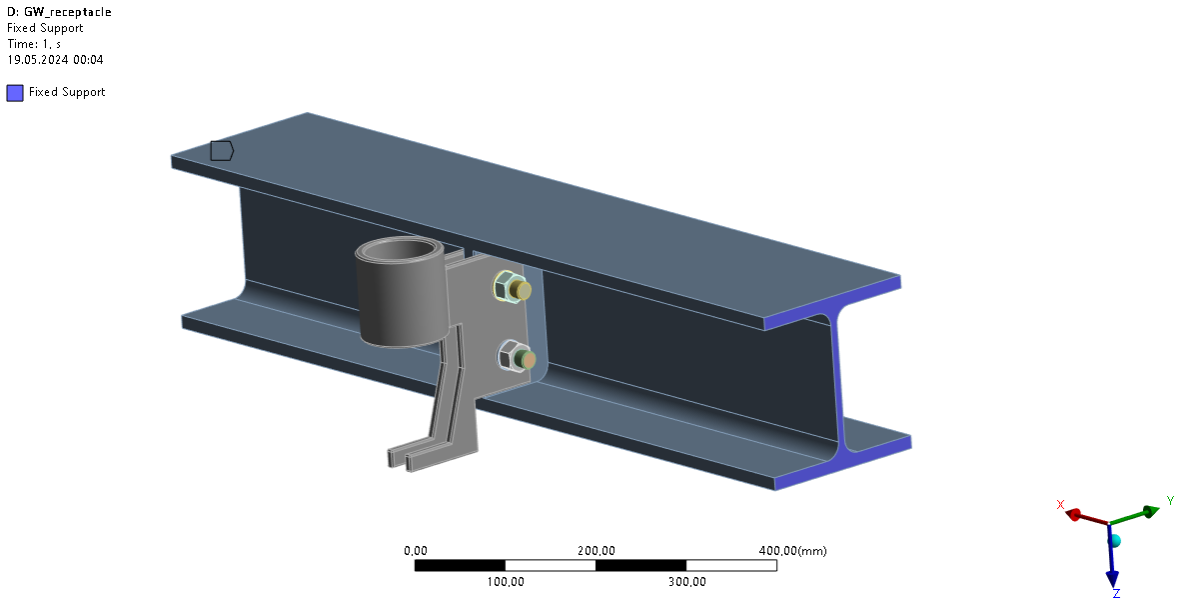

Figure 93 - Boundary condition of receptacle analysis.

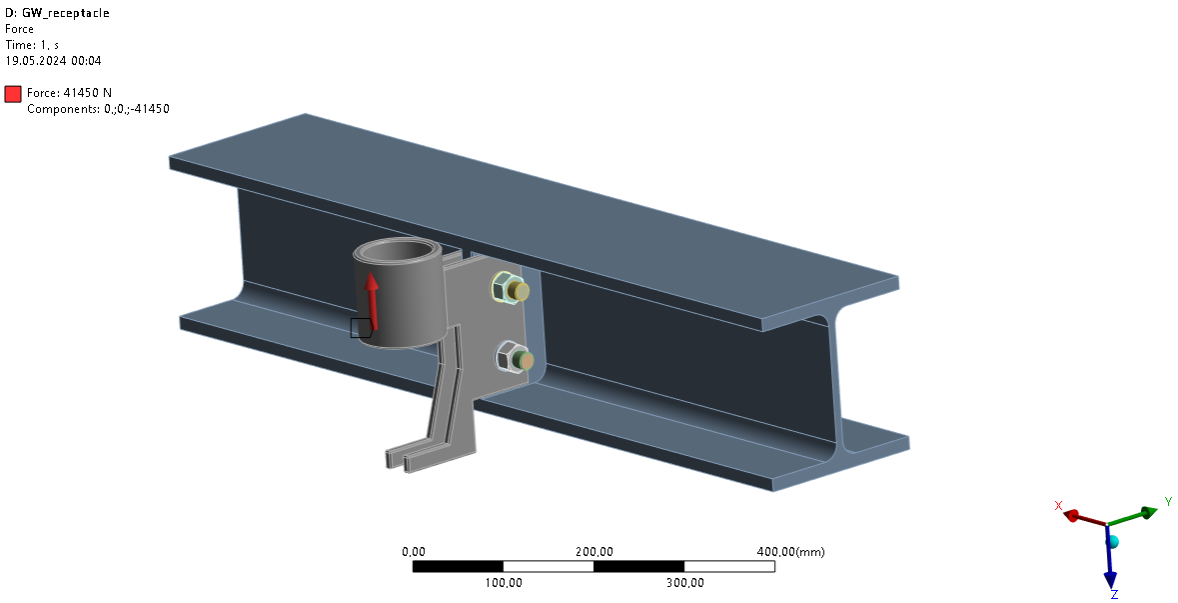

Figure 94 - Applied force on the receptacle.

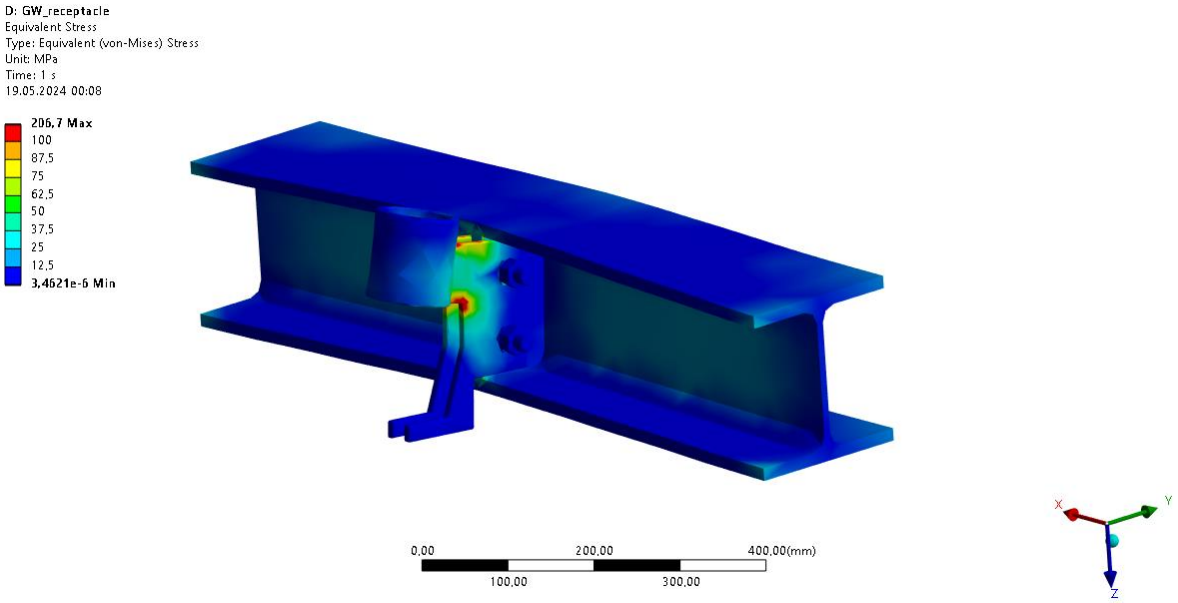

Figure 95 - Receptacle analysis results.

From the FEM simulation, the design is validated for further use in the subsea basket by including the load conditions and breakout force. The analysis results are presented in Figure 95. Compared with the allowable stress (3.3.3), the utilization factor results in 68,5% of the guidewire's capacity against the applied loads.

4.5.2. Sea fastening

(DNV-ST-E273 [3.7.2]) During transportation on deck, the basket is secured in each corner. The sea fastening points are D-rings. The pair of D-rings on each side are secured to a single connection point mounted on the deck via 16mm chains, as shown in Figure 96. The ISO corners also contribute as sea fastening on deck and are mounted on a rail system with a twist-lock locking mechanism. The extra weight and the basket are supplied with this feature.

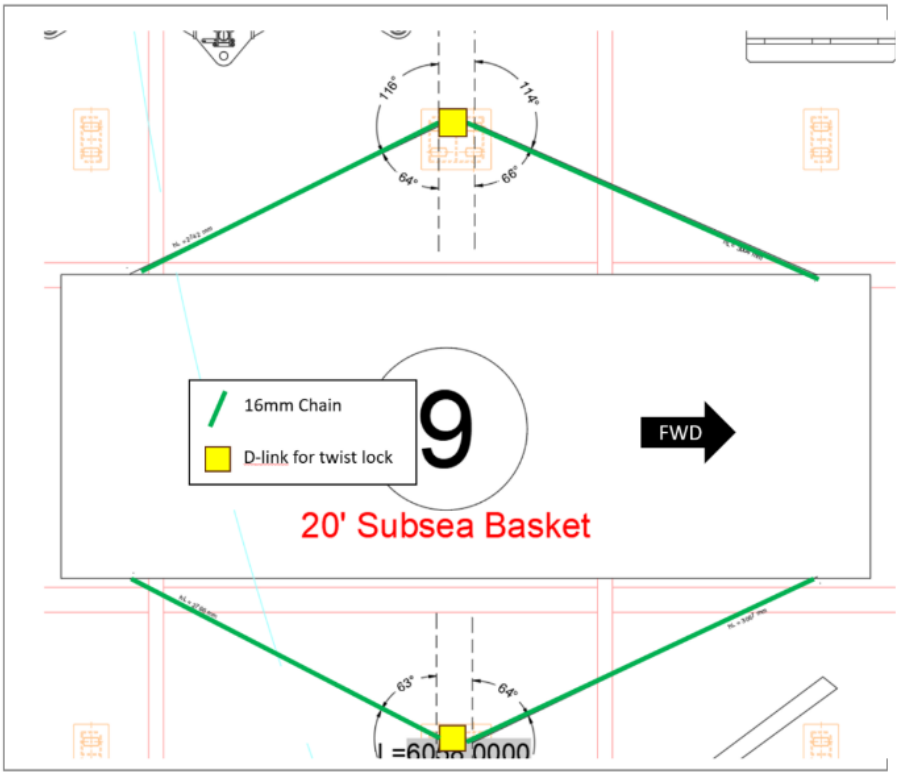

Figure 96 - Location of deck fastening. The picture is obtained from DeepOcean.

4.5.3. Grating

GRP grating

The floor grating must withstand the load of the tooling. Fiber-glass grating will be used as it is strong, as well as easy to cut and assemble. The assembly is done by using 316L steel M-clamps shown in. The M-clamps are bolted through the HEB100 beams below. The floor consists of 9 GRP grating plates with four different dimensions as illustrated in drawing number 7(67). Suitable GRP grating plate dimensions are listed in Supplementary Figure 5.

Expanded Metal

For the sides of the basket and the doors, expanded metal is applied. If something gets loose in the basket, the expanded metal will be able to stop the item from falling outside of the basket. These sheets of metal are easy to spot weld onto the basket, and cheap to replace if needed.

4.5.4. Shackles

The shackle sizes are determined by establishing their respective workload limit (WLL) in tons by adding a safety factor of less than 6 [7, Ch. 7.3.3]. A factor of 3 is used in the calculations below. CERTEX

provides all shackles with a safety factor of 6 [20]. The WLL of the four load point shackles on the basket and the two on the spread bar are limited to:

$$WLL \geq \frac{2,25}{SF} \cdot \frac{RSF}{g} = \frac{2,25}{2} \cdot \frac{124,4\ kN}{9,81^{m}/_{s^2}} = 9,51\ tons$$

The shackles between the crane hook and the main pad-eye are limited to:

$$WLL \geq \frac{2,25}{SF} \cdot \frac{RSF}{g} = \frac{2,25}{3} \cdot \frac{324\ kN}{9,81^{m}/_{s^2}} = 24,77\ tons$$

Shackles with a WLL of 9,5 tons and 25 tons are acceptable in this construction. The shackles used are designed and manufactured by CERTEX, according to EN 13889, which is suitable for offshore units in the North Sea [20]. Shackles dimensions and their respective parameters are given in Supplementary Table 5 and Supplementary Figure 3.

4.5.5. Chain Slings

DNV standards demand a safety factor of 2 to be multiplied by the *LL* when dimensioning the chain slings [7, Ch. 7.3.2]. The safety factor of CERTEX chain slings used in this design is 4 [21]. Therefore, it is not necessary to add a safety factor of 2 to the *LL*. Chain slings are found in tables by choosing an MBL closest to the respective *LL*. As shown in Supplementary Table 4, the smallest diameter of chain slings in class R45 for multiple use is 8mm.

The A-frame pad-eyes have a *LL* of 124,4kN. When choosing a suitable chain sling, the closest minimal breaking load more significant than the respective *LL*, is usually used. The chain size is found using the dimensions of the shackle to make the assembly possible. Therefore, the chain chosen for the A-frame has a minimal breaking strength of 760kN, which is sufficient. The chain dimensions and parameters are given in Supplementary Figure 2.

4.6. Total weight

The basket including the A-frame and accessories has a weight of 4,5 tons, as shown in Figure 97. When adding the weight of the tooling of 1500kg this results in a total weight of 5,5 tons. When adding the extra weight to the structure, the total weight becomes approximately 10,5 tons, and fulfills the criteria to be used as a DMA.

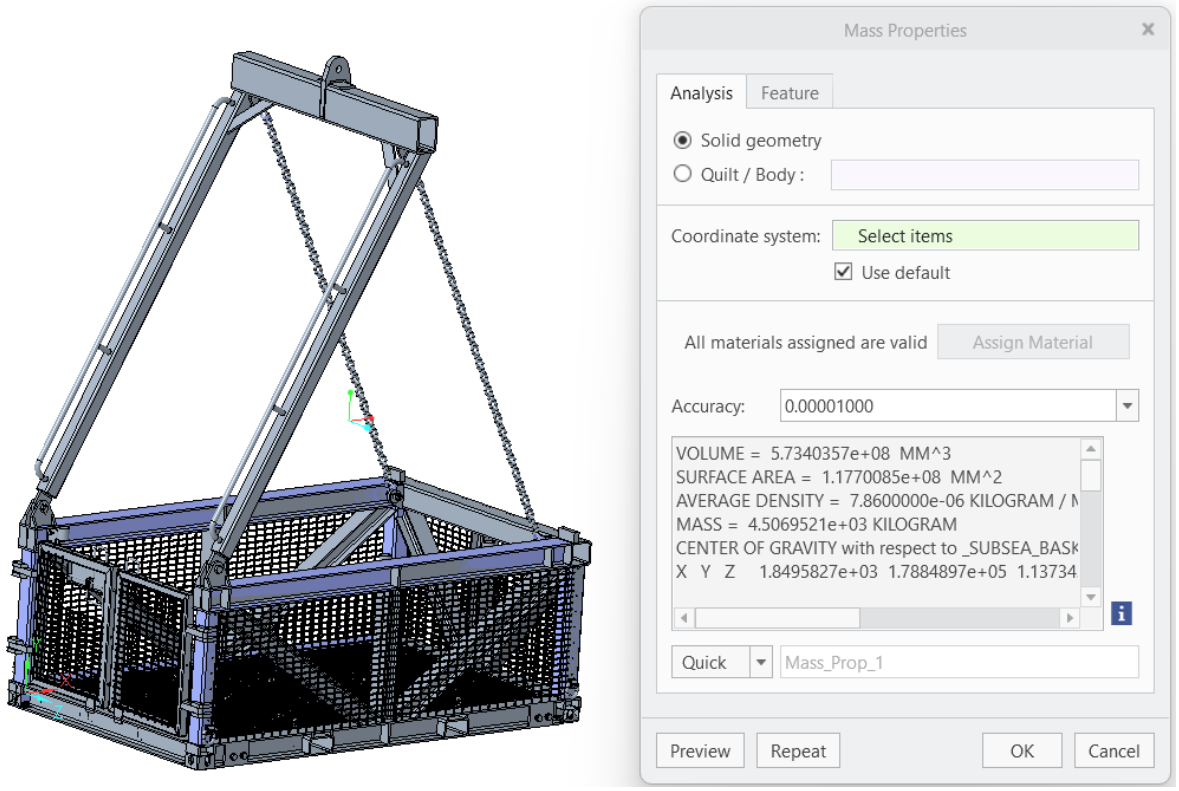

Figure 97 - Weight of the basket, A-frame and accessories.

5. Discussion

5.1. Contributions

A contribution to the structural analysis was made when a supervisor performed an analysis using Staad.Pro, which offers node analysis capabilities. This data has been valuable for the welding calculations, as mentioned in chapter 4.1.5. The contributed structural analysis provided connection properties and beam results, such as axial forces and bending moments along (x, y, z) components.

The analysis inserted horizontal forces perpendicular to the A-frame, specified as a Serviceability Limit State (SLS) [11]. Based on the design loads, a high utilization ratio for the longitudinal beam sections of $\eta(HEB140) > 1$, indicated that they were operating above the cross-section's capacity of 100%. As a solution, replacing HEB140 beams with SHS140 beams reduced the utilization ratio to 36%.

5.2. Result Discussion

Table 11 presents the results from the simulations, where the results with the highest utilization factor are highlighted in a darker color. The calculated forces used in the simulations are all worst-case scenarios, where multiple factors have been included in accordance with standards (3.4). If the stress results are below the utilization factor of 1, even with the worst-case forces, failure is unlikely to occur.

Load Case 1 of the Door Hinge was closest to the maximum allowed value, with a utilization factor of 0,84. As mentioned in subchapter 4.1.3, this hinge simulation had an unrealistic stress concentration where the highest value appeared. Realistically, the stress result is lower than what is presented in the table. However, the value remains within the limit despite the unrealistic stress concentration.

This also applies to the A-frame Total simulation in Table 11, which had the highest stress value where a stiffener was placed. The stiffener was not included in this simulation to simplify the geometry. The stiffener was, however, included in the A-frame Spreader Bar simulation, where the value at that point was significantly lower than for the A-frame Total simulation.

Overall, the values are within the limitation of 1, revealing that the basket withstands the forces that can appear. The parts not included in FEM simulations are either hand calculated, dimensioned according to tables, or both.

Table 11 - Results from simulations.

FEM Simulation	Stress result (MPa)	Max allowed stress (MPa)	Utilization Factor (UF)
Basket	157,11	301,75	0,52
Door Hinge (Load Case 1)	254,24	301,75	0,84
Door Hinge (Load Case 2)	131,74	301,75	0,44
Door Handle	173,63	301,75	0,58
A-frame Total	217,72	301,75	0,72
A-frame Spreader Bar	183,24	301,75	0,61
Extra Weight	122,99	301,75	0,41
Pad-eye Nr.1	183,24	301,75	0,61
Pad-eye Nr.2	130,35	301,75	0,43
Pad-eye Nr.3	153,97	301,75	0,51
Pad-eye Nr.4	146,97	301,75	0,49
Pad-eye Nr.5	209,95	301,75	0,70

5.3. Future Work

Testing and certification of the basket upon completion is crucial to ensure the design is suitable and safe for subsea operations. These processes serve to validate the accuracy of the FEM analysis and manual calculations performed during the design phase. Subjecting the basket to real-world conditions and rigorous testing, can confirm that it meets all necessary standards and specifications, verifying the structural integrity and functionality. It ensures the reliability and safety of the basket in demanding underwater environments, identifying any potential defects or weaknesses before deployment.

It is recommended to address the design challenge posed by the high edges of the basket, which currently hinder the use of a pallet jack for loading and unloading equipment. Exploring solutions to improve accessibility will have to be considered. One potential solution to consider is the use of a ramp.

6. Conclusion

Developing a multifunctional subsea basket for XT operations potentially improves subsea tool and equipment management. The proposed design combines the ability to act as a transport module for tools and equipment and as a DMA, ensuring safe and efficient subsea tree installations. This multifunctional approach addresses the high rental costs and market shortage of subsea baskets, offering a cost-effective and sustainable solution. By enabling the adjustment of the basket's mean gross weight, the design supports using the whip-line, enhancing operational efficiency on the construction vessel Normand Ocean.

The design can reduce time during operations, which aligns with DeepOcean's goal of reducing CO2 emissions by 45% before 2030. The enhancements not only meet the company's specific needs but also position the product as a unique offering in the market. In accordance with relevant standards, the company's requirements and wishes have been met. Technical drawings for all parts are included, making the product ready for production.

List of figures

List of tables

Bibliography

[1] DeepOcean, “About DeepOcean.” Accessed: Apr. 15, 2024. [Online]. Available: https://www.deepoceangroup.com/about/esg

[2] “Normand Ocean,” DeepOcean. Accessed: May 16, 2024. [Online]. Available: https://www.deepoceangroup.com//vessels/normand-ocean

[3] “1.pdf.” Accessed: May 13, 2024. [Online]. Available: https://cargotec.picturepark.com/Go/Nnm6V12E/V/66161/1

[4] SagaSubsea, “BASKET,” SAGA SUBSEA. Accessed: May 16, 2024. [Online]. Available: https://www.sagasubsea.com/basket

[5] P. Ungvary, “Which Subsea Basket alternative do you find most effective for IMR operations?,” SurveyMonkey. Accessed: May 19, 2024. [Online]. Available: https://no.surveymonkey.com/r/726C87T?fbclid=IwZXh0bgNhZW0CMTAAAR0w8GNiQtvh9JWI1LFhXwszC-bIxU_snEyQ_RlLO7hWMYVHDyj4jzn8ptY_aem_AUNQv6MoVdip6bjqI6m4F76iLb7smfSrseoWzF7u5o_JYe_2jRytN-w-9uYkIQu2ZLJOENzgji5l5YT6J0A4q89p

[6] Det Norske Veritas, “DNVGL-ST-N001: Marine operations and marine warranty.” Høvik, Norway, Desember 2023.

[7] Det Norske Veritas (DNV), “DNVGL-ST-E273: Portable offshore units.” Det Norske Veritas (DNV), Høvik, Norway, Apr. 2016.

[8] BMSteel, “Low-Carbon Steel.” Accessed: Apr. 14, 2024. [Online]. Available: https://www.bmsteel.co.uk/article/guide-to-low-carbon-steel

[9] CWBGroup, “Charpy V-notch test.” Accessed: May 16, 2024. [Online]. Available: https://www.cwbgroup.org/association/how-it-works/what-charpy-v-notch-cvn-impact-test

[10] Metinvest, “Steel S355J2: characteristics, properties, analogues - Metinvest.” Accessed: Feb. 16, 2024. [Online]. Available: https://metinvestholding.com/en/products/steel-grades/s355j2

[11] Eurocode3, “en.1993.1.1.2005.” Accessed: Apr. 12, 2024. [Online]. Available: https://www.phd.eng.br/wp-content/uploads/2015/12/en.1993.1.1.2005.pdf

[12] AISC, “Lateral Torsional Buckling.” Accessed: Apr. 15, 2024. [Online]. Available: https://www.aisc.org/globalassets/continuing-education/ssrc-proceedings/2016/lateral-torsional-buckling-of-welded-wide-flange-beams.pdf

[13] T. G. Idsøe, “Vipping, Eurocode 3 mot forenklet metode uten standard,” Institutt for Matematiske realfag og Teknologi. Accessed: May 16, 2024. [Online]. Available: https://nmbu.brage.unit.no/nmbu-xmlui/bitstream/handle/11250/221667/TorIdsoe2014-Gradsoppgave.pdf?sequence=1

[14] “en.1993.1.8.2005-1.pdf.” Accessed: May 03, 2024. [Online]. Available: https://www.phd.eng.br/wp-content/uploads/2015/12/en.1993.1.8.2005-1.pdf

[15] “Shear Lag Effects in Steel Tension Members | American Institute of Steel Construction.” Accessed: May 10, 2024. [Online]. Available: https://www.aisc.org/Shear-Lag-Effects-in-Steel-Tension-Members

[16] “en.1993.1.5.2006.pdf.” Accessed: May 18, 2024. [Online]. Available: https://www.phd.eng.br/wp-content/uploads/2015/12/en.1993.1.5.2006.pdf

[17] H. Hartvigsen, R. Lorenstsen, K. Michelsen, and S. Seljevoll, *Verktstedshåndboka*, 3rd. Aurskog: PDC Printing Data Center AS, 1994. Accessed: May 19, 2024. [Online]. Available: https://www.nb.no/items/5f6c5fce4e105fe011bdb21e80cc1f60?page=251&searchText=maskinteknikk

[18] E. team, “Table of design properties for metric steel bolts M5 to M39 - Eurocode 3,” EurocodeApplied.com. Accessed: Mar. 07, 2024. [Online]. Available: https://eurocodeapplied.com/design/en1993/bolt-design-properties

[19] Karl-Heinrich Grote and H. Hefazi, *Handbook of Mechanical Engineering*, 2nd. Switzerland: Springer Nature Switzerland AG, 2021.

[20] “80889.pdf.” Accessed: Apr. 16, 2024. [Online]. Available: https://www.certex.no/en_GB/download/productpage/80889?categoryId=495998

[21] "TECHNICAL NOTE 007 Structural Steel Sub-Grades JR, J0 and J2 Does It Matter.pdf." Accessed: Feb. 16, 2024. [Online]. Available: https://fs.hubspotusercontent00.net/hubfs/8729158/_TechnicalNotes/TECHNICAL%20NOTE%20007%20Structural%20Steel%20Sub-Grades%20JR%2C%20J0%20and%20J2%20Does%20It%20Matter.pdf

[22] "en.1993.1.8.2005-1.pdf." Accessed: May 14, 2024. [Online]. Available: https://www.phd.eng.br/wp-content/uploads/2015/12/en.1993.1.8.2005-1.pdf

[23] Glassiber Produkter, "Art.No.15022 - H 25mm, 38x38, yellow, meniscus, ve FR," Glassfiber Produkter. Accessed: May 20, 2024. [Online]. Available: https://glassfiber.no/en/product/artikkel-nr-15022-25-mm-gul/

[24] J. A. Breistig and E. K. M. Schmall, "Konstruksjon av subsea rør-basket med 100 metriske tonn løftekapasitet," *Høgsk. På Vestl.*, p. 105, May 2021.

[25] E. team, "Table of design properties for Square Hollow Sections (SHS)," EurocodeApplied.com. Accessed: May 10, 2024. [Online]. Available: https://eurocodeapplied.com/design/en1993/shs-design-properties

[26] E. team, "Table of properties for IPE,HEA,HEB,HEM,UB,UC,UBP profiles - Eurocode 3," EurocodeApplied.com. Accessed: May 10, 2024. [Online]. Available: https://eurocodeapplied.com/design/en1993/ipe-hea-heb-hem-design-properties

Appendix

POU length - L (m)	*Min. distance between centres of pockets (mm)*	*Comments*
L < 6	25% of L, minimum 900	Loaded handling
	900	Empty handling only
6 ≤ L ≤ 12	25% of L, maximum 2050	Loaded handling
	15% of L	Empty handling only
12 < L ≤ 18	2050	Empty handling only
L > 18	-	No pockets

Supplementary Table 1 - Recommended fork pocket distances and operational limitations. [7, Ch. 3.9.3]

	Dimensions		**Hole diameter d_0 [mm]**				**Areas**	
Size	**Nominal diameter d [mm]**	**Nut width across flats s [mm]**	**Normal round hole**	**Oversize round hole**	**Short slotted hole**	**Long slotted hole**	**Gross area (unthreaded part) A_g [mm^2]**	**Stress area (threaded part) A_s [mm^2]**
M24	24	36	26	30	32×26	60.0×26	452	353
M27	27	41	30	35	37×30	67.5×30	573	459
M30	30	46	33	38	40×33	75.0×33	707	561
M33	33	50	36	41	43×36	82.5×36	855	694
M36	36	55	39	44	46×39	90.0×39	1020	817
M39	39	60	42	47	49×42	97.5×42	1190	976

Supplementary Table 2 - Bolt and hole dimensions. [18]

Distances and spacings, see Figure 3.1	Minimum	Maximum[1) 2) 3)]		
		Structures made from steels conforming to EN 10025 except steels conforming to EN 10025-5		Structures made from steels conforming to EN 10025-5
		Steel exposed to the weather or other corrosive influences	Steel not exposed to the weather or other corrosive influences	Steel used unprotected
End distance e_1	$1{,}2d_0$	$4t + 40$ mm		The larger of $8t$ or 125 mm
Edge distance e_2	$1{,}2d_0$	$4t + 40$ mm		The larger of $8t$ or 125 mm
Distance e_3 in slotted holes	$1{,}5d_0$ [4)]			
Distance e_4 in slotted holes	$1{,}5d_0$ [4)]			
Spacing p_1	$2{,}2d_0$	The smaller of $14t$ or 200 mm	The smaller of $14t$ or 200 mm	The smaller of $14t_{min}$ or 175 mm
Spacing $p_{1,0}$		The smaller of $14t$ or 200 mm		
Spacing $p_{1,i}$		The smaller of $28t$ or 400 mm		
Spacing p_2 [5)]	$2{,}4d_0$	The smaller of $14t$ or 200 mm	The smaller of $14t$ or 200 mm	The smaller of $14t_{min}$ or 175 mm

1) Maximum values for spacings, edge and end distances are unlimited, except in the following cases:
- for compression members in order to avoid local buckling and to prevent corrosion in [AC2] exposed members (the limiting values are given in the table) and; [AC2]
- for exposed tension members [AC2] to prevent corrosion (the limiting values are given in the table). [AC2]

2) The local buckling resistance of the plate in compression between the fasteners should be calculated according to EN 1993-1-1 using $0{,}6\ p_1$ as buckling length. Local buckling between the fasteners need not to be checked if p_1/t is smaller than $9\ \varepsilon$. The edge distance should not exceed the local buckling requirements for an outstand element in the compression members, see EN 1993-1-1. The end distance is not affected by this requirement.

3) t is the thickness of the thinner outer connected part.

4) The dimensional limits for slotted holes are given in 1.2.7 Reference Standards: Group 7.

5) For staggered rows of fasteners a minimum line spacing of $p_2 = 1{,}2d_0$ may be used, provided that the minimum distance, L, between any two fasteners is greater or equal than $2{,}4d_0$, see Figure 3.1b).

Supplementary Table 3 - Minimum and maximum spacing, end and edge distances. [22, Ch. 3.5]

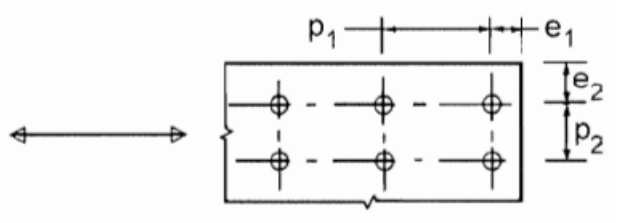

Supplementary Figure 1 - Hole positioning parameters. [22, Ch. 3.5]

Class	Wire rope slings		Chain slings	
	Single event	Multiple use	Single event	Multiple use
R60	D ≥ 13 mm	D ≥ 16 mm	D ≥ 8 mm	D ≥ 10 mm
R45	D ≥ 11 mm	D ≥ 13 mm	D ≥ 7 mm	D ≥ 8 mm
R30	D ≥ 9 mm	D ≥ 11 mm	D ≥ 6 mm	D ≥ 7 mm

Supplementary Table 4 – Minimum sling diameter. [7, Ch. 7.3.2]

Art. nr.	Chain diameter mm	WLL tonn	Min. bruddstyrke kN	Pitch Length	d mm	p mm	w1 mm	w2	Vekt
203500600000160	6	1,4	56,5	-	6	18	7,8	22,2	0,83
203501000000160	10	4	157	-	10	30	13	37	2,27
203501600000160	16	10	402	48	16	48	20,8	59,2	5,79
203502000000160	20	16	628	60	20	60	26	74	8,9
203502200000160	22	19	760	66	22	66	28,6	81,4	11,4
203502600000160	26	26,5	1 060	78	26	78	33,8	96,2	16
203503200000160	32	40	1 610	96	32	96	41,6	118	24,1

Måltabell

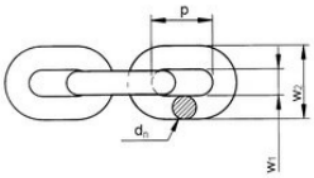

Supplementary Figure 2 - Chain sling parameters. [21]

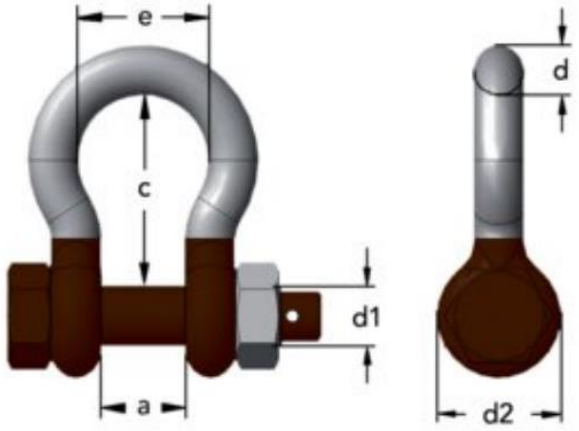

Supplementary Figure 3 – Shackle parameters. [20]

Part Code	WLL ton	a mm	c mm	d mm	d1 mm	d2 mm	e mm	Weight kg
420100200420	2	21	47	1/2" - 13	16	33	33	0.42
420100330420	3.25	27	60	5/8" - 16	19	40	42	0.7
420100480420	4.75	31	71	3/4" - 19	22	48	49	1.2
420100650420	6.5	37	84	7/8" - 22	25	52	60	1.7
420100850420	8.5	43	95	1" - 25	28	60	68	2.5
420100950420	9.5	46	108	1 1/8" - 28	32	64	74	3.4
420101200420	12	52	119	1 1/4" - 32	35	72	83	4.8
420101350420	13.5	57	132	1 3/8" - 35	38	76	89	7
420101700420	17	60	146	1 1/2" - 38	42	84	98	9
420102500420	25	74	178	1 3/4" - 45	50	105	127	15
420103500420	35	83	197	2" - 50	57	116	138	21
420105500420	55	105	260	2 1/2" - 65	70	145	180	39

Supplementary Table 5 – Shackle dimension values. [20]

Static hook load (SHL) (tonnes)			*DAF*		
			Onshore [2), 3)]	Inshore [4), 6)]	Offshore [5), 6)]
3 [1)]	< *SHL* ≤	100	1.10	$1.07+0.05\sqrt{100/SHL}$	$1+0.25\sqrt{100/SHL}$
100	< *SHL* ≤	300	1.05	1.12	1.25
300	< *SHL* ≤	1000	1.05	1.10	1.20
1000	< *SHL* ≤	2500	1.03	1.08	1.15
SHL > 2500			1.03	1.05	1.10

1) For lifted items weighing less than 3 tonnes, it is recommended to assume that the item weighs 3 tonnes and this is used throughout the calculations for the rigging design.
2) For onshore crawler cranes travelling with load, possible dynamic effects should be evaluated thoroughly. Crane speeds and surface conditions should be considered. If not documented, the factors for 'inshore lifts' should be used
3) Onshore is also applicable to a lift to/from a vessel moored alongside a quay using a land-based crane. If a ship's crane is used, inshore factors apply.
4) Inshore is applicable to a lift with a crane vessel to/from a vessel in sheltered waters and is also applicable to lifting from the deck of a crane vessel onto a fixed platform at an offshore location
5) Offshore is applicable to a lift by a crane vessel from another vessel to a fixed platform.
6) *SHL* refers to the static hook load (see [16.3.2.2] and [16.3.2.3]).

Supplementary Table 6 – DNV table for establishing DAF. [6, Ch. 16.2.5.6]

Supplementary Figure 4 - Metal clamps used for GRP grating. [18]

Supplementary Figure 5 - GRP grating specifications. [23]

Basis for Welding Calculations

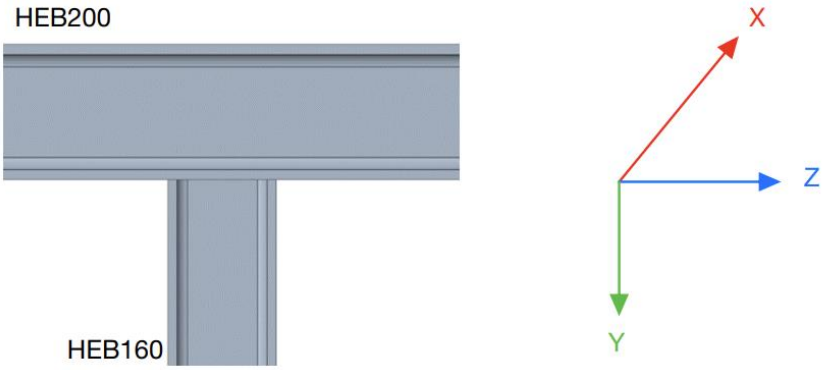

Supplementary Figure 6 - T-joint with axes aligned with Staad Pro coordinates.

Cross-section	Fx(kN)	Fy(kN)	Fz(kN)	Mx(kNm)	My(kNm)	Mz(kNm)
HEB160	-85.212	1.624	-0.406	-0.007	0.892	-0.389
	86.568	0.442	0.406	0.007	0.071	1.788
	-88.418	-0.03	-0.613	-0.007	1.058	-1.371
	89.774	2.097	0.613	0.007	0.394	-1.149
SHS140x12,5	109.621	0.923	-2.389	1.7	-7.574	0.164
	107.455	1.013	0.906	-1.174	4.623	-0.164

Supplementary Table 7 – Highest Node stress values from Supplementary Table 11.

Design properties of HEB and SHS profiles

The cross-sectional values of the HEB profile have been simplified as it follows the same procedure the company has utilized from a previous bachelor thesis [23, app. IX].

$$l_{weld,z} = h - 2 \cdot tf = (160 - 2 \cdot 15) = 130\text{mm}$$
$$l_{weld,x} = 160\text{mm}$$
$$h_{eff} = h_{HEB160} - tf + 2 \cdot a = 160 - 13 + 2 \cdot 5 = 157\text{mm}$$

$$W_{eff,x} = \frac{w \cdot h_{eff}^2}{6} - \frac{(w - t_{(2a)}) \cdot (h_{eff} - 2t_{(2a)})^3}{6h_{eff}}$$
$$W_{eff,x} = \frac{160 \cdot 157^2}{6} - \frac{(160 - 10) \cdot (157 - 2 \cdot 10)^3}{6 \cdot 157} = 247{,}85 \cdot 10^3\,\text{mm}^3$$
$$W_{eff,z} = \frac{2t_{(2a)} \cdot w^2}{6} + \frac{t_{(2a)}^3 \cdot (h_{eff} - 2t_{(2a)})^3}{6w}$$
$$W_{eff,z} = \frac{2 \cdot 10 \cdot 160^2}{6} + \frac{10^3 \cdot (157 - 2 \cdot 10)}{6 \cdot 160} = 85{,}48 \cdot 10^3\,\text{mm}^3$$
$$A_{eff} = 2(10 \cdot 160) + 10(160 - 2 \cdot 10) = 4600\,\text{mm}^2$$

The design properties of SHS [25].

$$W_{el} = 236{,}1 \cdot 10^3\,\text{mm}^3$$
$$A = 6207\,\text{mm}^2$$
$$l_{weld,x,z} = 150\,\text{mm}$$

Where:

$W_{eff,x,z}$: Effective section modulus for major(x) and minor(z) axis, in the elastic region

W_{el} : Elastic section modulus

A_{eff} : Effective Area of cross-section (HEB)

A : Area of cross-section (SHS)

l_{weld} : Length of the weld

Further design properties for its cross-section can be found in tables from Eurocode Applied [26].

Weld type	*Location of welding operation*	*Weld material factor, γ_{mw}*	
		Yield stress	*Ultimate stress*
Full penetration	Any	Use design resistance of the weaker of the joined parts	
Partial penetration and fillet	Fabrication site	1.15	1.3
	Onboard the vessel	1.3	1.5

Guidance note:

For welds made on board the vessel γ_{mw} for welds made at a fabrication site is acceptable provided that the welding conditions are good, see [5.10.2.2], and there is good weld fit-up (e.g. control of correct/no gaps to deck plate).

---e-n-d---o-f---g-u-i-d-a-n-c-e---n-o-t-e---

Supplementary Table 8 - Correlation factor for fillet welds. [6, Ch. 5.9.8.4.5]

Standard and steel grade			Correlation factor β_w
EN 10025	**EN 10210**	**EN 10219**	
S 235 S 235 W	S 235 H	S 235 H	0,8
S 275 S 275 N/NL S 275 M/ML	S 275 H S 275 NH/NLH	S 275 H S 275 NH/NLH S 275 MH/MLH	0,85
S 355 S 355 N/NL S 355 M/ML S 355 W	S 355 H S 355 NH/NLH	S 355 H S 355 NH/NLH S 355 MH/MLH	0,9
S 420 N/NL S 420 M/ML		S 420 MH/MLH	1,0
S 460 N/NL S 460 M/ML S 460 Q/QL/QL1	S 460 NH/NLH	S 460 NH/NLH S 460 MH/MLH	1,0

Supplementary Table 9 – Correlation factor for fillet welds[14, Ch. 4.5.3.2]

Weld type	*Location of welding operation*	*Weld permissible usage factor, η*	
		Yield stress	*Ultimate stress*
Full penetration	Any	Use design resistance of the weaker of the joined parts	
Partial penetration and fillet	Fabrication site	0.60	0.53
	Onboard the vessel	0.52	0.46
1) Where the loads are determined using IMO, then the strength shall be checked using IMO requirements. 2) Where the Sec.11 loads are due to accelerations determined according to DNV class rules, see [11.6.2] or [11.6.3] (as applicable), LS1 or LS2A shall be used as per [11.6.6].			

Supplementary Table 10 - Permissible usage factor for welds for ASD/WSD. [6, Ch. 5.9.7.6]

FEM simulation basis for ULS Calculations

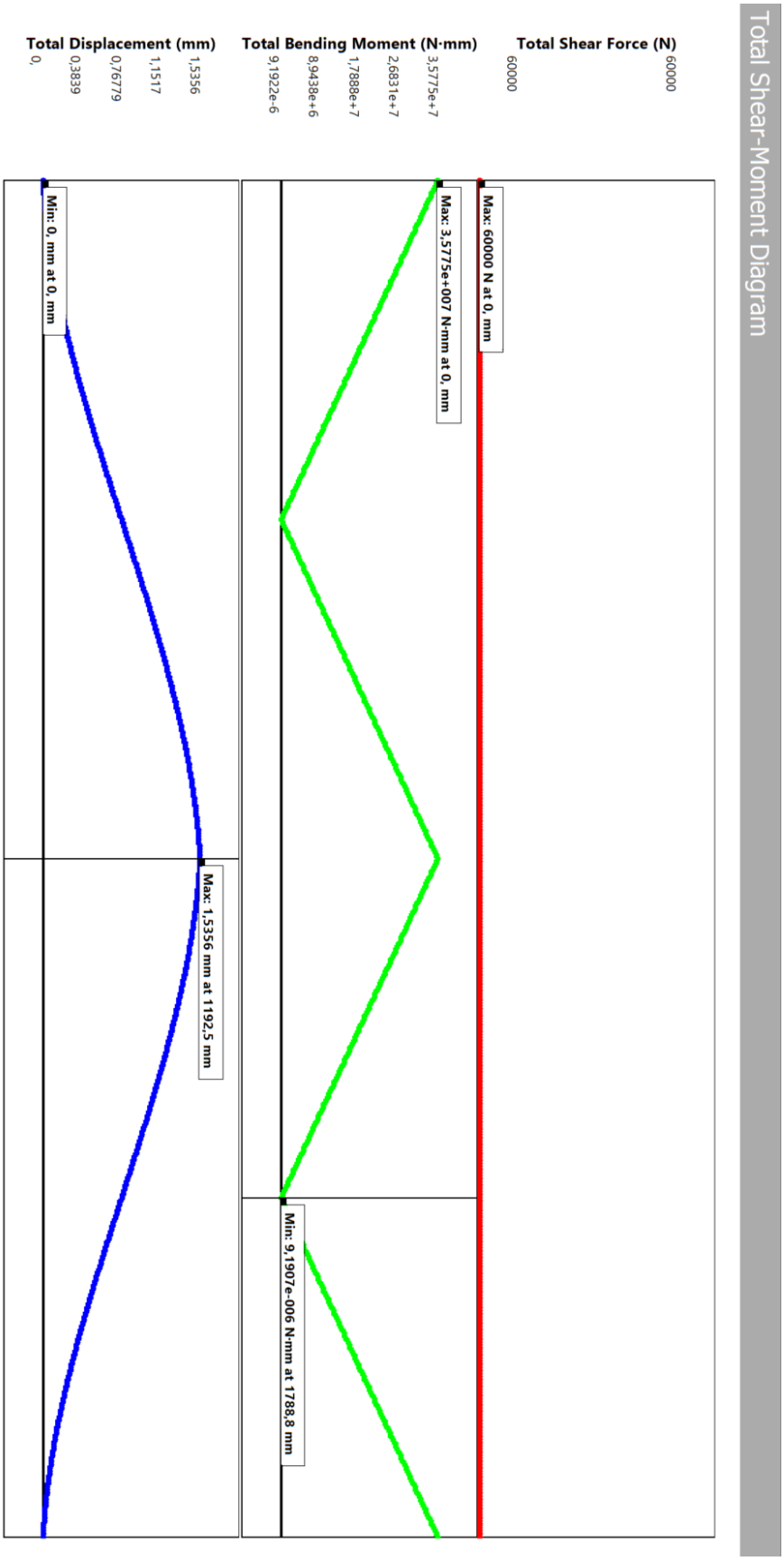

Supplementary Figure 7 - Shear and moment diagram for HEB100 under concentrated load.

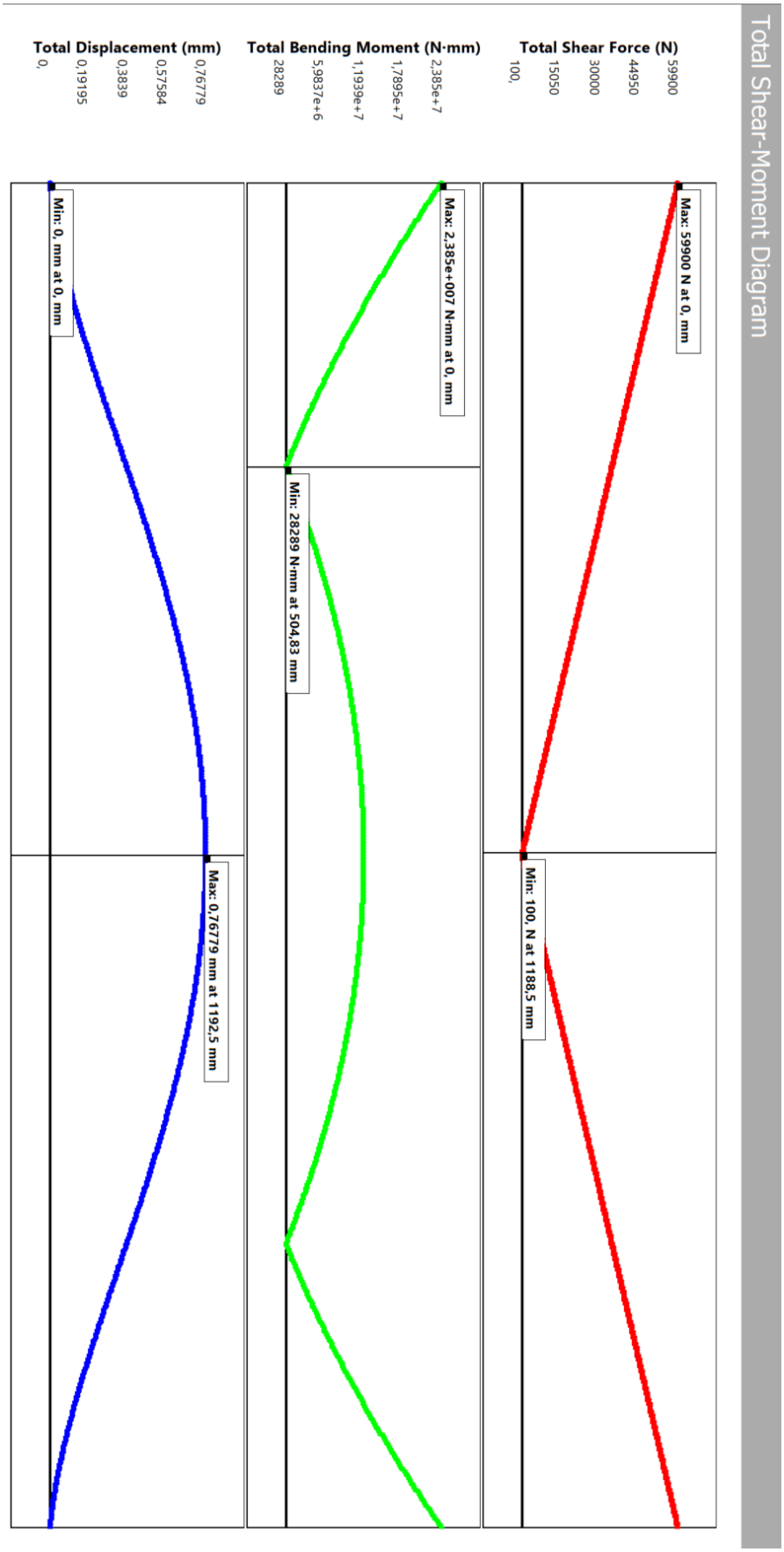

Supplementary Figure 8 - Shear and moment diagram for HEB100 under uniformly distributed load.

Supplementary Figure 9 – Shear and moment diagram for RHS250x150 under concentrated load.

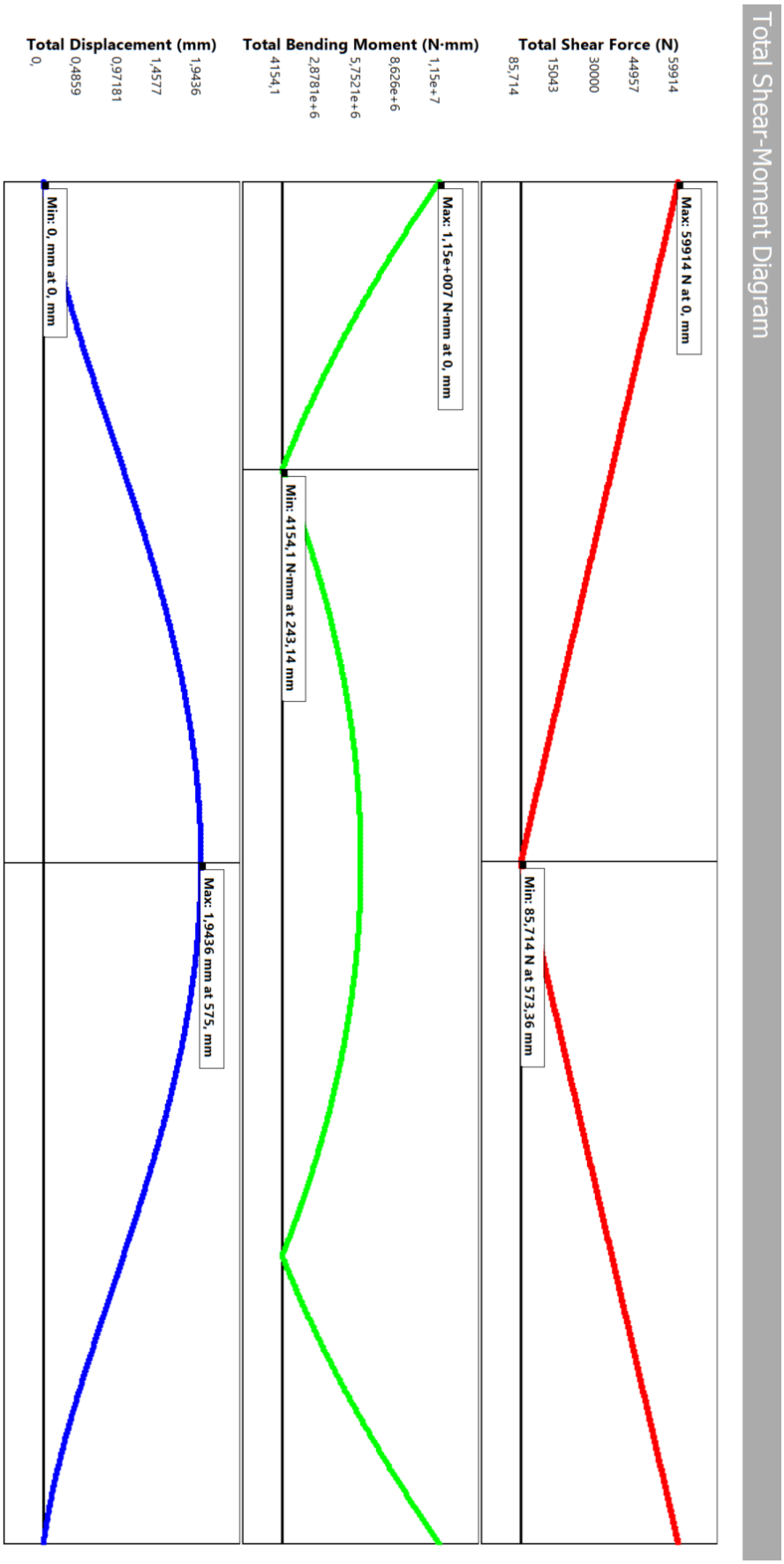

Supplementary Figure 10 - Shear and moment diagram for RHS250x150 under uniformly distributed load.

Staad.Pro analysis

DEEPOCEAN

◇ NOTES

Originator:	Anders Haga
Date:	23.04.2024
Project:	Bachelor Students
Subject:	Beam-end-forces for Subsea Basket

The Staad Pro analysis was performed to obtain the beam-end-forces for a subsea basket which is part of a bachelor thesis.

1.3 ANALYSIS LOAD

The load is applied as member loads on the bottom beams of the structure. The member load equals a payload of 120kN. This load is combined with the self weight and multiplied with 2.5 for the analysis of beam-end-forces.

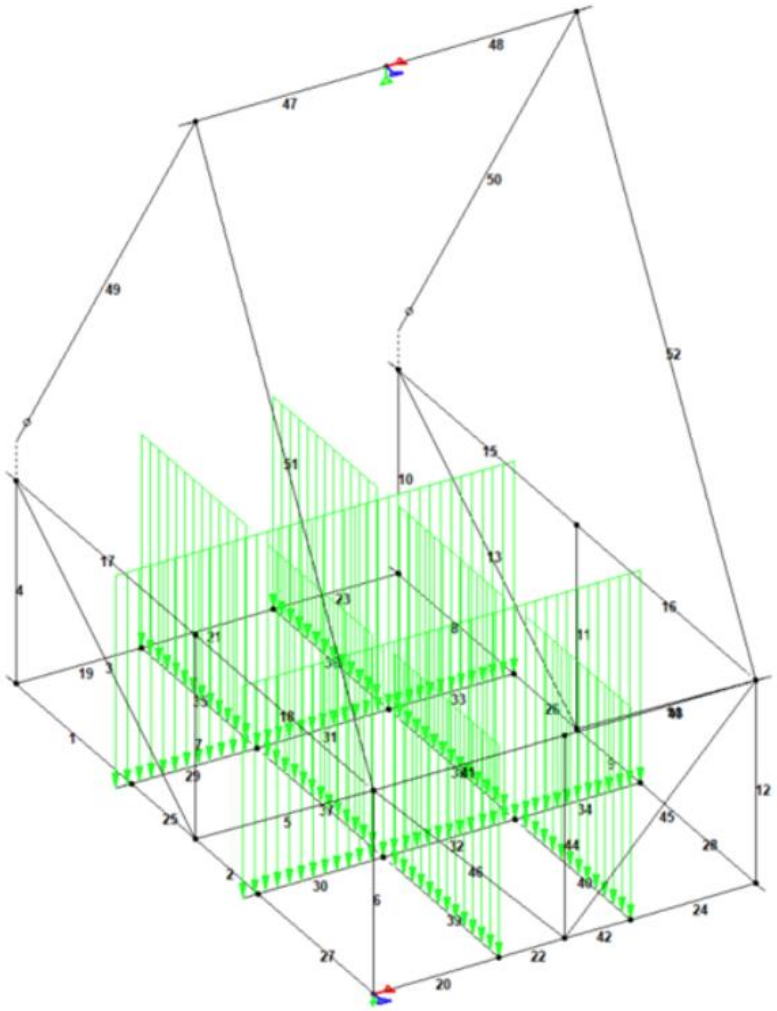

Supplementary Figure 11 - Applied load and beam numbers in Staad.Pro analysis.

DEEPOCEAN

1.4 BEAM-END-FORCES RESULTS

Beam	L/C	Node	Fx kN	Fy kN	Fz kN	Mx kN-m	My kN-m	Mz kN-m
1	3 COMBINATION LOAD CASE 3	1	-13.744	19.52	0.267	0.127	-0.249	9.978
		17	13.744	-17.449	-0.267	-0.127	-0.12	15.553
2	3 COMBINATION LOAD CASE 3	2	-10.847	47.898	1.498	0.275	-0.952	14.487
		19	10.847	-46.849	-1.498	-0.275	-0.097	18.674
3	3 COMBINATION LOAD CASE 3	2	-85.212	1.624	-0.406	-0.007	0.892	-0.389
		4	86.568	0.442	0.406	0.007	0.071	1.788
4	3 COMBINATION LOAD CASE 3	1	-36.79	0.87	13.943	0.251	-8.291	1.72
		4	38.59	-0.87	-13.943	-0.251	-9.835	-0.589
5	3 COMBINATION LOAD CASE 3	2	-88.418	-0.03	-0.613	-0.007	1.058	-1.371
		6	89.774	2.097	0.613	0.007	0.394	-1.149
6	3 COMBINATION LOAD CASE 3	3	-22.543	-1.533	-8.563	0.213	6.636	-1.178
		6	24.343	1.533	8.563	-0.213	4.496	-0.815
7	3 COMBINATION LOAD CASE 3	2	-0.76	-0.368	-0.569	0.012	0.308	-0.475
		5	2.116	0.368	0.569	-0.012	0.432	-0.004
8	3 COMBINATION LOAD CASE 3	7	-13.052	18.21	-0.424	-0.141	0.354	9.438
		18	13.052	-16.139	0.424	0.141	0.231	14.283
9	3 COMBINATION LOAD CASE 3	8	-8.211	45.729	-1.36	-0.297	0.449	13.817
		20	8.211	-44.679	1.36	0.297	0.502	17.825
10	3 COMBINATION LOAD CASE 3	7	-37.395	-0.635	13.395	-0.192	-7.889	0.629
		10	39.196	0.635	-13.395	0.192	-9.524	-1.454
11	3 COMBINATION LOAD CASE 3	8	-0.722	0.402	-0.586	-0.005	0.311	0.527
		11	2.078	-0.402	0.586	0.005	0.451	-0.004
12	3 COMBINATION LOAD CASE 3	9	-22.061	1.676	-8.118	-0.326	6.374	1.252
		12	23.862	-1.676	8.118	0.326	4.179	0.927
13	3 COMBINATION LOAD CASE 3	8	-81.081	1.654	0.222	0	-0.369	-0.313
		10	82.436	0.412	-0.222	0	-0.157	1.785
14	3 COMBINATION LOAD CASE 3	8	-85.949	-0.076	0.207	0.002	-0.495	-1.376
		12	87.304	2.142	-0.207	-0.002	0.005	-1.253
15	3 COMBINATION LOAD CASE 3	10	139.936	2.252	0.049	0.003	-0.319	-2.811
		11	139.936	0.87	-0.049	-0.003	0.216	4.249
16	3 COMBINATION LOAD CASE 3	11	139.35	-2.948	0.452	0.007	-0.221	-4.7
		12	-139.35	5.77	-0.452	-0.007	-0.629	-3.5
17	3 COMBINATION LOAD CASE 3	4	145.181	2.331	-1.112	-0.021	2.317	-2.801
		5	145.181	0.791	1.112	0.021	-0.002	4.404
18	3 COMBINATION LOAD CASE 3	5	144.611	-2.907	-1.48	-0.017	0.014	-4.837
		6	144.611	5.728	1.48	0.017	2.77	-3.285
19	3 COMBINATION LOAD CASE 3	1	1.137	17.27	-0.199	-0.265	-0.028	-1.847
		13	-1.137	-16.07	0.199	0.265	0.187	15.182
20	3 COMBINATION LOAD CASE 3	3	-3.035	5.626	0.45	0.293	-0.201	1.014
		14	3.035	-4.426	-0.45	-0.293	-0.16	3.007
21	3 COMBINATION LOAD CASE 3	13	1.134	-0.323	0.093	0.004	-0.187	-15.195
		15	-1.134	1.583	-0.093	-0.004	0.109	14.394
22	3 COMBINATION LOAD CASE 3	14	-3.032	-13.343	-1.334	-0.589	0.158	-3.023

46	3 COMBINATION LOAD CASE 3	25	-18.919	0.49	0.754	0.001	-0.592	-0.043
		6	20.274	0.783	-0.754	-0.001	-0.753	-0.218
47	3 COMBINATION LOAD CASE 3	27	-2.389	191.574	0.729	0.164	2.641	-26.43
		29	2.389	195.3	-0.729	-0.164	-3.603	-228.907
48	3 COMBINATION LOAD CASE 3	29	-0.906	193.039	-1.689	0.164	3.603	228.907
		28	0.906	189.313	1.689	-0.164	-1.373	23.445
49	3 COMBINATION LOAD CASE 3	4	106.651	1.013	2.389	-1.7	-1.09	0
		27	109.621	0.923	-2.389	1.7	-7.574	0.164
50	3 COMBINATION LOAD CASE 3	10	104.484	0.923	-0.906	1.174	-1.337	0
		28	107.455	1.013	0.906	-1.174	4.623	-0.164
51*	3 COMBINATION LOAD CASE 3	27	115.886	0	0	0	0	0
		6	115.886	0	0	0	0	0
52	3 COMBINATION LOAD CASE 3	28	115.307	0	0	0	0	0
		12	115.307	0	0	0	0	0
* Tension Only Members – representing sling.								

Supplementary Table 11 - Beam end forces results.

Crane specifications

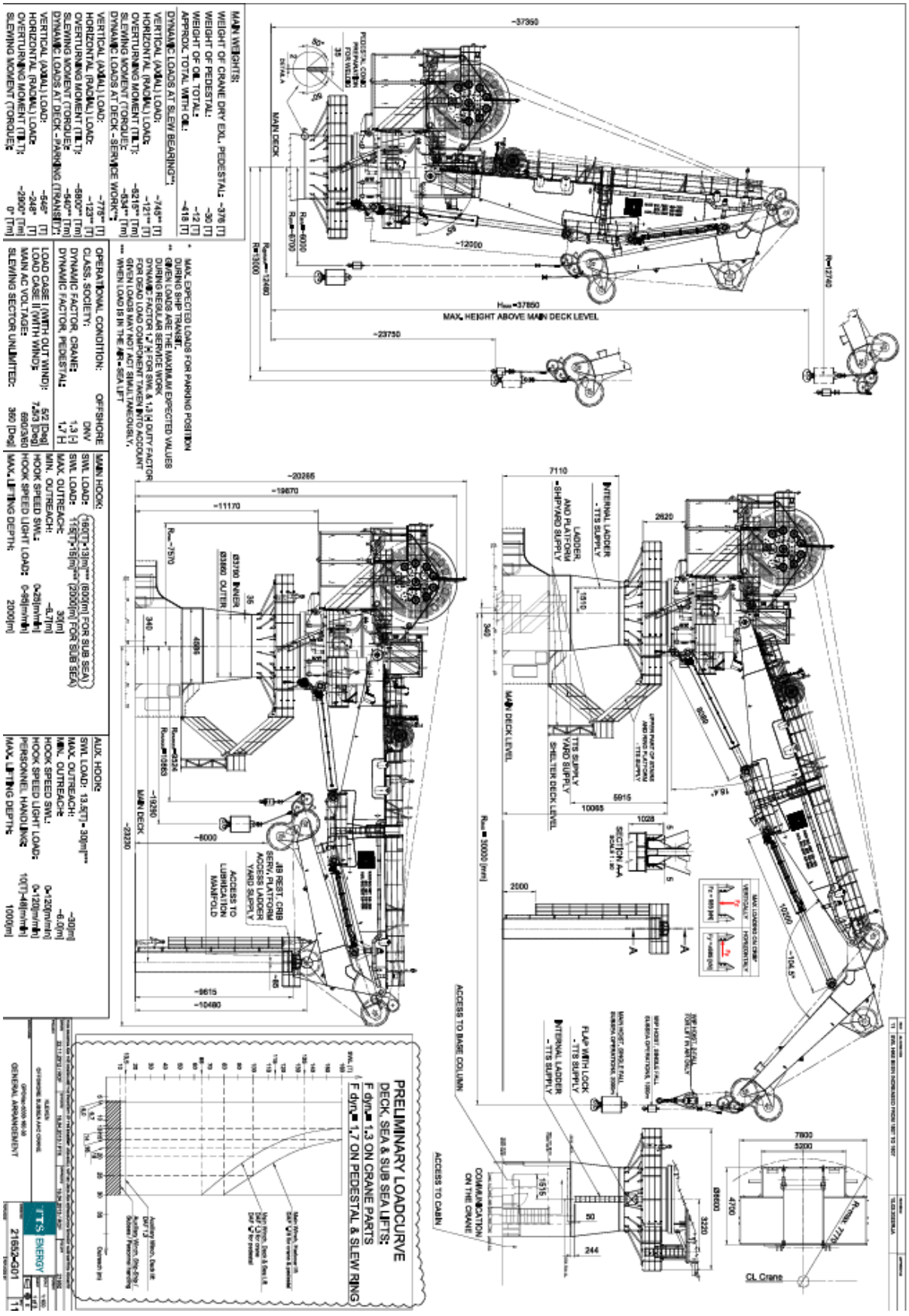

Supplementary Figure 12 - Crane specification, obtained from DeepOcean.

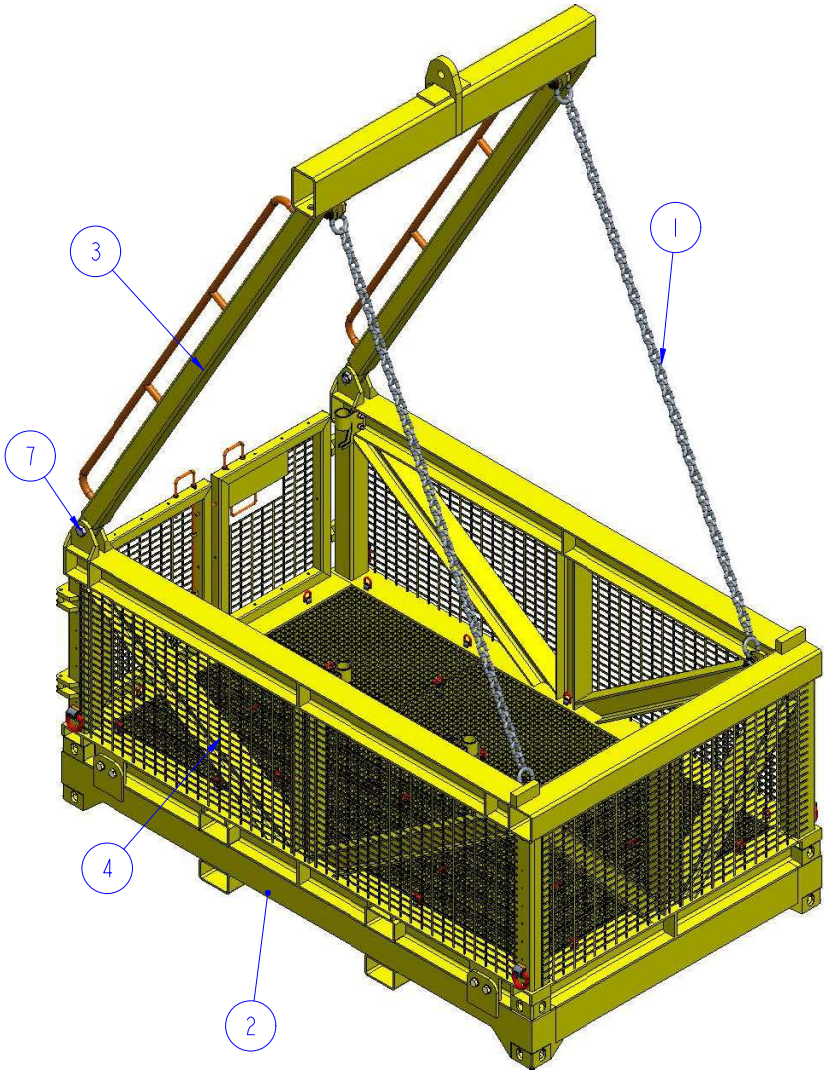

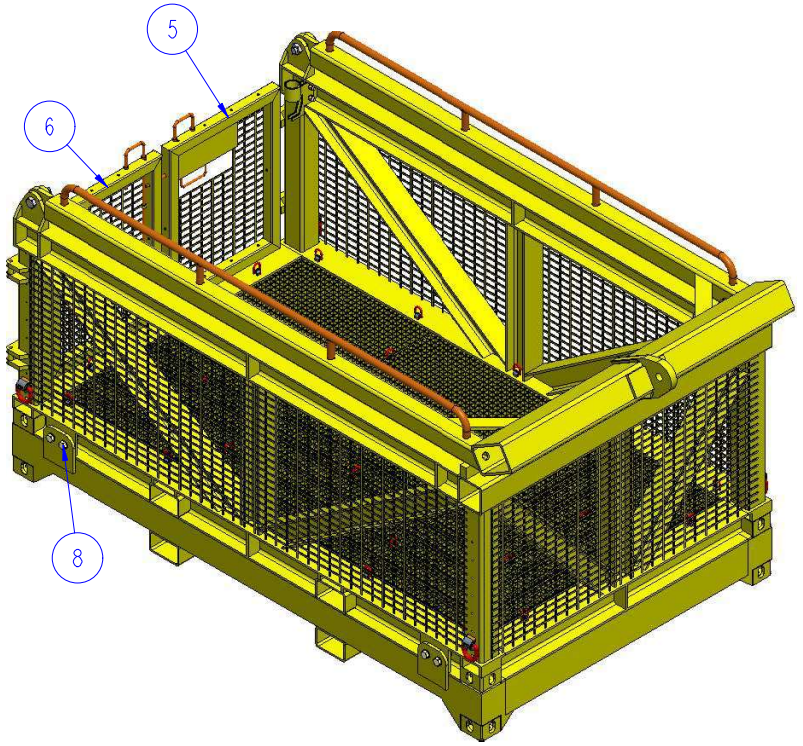

Pos	Ant	Artikell/Modell	Beskrivelse	Materiale	Dimensjon
8	8	M30_BOLT	-	S355J2	-
7	2	M39_BOLT	-	S355J2	-
6	1	Right Door	-	S355J2	-
5	1	Left Door	-	S355J2	-
4	1	Basket	-	S355J2	-
3	1	A Frame	-	S355J2	-
2	1	Extra Weight	-	S355J2	-
1	2	Chain	-	Grade 8	L=3500

Konstr	Tegnet VSF	Revisjon	Vekt	Skala 1:30	Format A3	Blad.nr 1(67)
Høgskulen på Vestlandet IMM	Artikell/Modell SUBSEA_BASKET				Dato 19-Apr-24	
	Beskrivelse				Tegning SUBSEA_BASKET	

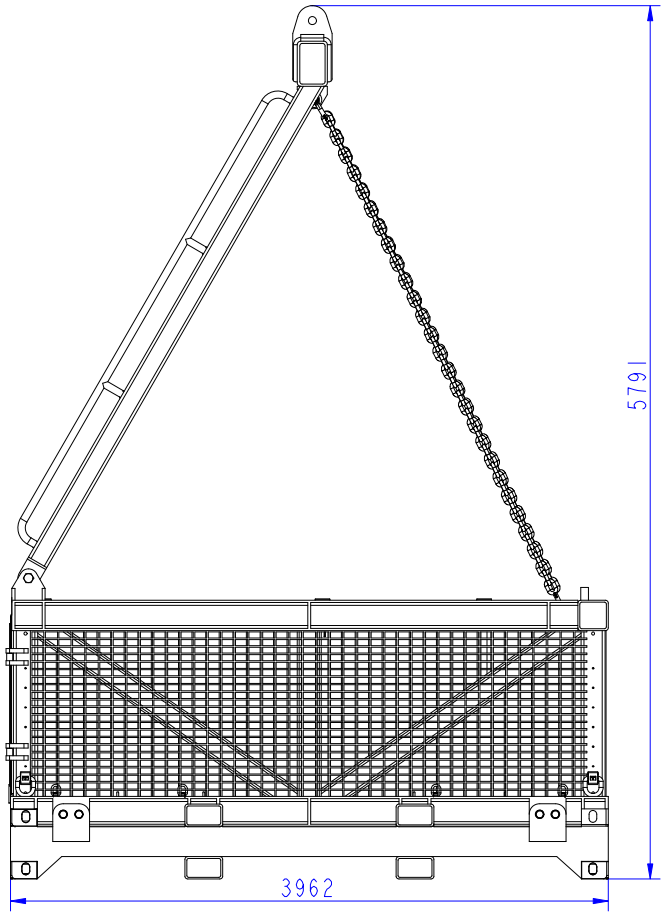

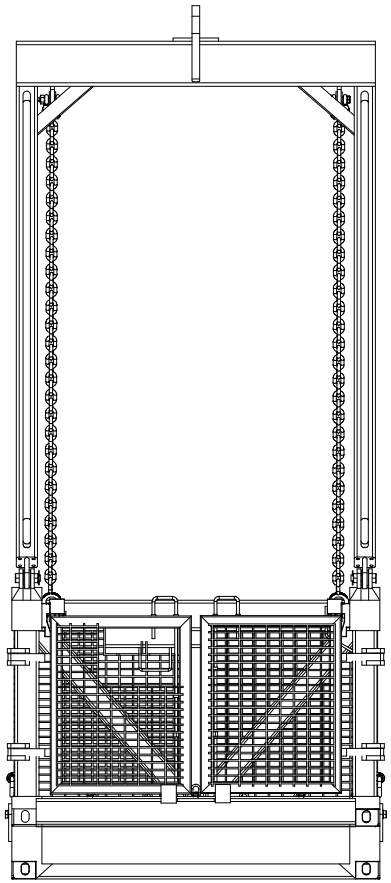

Notes:
1. Material certificates according to NS-EN 10204 3.1.
2. Break sharp edges.
3. All welds need to be sealed.
4. Fabrication, welding and inspection according to NORSOK Standard M-101, stuctural steel.
5. NDT: Category "C" U.O.S.
6. Surface treatment: Galvanization.

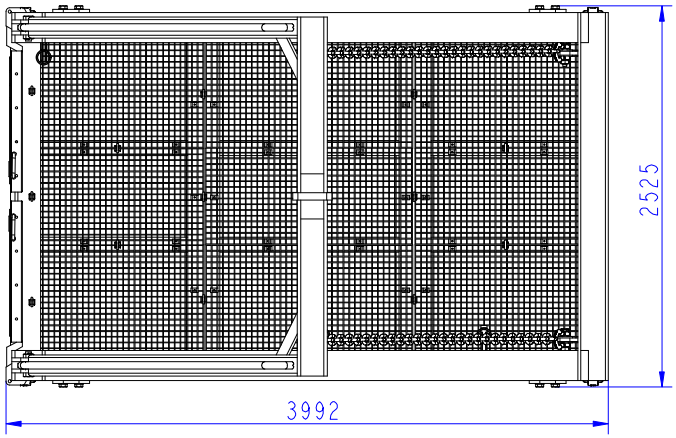

Pos	Ant	Artikell/Modell	Beskrivelse	Materiale	Dimensjon

Konstr	Tegnet	Revisjon	Vekt	Skala	Format	Blad.nr
	VSF			0.030	A3	2(67)

	Artikell/Modell	Dato
Høgskulen på Vestlandet IMM	SUBSEA_BASKET	19-Apr-24
	Beskrivelse	Tegning
		SUBSEA_BASKET

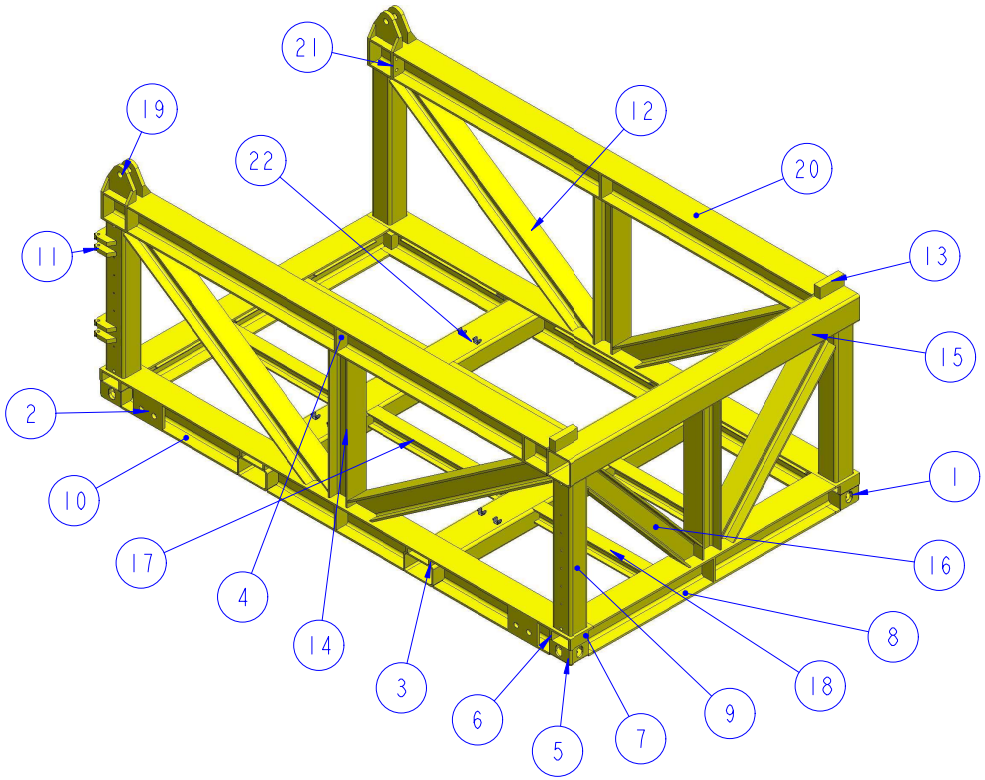

Pos	Ant	Artikell/Modell	Beskrivelse	Materiale	Dimensjon
22	2	BEAM_11	RHS 250x150x12,5	S355J2	L=2440
21	3	GW_STIFFENER	-	S355J2	-
20	2	BEAM_10	HEB200	S355J2	L=3752
19	4	PADEYE4ASS	-	S355J2	-
18	4	BEAM_9	HEB100	S355J2	L=1052
17	2	BEAM_8	HEB200	S355J2	L=1150
16	2	BEAM_7	HEB160	S355J2	-
15	1	BEAM_6	SHS 200x200x12,5	S355J2	L=2440
14	3	BEAM_5	HEB160	S355J2	L=1100
13	2	A-FRAME_BLOCK	PL200x50x85	S355J2	200x50x85
12	4	BEAM_4	HEB160	S355J2	-
11	8	DOOR_HINGE_2	-	S355J2	-
10	2	BEAM_3	HEB200	S355J2	-
9	4	BEAM_2	SHS160	S355J2	-
8	2	BEAM_1	HEB200	S355J2	-
7	4	STIFFENER_ISO_1	-	S355J2	-
6	8	STIFFENER_ISO_2	-	S355J2	-
5	2	ISO_CORNER_BL	-	CAST IRON	-
4	12	STIFFENER_200	-	S355J2	-
3	8	FORKLIFT_POCKET_STIFFENER		S355J2	-
2	4	BOLT_PLATE	-	S355J2	-
1	2	ISO_CORNER_BR	-	CAST IRON	-

Konstr	Tegnet VSF	Revisjon	Vekt	Skala 0.033	Format A3 / Blad.nr 3(67)
Høgskulen på Vestlandet IMM	Artikell/Modell SUBSEA_BASKET				Dato 24-Apr-24
	Beskrivelse				Tegning SUBSEA_BASKET

Note: Joint edges below 60° can be welded as butt welds. Joint edges above 60° are welded as fillet welds.

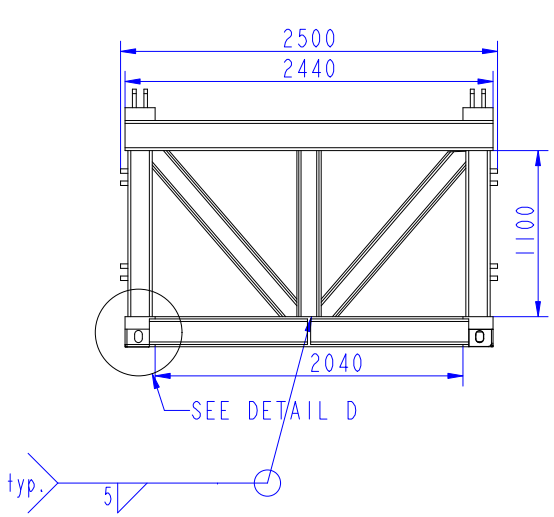

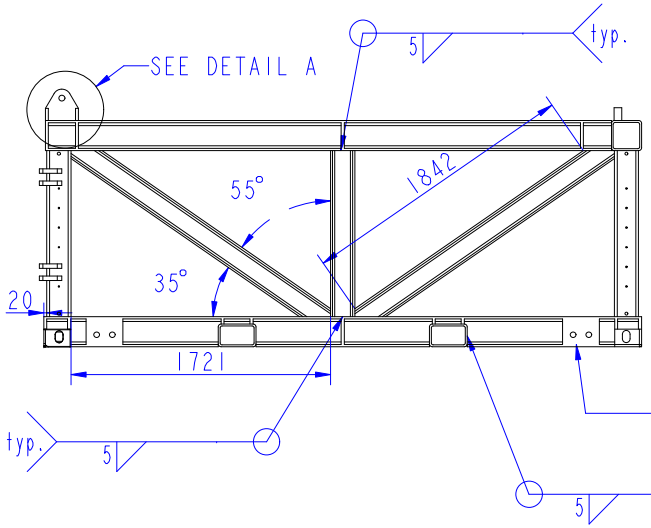

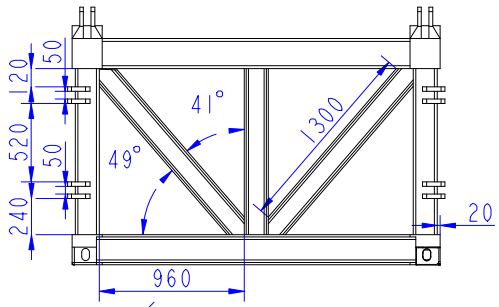

typ.
5
typ.

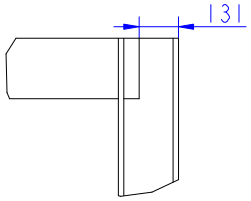

DETAIL C
SCALE 0.060

SEE DETAIL C

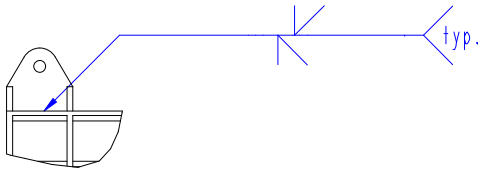

DETAIL A
SCALE 0.060

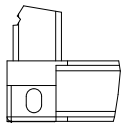

DETAIL D
SCALE 0.060

Pos	Ant	Artikell/Modell	Beskrivelse	Materiale	Dimensjon

Konstr	Tegnet VSF	Revisjon	Vekt	Skala 0.030	Format A3	Blad.nr 4(67)
Høgskulen på Vestlandet IMM		Artikell/Modell SUBSEA_BASKET			Dato 24-Apr-24	
		Beskrivelse			Tegning SUBSEA_BASKET	

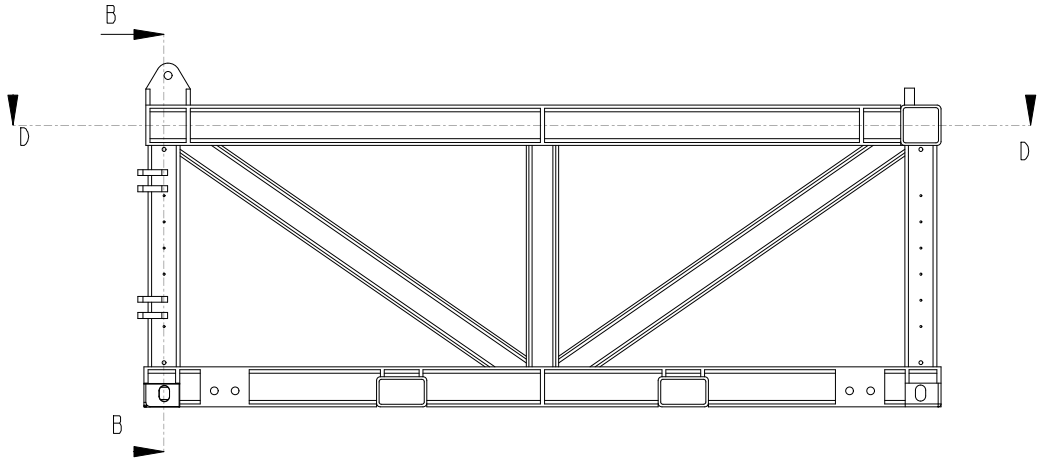

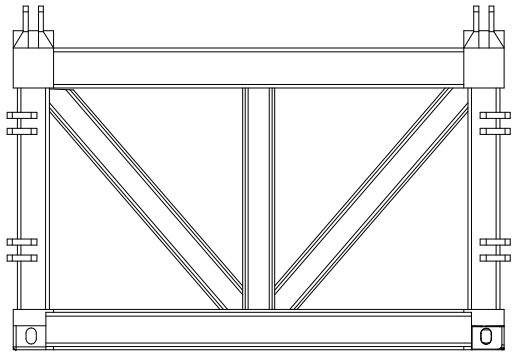

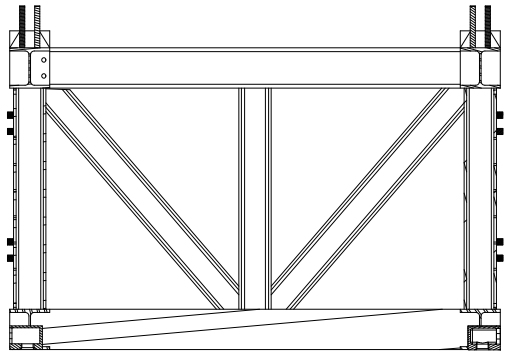

Section B-B

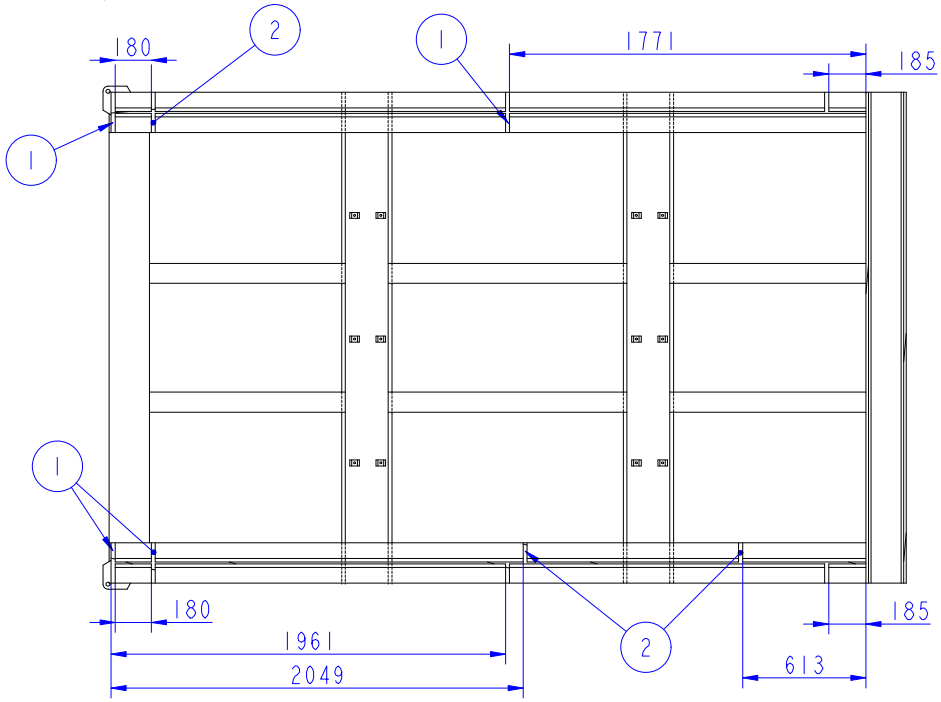

Section D-D

2	3	GW_STIFFENER	-	S355J2	-
1	12	STIFFENER_200	-	S355J2	-
Pos	Ant	Artikell/Modell	Beskrivelse	Materiale	Dimensjon

Konstr	Tegnet VSF	Revisjon	Vekt	Skala 0.040	Format A3	Blad.nr 5(67)
Høgskulen på Vestlandet IMM	Artikell/Modell SUBSEA_BASKET				Dato 24-Apr-24	
	Beskrivelse				Tegning SUBSEA_BASKET	

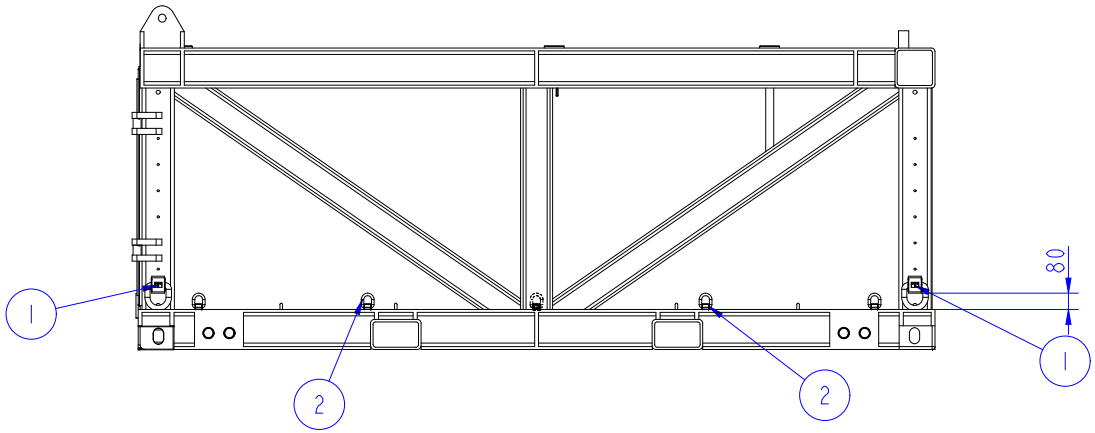

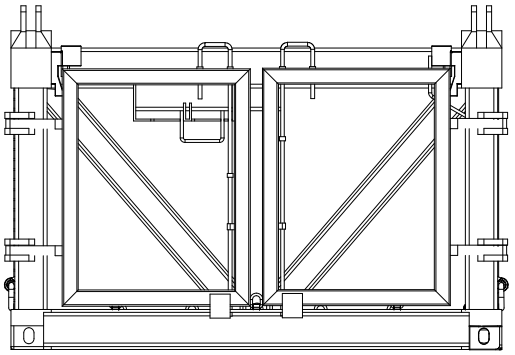

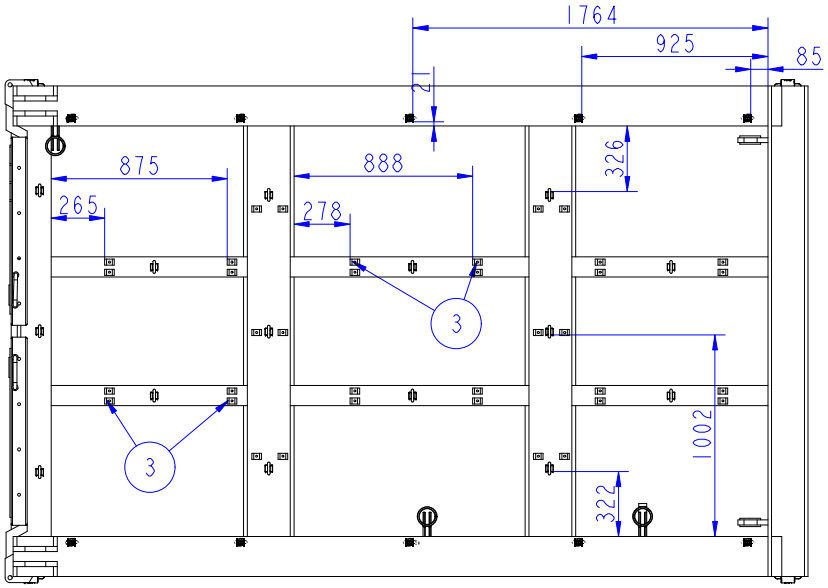

Pos	Ant	Artikell/Modell	Beskrivelse	Materiale	Dimensjon
3	24	Grating clamp	-	-	-
2	35	Small D-ring	-	-	-
1	4	Large D-ring	-	-	-

Konstr	Tegnet VSF	Revisjon	Vekt	Skala 0.040	Format A3	Blad.nr 6(67)
Høgskulen på Vestlandet IMM	Artikell/Modell SUBSEA_BASKET				Dato 29-Apr-24	
	Beskrivelse				Tegning SUBSEA_BASKET	

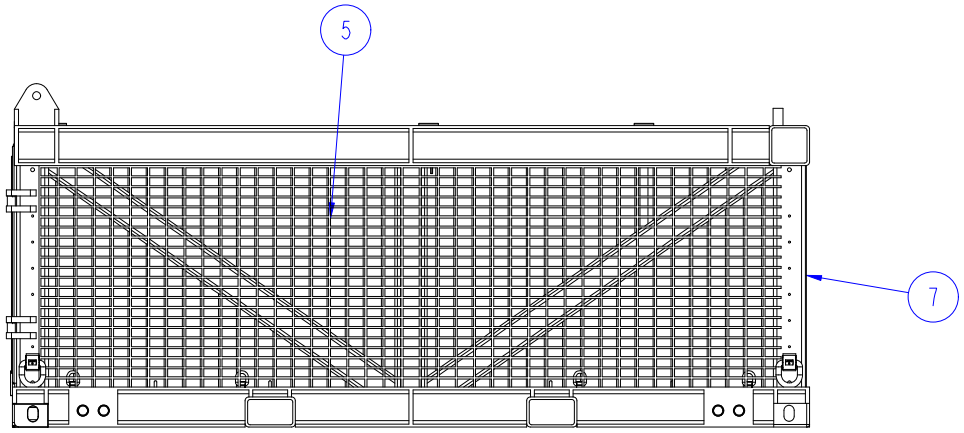

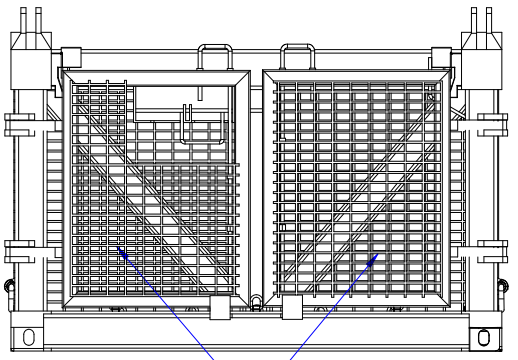

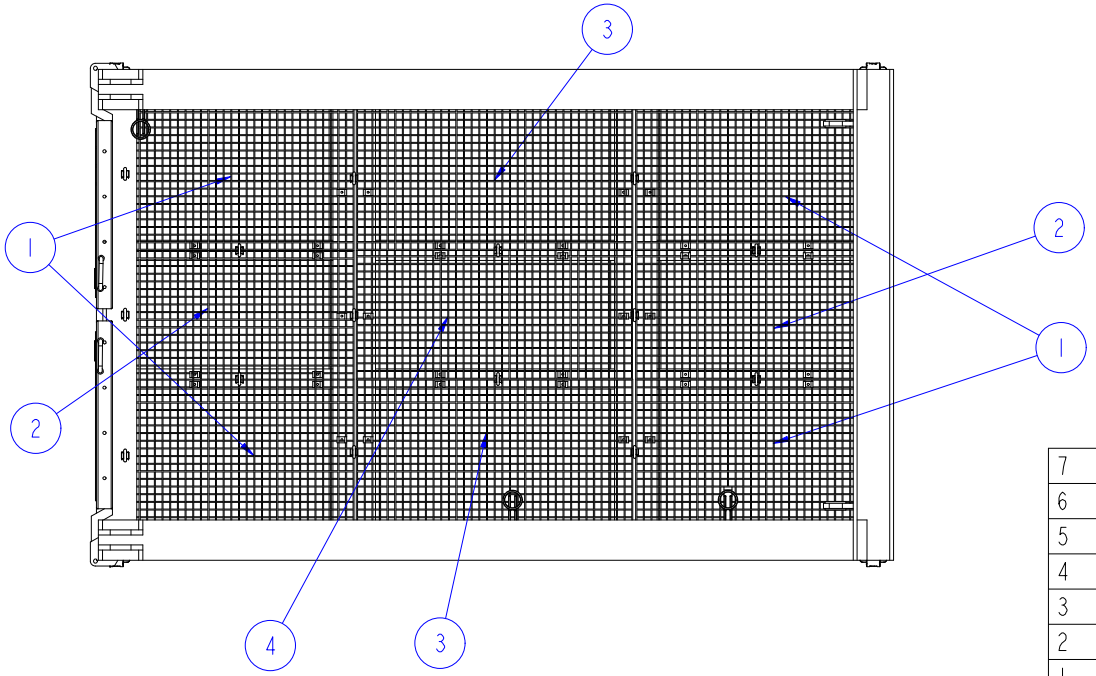

Pos	Ant	Artikell/Modell	Beskrivelse	Materiale	Dimensjon
7	1	METAL_GRATING	Expanded metal		2240x1100
6	2	METAL GRATING	Expanded metal		840x1075
5	2	METAL_GRATING	Expanded metal		3690x1100
4	1	GRP_GRATING	-	GRP	640x1373x25
3	2	GRP_GRATING	-	GRP	765x1373x25
2	2	GRP_GRATING	-	GRP	649x1159x25
1	4	GRP_GRATING	-	GRP	765x1159x25

Konstr	Tegnet VSF	Revisjon	Vekt	Skala 0.040	Format A3	Blad.nr 7(67)
Høgskulen på Vestlandet IMM	Artikell/Modell SUBSEA_BASKET				Dato 29-Apr-24	
	Beskrivelse				Tegning SUBSEA_BASKET	

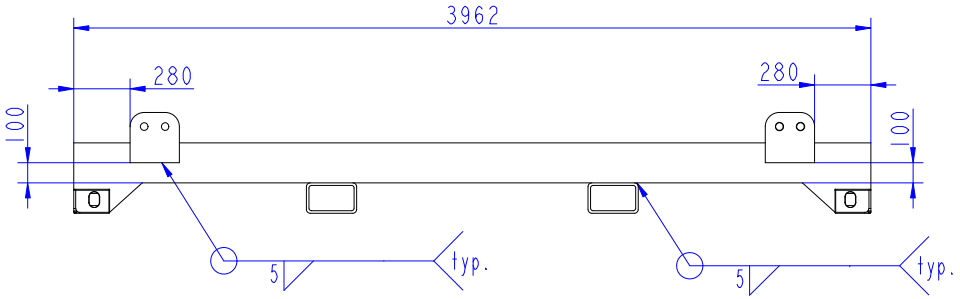

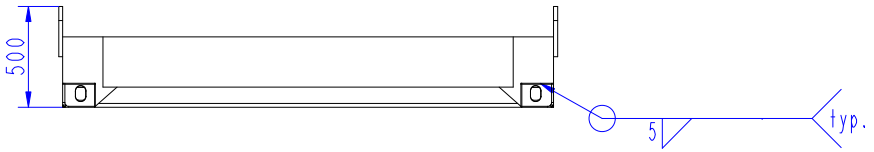

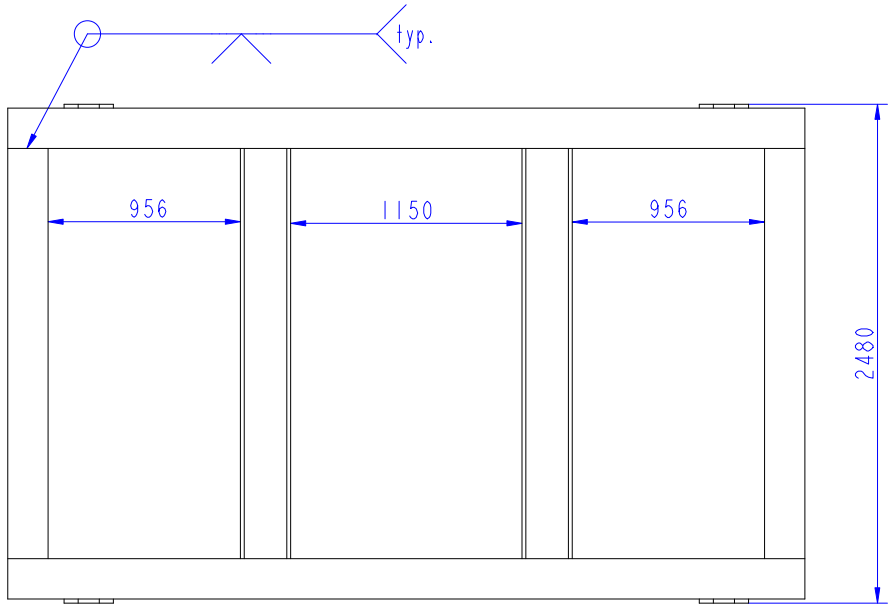

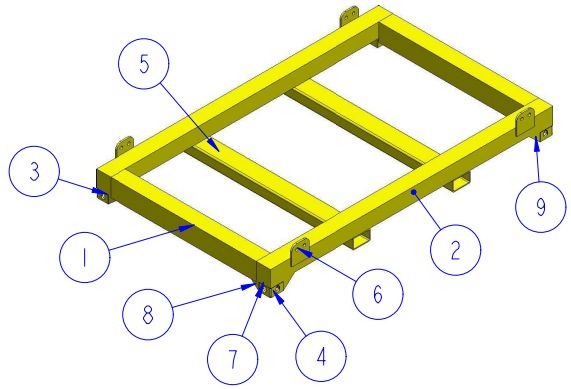

Pos	Ant	Artikell/Modell	Beskrivelse	Materiale	Dimensjon
9	4	ISO_STIFFENER_2	-	S355J2	-
8	4	ISO_STIFFENER	-	S355J2	-
7	4	ISO_PLATE	PL20x200x200	S355J2	20x200x200
6	4	Bolt_Plate_2	-	S355J2	-
5	2	BEAM_11	-	S355J2	-
4	2	ISO_CORNER	-	Cast Iron	-
3	2	ISO_CORNER	-	Cast Iron	-
2	2	PLATE_STEEL	PL200x200x3962	S355J2	200x200x3962
1	2	PLATE_STEEL	PL200x250x2040	S355J2	200x250x2040

Konstr	Tegnet	Revisjon	Vekt	Skala	Format	Blad.nr
	VSF			0.040	A3	8(67)

Høgskulen på Vestlandet
IMM

Artikell/Modell: EXTRA__WEIGHT
Beskrivelse:

Dato: 29-Apr-24
Tegning: SUBSEA_BASKET

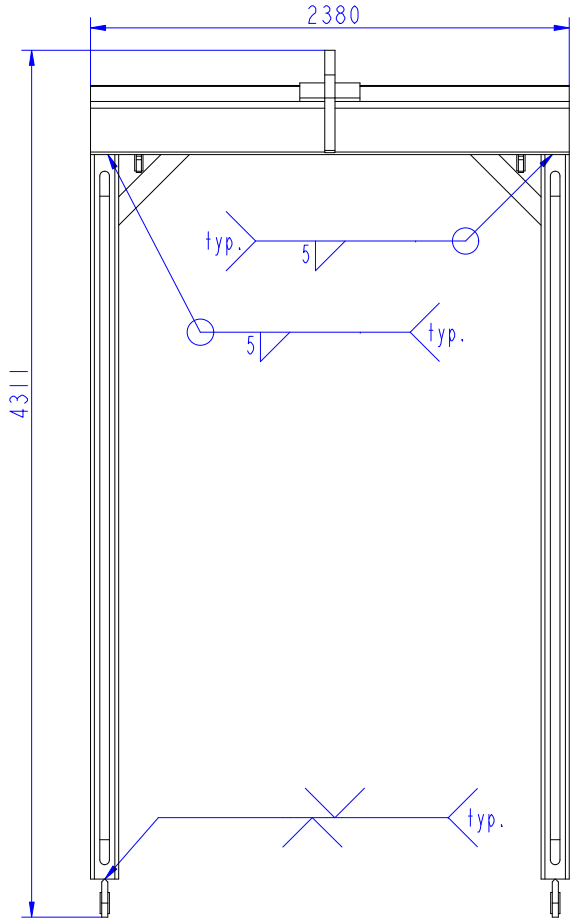

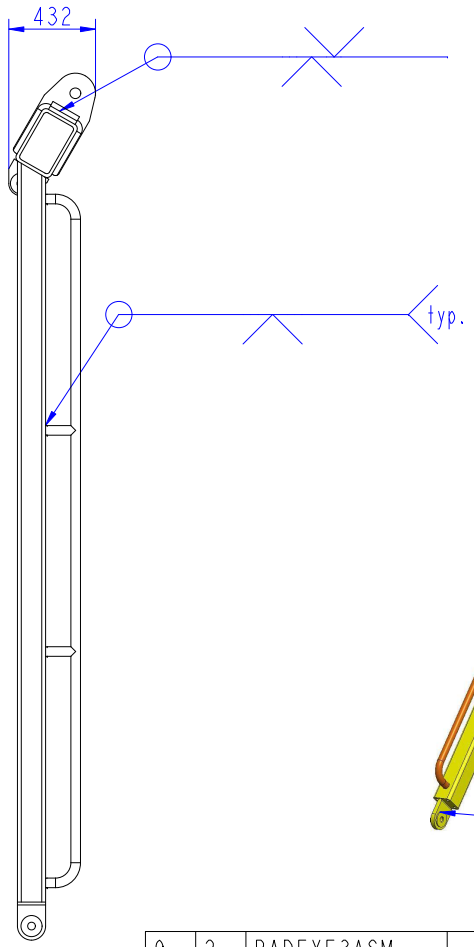

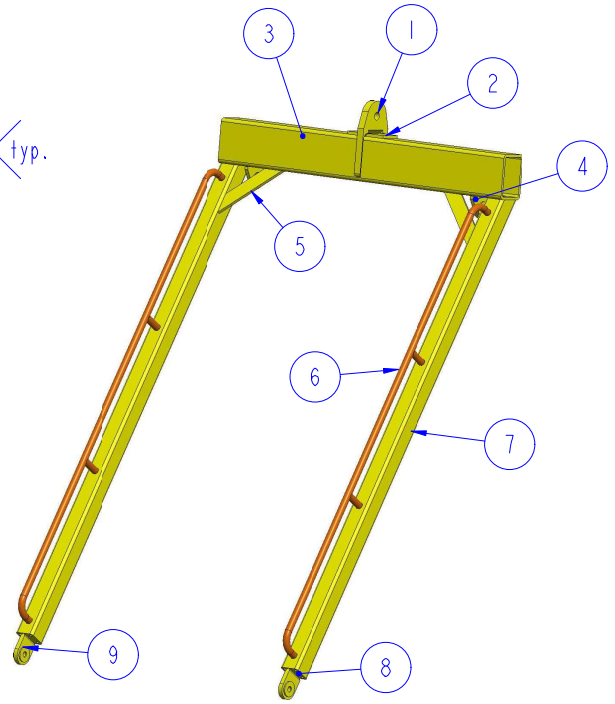

Pos	Ant	Artikell/Modell	Beskrivelse	Materiale	Dimensjon
9	2	PADEYE3ASM	-	S355J2	-
8	2	ENDPLATE_AFRAME	-	S355J2	-
7	2	AFRAME_SHS	-	S355J2	-
6	1	RAIL_AFRAME	-	S355J2	-
5	2	A_FRAME_STIFFENER	-	S355J2	-
4	2	PADEYE2ASS	-	S355J2	-
3	1	SPREAD_BEAM	-	S355J2	-
2	1	PADEYE1_PATCH	PL20x152x300	S355J2	300x152x20
1	1	PADEYE1	-	S355J2	-

Konstr	Tegnet	Revisjon	Vekt	Skala	Format	Blad.nr
	VSF			0.040	A3	9(67)

Høgskulen på Vestlandet IMM	Artikell/Modell: A_FRAME Beskrivelse:	Dato: 30-Apr-24 Tegning: SUBSEA_BASKET

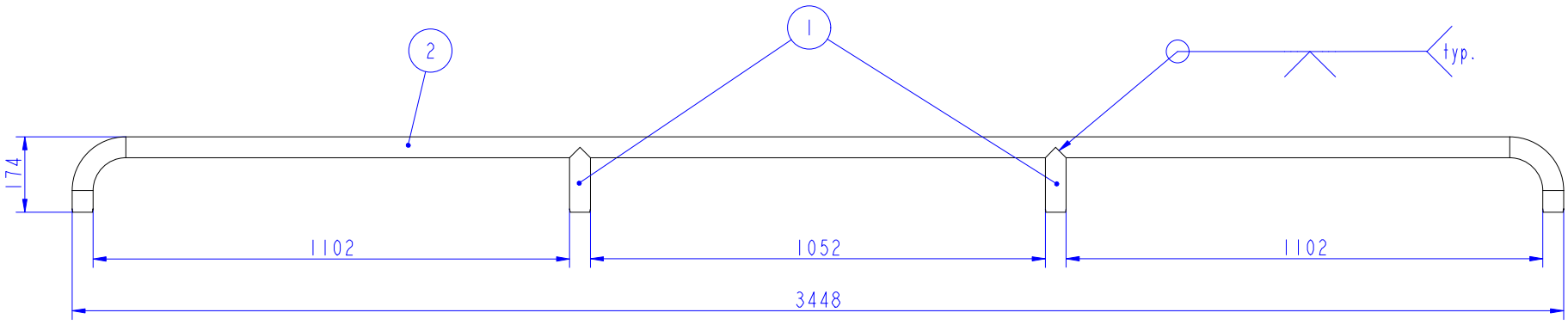

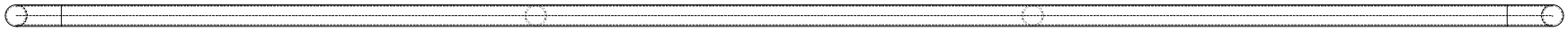

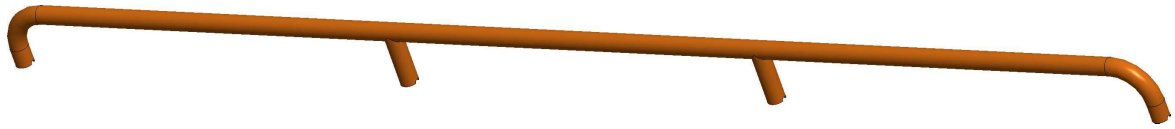

Pos	Ant	Artikell/Modell	Beskrivelse	Materiale	Dimensjon
2	1	RAIL_AFRAME	Welded steel pipe	S235JRH	48,3x2,9
1	2	RAIL_AFRAME2	Welded steel pipe	S235JRH	48,3x2,9

Konstr	Tegnet VSF	Revisjon	Vekt	Skala 0.100	Format A3	Blad.nr 10(67)
Høgskulen på Vestlandet IMM	Artikell/Modell RAIL_AFRAME				Dato 24-Apr-24	
	Beskrivelse				Tegning SUBSEA_BASKET	

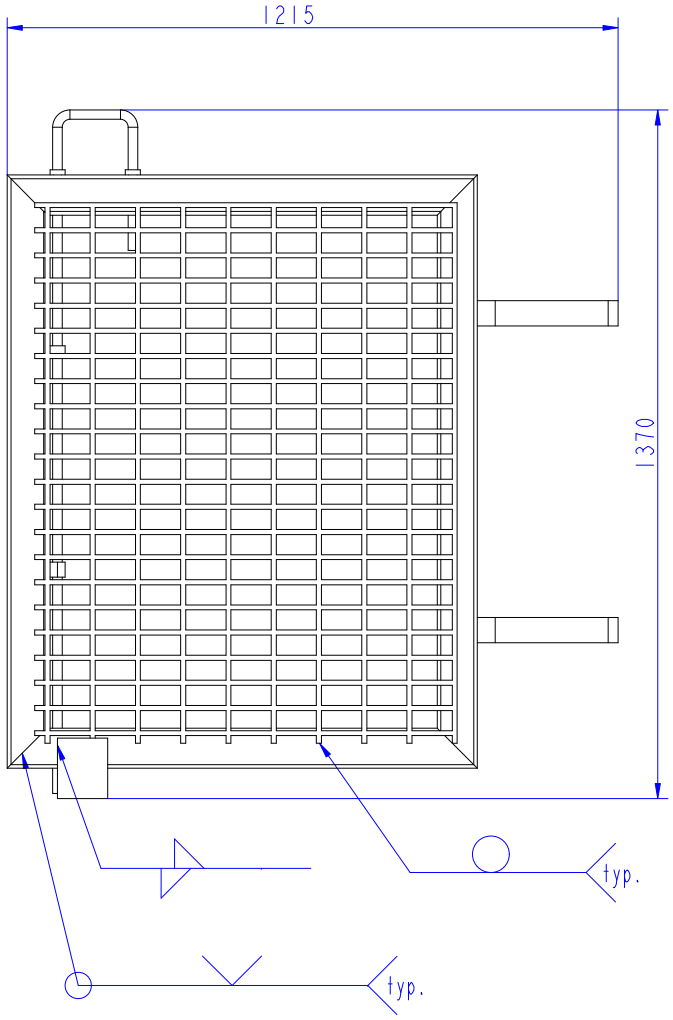

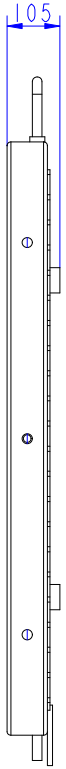

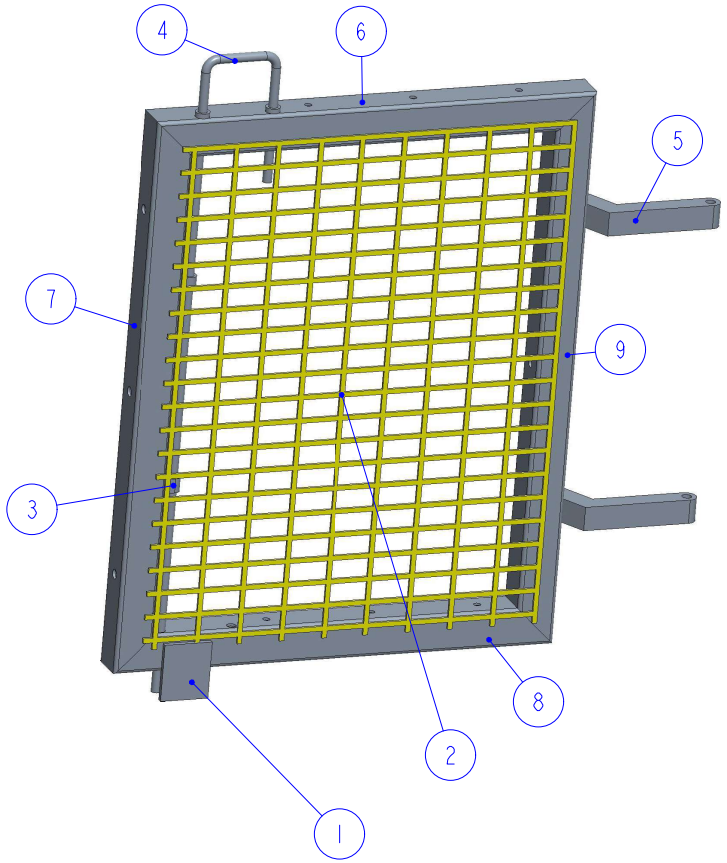

Pos	Ant	Artikell/Modell	Beskrivelse	Materiale	Dimensjon
9	1	DOOR_BEAM_4	SHS80x80x5	S355J2	-
8	1	DOOR_BEAM_3	SHS80x80x5	S355J2	-
7	1	DOOR_BEAM_2	SHS80x80x5	S355J2	-
6	1	DOOR_BEAM_1	SHS80x80x5	S355J2	-
5	2	HINGEDOOR	-	S355J2	-
4	1	HANDLEDOORRIGHT	-	S355J2	-
3	1	GUIDEFORLOCK	-	S355J2	-
2	1	GRATINGRIGHT2	EXPANDED METAL	SAE-304	-
1	1	DOORSTOPPER	-	S355J2	10x120x100

Konstr	Tegnet	Revisjon	Vekt	Skala	Format	Blad.nr
	OOB			0.130	A3	11(67)

Høgskulen på Vestlandet IMM	Artikell/Modell: DOORASSRIGHT Beskrivelse:	Dato: 01-May-24 Tegning: SUBSEA_BASKET

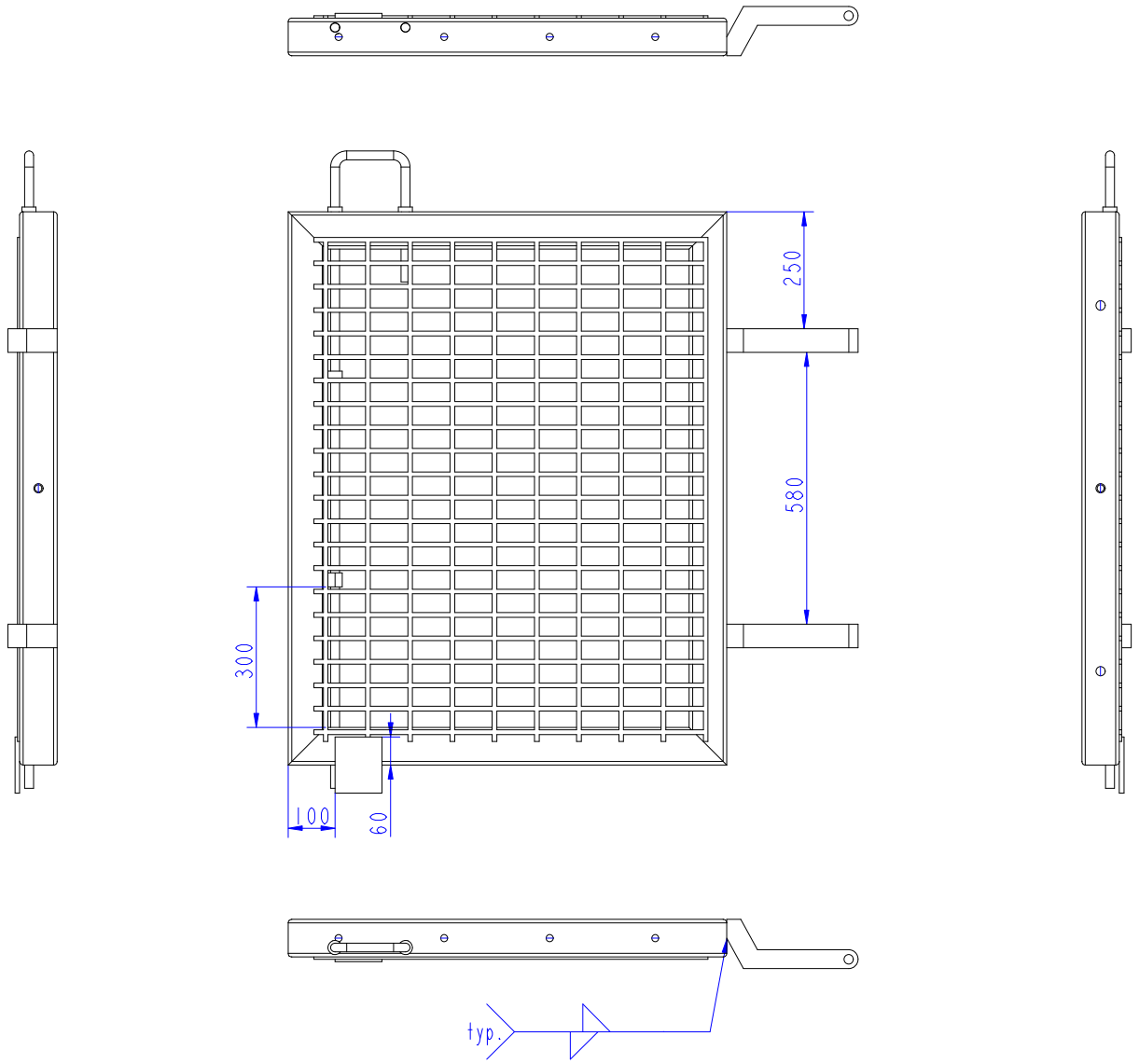

Pos	Ant	Artikell/Modell	Beskrivelse	Materiale	Dimensjon
Konstr	Tegnet OOB	Revisjon	Vekt	Skala 0.100	Format A3	Blad.nr 12(67)
Høgskulen på Vestlandet IMM		Artikell/Modell DOORASSRIGHT			Dato 01-May-24
		Beskrivelse			Tegning SUBSEA_BASKET

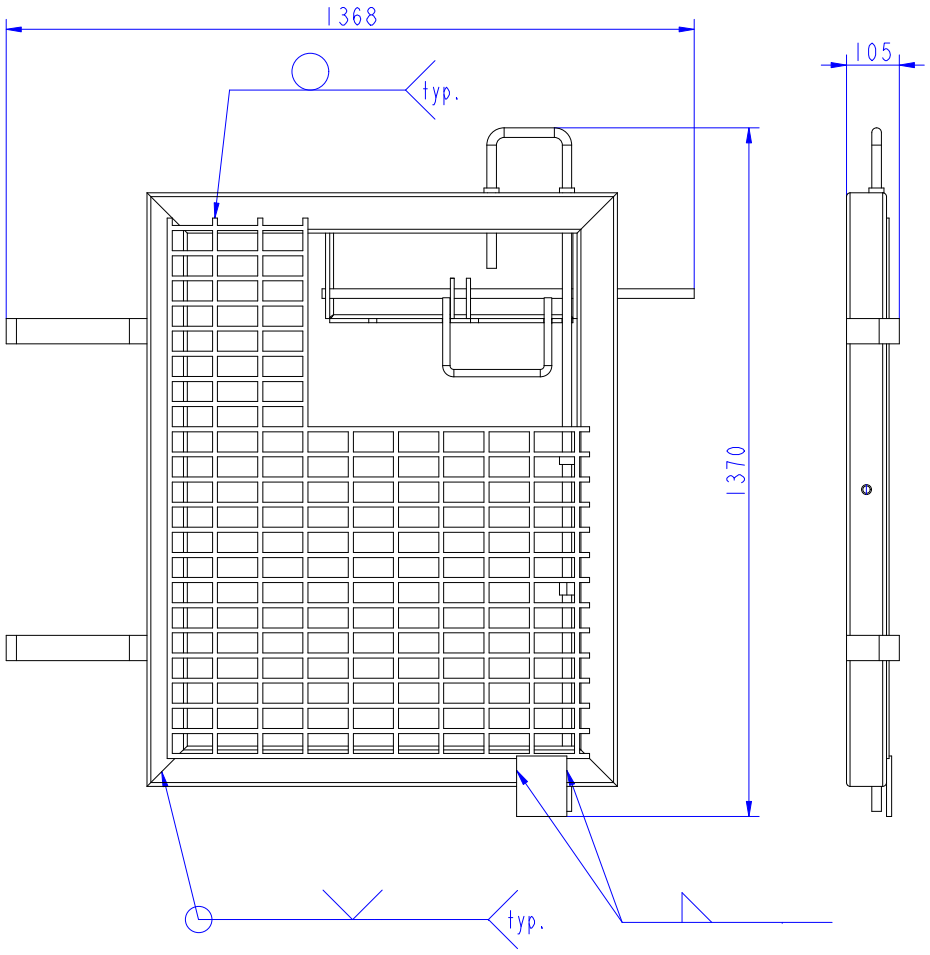

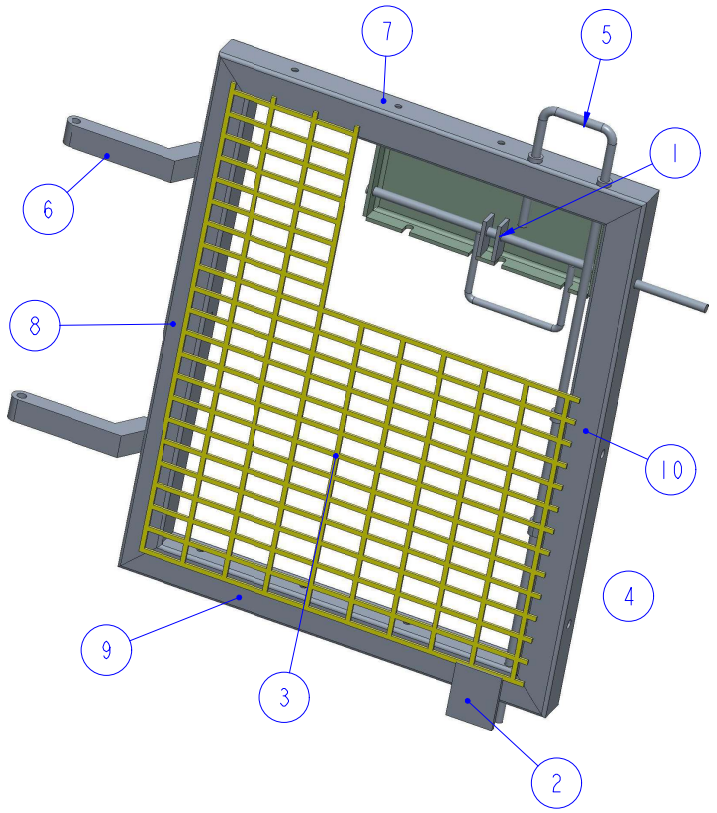

Pos	Ant	Artikell/Modell	Beskrivelse	Materiale	Dimensjon
10	1	DOOR_BEAM_4	SHS 80x80x5	S355J2	-
9	1	DOOR_BEAM_3	SHS 80x80x5	S355J2	-
8	1	DOOR_BEAM_2	SHS 80x80x5	S355J2	-
7	1	DOOR_BEAM_1	SHS 80x80x5	S355J2	-
6	2	HINGEDOOR	-	S355J2	-
5	1	HANDLEDOORLEFT	-	S355J2	-
4	1	GUIDEFORLOCK	-	S355J2	-
3	1	GRATING	EXPANDED METAL	SAE-304	-
2	1	DOORSTOPPER	-	S355J2	10x120x100
1	1	ASSEMBLYLOCK	-	S355J2	-

Konstr	Tegnet	Revisjon	Vekt	Skala	Format	Blad.nr
	OOB			0.100	A3	13(67)

Høgskulen på Vestlandet IMM	Artikell/Modell DOORASSLEFT	Dato 29-Apr-24
	Beskrivelse	Tegning SUBSEA_BASKET

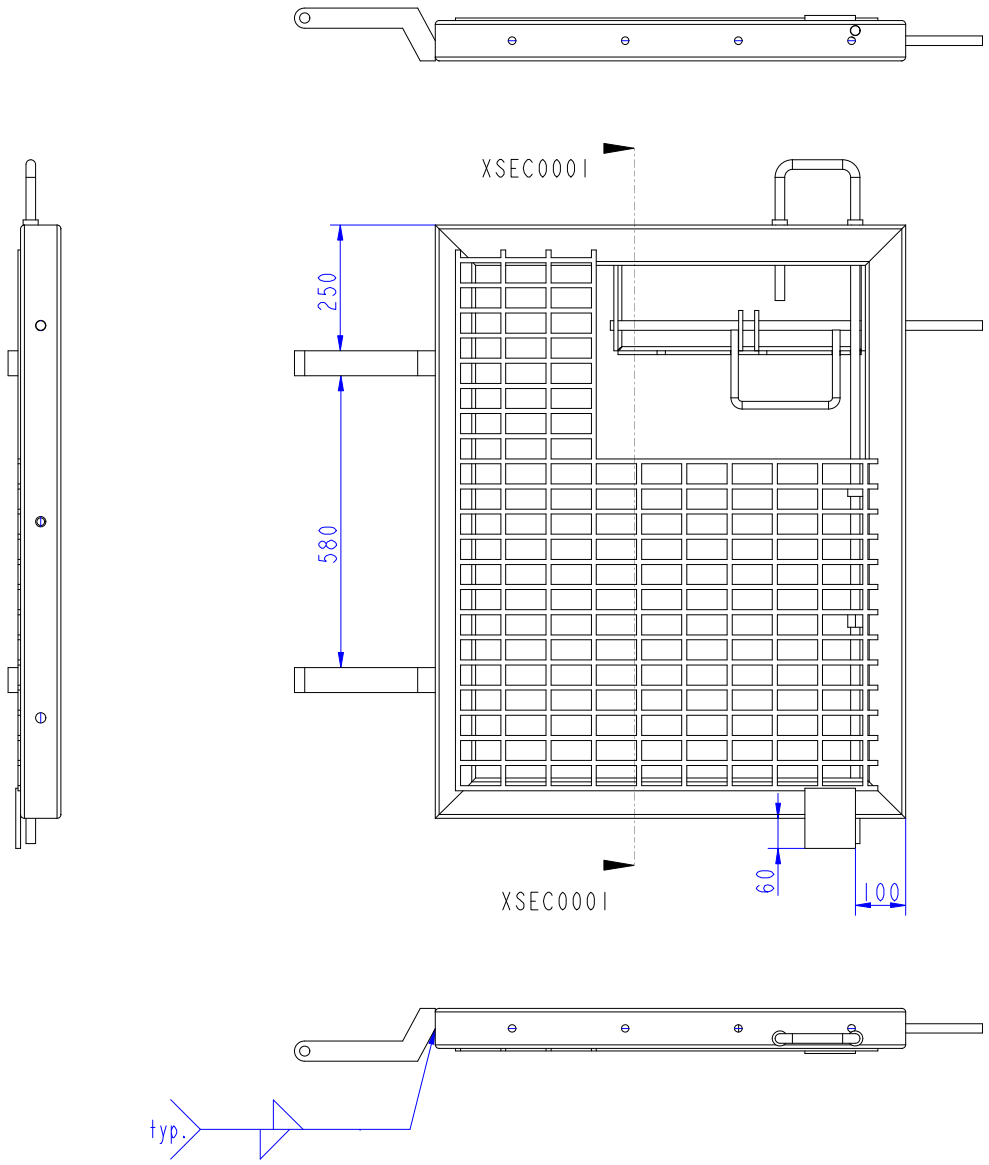

SECTION XSEC0001-XSEC0001

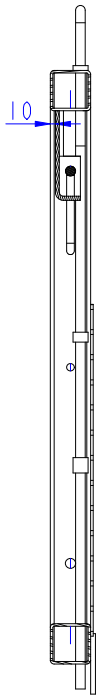

Pos	Ant	Artikell/Modell	Beskrivelse	Materiale	Dimensjon
Konstr	Tegnet: OOB	Revisjon	Vekt	Skala: 0.100	Format: A3	Blad.nr: 14(67)
Høgskulen på Vestlandet IMM		Artikell/Modell: DOORASSLEFT			Dato: 29-Apr-24
		Beskrivelse			Tegning: SUBSEA_BASKET

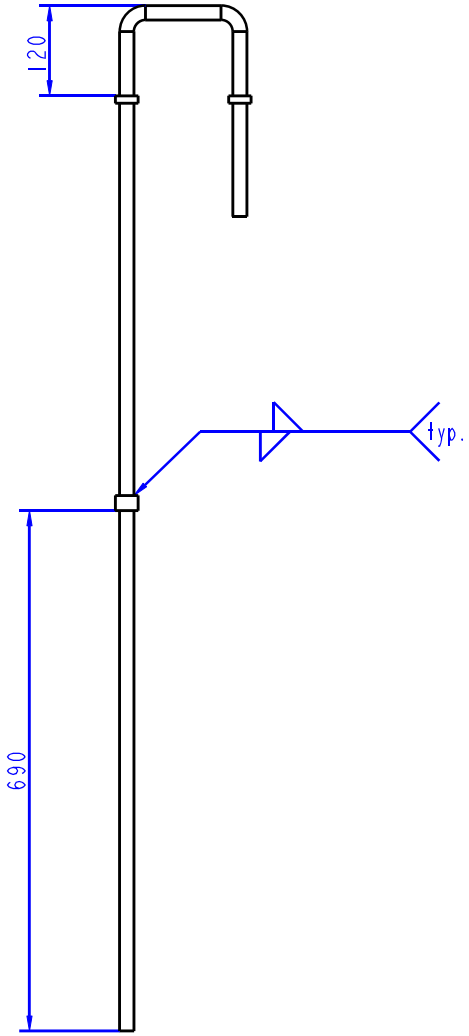

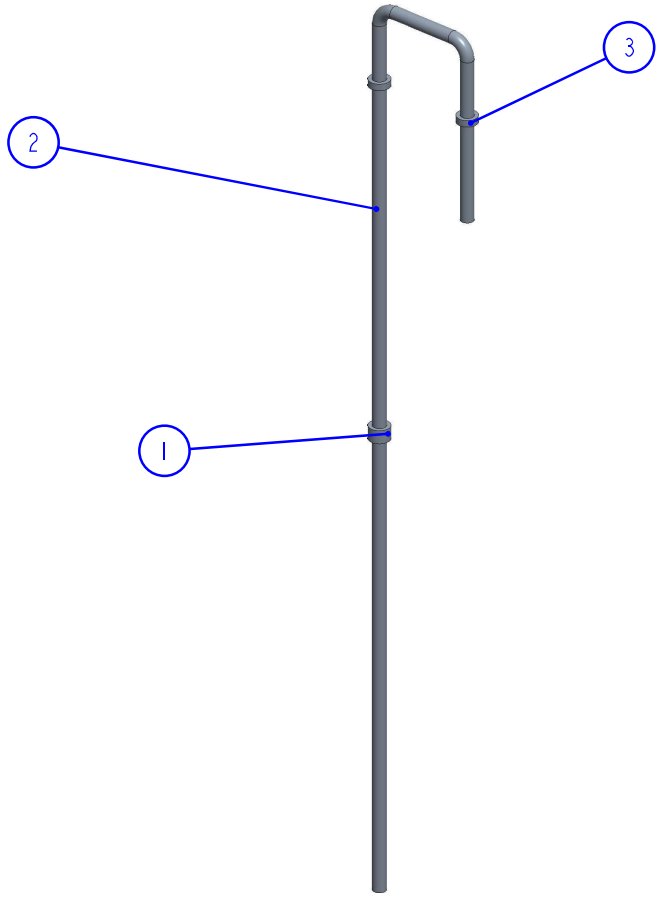

Pos	Ant	Artikell/Modell	Beskrivelse	Materiale	Dimensjon
2	1	HANDLEDOOR	-	S355J2	-
1	1	RINGFORLOCK	-	S355J2	-

Konstr	Tegnet: OOB	Revisjon	Vekt	Skala: 0.150	Format: A3 / Blad.nr: 15(67)
Høgskulen på Vestlandet IMM	Artikell/Modell: HANDLEDOORLEFT	Beskrivelse			Dato: 29-Apr-24
					Tegning: SUBSEA_BASKET

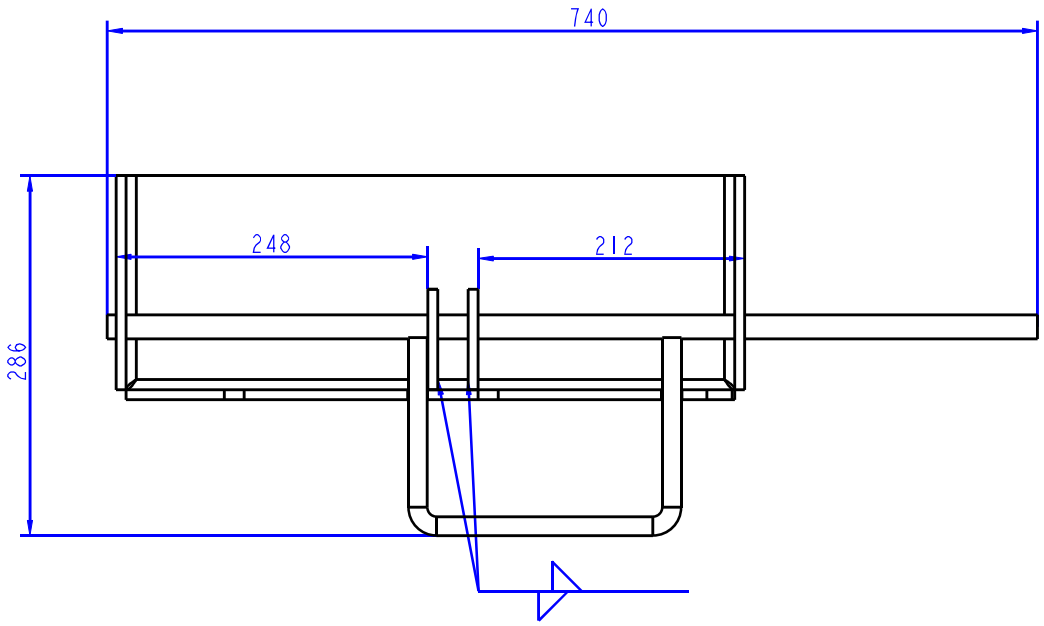

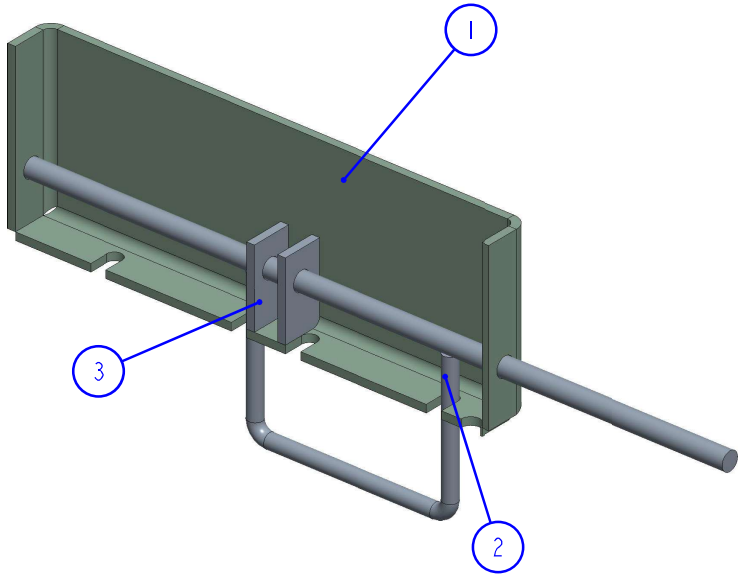

Pos	Ant	Artikell/Modell	Beskrivelse	Materiale	Dimensjon
3	2	LOCKSTOPPER	-	S355J2	-
2	1	HANDLELOCKASS	-	S355J2	-
1	1	CASELOCK	-	SHEETMETAL	-

Konstr	Tegnet: OOB	Revisjon	Vekt	Skala: 0.250	Format: A3 / Blad.nr: 16(67)
Høgskulen på Vestlandet IMM	Artikell/Modell: ASSEMBLYLOCK			Dato: 10-May-24	
	Beskrivelse			Tegning: SUBSEA_BASKET	

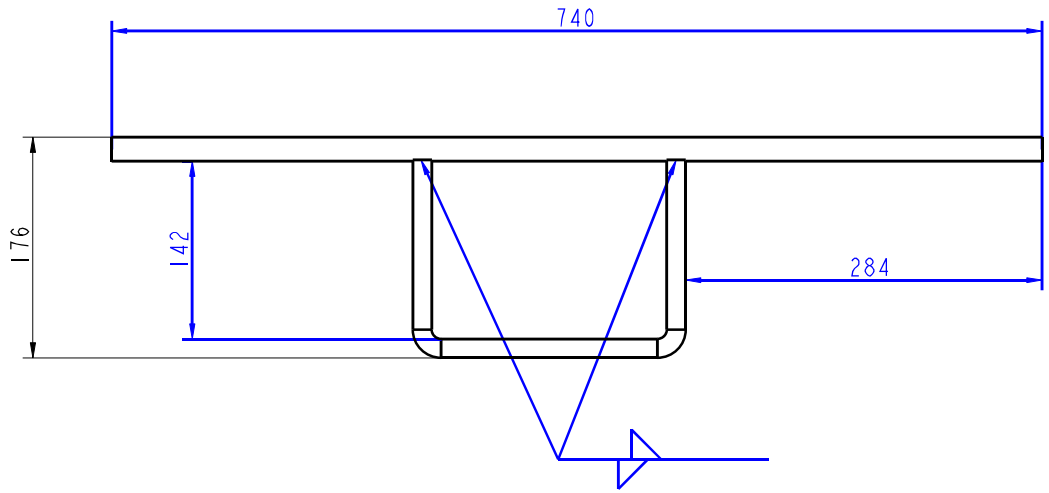

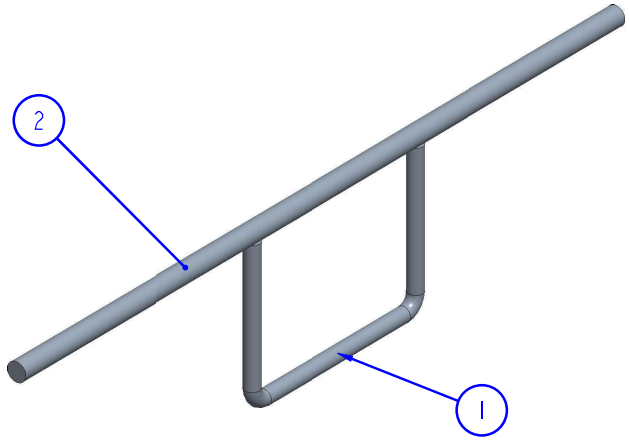

Pos	Ant	Artikell/Modell	Beskrivelse	Materiale	Dimensjon
2	1	LOCKSTICK	-	S355J2	740xØ19
1	1	LOCKHANDLE	-	S355J2	-

Konstr	Tegnet: OOB	Revisjon	Vekt	Skala: 0.110	Format: A3 / Blad.nr: 17(67)
Høgskulen på Vestlandet IMM	Artikell/Modell: HANDLELOCKASS			Dato: 10-May-24	
	Beskrivelse			Tegning: SUBSEA_BASKET	

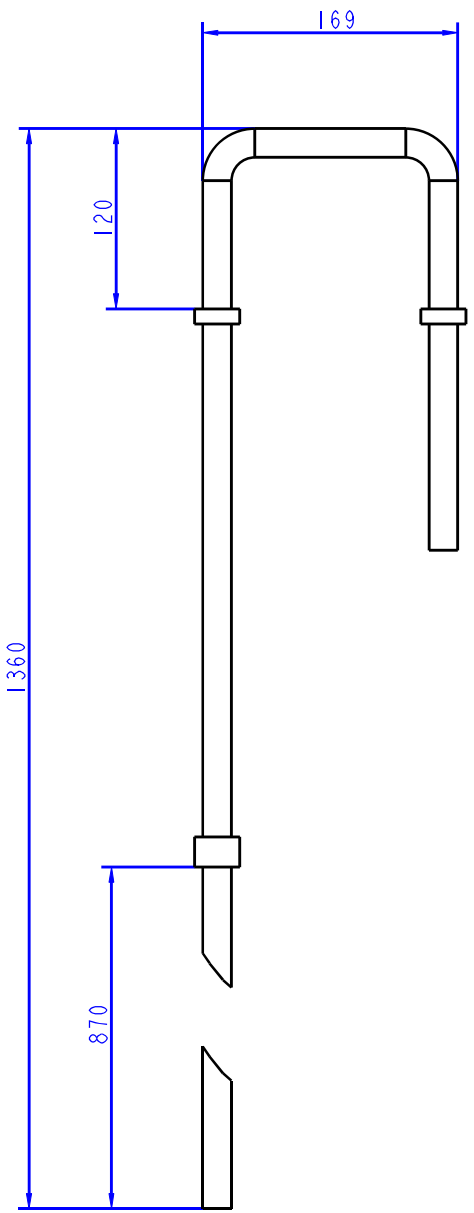

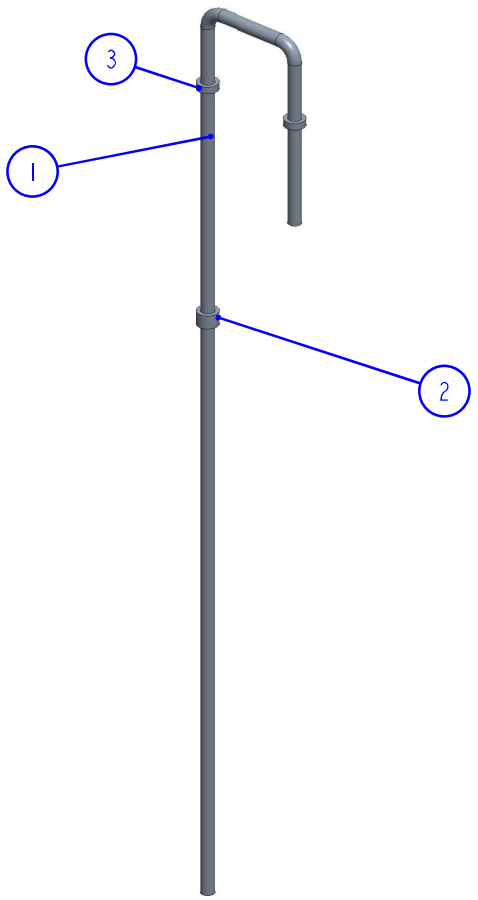

Pos	Ant	Artikell/Modell	Beskrivelse	Materiale	Dimensjon
3	2	RINGFORLOCK2	-	S355J2	-
2	1	RINGFORLOCK	-	S355J2	-
1	1	HANDLEDOOR	-	S355J2	-

Konstr	Tegnet: OOB	Revisjon	Vekt	Skala: 0.300	Format: A3 / Blad.nr: 18(67)
Høgskulen på Vestlandet IMM		Artikell/Modell: HANDLEDOORRIGHT			Dato: 01-May-24
		Beskrivelse			Tegning: SUBSEA_BASKET

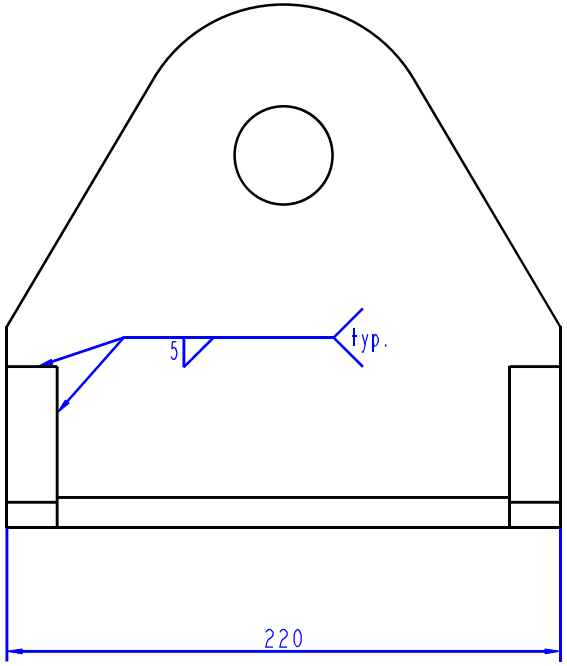

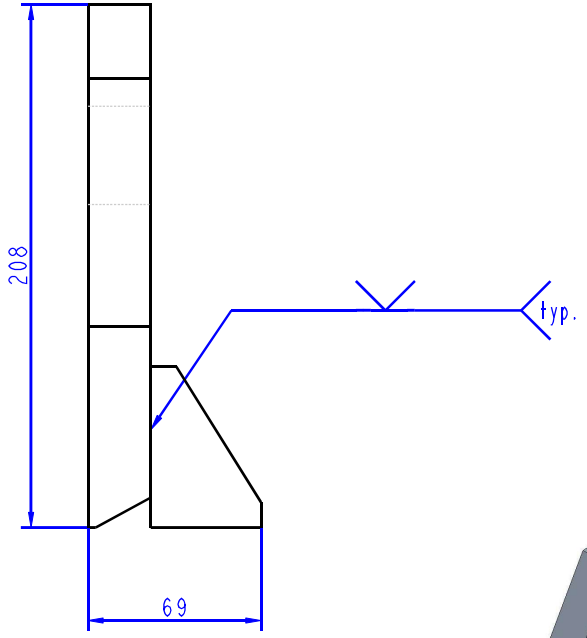

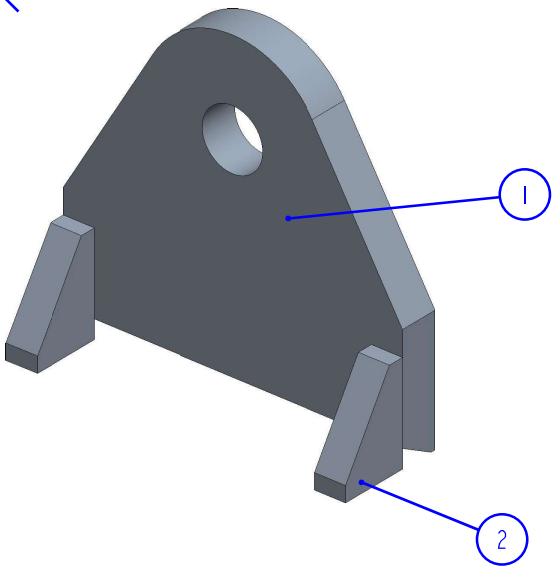

Pos	Ant	Artikell/Modell	Beskrivelse	Materiale	Dimensjon
2	2	PADEYE4_STIFFENER	-	S355J2	-
1	1	PADEYE4	-	S355J2	-

Konstr	Tegnet: OOB	Revisjon	Vekt	Skala: 0.500	Format: A3 / Blad.nr: 19(67)
Høgskulen på Vestlandet IMM	Artikell/Modell: PADEYE4ASS			Dato: 22-Apr-24	
	Beskrivelse			Tegning: SUBSEA_BASKET	

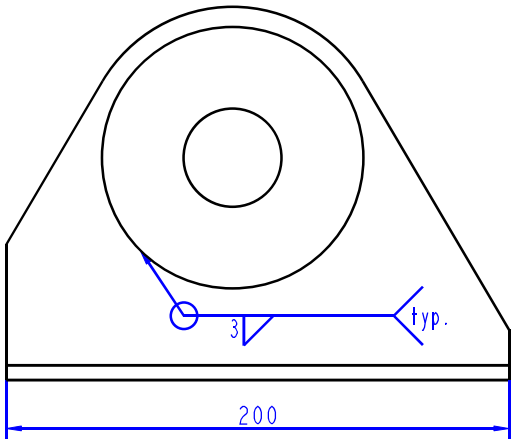

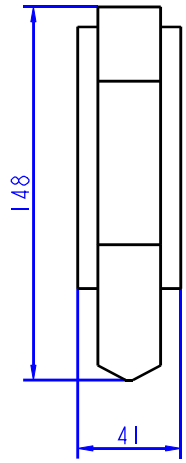

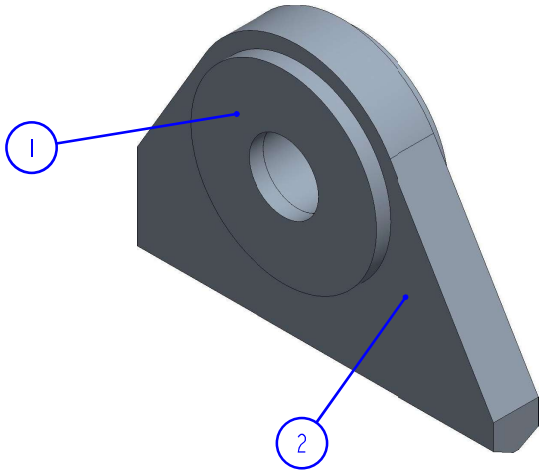

Pos	Ant	Artikell/Modell	Beskrivelse	Materiale	Dimensjon
2	1	PADEYE_2	-	S355J2	-
1	2	PADEYE2CHEEK	-	S355J2	-

Konstr	Tegnet: OOB	Revisjon	Vekt	Skala: 0.500	Format: A3 / Blad.nr: 20(67)
Høgskulen på Vestlandet IMM	Artikell/Modell: PADEYE2ASS				Dato: 22-Apr-24
	Beskrivelse				Tegning: SUBSEA_BASKET

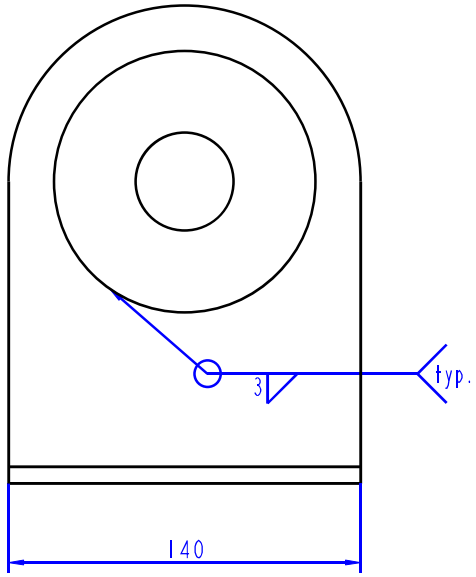

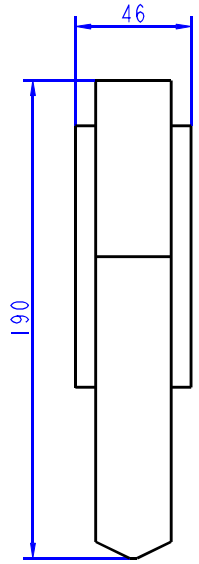

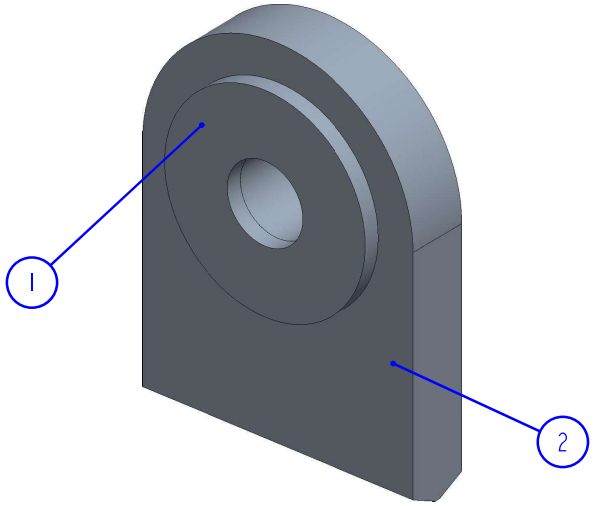

Pos	Ant	Artikell/Modell	Beskrivelse	Materiale	Dimensjon
2	1	PADEYE3	-	S355J2	-
1	2	PADEYE3_CHEEK	-	S355J2	-

Konstr	Tegnet: OOB	Revisjon	Vekt	Skala: 0.500	Format: A3 / Blad.nr: 21(67)
Høgskulen på Vestlandet IMM	Artikell/Modell: PADEYE3ASM			Dato: 19-Apr-24	
	Beskrivelse			Tegning: SUBSEA_BASKET	

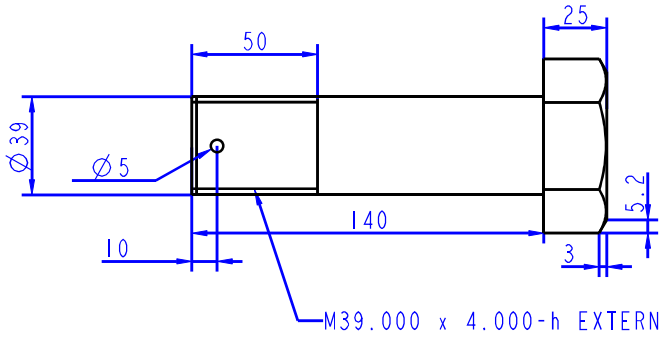

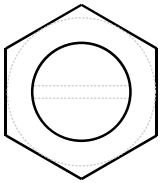

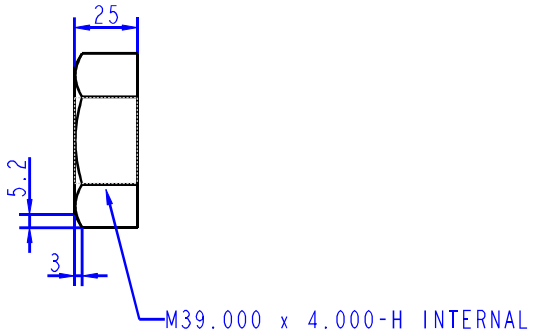

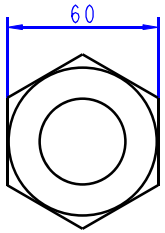

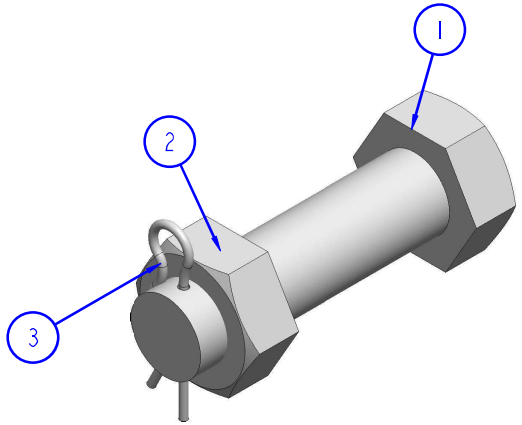

Pos	Ant	Artikell/Modell	Beskrivelse	Materiale	Dimensjon
3	2	M39_R-CLIP	-	S355J2	-
2	2	M39_NUT	-	S355J2	-
1	2	M39_BOLT	-	S355J2	-

Konstr	Tegnet: VSF	Revisjon	Vekt	Skala: 0.500	Format: A3 / Blad.nr: 22(67)
Høgskulen på Vestlandet IMM	Artikell/Modell: M39_BOLT				Dato: 13-May-24
	Beskrivelse				Tegning: SUBSEA_BASKET

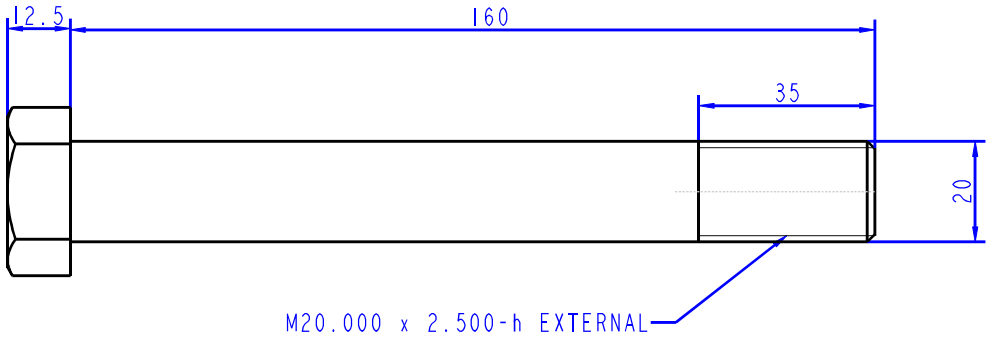

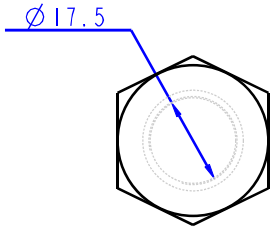

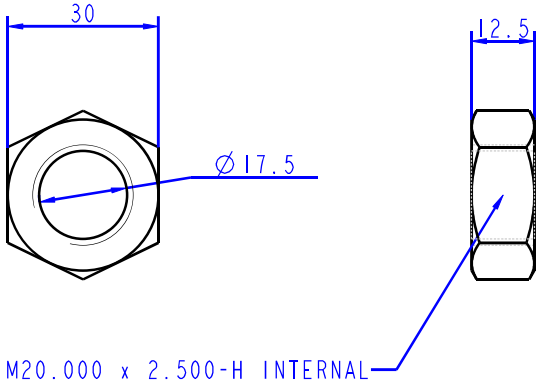

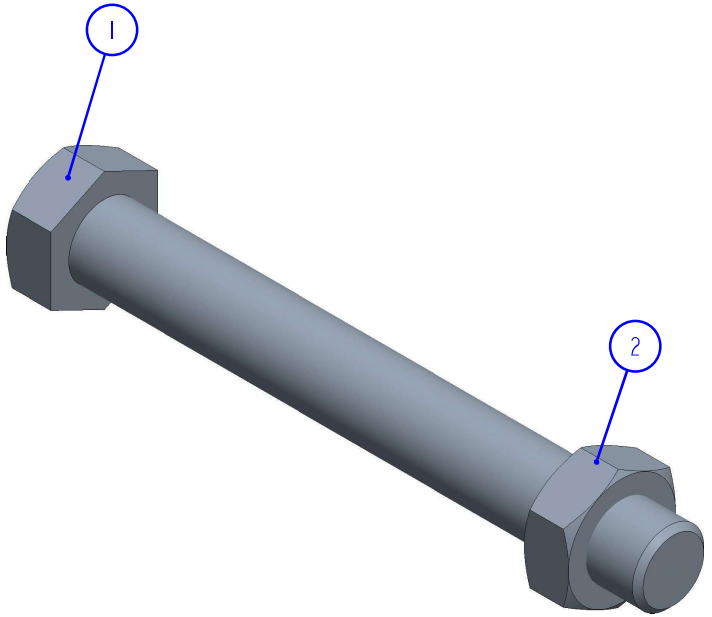

2	1	NUTDOOR	-	S355J2	-
1	1	BOLTDOOR	-	S355J2	-
Pos	Ant	Artikell/Modell	Beskrivelse	Materiale	Dimensjon

Konstr	Tegnet: OOB	Revisjon	Vekt	Skala: 1.000	Format: A3	Blad.nr: 23(67)
Høgskulen på Vestlandet IMM	Artikell/Modell: DOORBOLTASS				Dato: 13-May-24	
	Beskrivelse				Tegning: SUBSEA_BASKET	

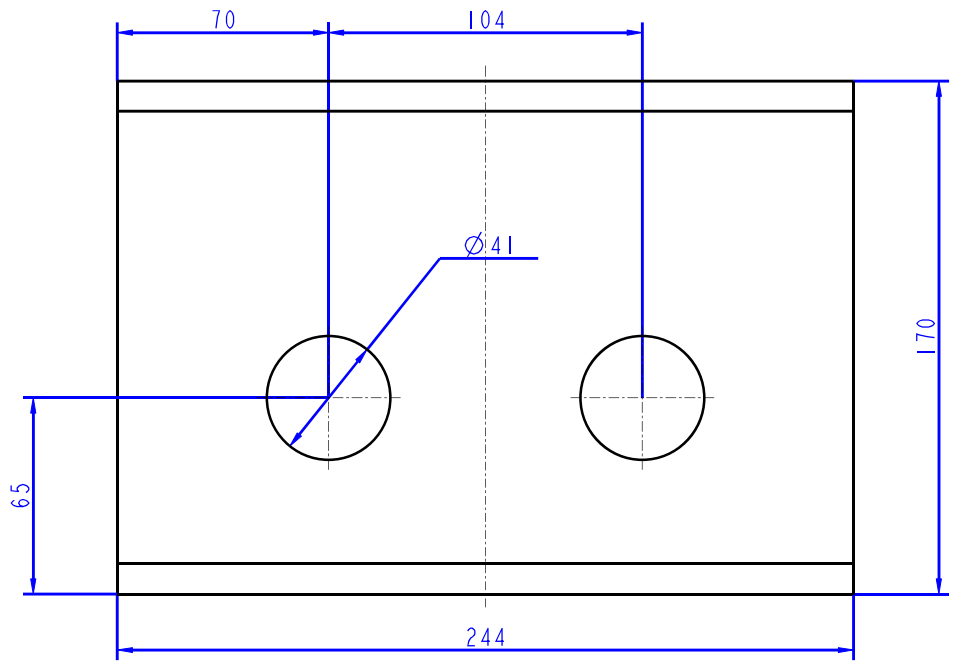

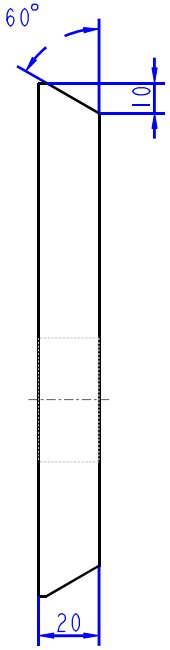

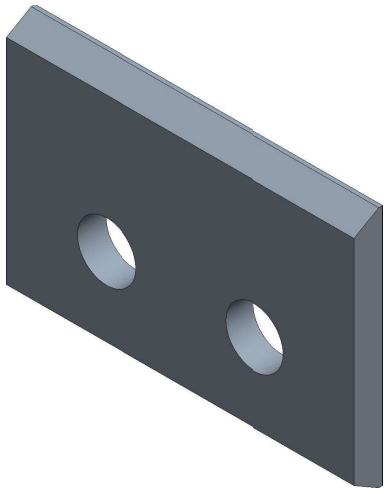

Pos	Ant	Artikell/Modell	Beskrivelse	Materiale	Dimensjon
Konstr	Tegnet VSF	Revisjon	Vekt	Skala 0.600	Format A3	Blad.nr 24(67)
Høgskulen på Vestlandet IMM	Artikell/Modell BOLT_PLATE				Dato 23-Apr-24
	Beskrivelse				Tegning SUBSEA_BASKET

SCALE 0.400

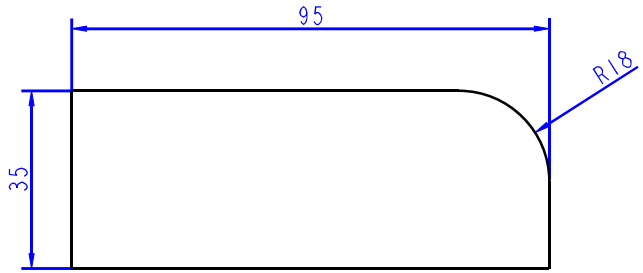

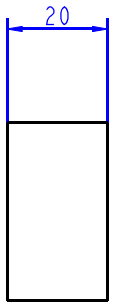

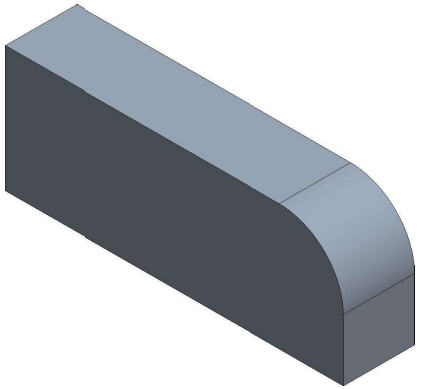

Pos	Ant	Artikell/Modell	Beskrivelse	Materiale	Dimensjon
Konstr	Tegnet VSF	Revisjon	Vekt	Skala 1.000	Format A3	Blad.nr 25(67)
Høgskulen på Vestlandet IMM		Artikell/Modell FORKLIFT_POCKET_STIFFENER			Dato 29-Apr-24
		Beskrivelse			Tegning SUBSEA_BASKET

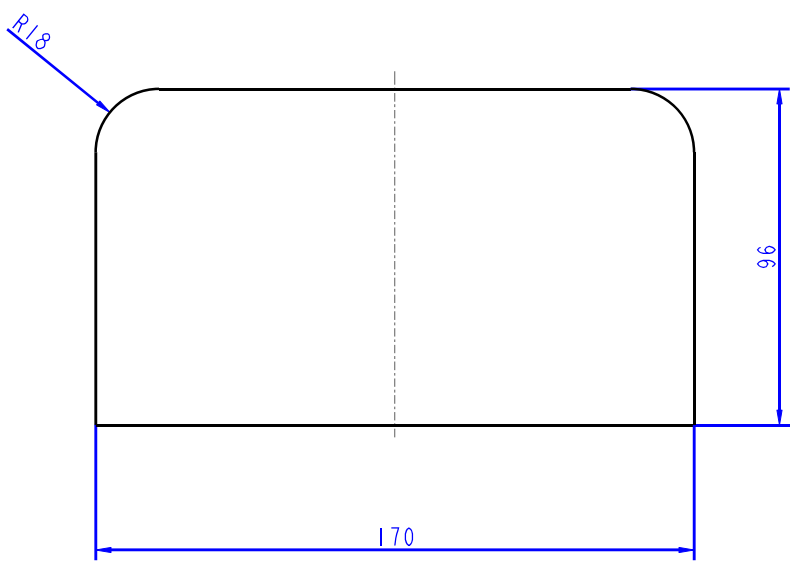

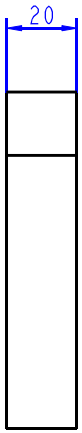

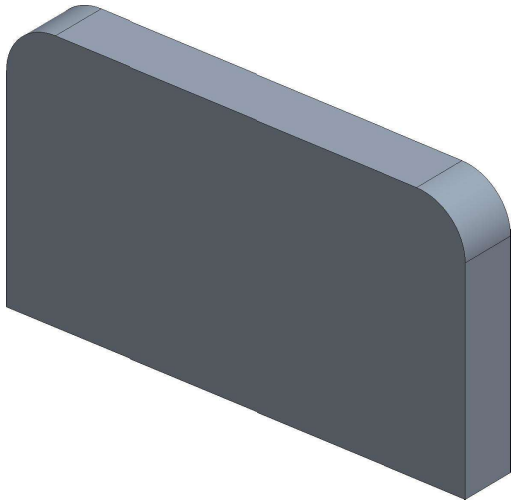

Pos	Ant	Artikell/Modell	Beskrivelse	Materiale	Dimensjon
Konstr	Tegnet VSF	Revisjon	Vekt	Skala 0.700	Format A3	Blad.nr 26(67)
Høgskulen på Vestlandet IMM	Artikell/Modell STIFFENER_200				Dato 23-Apr-24
	Beskrivelse				Tegning SUBSEA_BASKET

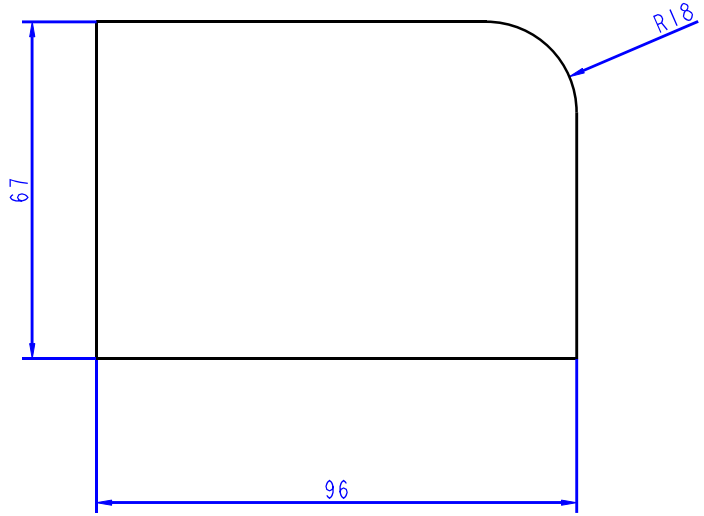

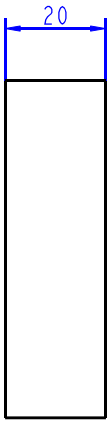

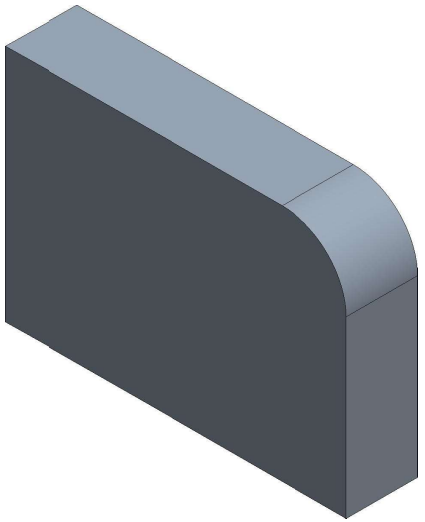

Pos	Ant	Artikell/Modell	Beskrivelse	Materiale	Dimensjon

Konstr	Tegnet	Revisjon	Vekt	Skala	Format	Blad.nr
	VSF			1.000	A3	27(67)

	Artikell/Modell	Dato
Høgskulen på Vestlandet IMM	STIFFENER_ISO_2	23-Apr-24
	Beskrivelse	Tegning: SUBSEA_BASKET

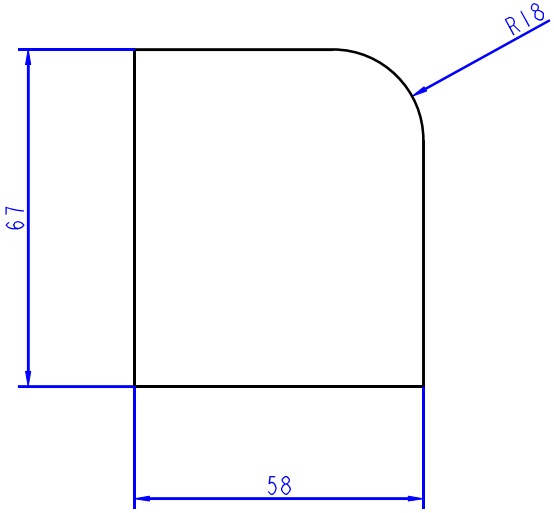

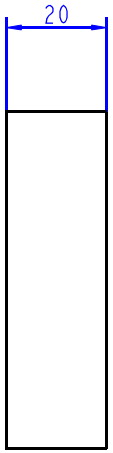

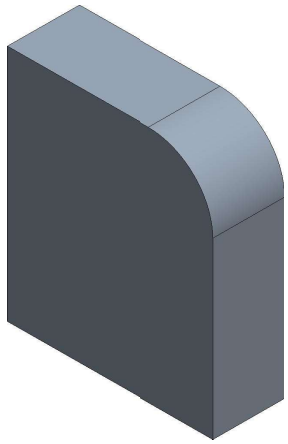

Pos	Ant	Artikell/Modell	Beskrivelse	Materiale	Dimensjon
Konstr	Tegnet VSF	Revisjon	Vekt	Skala 1.000	Format A3	Blad.nr 28(67)
Høgskulen på Vestlandet IMM	Artikell/Modell STIFFENER_ISO_1				Dato 23-Apr-24
	Beskrivelse				Tegning SUBSEA_BASKET

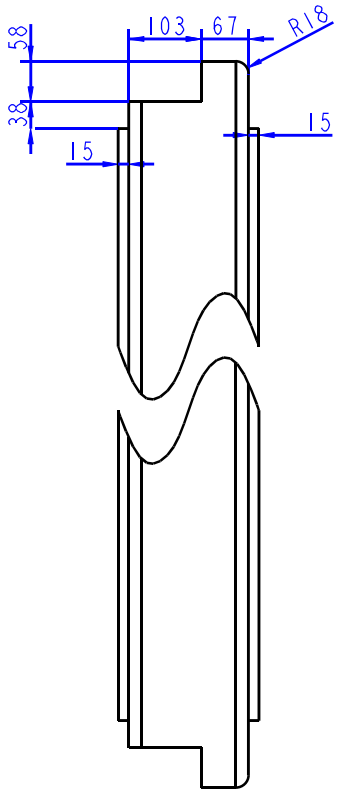

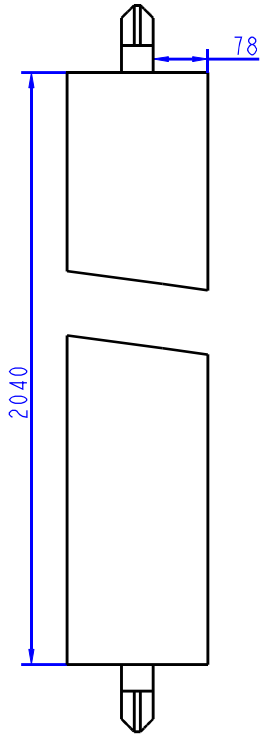

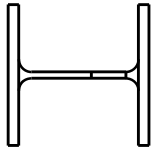

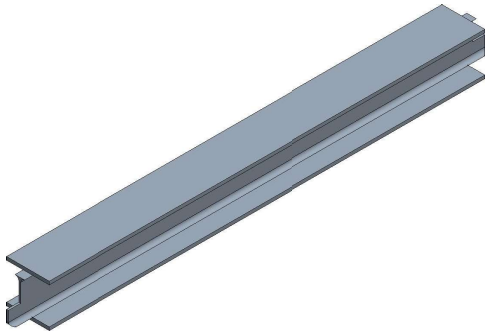

Pos	Ant	Artikell/Modell	Beskrivelse	Materiale	Dimensjon
Konstr	Tegnet VSF	Revisjon	Vekt	Skala 0.140	Format A3	Blad.nr 29(67)
Høgskulen på Vestlandet IMM		Artikell/Modell PRT0012			Dato 29-Apr-24
		Beskrivelse			Tegning SUBSEA_BASKET

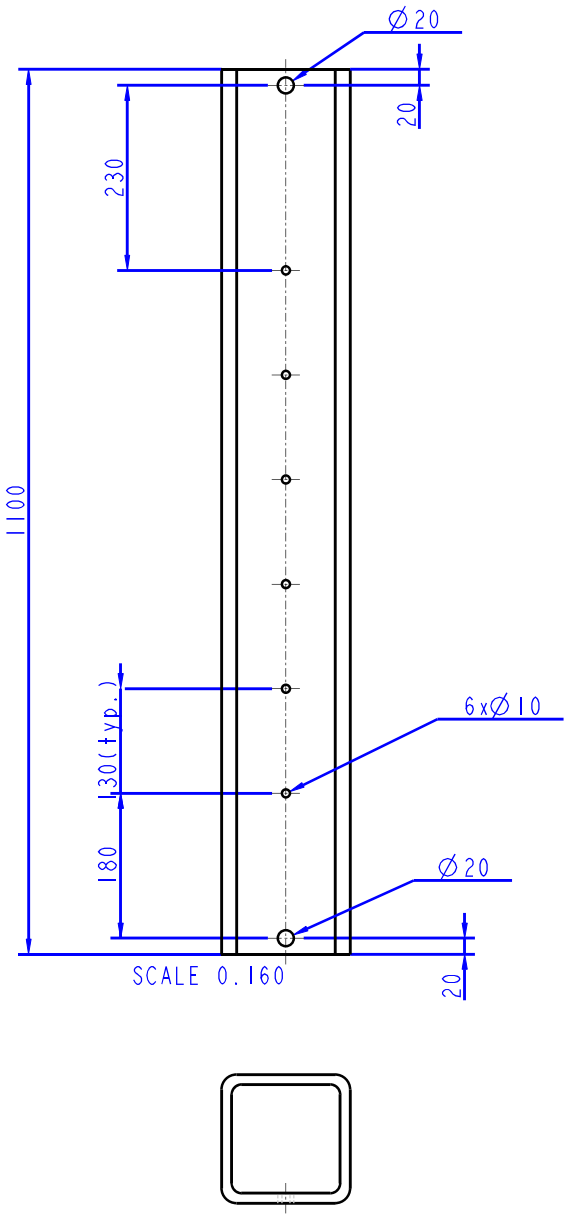

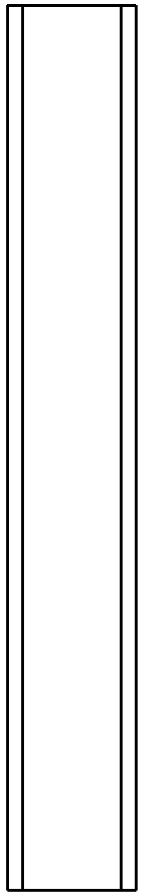

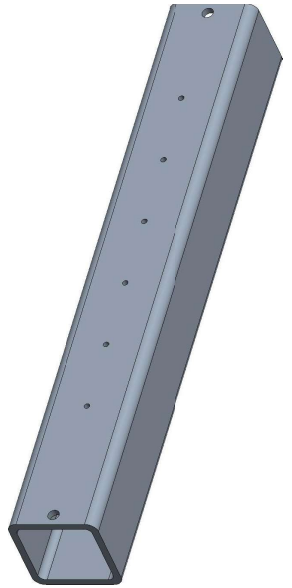

Pos	Ant	Artikell/Modell	Beskrivelse	Materiale	Dimensjon

Konstr	Tegnet	Revisjon	Vekt	Skala	Format	Blad.nr
	VSF			0.080	A3	30(67)

	Artikell/Modell	Dato
Høgskulen på Vestlandet IMM	BEAM_2	29-Apr-24
	Beskrivelse	Tegning: SUBSEA_BASKET

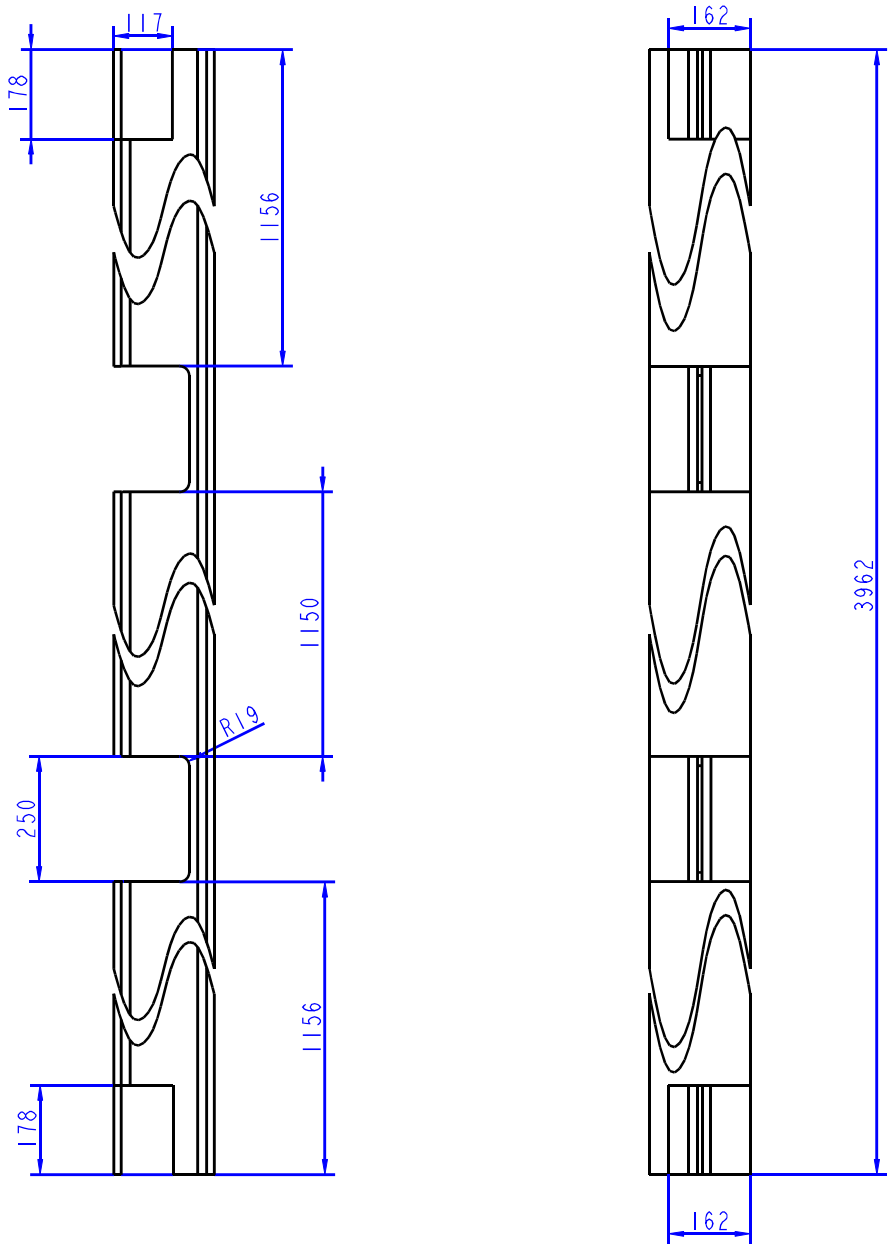

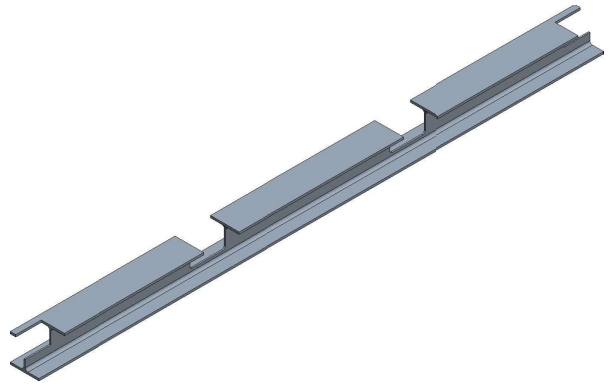

SCALE 0.040

Pos	Ant	Artikell/Modell	Beskrivelse	Materiale	Dimensjon
Konstr	Tegnet VSF	Revisjon	Vekt	Skala 0.100	Format A3	Blad.nr 31(67)
Høgskulen på Vestlandet IMM		Artikell/Modell BEAM_3			Dato 29-Apr-24
		Beskrivelse			Tegning SUBSEA_BASKET

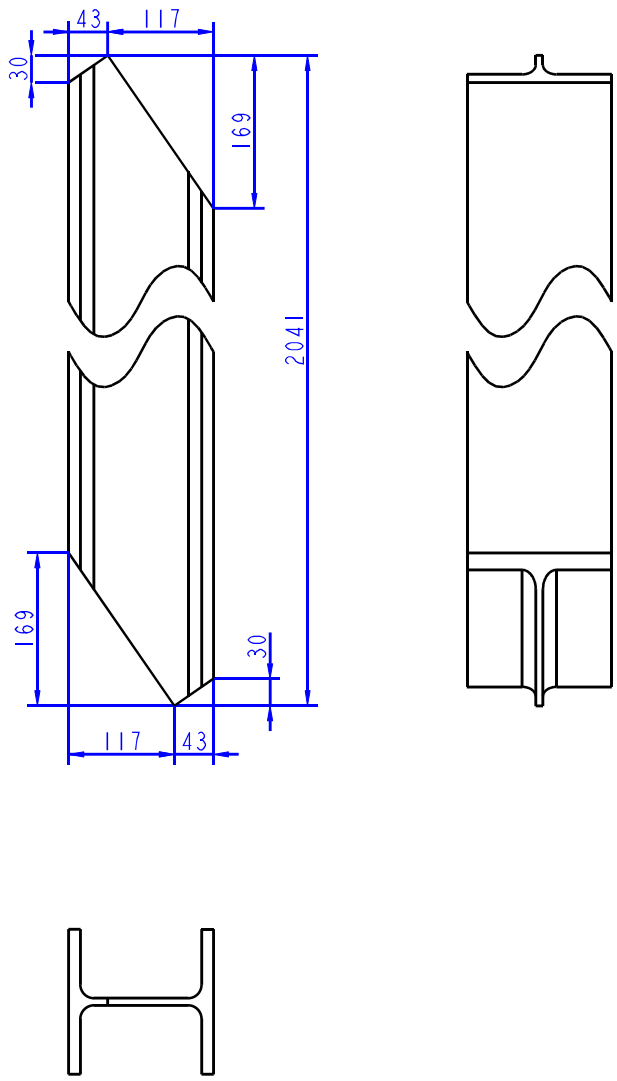

Pos	Ant	Artikell/Modell	Beskrivelse	Materiale	Dimensjon
Konstr	Tegnet VSF	Revisjon	Vekt	Skala 0.180	Format A3	Blad.nr 32(67)
Høgskulen på Vestlandet IMM	Artikell/Modell BASKET_I_BEAM_5_ANL__			Dato 29-Apr-24
	Beskrivelse			Tegning SUBSEA_BASKET

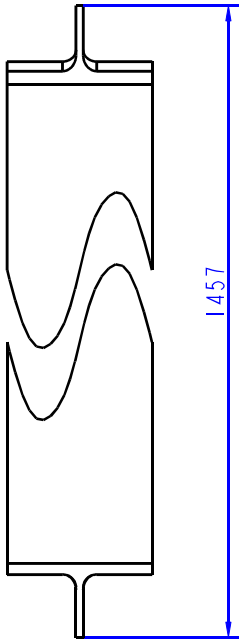

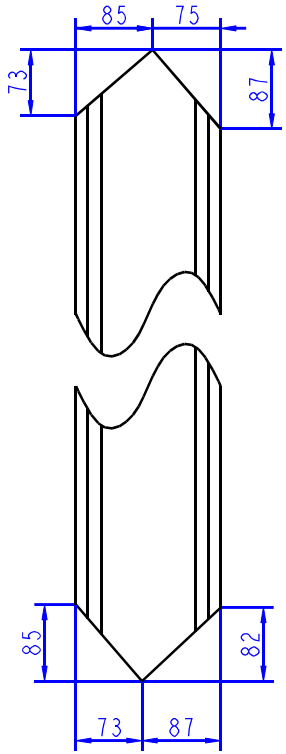

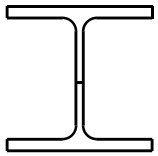

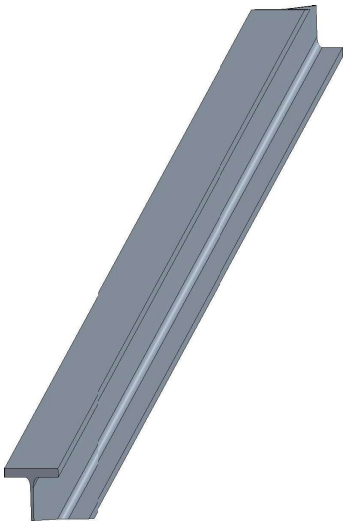

Pos	Ant	Artikell/Modell	Beskrivelse	Materiale	Dimensjon
Konstr	Tegnet VSF	Revisjon	Vekt	Skala 0.180	Format A3	Blad.nr 33(67)
Høgskulen på Vestlandet IMM		Artikell/Modell BASKET_I_BEAM_10_ANL__			Dato 29-Apr-24
		Beskrivelse			Tegning SUBSEA_BASKET

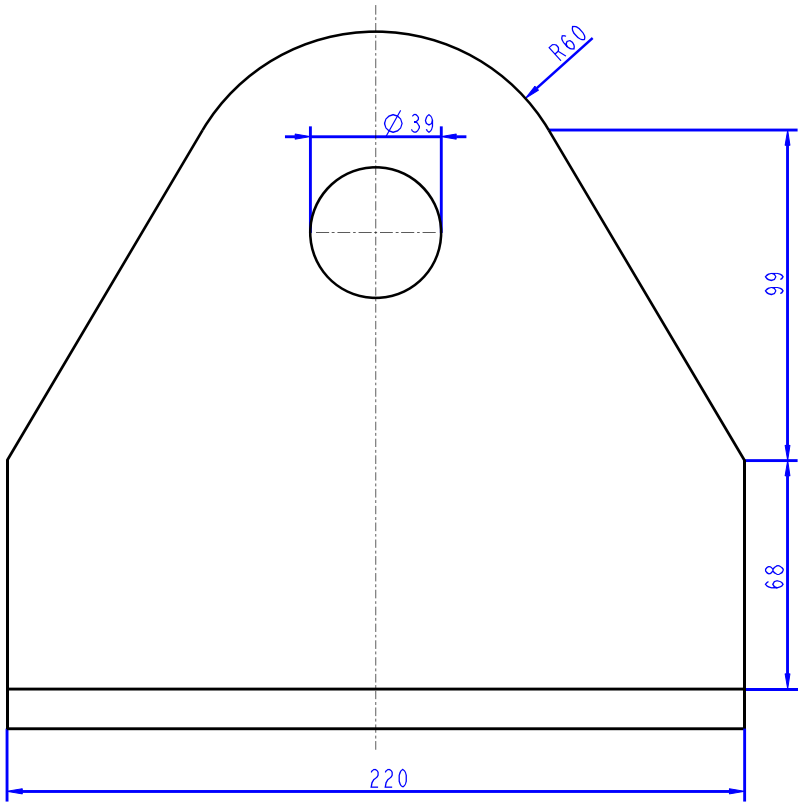

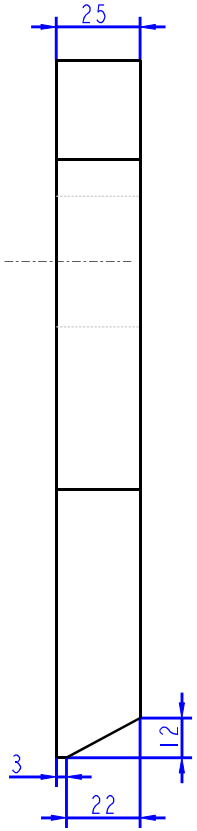

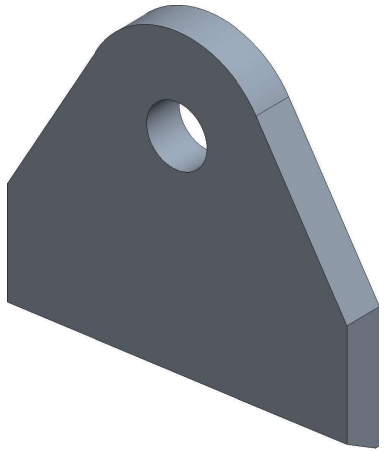

Pos	Ant	Artikell/Modell	Beskrivelse	Materiale	Dimensjon

Konstr	Tegnet	Revisjon	Vekt	Skala	Format	Blad.nr
	OOB			0.670	A3	34(67)

	Artikell/Modell	Dato
Høgskulen på Vestlandet IMM	PADEYE4_1	22-Apr-24
	Beskrivelse	Tegning: SUBSEA_BASKET

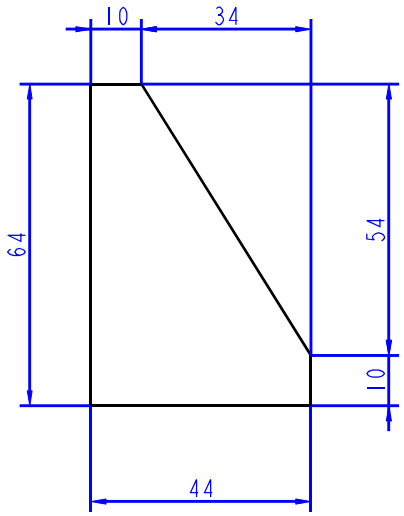

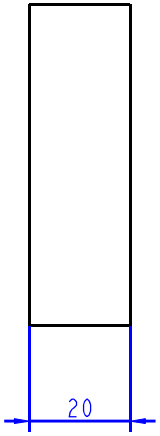

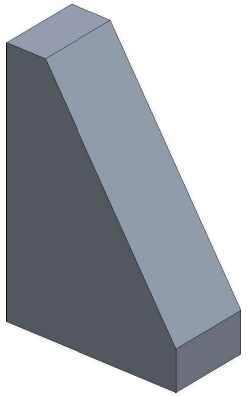

Pos	Ant	Artikell/Modell	Beskrivelse	Materiale	Dimensjon
Konstr	Tegnet OOB	Revisjon	Vekt	Skala 1.000	Format A3	Blad.nr 35(67)
Høgskulen på Vestlandet IMM		Artikell/Modell PASEYE4_STIFFENER_1			Dato 22-Apr-24
		Beskrivelse			Tegning SUBSEA_BASKET

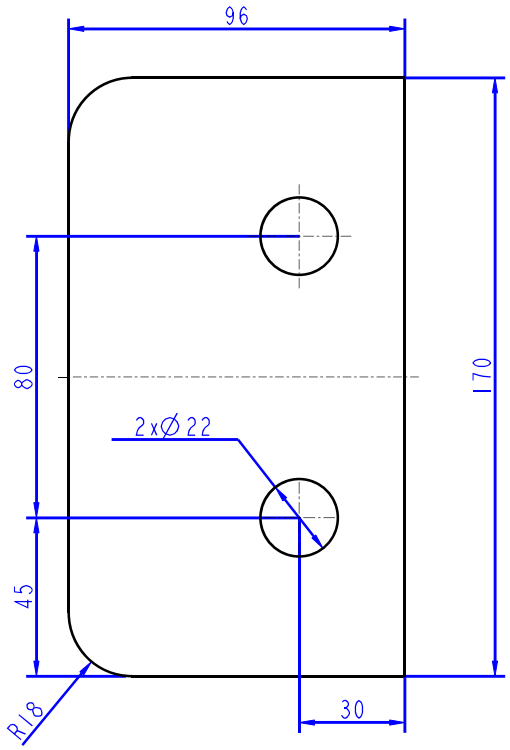

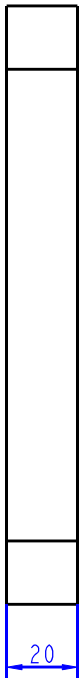

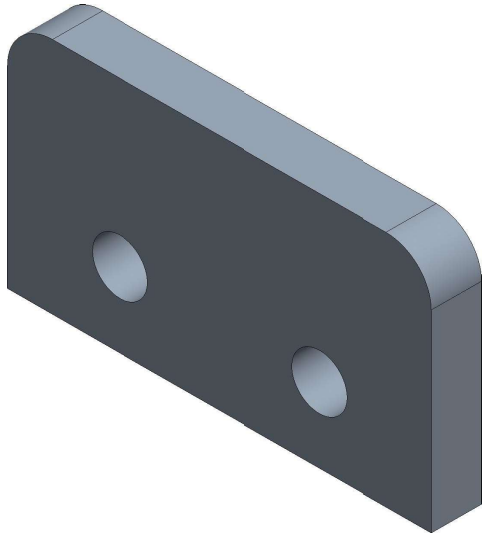

Pos	Ant	Artikell/Modell	Beskrivelse	Materiale	Dimensjon

Konstr	Tegnet	Revisjon	Vekt	Skala	Format	Blad.nr
	VSF			0.700	A3	36(67)

	Artikell/Modell	Dato
Høgskulen på Vestlandet IMM	GW_STIFFENER	29-Apr-24
	Beskrivelse	Tegning: SUBSEA_BASKET

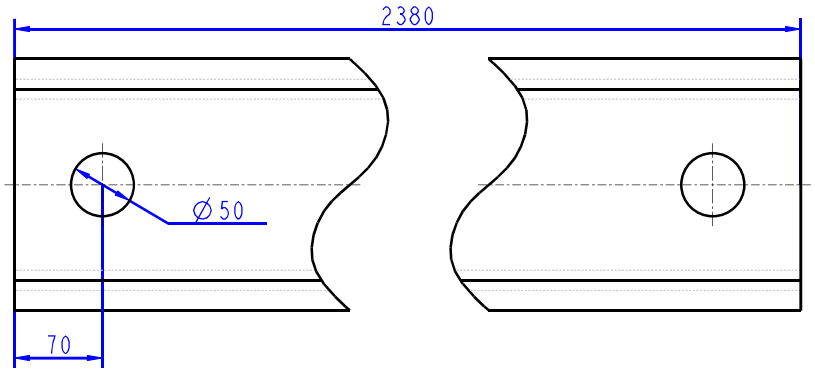

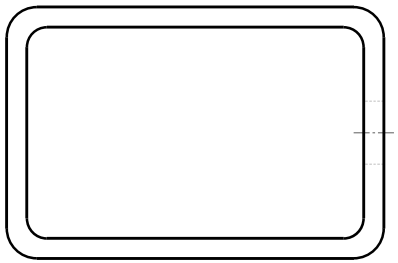

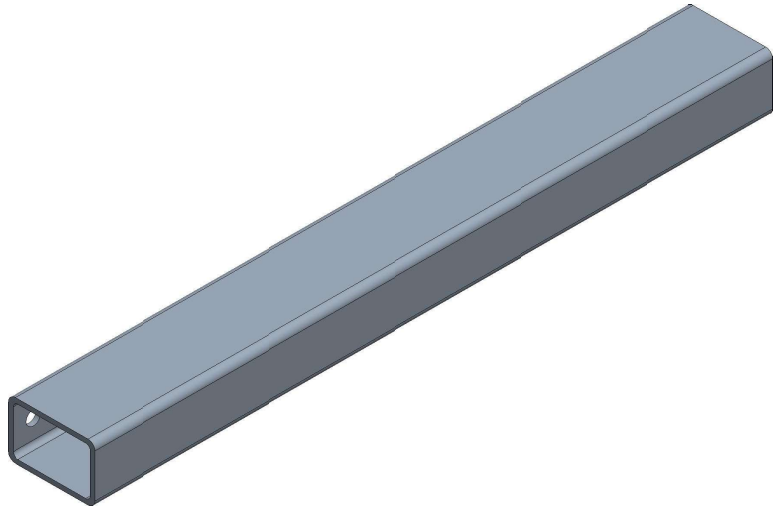

Pos	Ant	Artikell/Modell	Beskrivelse	Materiale	Dimensjon
Konstr	Tegnet VSF	Revisjon SCALE0.080		Skala 0.250	Format A3	Blad.nr 37(67)
Høgskulen på Vestlandet IMM		Artikell/Modell SPREAD_BEAM		Dato 01-May-24	
		Beskrivelse		Tegning SUBSEA_BASKET	

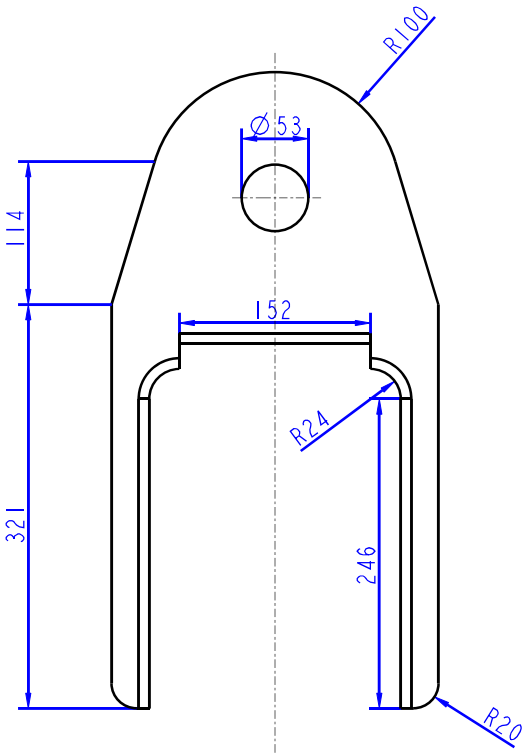

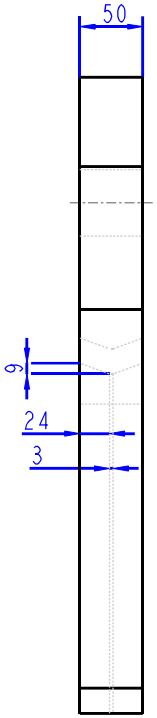

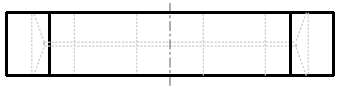

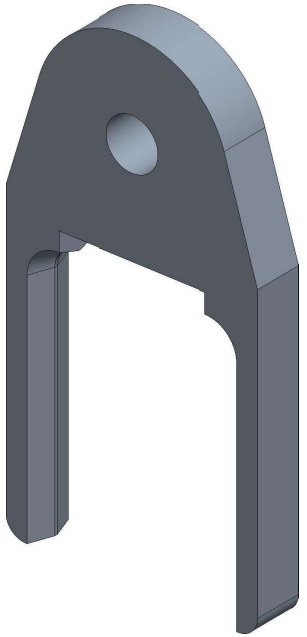

Pos	Ant	Artikell/Modell	Beskrivelse	Materiale	Dimensjon
Konstr	Tegnet OOB	Revisjon	Vekt	Skala 0.330	Format A3	Blad.nr 38(67)
Høgskulen på Vestlandet IMM	Artikell/Modell PADEYE1			Dato 22-Apr-24
	Beskrivelse			Tegning SUBSEA_BASKET

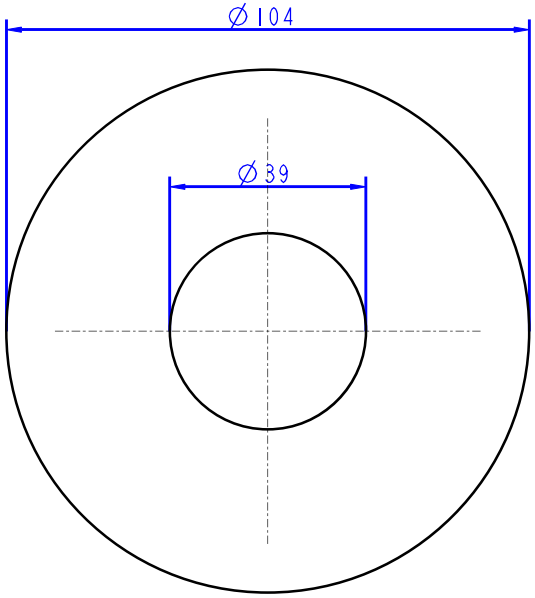

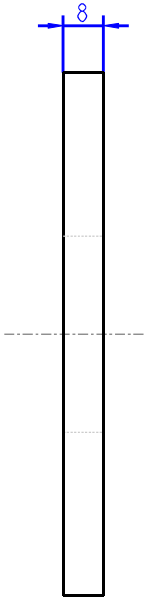

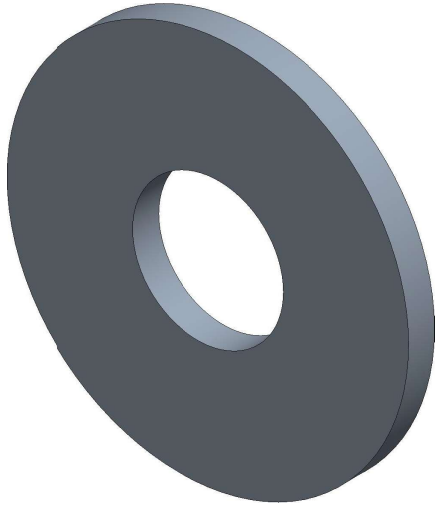

Pos	Ant	Artikell/Modell	Beskrivelse	Materiale	Dimensjon
Konstr	Tegnet OOB	Revisjon	Vekt	Skala 1.000	Format A3	Blad.nr 39(67)
Høgskulen på Vestlandet IMM		Artikell/Modell PADEYE2CHEEK			Dato 22-Apr-24
		Beskrivelse			Tegning SUBSEA_BASKET

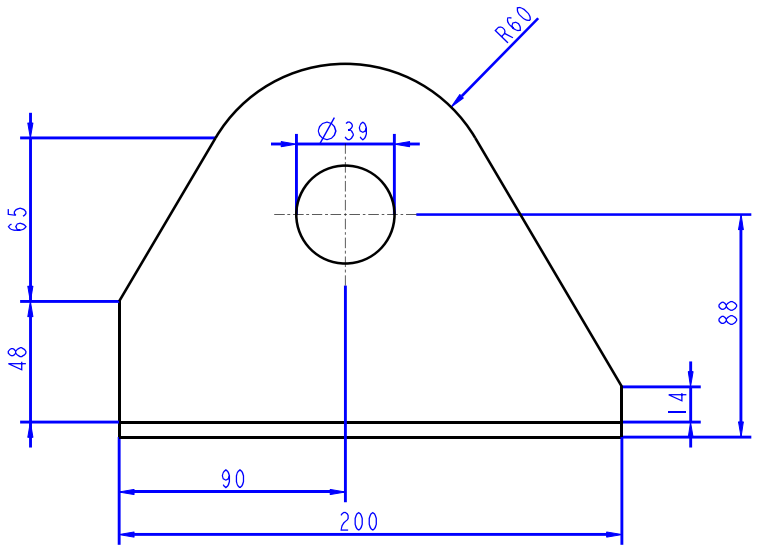

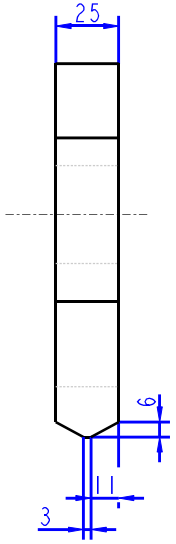

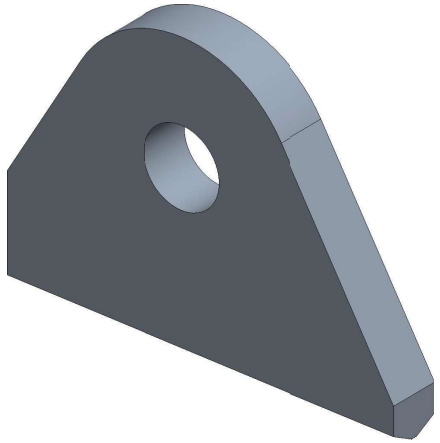

Pos	Ant	Artikell/Modell	Beskrivelse	Materiale	Dimensjon
Konstr	Tegnet OOB	Revisjon	Vekt	Skala 1.000	Format A3	Blad.nr 40(67)
Høgskulen på Vestlandet IMM		Artikell/Modell Padeye_2			Dato 22-Apr-24
		Beskrivelse			Tegning SUBSEA_BASKET

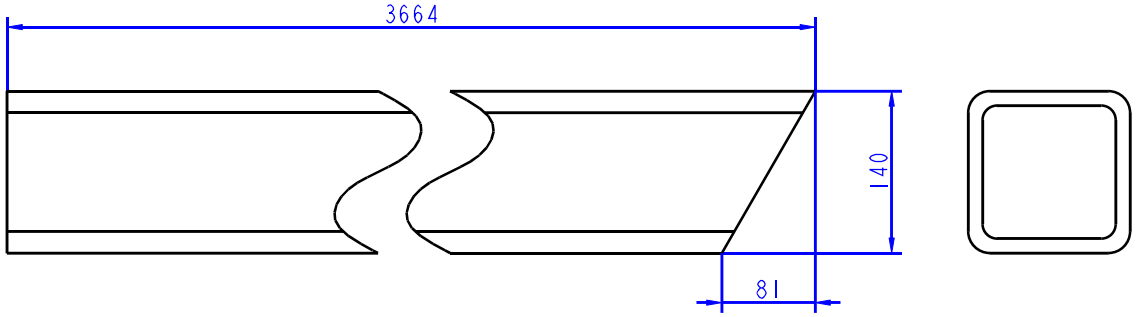

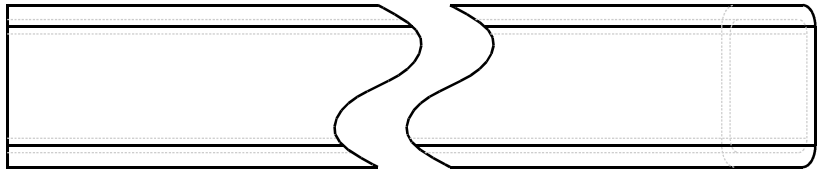

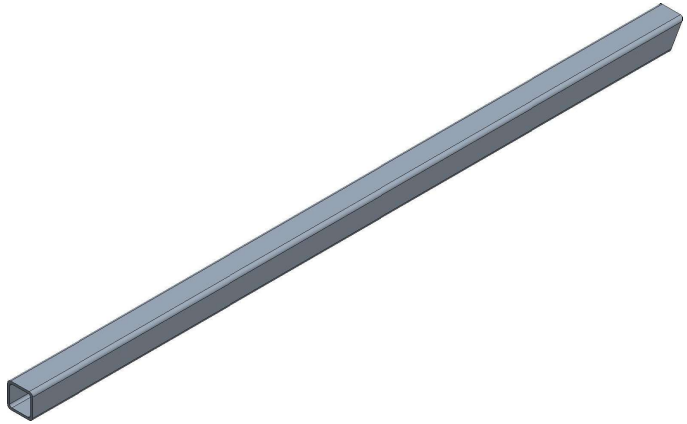

SCALE 0.050

Pos	Ant	Artikell/Modell	Beskrivelse	Materiale	Dimensjon

Konstr	Tegnet	Revisjon	Vekt	Skala	Format	Blad.nr
	VSF			0.230	A3	41(67)

	Artikell/Modell	Dato
Høgskulen på Vestlandet IMM	A-FRAME_SHS	01-May-24
	Beskrivelse	Tegning SUBSEA_BASKET

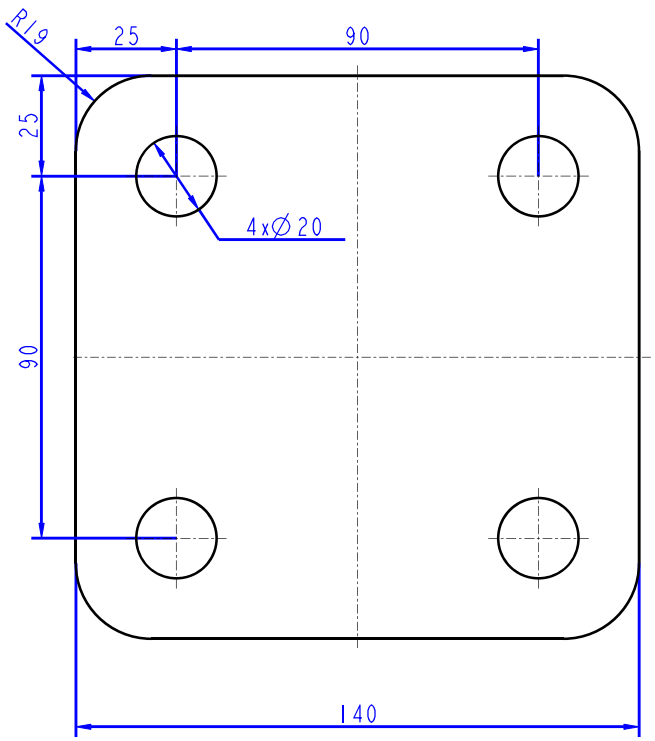

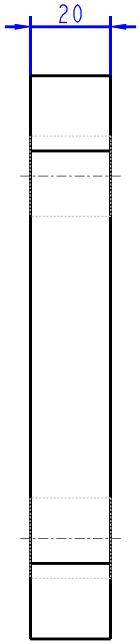

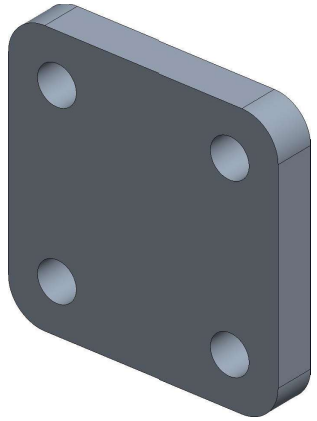

Pos	Ant	Artikell/Modell	Beskrivelse	Materiale	Dimensjon
Konstr	Tegnet VSF	Revisjon	Vekt	Skala 0.800	Format A3	Blad.nr 42(67)
Høgskulen på Vestlandet IMM	Artikell/Modell ENDPLATE_A-FRAME			Dato 30-Apr-24
	Beskrivelse			Tegning SUBSEA_BASKET

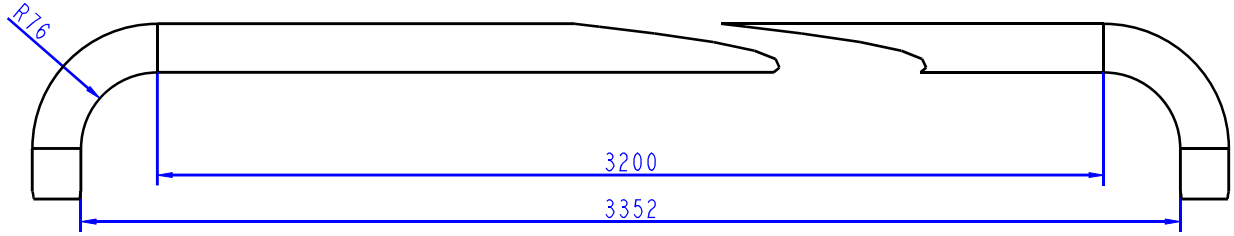

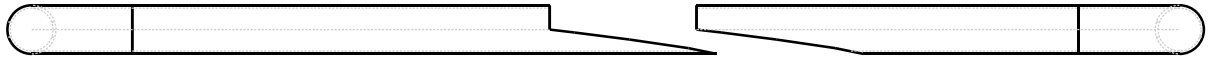

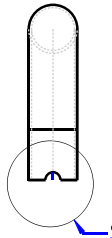

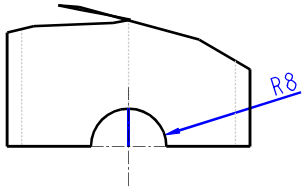

DETAIL **A**
SCALE 1.000

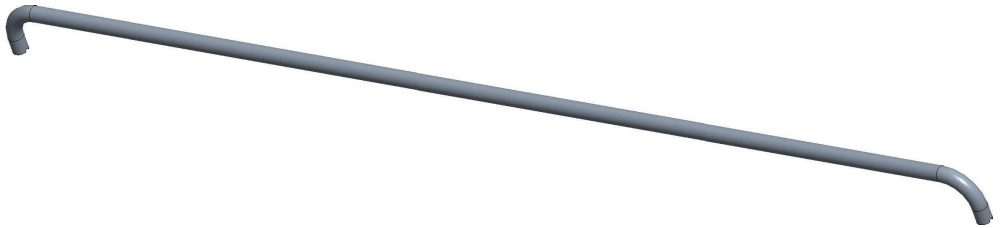

Pos	Ant	Artikell/Modell	Beskrivelse	Materiale	Dimensjon
Konstr	Tegnet VSF	Revisjon	Vekt	Skala 0.200	Format A3	Blad.nr 43(67)
Høgskulen på Vestlandet IMM	Artikell/Modell RAIL_AFRAME			Dato 24-Apr-24
	Beskrivelse			Tegning SUBSEA_BASKET

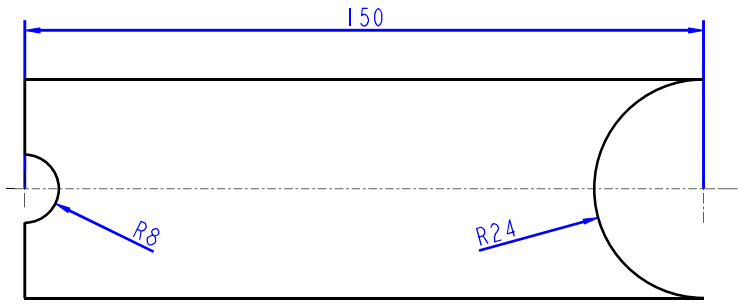

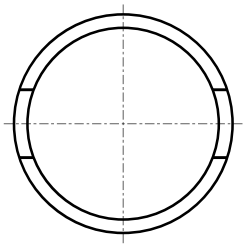

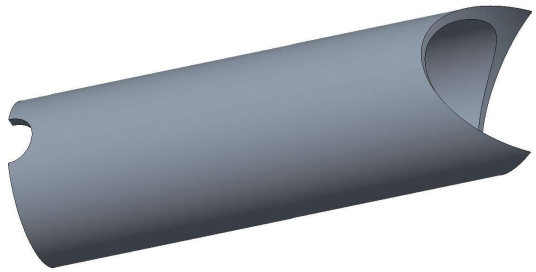

Pos	Ant	Artikell/Modell	Beskrivelse	Materiale	Dimensjon
Konstr	Tegnet VSF	Revisjon	Vekt	Skala 0.900	Format A3	Blad.nr 44(67)
Høgskulen på Vestlandet IMM		Artikell/Modell RAIL_AFRAME2_			Dato 24-Apr-24
		Beskrivelse			Tegning SUBSEA_BASKET

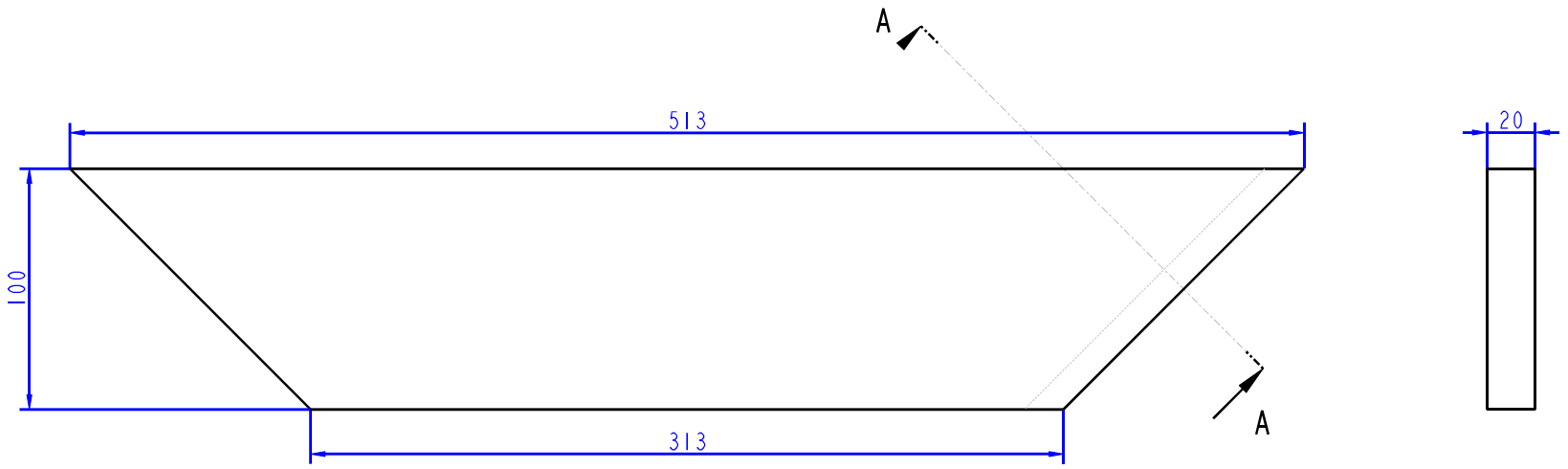

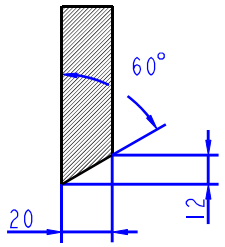

SECTION A-A

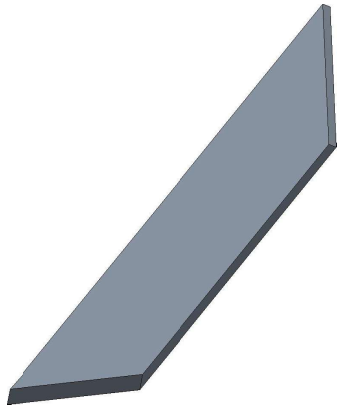

Pos	Ant	Artikell/Modell	Beskrivelse	Materiale	Dimensjon

Konstr	Tegnet	Revisjon	Vekt	Skala	Format	Blad.nr
	VSF			0.500	A3	45(67)

	Artikell/Modell	Dato
Høgskulen på Vestlandet IMM	A-FRAME_STIFFENER	01-May-24
	Beskrivelse	Tegning SUBSEA_BASKET

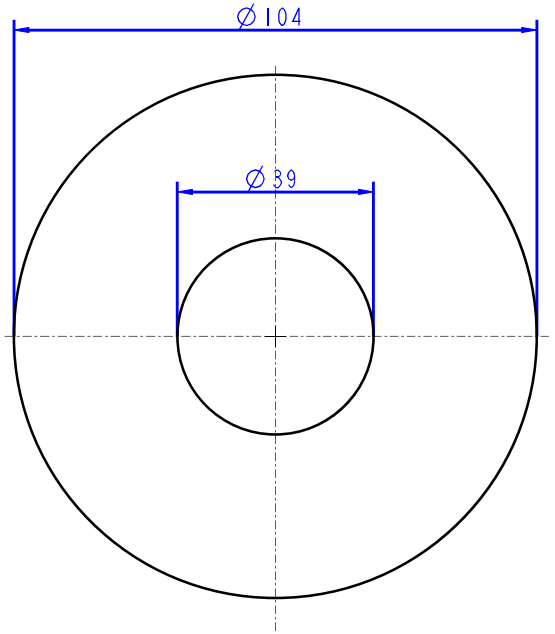

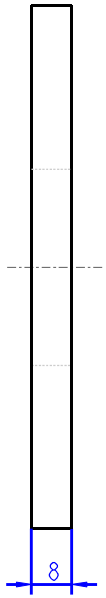

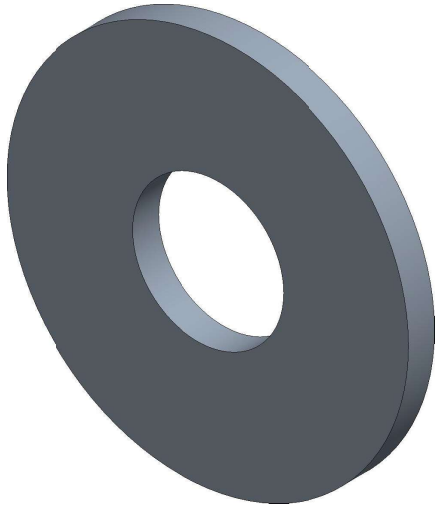

Pos	Ant	Artikell/Modell	Beskrivelse	Materiale	Dimensjon

Konstr	Tegnet	Revisjon	Vekt	Skala	Format	Blad.nr
	OOB			1.000	A3	46(67)

	Artikell/Modell	Dato
Høgskulen på Vestlandet IMM	PADEYE3_CHEEK	19-Apr-24
	Beskrivelse	Tegning
		SUBSEA_BASKET

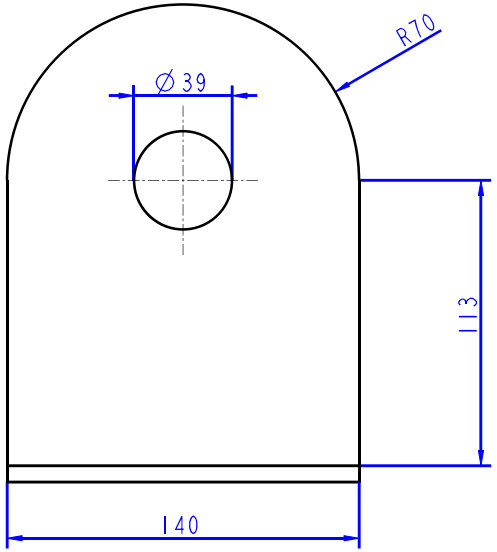

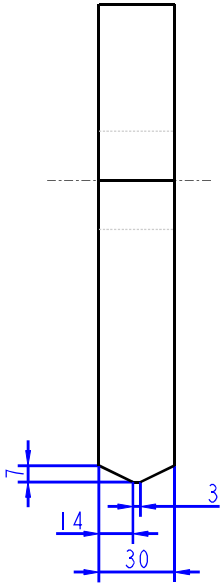

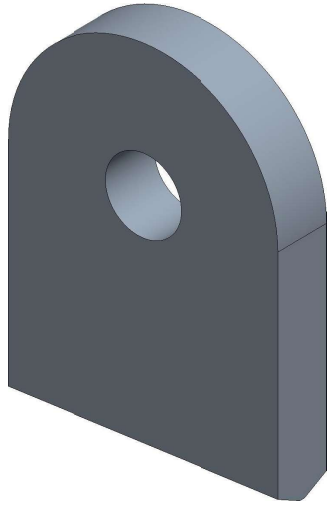

Pos	Ant	Artikell/Modell	Beskrivelse	Materiale	Dimensjon
Konstr	Tegnet OOB	Revisjon	Vekt	Skala 1.000	Format A3	Blad.nr 47(67)
Høgskulen på Vestlandet IMM		Artikell/Modell PRT0002			Dato 19-Apr-24
		Beskrivelse			Tegning SUBSEA_BASKET

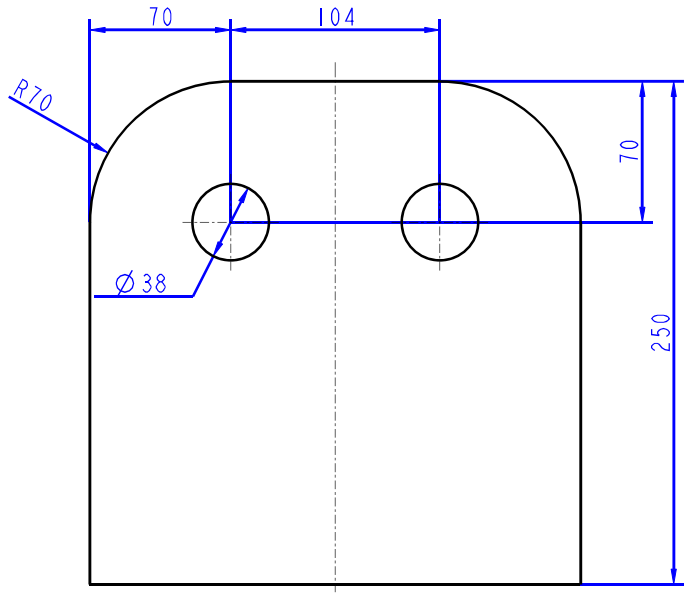

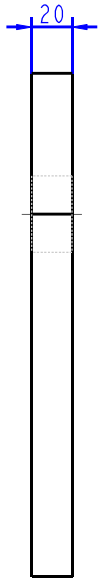

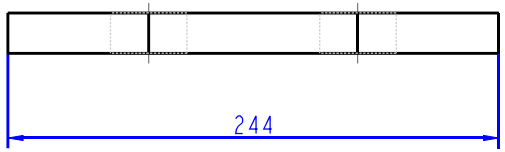

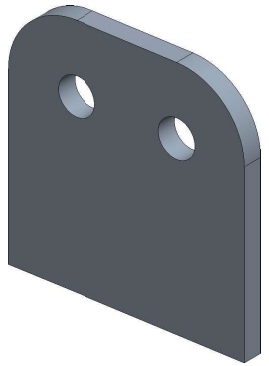

Pos	Ant	Artikell/Modell	Beskrivelse	Materiale	Dimensjon

Konstr	Tegnet	Revisjon	Vekt	Skala	Format	Blad.nr
	VSF			0.400	A3	48(67)

	Artikell/Modell	Dato
Høgskulen på Vestlandet IMM	BOLT_PLATE_2	29-Apr-24
	Beskrivelse	Tegning SUBSEA_BASKET

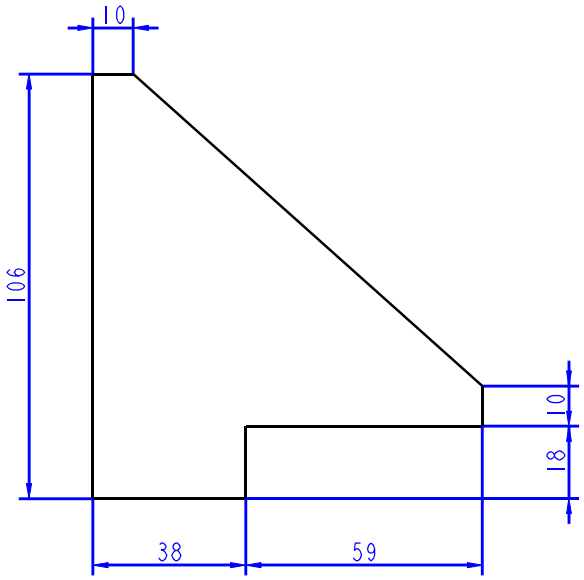

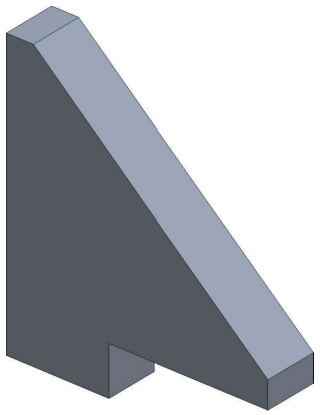

Pos	Ant	Artikell/Modell	Beskrivelse	Materiale	Dimensjon
Konstr	Tegnet VSF	Revisjon	Vekt	Skala 0.800	Format A3	Blad.nr 49(67)
Høgskulen på Vestlandet IMM	Artikell/Modell ISO_STIFFENER				Dato 01-May-24
	Beskrivelse				Tegning SUBSEA_BASKET

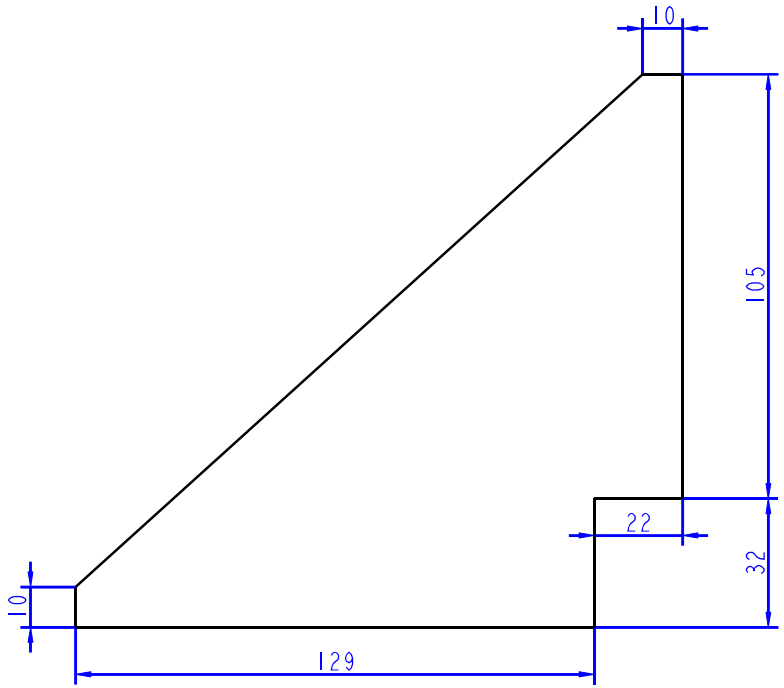

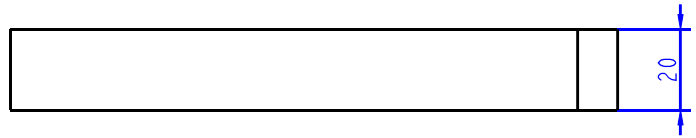

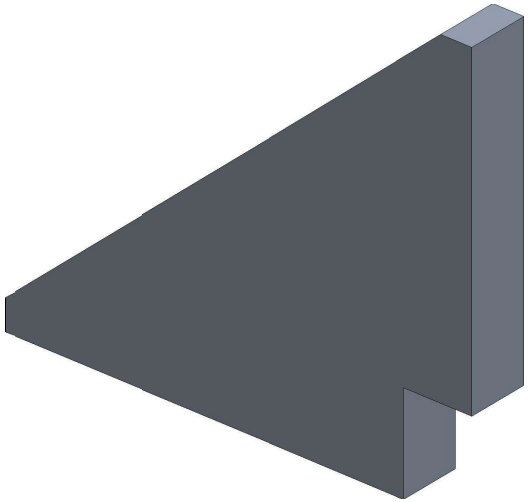

Pos	Ant	Artikell/Modell	Beskrivelse	Materiale	Dimensjon
Konstr	Tegnet VSF	Revisjon	Vekt	Skala 0.800	Format A3	Blad.nr 50(67)
Høgskulen på Vestlandet IMM		Artikell/Modell ISO_STIFFENER_2			Dato 01-May-24
		Beskrivelse			Tegning SUBSEA_BASKET

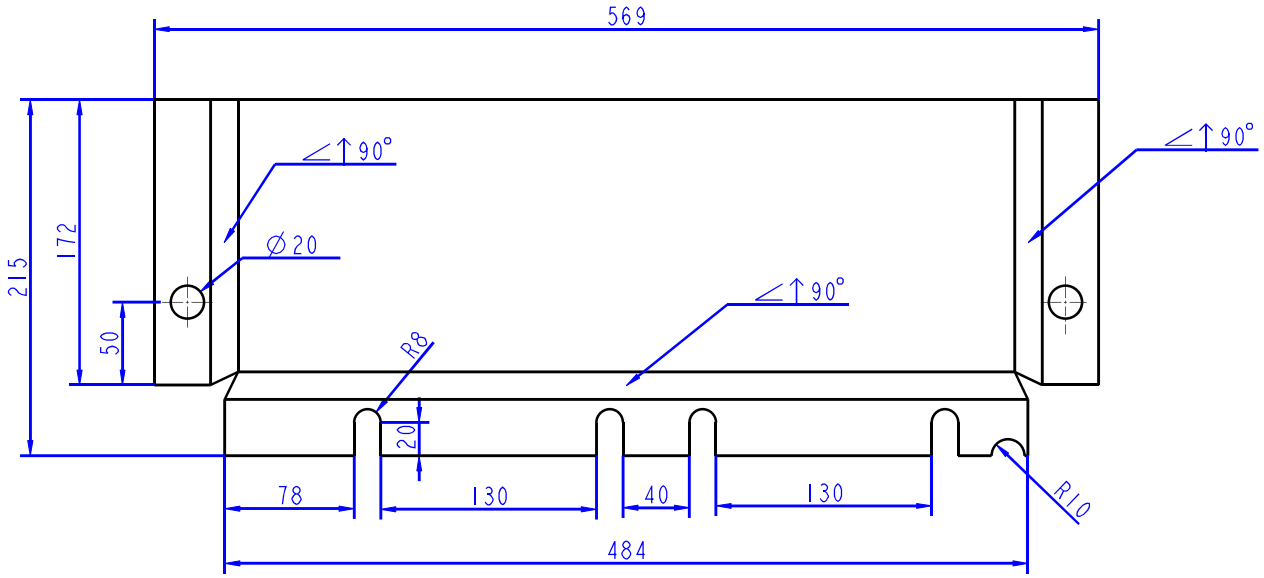

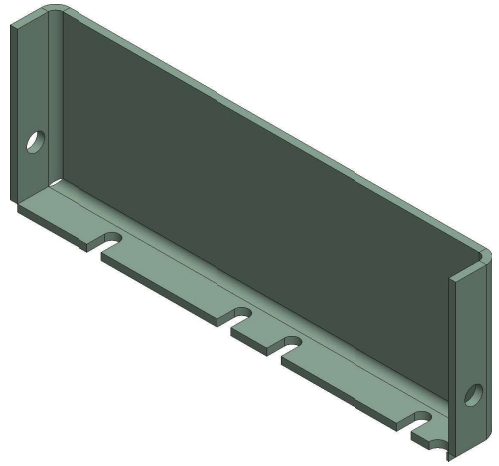

Pos	Ant	Artikell/Modell	Beskrivelse	Materiale	Dimensjon
Konstr	Tegnet OOB	Revisjon	Vekt	Skala 1.000	Format A3	Blad.nr 51(67)
Høgskulen på Vestlandet IMM		Artikell/Modell CASELOCK			Dato 29-Apr-24
		Beskrivelse			Tegning SUBSEA_BASKET

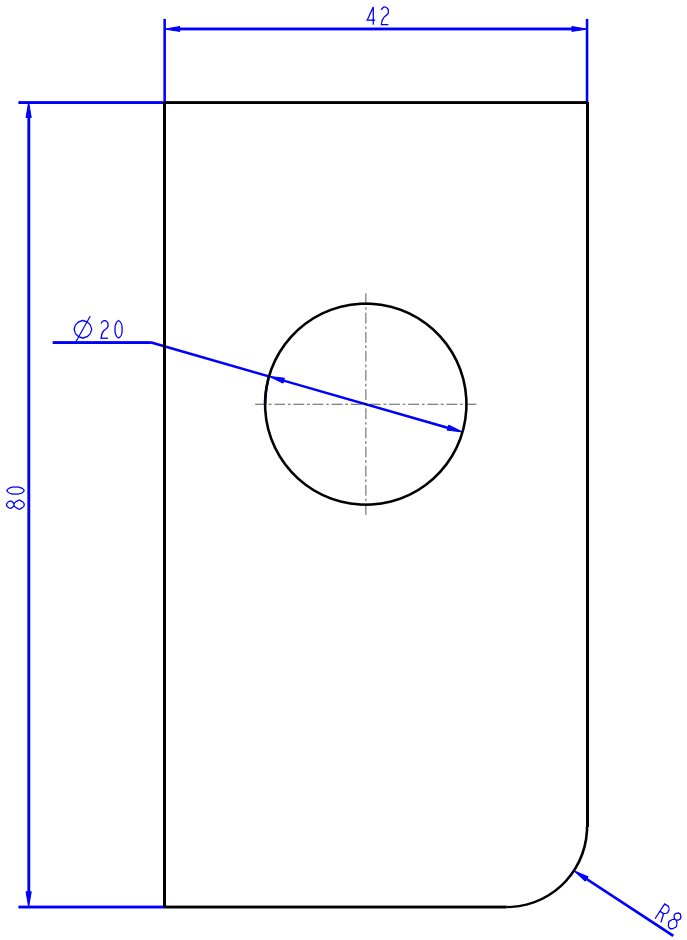

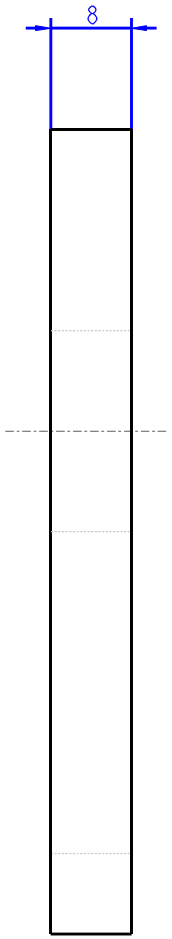

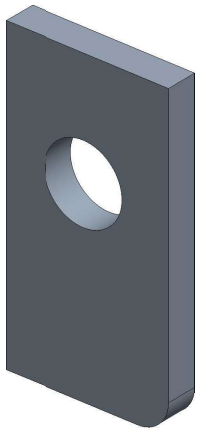

Pos	Ant	Artikell/Modell	Beskrivelse	Materiale	Dimensjon
Konstr	Tegnet OOB	Revisjon	Vekt	Skala 2.000	Format A3	Blad.nr 52(67)
Høgskulen på Vestlandet IMM		Artikell/Modell LOCKSTOPPER			Dato 10-May-24
		Beskrivelse			Tegning SUBSEA_BASKET

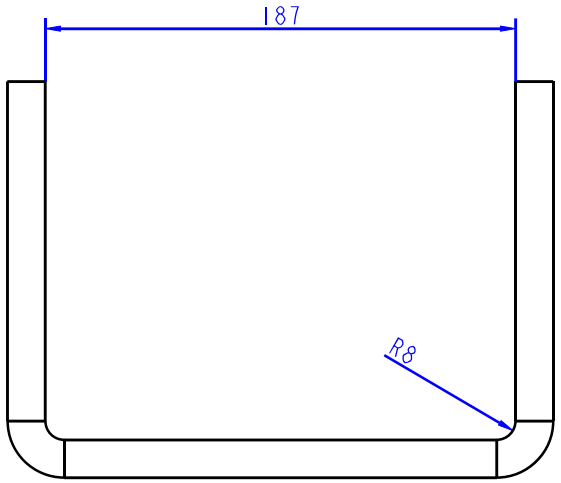

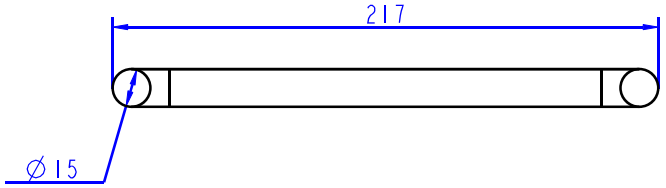

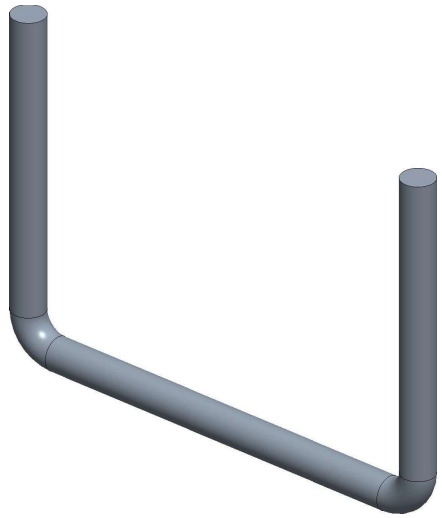

Pos	Ant	Artikell/Modell	Beskrivelse	Materiale	Dimensjon
Konstr	Tegnet OOB	Revisjon	Vekt	Skala 0.500	Format A3	Blad.nr 53(67)
Høgskulen på Vestlandet IMM		Artikell/Modell LOCKHANDLE			Dato 10-May-24
		Beskrivelse			Tegning SUBSEA_BASKET

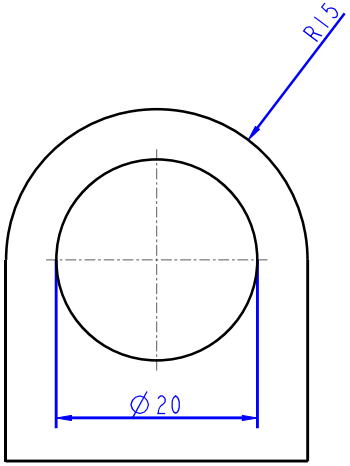

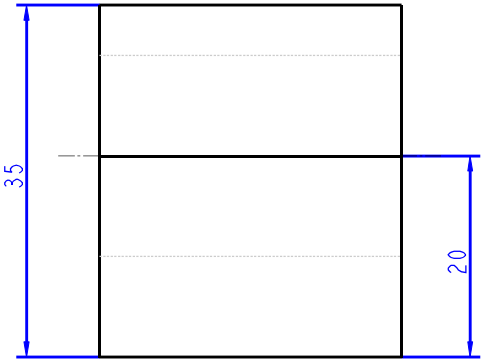

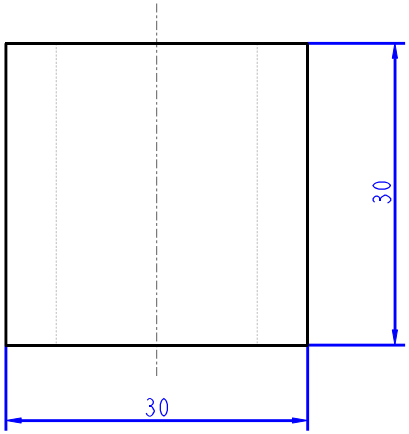

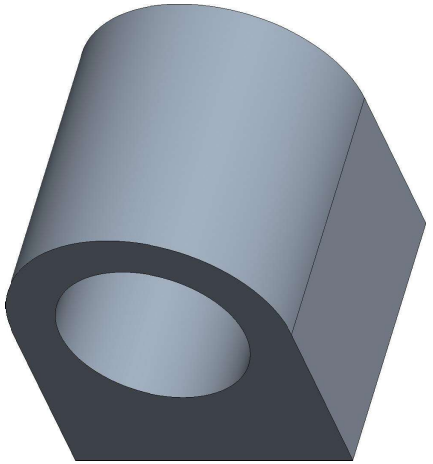

Pos	Ant	Artikell/Modell	Beskrivelse	Materiale	Dimensjon

Konstr	Tegnet	Revisjon	Vekt	Skala	Format	Blad.nr
	OOB			2.000	A3	54(67)

	Artikell/Modell	Dato
Høgskulen på Vestlandet IMM	GUIDEFORLOCK	29-Apr-24
	Beskrivelse	Tegning SUBSEA_BASKET

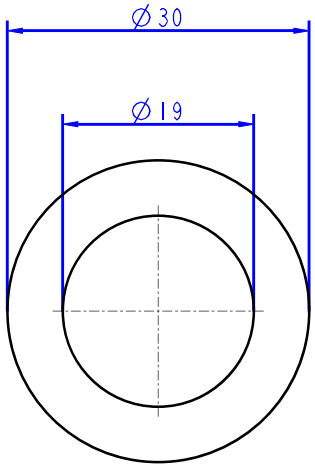

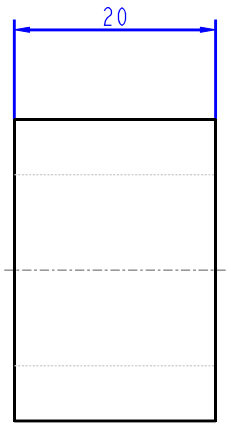

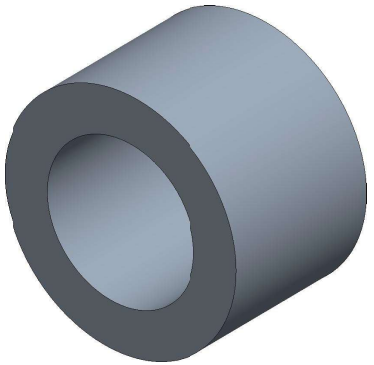

Pos	Ant	Artikell/Modell	Beskrivelse	Materiale	Dimensjon
Konstr	Tegnet OOB	Revisjon	Vekt	Skala 2.000	Format A3	Blad.nr 55(67)
Høgskulen på Vestlandet IMM		Artikell/Modell RINGFORLOCK			Dato 29-Apr-24
		Beskrivelse			Tegning SUBSEA_BASKET

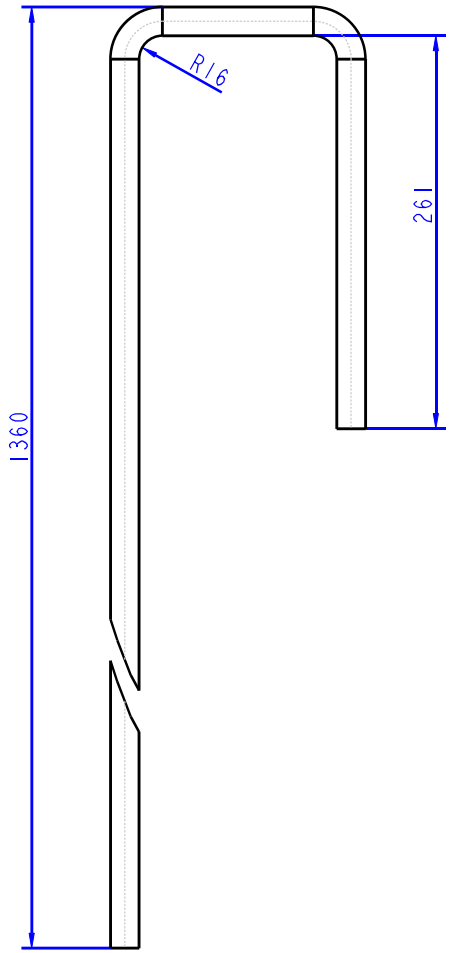

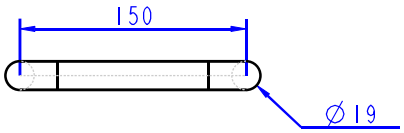

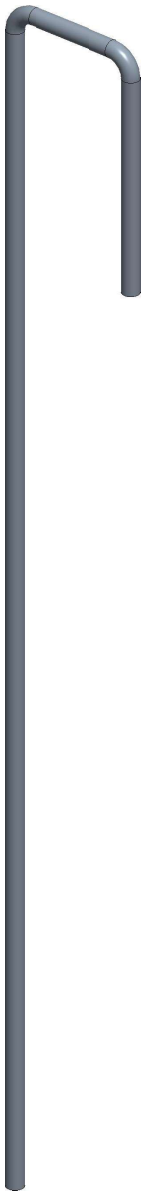

Pos	Ant	Artikell/Modell	Beskrivelse	Materiale	Dimensjon

Konstr	Tegnet	Revisjon	Vekt	Skala	Format	Blad.nr
	00B			0.300	A3	56(67)

	Artikell/Modell	Dato
Høgskulen på Vestlandet IMM	HANDLEDOOR	29-Apr-24
	Beskrivelse: -	Tegning: SUBSEA_BASKET

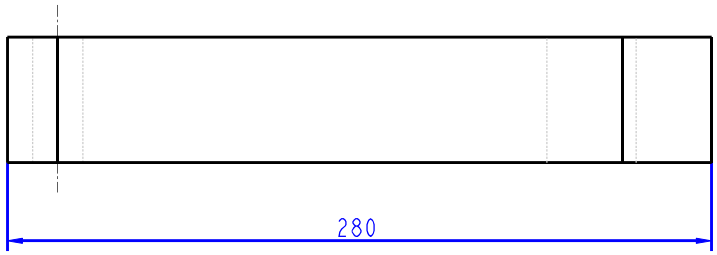

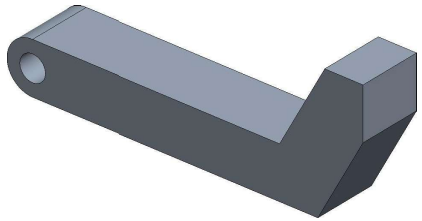

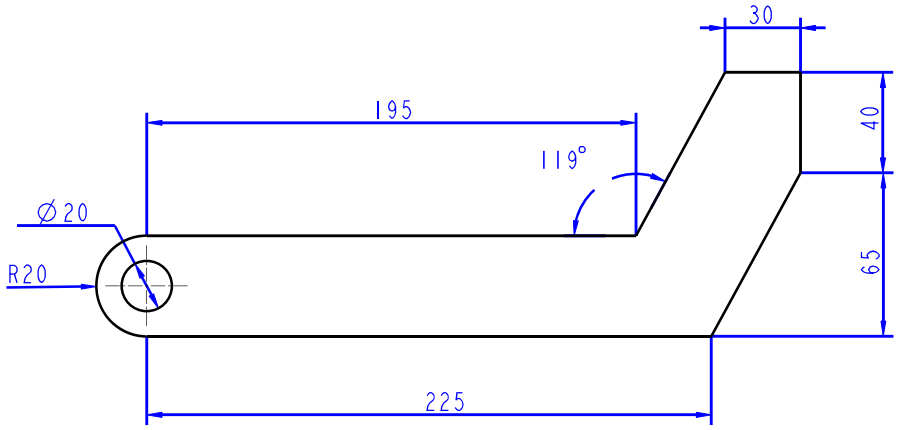

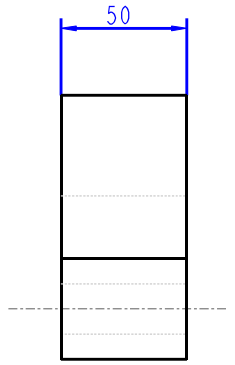

Pos	Ant	Artikell/Modell	Beskrivelse	Materiale	Dimensjon
Konstr	Tegnet: OOB	Revisjon	Vekt	Skala: 0.500	Format: A3	Blad.nr: 57(67)
Høgskulen på Vestlandet IMM		Artikell/Modell: HINGEDOOR			Dato: 01-May-24
		Beskrivelse			Tegning: SUBSEA_BASKET

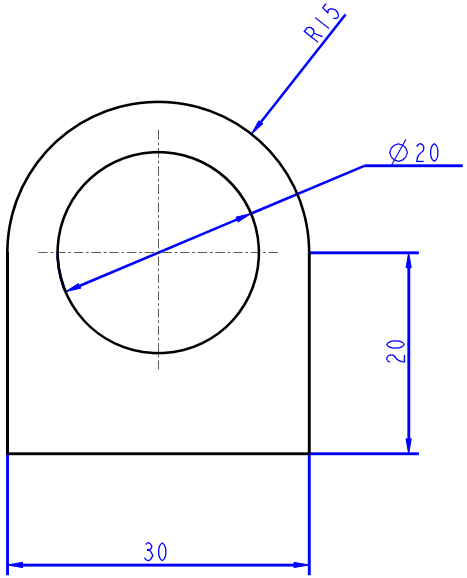

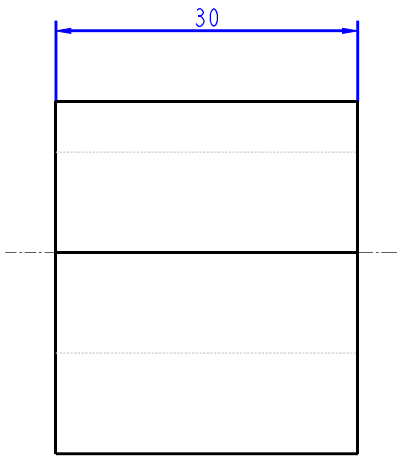

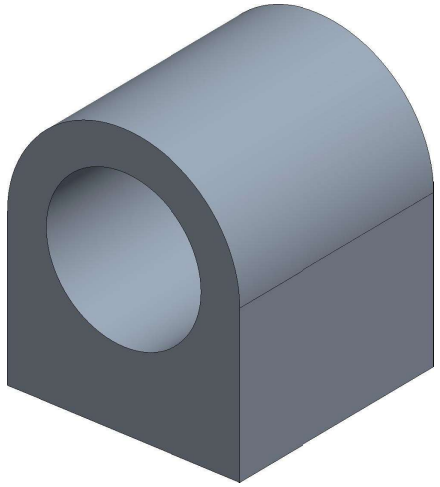

Pos	Ant	Artikell/Modell	Beskrivelse	Materiale	Dimensjon
Konstr	Tegnet OOB	Revisjon	Vekt	Skala 2.000	Format A3	Blad.nr 58(67)
Høgskulen på Vestlandet IMM		Artikell/Modell GUIDEFORLOCK			Dato 01-May-24
		Beskrivelse			Tegning SUBSEA_BASKET

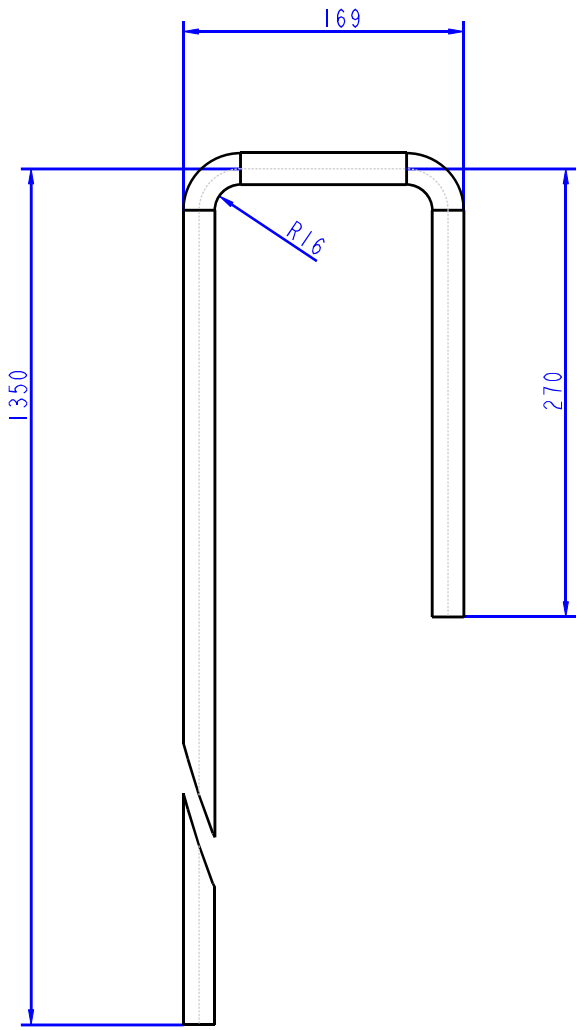

Pos	Ant	Artikell/Modell	Beskrivelse	Materiale	Dimensjon

Konstr	Tegnet	Revisjon	Vekt	Skala	Format	Blad.nr
	OOB			0.200	A3	59(67)

	Artikell/Modell	Dato
Høgskulen på Vestlandet IMM	HANDLEDOOR	01-May-24
	Beskrivelse	Tegning SUBSEA_BASKET

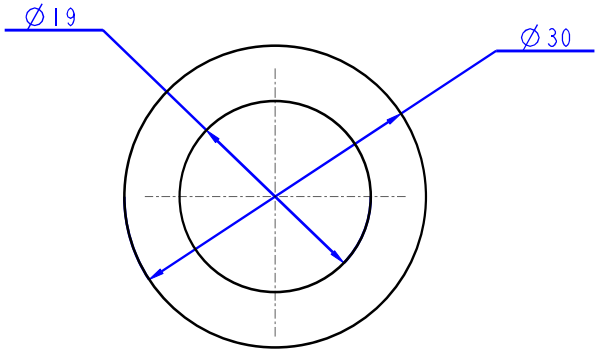

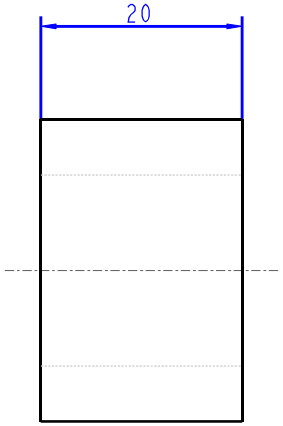

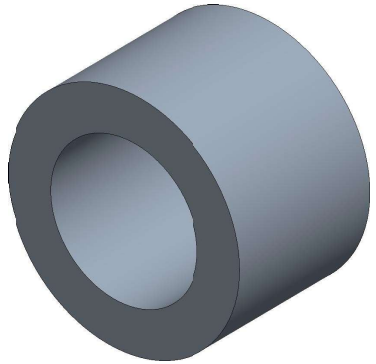

Pos	Ant	Artikell/Modell	Beskrivelse	Materiale	Dimensjon
Konstr	Tegnet OOB	Revisjon	Vekt	Skala 2.000	Format A3	Blad.nr 60(67)
Høgskulen på Vestlandet IMM		Artikell/Modell RINGFORLOCK			Dato 01-May-24
		Beskrivelse			Tegning SUBSEA_BASKET

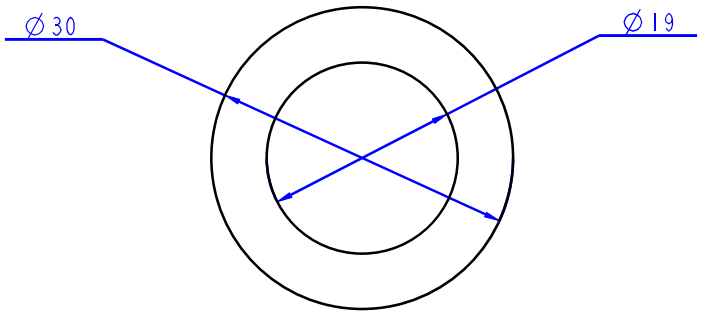

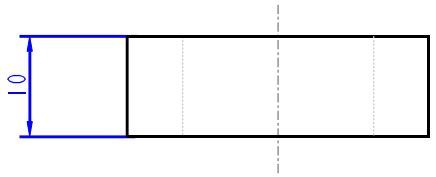

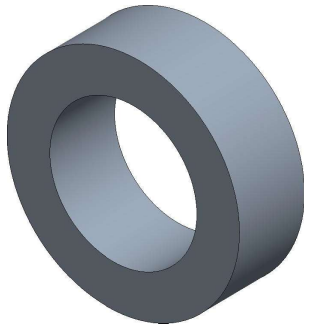

Pos	Ant	Artikell/Modell	Beskrivelse	Materiale	Dimensjon
Konstr	Tegnet OOB	Revisjon	Vekt	Skala 2.000	Format A3	Blad.nr 61(67)
Høgskulen på Vestlandet IMM		Artikell/Modell RINGFORLOCK2			Dato 08-May-24
		Beskrivelse -			Tegning SUBSEA_BASKET

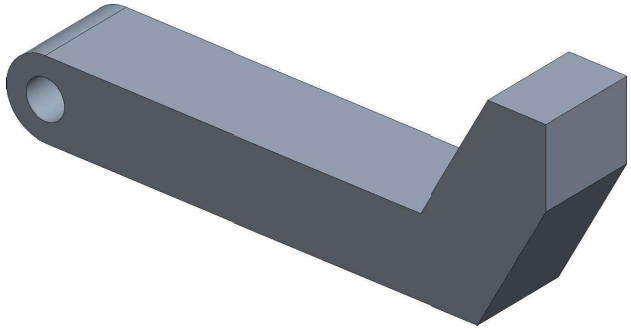

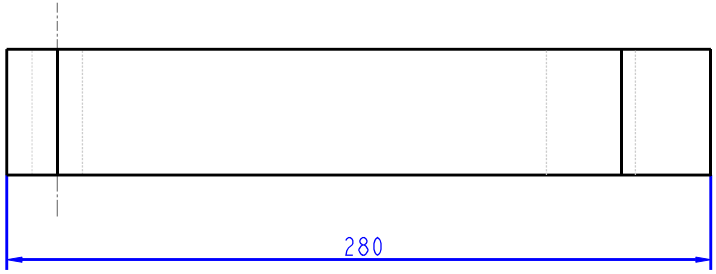

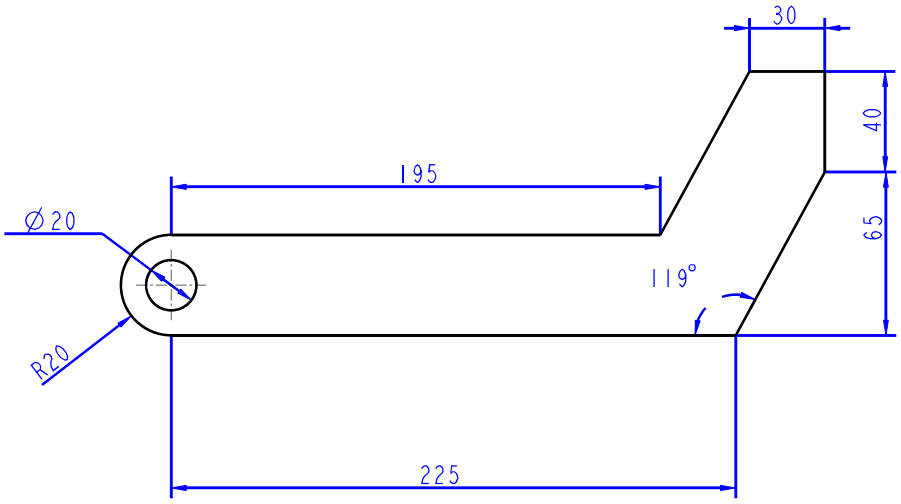

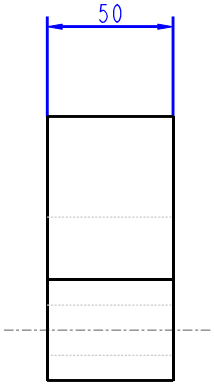

Pos	Ant	Artikell/Modell	Beskrivelse	Materiale	Dimensjon

Konstr	Tegnet	Revisjon	Vekt	Skala	Format	Blad.nr
	OOB			0.500	A3	62(67)

	Artikell/Modell	Dato
Høgskulen på Vestlandet IMM	HINGEDOOR	01-May-24
	Beskrivelse: -	Tegning: SUBSEA_BASKET

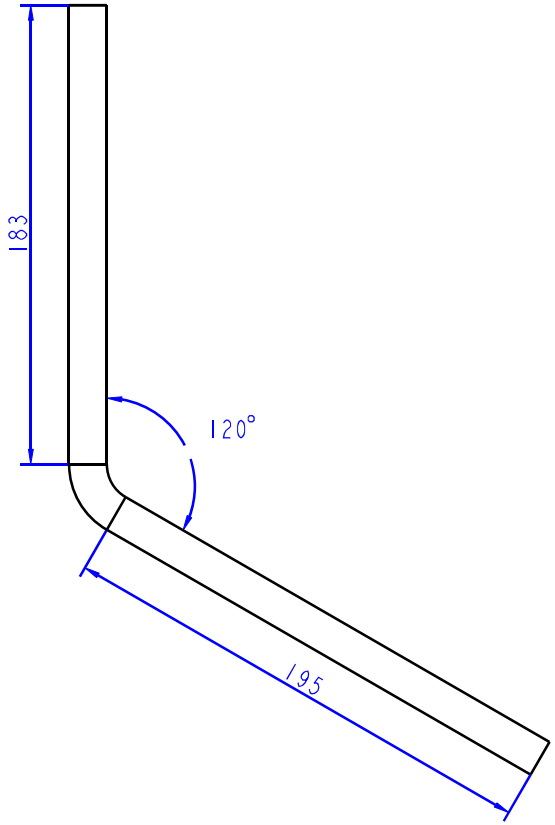

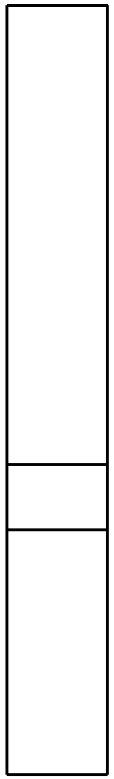

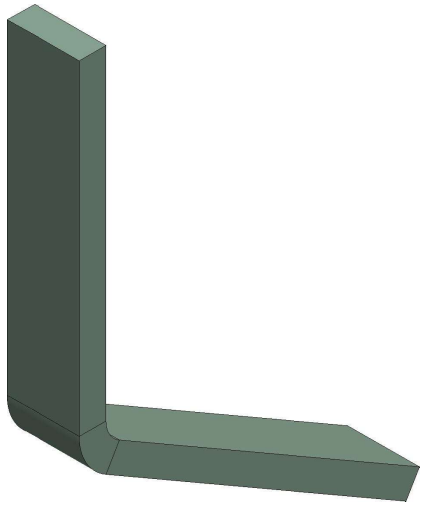

Pos	Ant	Artikell/Modell	Beskrivelse	Materiale	Dimensjon
Konstr	Tegnet VSF	Revisjon	Vekt	Skala 0.500	Format A3	Blad.nr 63(67)
Høgskulen på Vestlandet IMM	Artikell/Modell CHAIN_GUIDE_PLATE	Dato 14-May-24
	Beskrivelse	Tegning SUBSEA_BASKET

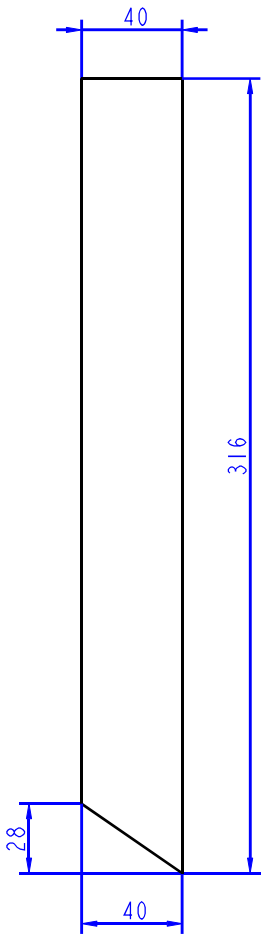

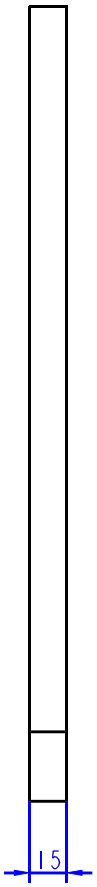

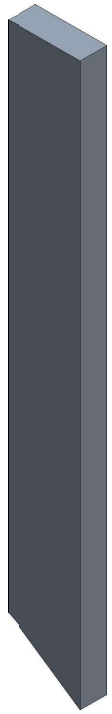

Pos	Ant	Artikell/Modell	Beskrivelse	Materiale	Dimensjon
Konstr	Tegnet VSF	Revisjon	Vekt	Skala 0.500	Format A3	Blad.nr 64(67)
Høgskulen på Vestlandet IMM	Artikell/Modell CHAIN_GUIDE_PLATE1				Dato 16-May-24
	Beskrivelse				Tegning SUBSEA_BASKET

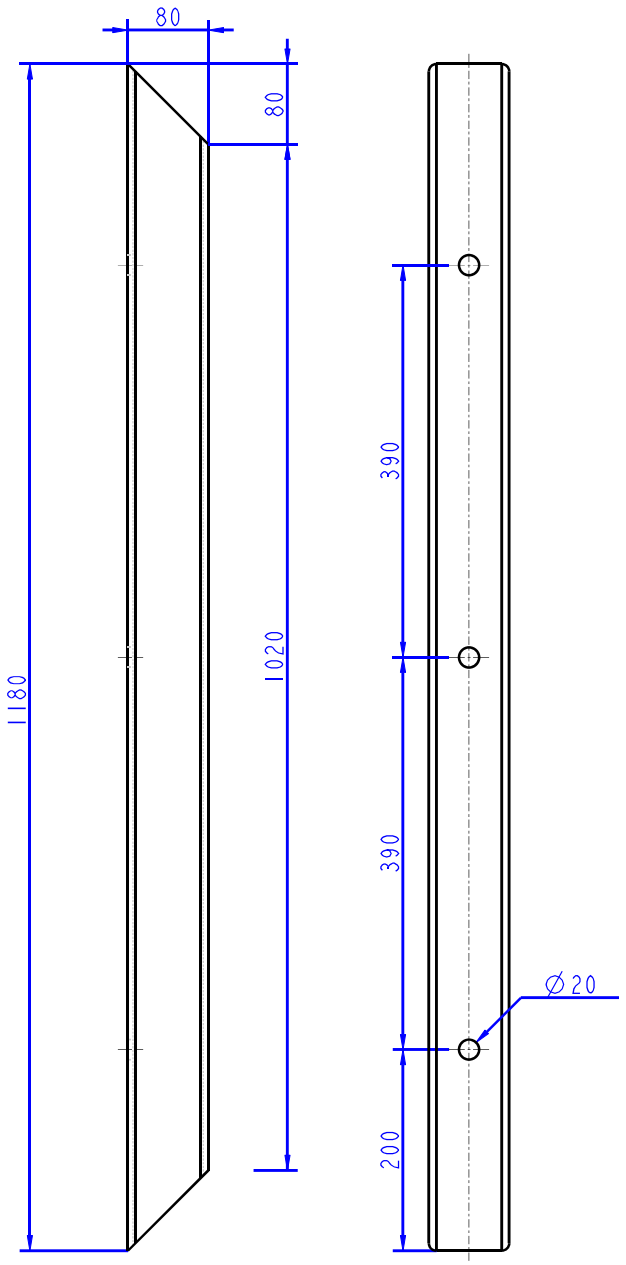

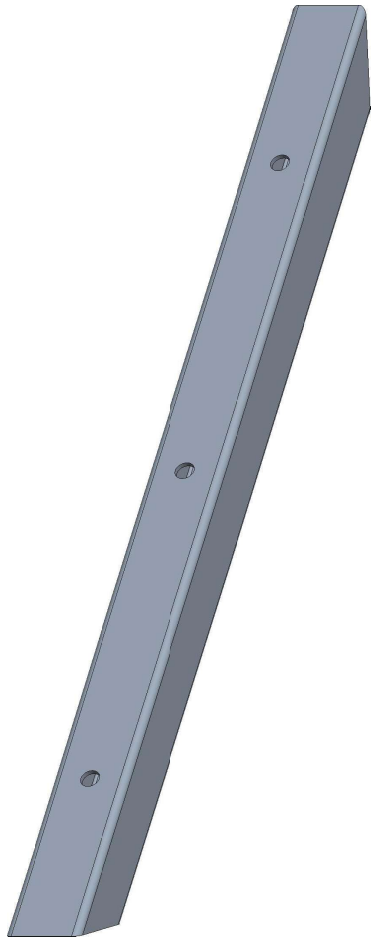

Pos	Ant	Artikell/Modell	Beskrivelse	Materiale	Dimensjon
Konstr	Tegnet OOB	Revisjon	Vekt	Skala 0.200	Format A3	Blad.nr 65(67)
Høgskulen på Vestlandet IMM	Artikell/Modell DOOR_BEAM_2			Dato 07-May-24
	Beskrivelse			Tegning SUBSEA_BASKET

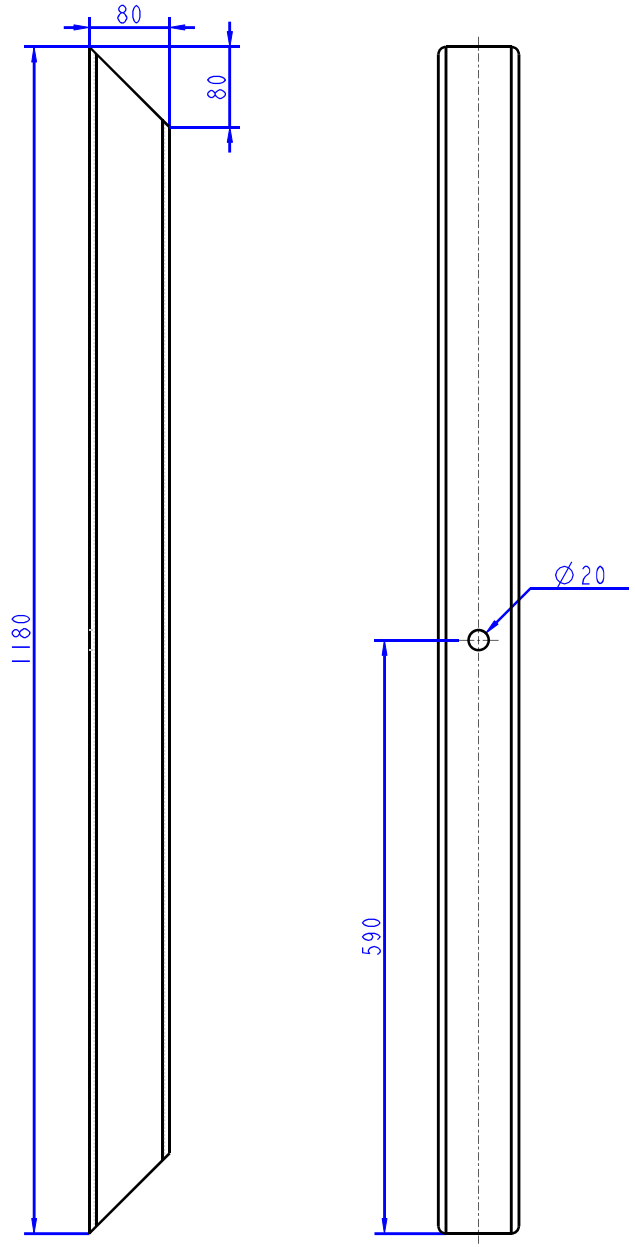

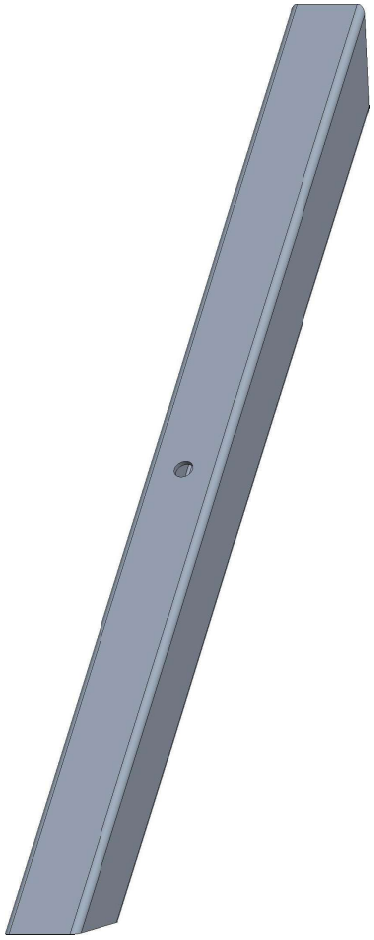

Pos	Ant	Artikell/Modell	Beskrivelse	Materiale	Dimensjon

Konstr	Tegnet	Revisjon	Vekt	Skala	Format	Blad.nr
	VSF			0.200	A3	66(67)

	Artikell/Modell	Dato
Høgskulen på Vestlandet IMM	DOOR_BEAM_4	14-May-24
	Beskrivelse	Tegning SUBSEA_BASKET

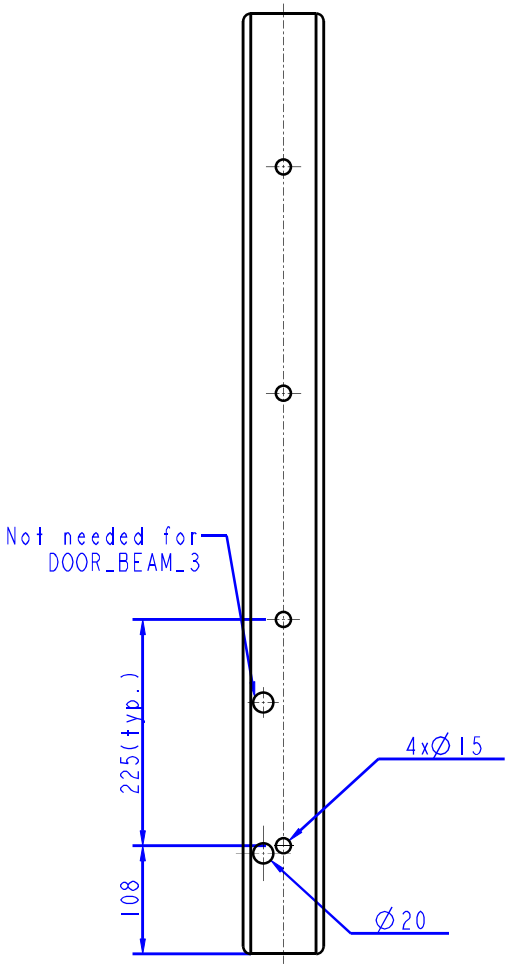

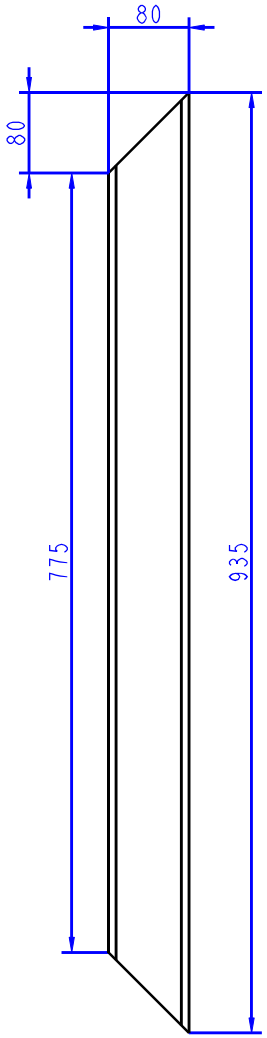

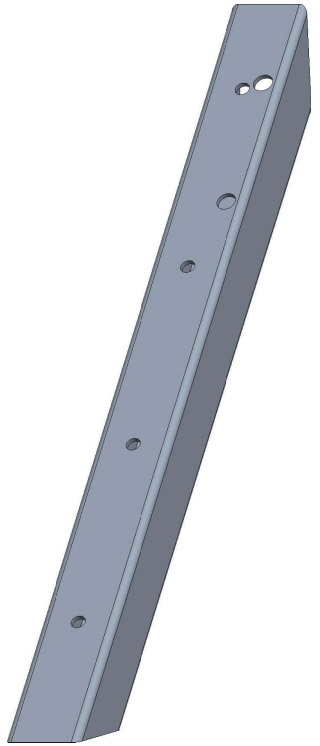

Pos	Ant	Artikell/Modell	Beskrivelse	Materiale	Dimensjon
Konstr	Tegnet OOB	Revisjon	Vekt	Skala 0.200	Format A3	Blad.nr 67(67)
Høgskulen på Vestlandet IMM		Artikell/Modell DOOR_BEAM_1 & DOORBEAM_3			Dato 07-May-24
		Beskrivelse			Tegning SUBSEA_BASKET